

Sheffield Hallam University

The identification and characterisation of antimicrobial peptides from snake and scorpion venom.

HARRISON, Patrick Liam.

Available from the Sheffield Hallam University Research Archive (SHURA) at:

<http://shura.shu.ac.uk/19762/>

A Sheffield Hallam University thesis

This thesis is protected by copyright which belongs to the author.

The content must not be changed in any way or sold commercially in any format or medium without the formal permission of the author.

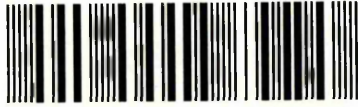
When referring to this work, full bibliographic details including the author, title, awarding institution and date of the thesis must be given.

Please visit <http://shura.shu.ac.uk/19762/> and <http://shura.shu.ac.uk/information.html> for further details about copyright and re-use permissions.

Learning and Information Services
Adsetts Centre, City Campus
Sheffield S1 1WD

(2000)

102 058 731 8



Sheffield Hallam University
Learning and Information Services
Adsetts Centre, City Campus
Sheffield S1 1WD

REFERENCE

ProQuest Number: 10697064

All rights reserved

INFORMATION TO ALL USERS

The quality of this reproduction is dependent upon the quality of the copy submitted.

In the unlikely event that the author did not send a complete manuscript and there are missing pages, these will be noted. Also, if material had to be removed, a note will indicate the deletion.



ProQuest 10697064

Published by ProQuest LLC (2017). Copyright of the Dissertation is held by the Author.

All rights reserved.

This work is protected against unauthorized copying under Title 17, United States Code
Microform Edition © ProQuest LLC.

ProQuest LLC.
789 East Eisenhower Parkway
P.O. Box 1346
Ann Arbor, MI 48106 – 1346

**THE IDENTIFICATION AND
CHARACTERISATION OF
ANTIMICROBIAL PEPTIDES
FROM SNAKE AND SCORPION
VENOM**

By

Patrick Liam Harrison

*Submitted in partial fulfilment for the degree of Doctor of
Philosophy (PhD)*

Biomedical Research Centre, Sheffield Hallam University

October 2014

Dedication

This thesis is dedicated to the memory of Thomas O'Shea and Trevor Harrison

Very different men, who shared common decency, a belief in fairness and pride in who they were. If everyone were like you the world would be a better place.

Quote

“It is not long since conditions in the mines were worse than they are now. There are still living a few very old women who in their youth have worked underground, with the harness round their waists, and a chain that passed between their legs, crawling on all fours and dragging tubs of coal. They used to go on doing this even when they were pregnant. And even now, if coal could not be produced without pregnant women dragging it to and fro, I fancy we should let them do it rather than deprive ourselves of coal. But-most of the time, of course, we should prefer to forget that they were doing it. It is so with all types of manual work; it keeps us alive, and we are oblivious of its existence. More than anyone else, perhaps, the miner can stand as the type of the manual worker, not only because his work is so exaggeratedly awful, but also because it is so vitally necessary and yet so remote from our experience, so invisible, as it were, that we are capable of forgetting it as we forget the blood in our veins. In a way it is even humiliating to watch coal-miners working. It raises in you a momentary doubt about your own status as an ‘intellectual’ and a superior person generally. For it is brought home to you, at least while you are watching, that it is only because miners sweat their guts out that superior persons can remain superior. You and I and the editor of the Times Lit. Supp., and the poets and the Archbishop of Canterbury and Comrade X, author of Marxism for Infants—all of us really owe the comparative decency of our lives to poor drudges underground, blackened to the eyes, with their throats full of coal dust, driving their shovels forward with arms and belly muscles of steel”

-George Orwell-The Road to Wigan Pier, 1932

Acknowledgments

First of all thank you to my supervisors Dr. Keith Miller & Prof. Peter Strong for all their support and willingness to allow me freedom of thought and to try new things. Not everything worked out but I hope the direction we have travelled, represented in this thesis, will be something we can look back on with fondness. Thank you also to Prof. Stephen Evans, Dr. George Heath and Dr. Ben Johnson at the University of Leeds you have been truly remarkable collaborators and this thesis would look radically different without you. Also where would I be without my friends and colleagues Dr. Mohamed Abdel-Rahman and Mohamed Tawfik.

To Prof. Thomas Smith, whose decision to employ me as placement student within his laboratory in 2008 represents the start of this journey and I certainly wouldn't be where I am today without your kindness, I must also thank Dr. Jeanette Gittens and Dr. Tim Nichol for their help, support and friendship over the last six years. I'm sorry for all the stolen pens, tip boxes, lab coats and mess I make-I only hope you can forgive me!

And to Nicola, I don't think you realise the high regard people hold you in. The passion for your research, your role within science and the position you hold is only transcended by the warmth and kindness you do it with. Thank you for all your help and support over the last six years.

This PhD experience wouldn't have been the same without (Dr) Robert Bradshaw and Adam Bagshaw, in the three years I have lived at Kelham Island you have provided more fun, laughter and true friendship than most people experience in a lifetime. I've spent all my money on Kelham best, incredibly bad football bets and slow horses and I wouldn't change it for the world.

To my friends for who this big purple book means absolutely nothing. You're an eclectic bunch to say the least and long may you stay that way. Never stop being who you are and become what society considers acceptable.

Apart from the fancy title, an even if I fail the viva, it matters little because without starting this PhD I wouldn't have met my beautiful girlfriend. Words can't express how much I love you. When I think of the future I don't for one second consider the job I will have or things I will own I think of us building a life and a family, spending time together because to be truly happy is the biggest prize of all.

But lastly I save the biggest thank you to my parents whom I love dearly. You have given me everything I could have ever wished for and this thesis is yours as much as mine. Wherever I am or whatever I'm doing I always think of being at home. The mark of happy home is it makes you relaxed and comfortable and whenever I am there I always do. To me it will always be home.

Abstract

The need for new antimicrobial agents is becoming one of the most urgent requirements in modern medicine. In the search for new antimicrobial drugs, in recent years, a large amount of research has been undertaken to both identify antimicrobial peptides (AMPs) and elucidate their mechanism of action. AMPs are ubiquitous in nature and have favourable properties that make them attractive for drug development including potent activity, low resistance rates due to their membrane disruptive mechanism of action, and selectivity to prokaryotic membranes.

Venoms are an under exploited source of AMPs, in this thesis AMPs have been identified, biologically characterised and their mechanism investigated. From snake venom two novel AMPs (6-7KDa) along with four potential phospholipase A2 (PLA2) proteins have been identified (12-14 KDa). One of these peptides, isolated from black mamba venom (*Dendroaspis polylepis*) exerts moderate antimicrobial activity and has low cytotoxic properties making it an ideal candidate for future drug development. From scorpion venom, three AMPs (1-4 KDa) have been biologically characterised, one of which, Smp43, is postulated to have a di-helical structure and exhibits good antimicrobial activity especially against Gram positive organisms (4-64 $\mu\text{g/ml}$) and exhibits negligible haemolytic properties at concentrations up to 512 $\mu\text{g/ml}$. The mechanism of action of Smp43 and a shorter peptide termed Smp24 has been determined using liposome leakage assays, atomic force microscopy (AFM) and quartz crystal microbalance-dissipation (QCM-D). Smp24 caused pore formation in synthetic prototypical prokaryotic membranes and induced the formation of non lamellar lipid structures and caused lipid segregation in a prototypical eukaryotic membrane whilst Smp43 exerted its effects through a mechanism of diffuse limited aggregation (DLA) which, until now, has not been described as an AMP mechanism of action.

In summary, this thesis has identified novel AMPs which can subsequently feed into drug development pipelines, provides further evidence of the membrane disruptive mechanism of AMPs whilst enhancing our understanding of these mechanisms.

Table of Contents

◇ Dedication – I ◇

Quote-II

◇ Acknowledgments-III

◇ Abstract – V ◇

◇ Table of contents – VII ◇

◇ List of figures – XII

◇ List of tables – XVII

◇ Abbreviations – XVIII

Dedication	i
Abstract	v
Table of Contents	vi
List of figures	ix
List of tables	xi
Abbreviations	xii
1 CHAPTER 1 INTRODUCTION TO ANTIMICROBIAL PEPTIDES	1
1.1 Introduction.....	2
1.2 Mechanisms of antimicrobial resistance.....	3
1.3 Strategies in antibiotic drug discovery	7
1.4 Antimicrobial Peptides	8
1.5 AMP conformation	9
1.6 Structural Characteristics of AMPs.....	12
1.7 Membrane characteristics.....	16
1.8 Natural resistance towards AMPs	20
1.9 Strategies for AMP production	21
1.10 AMP mechanism of action	23
1.11 AMPs from venom.....	35
1.11.1 AMPs from snake venom	36
1.11.2 AMPs from scorpion venom.....	41
1.12 Atomic force microscopy.....	68
1.12.1 Operation characteristics of AFM.....	69

1.12.2	Force volume curves	72
1.13	Quartz crystal microbalance-dissipation (QCM-D).....	74
1.14	Scope of the present study	76
2	CHAPTER 2 MATERIALS AND METHODS.....	77
2.1	Purification and characterisation	78
2.1.1	Venom	78
	Table 2.1: Venoms used within this study	79
2.2	Purification of venom constituents.....	80
2.2.1	Peptide synthesis.....	81
	Table 2.2 Peptides used within the study.	82
2.2.2	MALDI-TOF analysis.....	83
2.3	Biological Characterisation.....	83
2.3.1	Antimicrobial assay	83
2.3.2	Haemolysis assay.....	84
2.3.3	Cytotoxicity assay.....	84
2.3.4	Membrane integrity assay (BacLight).....	85
2.3.5	Intracellular bio-reporter gene assay	86
2.4	Biophysical determination of mechanism of action.....	86
2.4.1	Lipids used within study	86
2.4.2	Bilayer preparation.....	88
2.4.3	AFM imaging of hydrated lipid bilayers	88
2.4.4	QCM-D protocol	88
2.4.5	Liposome leakage assay	90
3	CHAPTER 3 IDENTIFICATION AND CHARACTERISATION OF ANTIMICROBIAL PEPTIDES FROM SNAKE VENOMS	92
3.1	Background and Aims.....	93
3.2	Method Summary.....	93
3.3	Results	94
3.3.1	Isolation and characterisation of an antimicrobial component of <i>Bitis arietans</i> venom	96
3.3.2	Isolation and characterisation of an antimicrobial component of <i>Crotalus</i> <i>adamanteus</i> venom.....	101
3.3.3	Isolation and characterisation of an antimicrobial component of <i>Naja haje</i> venom	104
3.3.4	Isolation and characterisation of an antimicrobial component of <i>Dendroaspis</i> <i>polylepis</i> venom.....	106
	107

3.3.5	Isolation and characterisation of an antimicrobial component of <i>Notechis scutatus</i> venom	108
3.3.6	Isolation and characterisation of an antimicrobial component of <i>Cerastes cerastes</i> venom	110
3.4	Discussion	112
4	CHAPTER 4 CHARACTERISATION OF ANTIMICROBIAL PEPTIDES FROM SCORPION VENOM	123
4.1	Background and aims	124
4.2	Method Summary.....	125
4.3	Results	125
4.3.1	Antimicrobial activity of AMPs from the <i>Scorpio maurus palmatus</i>	125
4.3.2	Haemolytic activity of AMPs from <i>Scorpio maurus palmatus</i>	127
4.3.3	Cytotoxic activity of AMPs from <i>Scorpio maurus palmatus</i>	130
4.3.4	Membrane disruptive potential of scorpion AMPs.....	132
4.3.5	Elucidation of intracellular targets of scorpion AMPs using the <i>B. subtilis</i> whole cell assay	134
4.4	Discussion	137
5	CHAPTER 5 BIOPHYSICAL CHARACTERISATION OF THE ANTIMICROBIAL PEPTIDES SMP24 & SMP43 FROM <i>SCORPIO MAURUS PALMATUS</i>	159
5.1	Background and Aims.....	160
5.2	Method Summary.....	162
5.3	Results	162
5.3.1	Analysis of Smp24 using liposome leakage assays.....	162
5.3.2	Analysis of Smp24 attack on hydrated lipid bilayers using AFM.....	166
	172
5.3.3	Analysis of Smp24 attack on hydrated lipid bilayers using QCM-D	177
	179
5.3.4	Analysis of Smp43 attack on liposomes	181
5.3.5	Analysis of the mechanism of action of Smp43 using the Dimension FastScan Bio™ AFM	185
5.4	Discussion	191
6	CHAPTER 6 CONCLUSIONS AND FUTURE WORK	215

List of figures

Figure 1.1: Structural conformation of the major classes of antimicrobial peptides.....	11
Figure 1.2: Physiochemical properties of AMPs.....	13
Figure 1.3: The major prototypical characteristics of both prokaryotic and eukaryotic membranes.	17
Figure 1.4: Differences of phospholipid geometry and the effect of lipid packing.....	19
Figure 1.5: Postulated mechanism of action of AMPs.....	27
Figure 1.6: Alternative models of AMP mechanism of action.....	32
Figure 1.7: Mechanism of action of Pandinin 2	48
Figure 1.8: Mechanism of action of Pandinin 1.	49
Figure 1.9: Schematic illustration of a scanned tip AFM system.....	71
Figure 1.10: Schematic of a force spectroscopy curve.....	73
Figure 1.11: Explanation of the QCM-D reading upon peptide attack.	75
Figure 3.1: Isolation and characterisation of a potential PLA2 antimicrobial protein from <i>Bitis arietans</i> venom.....	98
Figure 3.2: Haemolytic effects of antimicrobial snake proteins against sheep erythrocytes.....	99
Figure 3.3: Membrane damaging effects of snake proteins against the eukaryotic cell line HepG2 determined by release of ATP..	100
Figure 3.4: Purification of a potential PLA2 protein from <i>Crotalus adamanteus</i> venom.....	103
Figure 3.5: Purification of a possible PLA2 protein from <i>Naja haje</i> venom	105
Figure 3.6: Purification of an antimicrobial protein from <i>Dendroaspis polylepis</i> venom.....	107
Figure 3.7: Purification of an AMP from <i>Notechis scutatus</i> venom	109
Figure 3.8: Purification of a potential antimicrobial protein from <i>Cerastes cerastes</i> venom ...	111
Figure 3.9: Structural motifs of snake venoms that could be used as AMPs	117
Figure 4.1: Haemolytic activities of peptides used within this study.....	129
Figure 4.2: Cytotoxic activities of peptides used within this study.....	131
Figure 4.3: Stress response of <i>B. subtilis</i> elucidated after incubation with scorpion AMPs using the luciferase/luciferin assay	136
Figure 4.4 Alignment of Smp43 with evolutionary related scorpion AMPs using ClustalW2 alignment software (EMBL)	138
Figure 4.5: Alignment of Smp24 & Smp43 with the Pandinin peptides using ClustalW2 alignment software (EMBL)	138
Figure 4.6: Helical wheel analysis of the predicted helical regions of Smp43 using the r3lab software from the University of California (WWW.r3lab.ucr.edu).	140
Figure 4.7: Comparison of the predicted helical regions of Smp24 and Smp24GVG using the Jpred 3 server	144
Figure 4.8: Spatial distribution of Smp24 modelled using the 3D Hydrophobic Moment Vector Calculator.	145
Figure 4.9: Spatial distribution of Smp24GVG modelled using the 3D Hydrophobic Moment Vector Calculator	145
Figure 4.10: C-terminal analysis of the effect of the GVG motif insertion in to both Smp24 and Pin 2 modelled using the 3D Hydrophobic Moment Vector Calculator	146
Figure 5.1: Effect of Smp24 against a number of PCPG bilayers at varying concentrations....	164
Figure 5.2: Effect of Smp24 against a number of PCPE bilayers at varying concentrations....	165
Figure 5.3: The effect of Smp24 on a phase separated bilayer at 1.0 μ M determined by AFM	

.....	167
Figure 5.4: The effect of Smp24 attack on a PCPG bilayer at 1.25 μ M determined by AFM..	168
Figure 5.5: Analysis of pore size detected within a PCPG bilayer after 1.25 μ M Smp24 attack..
.....	169
Figure 5.6: The effect of Smp24 attack on a PCPG bilayer at 2 μ M determined by AFM	170
Figure 5.7: The effect of Smp24 on a PCPE bilayer at 1.25 μ M determined by AFM.....	172
Figure 5.8: The analysis of PCPE bilayer disruption after Smp24 attack at 1.25 and 2.0 μ M..	173
Figure 5.9: The effect of Smp24 on a PC:PE bilayer at 2.0 μ M determined by AFM.....	174
Figure 5.10: The effect of the incorporation of 10 % cholesterol into a PCPG bilayer has on Smp24 attack at 1.25 μ M determined by AFM.....	176
Figure 5.11: QCM-D analysis of Smp24 attack on a PCPG bilayer	179
Figure 5.12 QCM-D analysis of Smp24 attack on a PC:PE bilayer.....	180
Figure 5.13: Effect of Smp43 against a number of PCPG bilayers at varying concentrations	182
Figure 5.14: Effect of NaCl on Smp43 lyses of PCPG liposomes.....	183
Figure 5.15: Effect of Smp43 against a number of PCPE liposomes at varying concentrations	184
Figure 5.16: Initial nucleation sites of Smp43 attack on a PCPG bilayer as determined by AFM	187
Figure 5.17: Initial nucleation site of Smp43 attack on a PCPE bilayer as determined by AFM.	188
Figure 5.18: The contrasting speed of membrane disruption after Smp43 attack after initial nucleation is observed on both PC:PG and PC:PE bilayers	189
Figure 5.19: The contrasting effects of Smp43 attack on PC:PG and PC:PE bilayers as determined by high speed AFM	190
Figure 5.20: Explanation of steric hindrance	196
Figure 5.21: Worm like structures detected by Lam <i>et al.</i> , 2012 using atomic force microscopy..	198
Figure 5.22: Non lamellar structures possibly present after Smp24 attack on PCPE bilayers..	202
Figure 5.23: The comparison of DLA type patterns seen with Smp43 attack and a typical DLA structure.).....	205
Figure 5.24: Expanding pore mechanism for amphipathic AMPs proposed by Rakowski <i>et al.</i> , 2013.....	210

List of tables

Table 1.1: Examples of antibiotic resistance mechanisms	4
Table 1.2: Table of selected AMPs isolated from snake venoms with known sequence	40
Table 1.3: Table of selected scorpion derived AMPs with known sequence	62
Table 2.1: Venoms used within this study	79
Table 2.2 Peptides used within the study.	82
Table 3.1: Molecular weight, antimicrobial activity and membrane damaging effect against <i>E.coli</i> and <i>S.aureus</i> of all the peptides isolated in this study	95
Table 4.1: Antimicrobial activity of AMPs (MIC) isolated from <i>Scorpio maurus palmatus</i> , Smp24 derivatives and Pin 2 from <i>P. imperator</i>	126
Table 4.2: Effect of Smp24 on a range of <i>S. aureus</i> strains	126
Table 4.3: Effect of scorpion AMPs on Gram positive and Gram negative membranes	133

Abbreviations

μg	micro gram
CPS	Capsule polysaccharide
AN-OH	Anoplin non amidated
AN-NH ₂	Anoplin amidated
HAS	Human serum albumin
μM	micro molar
AC	Alternate current
AFM	atomic force microscopy
ALPS	amphipatic lipid packing sensor
AMP	Antimicrobial peptide
ATP	Adenosine triphosphate
BLAST	Basic Local Alignment Search Tool
CD	Circular dichroism
CF	Carboxyfluorescein
CHCA	Cyno-4-hydroxycinnamic acid
CL	Cholesterol
CR	Cardiolipin
CV	Column volume
D	Dissipation
Da	Daltons
DLA	Diffuse limited aggregation
DMEM	Dulbecco modified Eagle's minimal essential medium
DMPC	Dimyristoyl-sn-glycero-3-phosphocholine
DNA	Deoxyribonucleic acid
DOPC	1,2-Dioleoyl-sn-glycero-3-phosphocholine
DOPE	1,2-Dioleoyl-sn-glycero-3-phosphoethanolamine

DOPG	1,2-Dioleoyl-sn-glycero-3-phospho-rac-(1-glycerol)
DPPE	1,2-Dipalmitoyl-sn-glycero-3-phosphoethanolamine
DPPG	1,2-Dipalmitoyl-sn-glycero-3-phosphoglycerol
DRG	Dorsal root ganglion
EDTA	Ethylenediaminetetraacetic acid
EMRSA	Epidemic Methicillin-resistant <i>Staphylococcus aureus</i>
f,	frequency
FM-KPFM	Frequency Modulated-Kelvin Probe Force Microscopy
FRET	Fluorescence resonance energy transfer
GAPDH	Glyceraldehyde 3-phosphate dehydrogenase
Gly	Glycine
GS	Gramicidin S
HepG2	Hepatic liver cells
HM	Hydrophobic moment
Hr	Hour
Hz	Hertz
Ile	Isoleucine
L _d	Lipid disordered domain
Leu	Leucine
LL-37	Cathelicidin LL-37
L _o	Lipid ordered domain
LPS	Lipopolysaccharide
Lys	Lysine
m/z	mass to charge ratio
mAChR	Muscarinic acetylcholine receptors
MALDI-TOF	Matrix-assisted laser desorption/ionization time of flight mass spectrometry
MAPK	mitogen-activated protein kinase

MIC	Minimum inhibitory concentration
mM	Milli molar
MRSA	Methicillin-resistant <i>Staphylococcus aureus</i>
NaChBac	Bacterial sodium channel
nAChRs	Nicotine acetylcholine receptors
NaCl	Sodium chloride
Na _v	Voltage gated sodium channel
NDYAG	Neodymium-doped yttrium aluminium garnet
Nm	Nano metre
NMR	Nuclear magnetic resonance
NTII	α -neurotoxin II
PBS	Phosphate buffered saline solution
PC/SM/CL	DOPC/ sphingomyelin/cholesterol
PC:PE	DOPC/DOPE
PC:PE:CL	DOPC/DOPE/cholesterol
PC:PG	DOPC/DOPG
PC:PG:CL	DOPC/DOPG/cholesterol
PC:PG:CR	DOPC:DOPG:cardiolipin
PE	Phosphatidylethanolamine
PG	Phosphatidylglycerol
PG-1	Protegrin-1
Phe	Phenylalanine
Pin 1	Pandinin 1
Pin 2	Pandinin 2
PKC	Protein Kinase C
PLA2	Phospholipase A2
POPE	1-palmitoyl-2-oleoyl-sn-glycero-3-phosphoethanolamine
Pro	Proline

PS	Phosphatidylserine
PZT	Piezoelectric
QCM-D-	quartz crystal microbalance
R_f	Resonant frequency
RNA	Ribonucleic acid
S	second
SDS	sodium lauryl sulfate
SEM	Scanning electron microscopy
SIMS	Secondary ion mass spectrometry
SM-	sphingomyelin
TEM	Transmission electron microcopy
TFE	2,2,2-Trifluoroethanol
Trp	Tryptophan
UV	Ultra violet
Val	Valine
WAFC	Whey acidic protein disulphide bridged core
α	alpha
β	beta
γ	gamma

1 CHAPTER 1
INTRODUCTION TO ANTIMICROBIAL PEPTIDES

1.1 Introduction

Over the last few decades an increasing number of pathogenic microorganisms have developed resistance to conventional antibiotics. This poses problems in the clinical management of infection, especially in immunocompromised individuals but also, increasingly, at the community level. During the same period, the development of new antibiotics has decreased. Recent publications by a number of leading public bodies have highlighted this issue. For example, the publication of the UK Five Year Antimicrobial Resistance Strategy (2013-2018) stated antimicrobial resistance to be one of the greatest threats to the health of society and setting out a number of goals that need to be reached to mitigate the problem include (i) having good infection prevention and control measures to help prevent infections becoming the norm in all sectors of human and animal health (ii) diagnosing infections quickly and using the right treatment strategy (iii) for patients and animal keepers to fully understanding the importance of antibiotic treatment regimens and to adhere to them (iv) for surveillance to be in place which quickly identifies new threats or changing patterns in resistance and (v) a sustainable supply of new, effective antimicrobials is developed (Department of Health, UK 2013) Importantly, these goals need to be achieved on a worldwide scale a notion recognised by the World Health Organization (WHO) in its 2014 antimicrobial resistance global surveillance report (WHO 2014) which ominously states that the once apocalyptic fantasy of a post antibiotic era is now a very real prospect. This worldwide problem is driven by the ability of mobile genetic elements of bacterial plasmids to spread through a population which increases the overall rate of resistance (Kumarasamy et al., 2010). While the media portrayal of an imminent crisis of untreatable infections is over simplistic, the position in reality is rather more complex and although treatment options for some pathogens have undoubtedly decreased, for others the position has actually reversed (Livermore. 2009). However recent high profile media coverage of

antimicrobial resistance have included prominent figures such as the prime minister David Cameron (Walsh 2014a), the UK's chief medical officer Dame Sally Davies and leading members of the scientific national charities antibiotic action and antibiotic research UK (BBC 2014b) highlighting the severity of the issue and the potential impact on public life. One of the major issues in combating antimicrobial resistance is developing antimicrobial agents that are not easily susceptible to resistance and therefore a new approach to drug development is required (Jenssen et al., 2006).

1.2 Mechanisms of antimicrobial resistance

Conventional antibiotics have been developed that either kill or inhibit the growth of bacteria by binding to specific targets within bacteria. Table 1.1 summarises these antimicrobial drug targets as well as the resistance mechanisms bacteria have developed to combat these drugs.

Resistance to antibiotics is neither a new phenomenon nor an unnatural process with no single antibiotic having complete broad spectrum activity. Rather, the selective pressures of antibiotic use promote the survival of resistant strains, indeed the spread of methicillin resistance in *Staphylococcus aureus* was reported as far back as the early 1960's (Chastre. 2008). Antibiotic resistance is complex and no single issue can be pin pointed. However, the widespread abuse of antibiotics around the world including uncontrolled administration (Conly. 1998) an ageing population within the developed world requiring more complex healthcare (Chopra *et al.*, 2008), increased global migration (Kumarasamy *et al.*, 2010) and the use of antibiotics within farming (Porrero *et al.*, 2007, Van den Bogaard *et al.*, 1999) especially when administered at a sub-therapeutic dosage (Ghosh *et al.*, 2007) have all contributed to the problem.

Table 1.1: Examples of antibiotic resistance mechanisms

Antimicrobial agent	Mechanism of drug	Mechanism of resistance	Example of clinically relevant resistant pathogens
Beta lactams <i>penicillins</i> <i>cephalosporins</i> <i>carbapenems</i> <i>monobactams</i>	Inhibition of cell wall synthesis	Beta-lactamase	<i>S. aureus</i> <i>N. gonorrhoeae</i> Enterococci Gram negative bacilli
		Altered penicillin binding protein	MRSA <i>S. pneumoniae</i>
		Reduced permeability	<i>P. aeruginosa</i> <i>E. cloacae</i>
Glycopeptides <i>vancomycin</i>	Inhibition of cell wall synthesis	Altered drug target	Enterococci
Fluoroquinolones <i>ciprofloxacin</i>	Inhibition of DNA synthesis	Altered DNA gyrase	<i>S. aureus</i> Gram negative bacilli <i>M. tuberculosis</i>
		Efflux	<i>S. aureus</i> Gram negative bacilli
Rifampin	Inhibition of RNA synthesis	Altered RNA polymerase	<i>M. tuberculosis</i>
Aminoglycosides <i>Gentamicin</i> <i>streptomycin</i> <i>kanamycin</i>	Inhibition of protein synthesis	Modifying enzymes	Enterococci Gram negative bacilli
		Altered ribosomal target	<i>M. tuberculosis</i>
		Reduced uptake	<i>P. aeruginosa</i>

Macrolides <i>erthromycin</i> <i>clarithomycin</i>	Inhibition of protein synthesis	Altered ribosomal target	<i>S. pneumonie</i>
Tetracyclines <i>tetracycline</i>	Inhibition of protein synthesis	Altered ribosomal target	<i>N. gonorrhoeae</i> <i>S. aureus</i>
		Efflux	<i>S. aureus</i> Gram negative bacilli
Oxazolidinones <i>linezolid</i>	Inhibition of protein synthesis	Efflux	<i>S. aureus</i> Enterococci
Folate inhibitors <i>sulfonamides</i>	Inhibition of folic acid	Novel target enzymes	Gram negative bacilli
Lipopeptides <i>daptomycin</i>	Cell membrane disruption	Changes in membrane composition	<i>S. aureus</i> Enterococci
Polymyxins	Inner and outer membrane disruption	Altered outer membrane	Gram negative

Resistance can develop in a number of ways, by horizontal gene transfer of mobile genetic elements (both inter and intra) and by point mutations within an antibiotic target (Bryan., 1989, Silver *et al.*, 1993 & Silver., 2011). Often it is assumed that the former is responsible for increased resistance levels of resistance, however as Woodford and Ellington. (2007) highlighted, organisms capable of hyper-mutation can readily acquire resistance without the need for horizontal gene transfer. Furthermore they are responsible for the continued evolution of plasmids containing resistance genes.

Along with acquired resistance bacteria can also exhibit phenotypic resistance which is often transient and dependent on their physiological condition. For example, if the bacteria are in a restive or dividing state effects susceptibility with a number of studies

showing reduced antibiotic efficacy against resting cells (Lee *et al.*, 1944, McDermott., 1958). A reduction in cell permeability due to environmental stress such as temperature, nutrient deficiency, the presence of reactive oxygen species can reduce susceptibility in a number of ways, firstly, changes in cell wall/membrane architecture, for example, by modification or reduction of LPS, capsule formation, secondly, the closure of porins which through antibiotics can gain access to intracellular targets antibiotics and thirdly an increased production of efflux pumps (McPhee *et al.*, 2003). The formation of a biofilm leads to decreased susceptibility facilitating survival against antibiotic attack as gradients of nutrients and oxygen within the biofilm change the metabolic states of the bacteria depending on their depth inside the biofilm. Also, compounds of the matrix can impair the diffusion of the antibiotic and eventually bind the drug thus reducing its free concentration. Quorum sensing, which can be triggered at dense regions of the biofilm, may also alter bacterial susceptibility to antibiotics. Also the presence of persistent cells within the bacterial population, there is a subpopulation that are not killed by antibiotics in conditions that kill the bulk of the population, however, once growth resumes, these cells become susceptible to antibiotics, indicating that the phenotype of resistance is transient.(Corona & Martinez. 2013)

Whilst there has been global misuse of antibiotic drugs, the situation has been compounded by the lack of development of new anti-infectives with no new class of drugs been developed since the 1980's (Livermore. 2009). Chopra *et al.* (2008) highlighted some of the key issues. The economic cost of drug development is considerable with capital of over \$800 million required to bring a drug to market and the development of drugs for chronic diseases is more attractive option for both long term use and fewer resistance problems. Tight regulation placed upon anti-infective agents with regards to their therapeutic index mean that drugs with possible adverse side

effects or moderate activities are not approved however these considerations are of reduced importance when considering other therapeutic agents such as cancer drugs.

1.3 Strategies in antibiotic drug discovery

Two major strategies of drug discovery are empirical screening, testing of compounds to determine effect (i.e. does it kill bacteria) and a more targeted approach (i.e. does it interact with a specific molecular target). With the exception of a few antibiotics (monobactams, carbapenems, and fosfomycin) nearly all antibiotics have come through empirical screening of natural chemicals and fermenting cultures rather than a targeted approach (Chopra. 2000). As described by Silver (2011) this shift has been part economic part philosophical. During the “golden age” of antibiotic discovery this empirical screening led researchers to discover new antibiotics on the basis of antimicrobial activity rather than their mechanism of action. This approach proved very fruitful however it was also recognised that it was inevitably going to lead to a situation of degeneracy. This led to a target based approach (Cohen., 1977) where compounds were assayed on the basis of their ability to interact with specific targets. Highly specialised groups taking responsibility for specific areas of research as opposed to a cohesive approach were also established, this loss of cohesion led to a situation where therapeutics competed against each other for development on the basis of their potential value to the company. This highly compartmentalised, intracellular targeted approach led to vast libraries of drug candidates and the natural drug development route was almost abandoned. The paradigm with a targeted approach is that you get what you are looking for. By either only screening against known antibiotic targets or taking genomic or structural approaches to determine activity based on molecular modelling of

previously known antibiotics the discovery of novel targets or structural motifs is essentially excluded (Harrison *et al.*, 2014).

This does not mean structural modification of existing classes has not been successful and this approach has resulted in lowered adverse effects and has combated resistance (Silver, 2011). Although the development of resistance has quickly become apparent; resistance to third and fourth generation cephalosporins and carbapenems in a number of bacteria has been the result of a number of mechanisms that include : the generation of extended-spectrum β -lactamases (ESBL) due to extension of the spectrum of already widely disseminated plasmid-encoded β -lactamases by amino acid substitution, acquisition of genes encoding ESBL from environmental bacteria as, increased expression of chromosome-encoded β -lactamase due to modifications in regulatory genes or mutations of the β -lactamase promoter sequence, horizontal transfer into other Gram-negative species, the dissemination of plasmid-mediated carbapenemases as KPC and metallo- β -lactamases and reduced expression of porin and/or efflux pump-proteins (Pfifer *et al.*, 2010).

1.4 Antimicrobial Peptides

AMPs represent an ancient defence mechanism that transverses the evolutionary spectrum and remain an effective strategy against invading pathogens in the animal kingdom they are commonly found in the blood, haemolymph, and mucus secretions and immunological cells, in the plant kingdom peptides have been isolated from roots, seeds, flowers, stems, and leaves. Because of their selectivity for prokaryotic membranes and their membrane-disruptive mechanisms for which microbes have little natural resistance, the spotlight in recent years has turned towards the development of novel antibiotics from these peptides (Zasloff., 2002).

AMP's can be broadly divided into 4 major groups; α helical, β sheet, extended peptides enriched with one or more amino acids and a small group of loop peptides (Powers., 2003) and have between around 10-70 amino acids. These conformations are represented in Figure 1.1.

1.5 AMP conformation

The α -helical peptides are by far the most intensely studied group; indeed nearly all the structural-functional relationship studies carried out have been undertaken on this class (Huang *et al.*, 2010). Unlike β sheet peptides they contain no disulphide bonds and lack tertiary structure and remain in extended, unstructured conformers until in the presence of membranes (Dennison *et al.*, 2005). They are best characterised by AMP helical families such as the magainins (Zasloff. 1987) isolated from amphibians, the insect derived cecropins (Christenson *et al.*, 1998), melittin from bee venom (Fennell *et al.*, 1968) and certain cathelcidins which have been isolated from a variety of species including humans, chickens, dogs, rats, frogs (Zanetti *et al.*, 2004) and recently snakes (Zhao *et al.*, 2008). These peptides can be both amidated and non amidated at the C-terminal, however longer chain peptides tend to be the latter (Harrison *et al.*, 2014) with shorter AMP amidation thought necessary for helical stability (Stranburg *et al.*, 2007). As well as amidation, α -helical peptides can either be a mono-helical structure or di-helical with the latter generally being far less cytotoxic. For example melittin is a mono-helical peptide with non specific lytic activity whilst maganin 2 is di-helical and is far less cytotoxic (Zasloff. 1987). Similarly pandinin 1 and 2 (Pin 1 & Pin 2) isolated from the venom of the scorpion *Pandinus imperator* (emperor scorpion) (Corzo *et al.*, 2001) show this phenomena with the di-helical pin 1 being far less haemolytic, which is postulated to be due to the increased flexibility around a central hinge region (Rodriguez *et al.*, 2011).

The β sheet peptides are largely represented by the defensins which are characterised by an anti-parallel β sheet fold that is stabilised by at least 3 disulphide bonds (Powers *et al.*, 2003). This tertiary structure is essential for activity with linearisation inhibiting activity (Matazuki *et al.*, 1993 & 1997). Along with this motif, β -sheet peptides can also be constrained by the cyclisation of the peptide backbone (i.e. gramicidin S and polymyxin B (Ashrafuzzaman *et al.*, 2009 & Tsubery *et al.*, 2000). Whilst the defensins contain minimal helical structure, other cysteine constrained AMPs such as the scorpine-like molecules isolated from scorpion venoms do have helical structure and, it has been postulated (Zhou *et al.*, 2004), that these peptides possess dual function, namely K^+ channel modulation with only the helical N-terminus being responsible for antimicrobial activity.

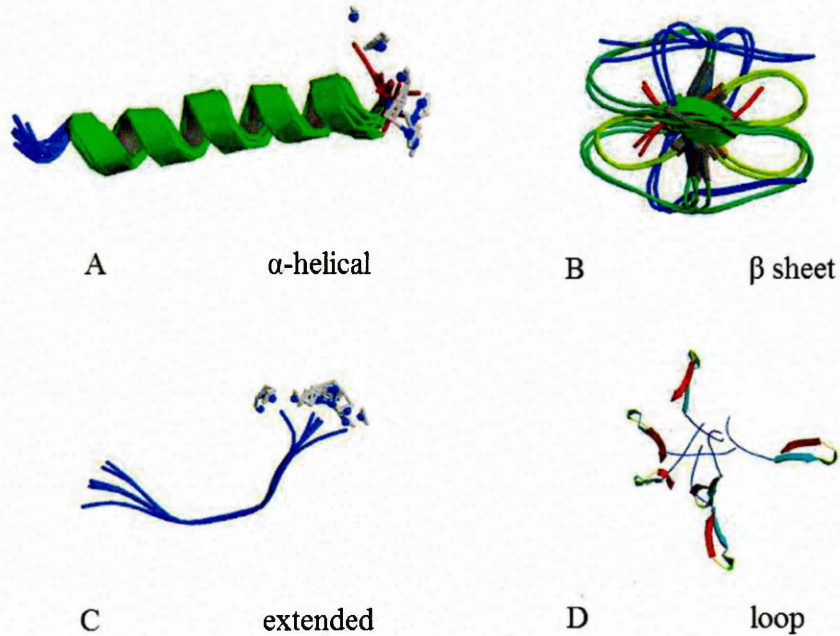


Figure 1.1: Structural conformation of the major classes of antimicrobial peptides-(A) The largest class of AMPs is the α -helical peptides represented by magainin 2 (PDB: MAG2) (Gessel *et al.*, 1997). (B) β -sheet peptides are the second largest group and are best represented by the defensins such as human β -defensin-1 (PDB: 1KJ5) (Schibili *et al.*, 2002). (C) & (D)- Two smaller but important groups are the extended peptides such as indolicidin (PDB: 1G89) (Rozek *et al.*, 2000) and the loop peptides such as thanatin (PDB: 8T8V) (Mandard *et al.*, 1998).

The extended peptides are best represented by the 13 residue tryptophan rich indolicidin (Selstrad *et al.*, 1992, Rozek *et al.*, 2000). These peptides lack secondary structure and only form weakly bound structures in the presence of membranes unlike α -helical peptides which form residue-residue non-covalent interactions, extended peptides form residue-lipid interactions (Powers *et al.*, 2003); indolicidin for example develops two kinks within its structure when in contact with DPC, however it remains in its straight conformation extended when in anionic SDS (Rozek *et al.*, 2000).

Loop peptides are the smallest of the classified groups with only one peptide being fully characterised. Thanatin (Fehlbaum *et al.*, 1996), a 21 residue peptide displays typical loop formation caused by the presence of a single bond disulphide bond between residue 11 and 18 that forms an anti-parallel β sheet loop between residues 8 and 21. Interestingly, it is not thought to be membrane disruptive as studies with D and L isoforms reveals stereospecificity with only the L-isoform being active, suggesting a receptor mediated mechanism.

1.6 Structural Characteristics of AMPs

An essential requirement of AMPs is to preferentially target the microbial membrane over the host membrane, therefore, the biochemical characteristics of AMPs are critical. To achieve this a number of interdependent physicochemical properties are found within AMPs these include amphipathicity, charge, hydrophobicity, polar angle and conformation (Yeaman *et al.*, 2003). This is represented below in figure 1.2.

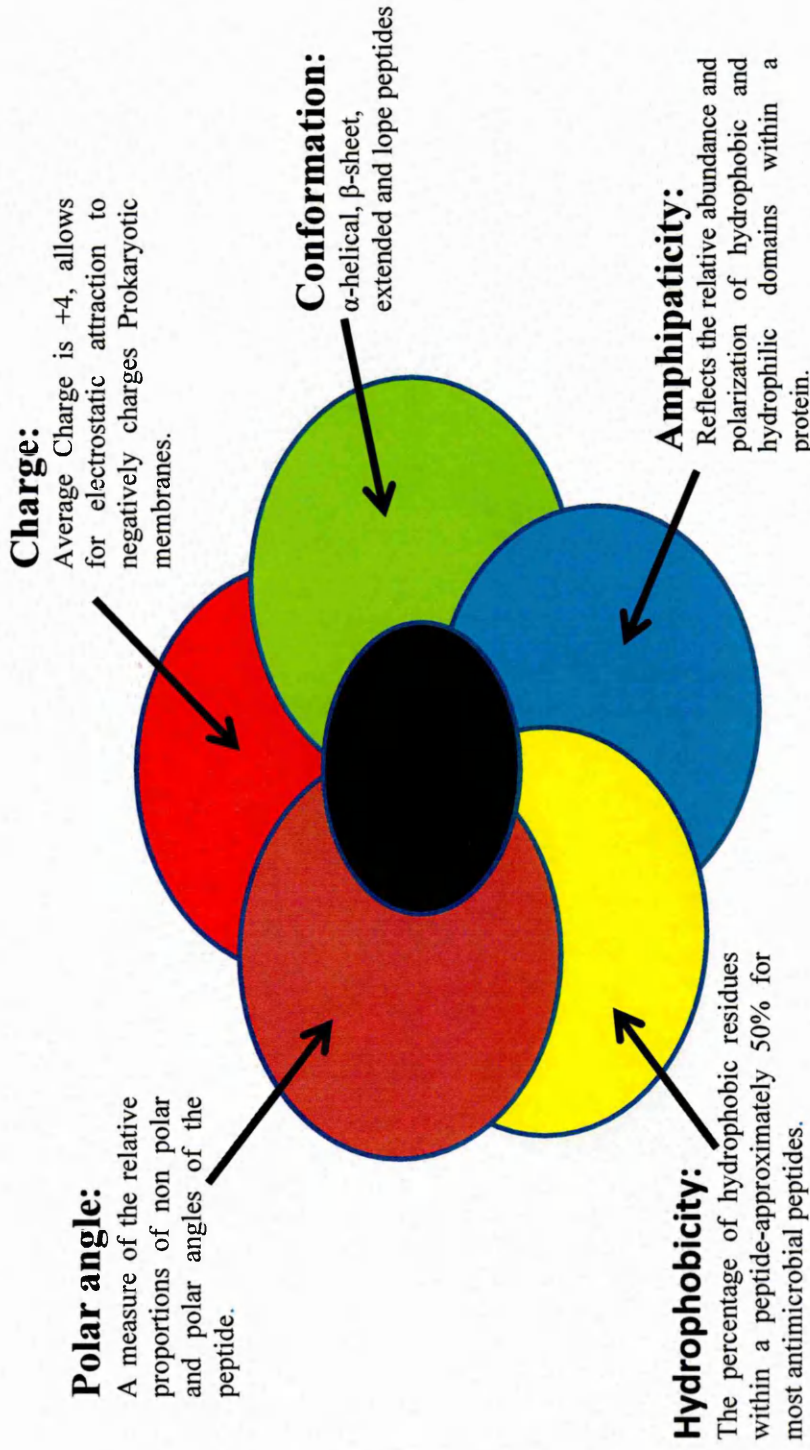


Figure 1.2: Physiochemical properties of AMPs adapted from Yeaman and Yount (2003). Interrelationship among structural determinants in antimicrobial peptides-fundamental composition and amino acid sequence influences not only the biochemical properties of the peptide (charge, amphipathicity, and hydrophobicity), but also govern their three dimensional configuration (conformation, polar angle and overall stereo geometry). Therefore, changes in composition, sequence, and intramolecular bonds may profoundly effect the structure-activity relationships of AMPs. Therefore AMP efficacy lies in the relevant coordination of these relationships (central black area) as they relate to microbial target versus host cells in a particular context of infection.

An amphipathic molecule has opposing polarities within its structure. Phospholipids are a classic example, with a hydrophilic phosphate head group and hydrophobic fatty acid chains, and, therefore, it is not surprising that peptides adapted to interact with these molecules share the same characteristic allowing interaction with the both head group and the membrane's hydrophobic core. Whilst an amphipathic conformation is essential for membrane interaction, too little and no incursion will occur, however, an increase beyond a critical point will decrease the specificity of the peptides towards prokaryotic membranes thus increasing their haemolytic potential (Pathak *et al.*, 1995). This has been observed using magainin, where increasing its amphipathic nature increased lysis of zwitterionic liposomes (Wieprecht *et al.*, 1997). Whilst the simplest form of amphipathic peptide is a helical structure (Eisenberg *et al.*, 1984), the β sheet peptides are also amphipathic, with anti-parallel β -strands organised to give polar and non-polar domains and are amphipathic in aqueous conditions, whilst α -helical peptides only adopt this characteristic in the presence of lipids (Huang *et al.*, 2010).

This amphipathic nature is highly linked to a peptide's polar angle, a measure of the relative proportions of polar and non polar areas with a maximal measurement of 180° if each area is at opposing ends of the peptide (Yeaman *et al.*, 2003). The polar angle of a peptide has been shown to be important in the permeabilisation of membranes, with a reduced polar angle leading to increased permeabilisation (Dathe *et al.*, 1997, Wieprecht *et al.*, 1997, Uematsu *et al.*, 2000). Amphipathicity has also been implicated in the stability of membrane pores with peptides with increased polar angles forming pores with greater half-lives (Uematsu *et al.*, 2000).

Preferential electrostatic attraction of an AMP towards the target membrane is fundamental to the mechanism of action therefore their charge state is critical. AMPs usually have a net positive charge of between +2 and +9. It is generally accepted that an

increase will increase potency although over a certain threshold antimicrobial activity does not increase, instead an increased in toxicity is observed (Jiang *et al.*, 2008). For example, an increase in the charge of magainin 2 from +4 to +5 increased antimicrobial activity but an increase to +7 did not correspond to further activity instead increasing haemolytic activity (Dathe *et al.*, 2001). Similarly Jiang *et al.* (2008), using the 26-residue helical peptide L-V13K showed that by altering both net charge and number of positively charged residues, profound effects on biological activity were seen, with just one positive charged increase (+8 to +9) on the polar surface increased the haemolytic activity 32 fold. Ginagaspero *et al.* (2001) and Jiang *et al.* (2008) also showed that increasing charge beyond a certain threshold can decrease overall activity due to electrostatic repulsion within the peptide hindering helical formation.

Whilst the vast majority of AMPs are cationic in nature, anionic peptides have also been isolated, for example, dermicidin from humans (Schitteck *et al.*, 2001). These peptides have a net charge between -1 and -7 and it is thought that they form salt bridges with metal ions and the negatively charged phospholipids present within the microbial membrane, which allows attraction to the surface (Harris *et al.*, 2009).

An AMP, on average, is comprised of approximately 50% hydrophobic residues, which is a critical parameter to allow partitioning of the peptide into the hydrophobic core (Tossi *et al.*, 2000). A number of studies have sought to understand the relationship between hydrophobicity and biological activity. Using magainin, Tachi *et al.* (2002) synthesised analogues with an Alanine replacing Leucine at the non-polar surface, revealing that higher hydrophobicity increased the haemolytic activity, whilst a decrease in hydrophobicity lowered the antimicrobial activity. Chen *et al.* (2007) concluded that AMPs have an optimal window and any deviation from this has a dramatic effect on biological activity. It has been postulated that these effects are due to the peptides

ability to self associate. In aqueous solution it is thermodynamically favourable for highly hydrophobic peptides to self associate and therefore a non specific lytic aggregate is formed rather than the monomeric form that is observed in AMP mechanism of action (Yeaman *et al.*, 2003).

1.7 Membrane characteristics

The precise nature of membrane composition and super molecular structure is essential to cell function. As well as acting as a barrier, it regulates nutrient flow, maintains osmotic balance, electrochemical gradient and is the site of many catalytic reactions fundamental to cell function and survival. Due to the nature of prokaryotic and eukaryotic cell function and environmental stresses, fundamental differences in this composition exist, it is these differences that allow the preferential activity of AMPs against prokaryotic membranes. A comparison of the prototypical characteristics of Gram positive, Gram negative and eukaryotic membranes are seen in Figure 1.3.

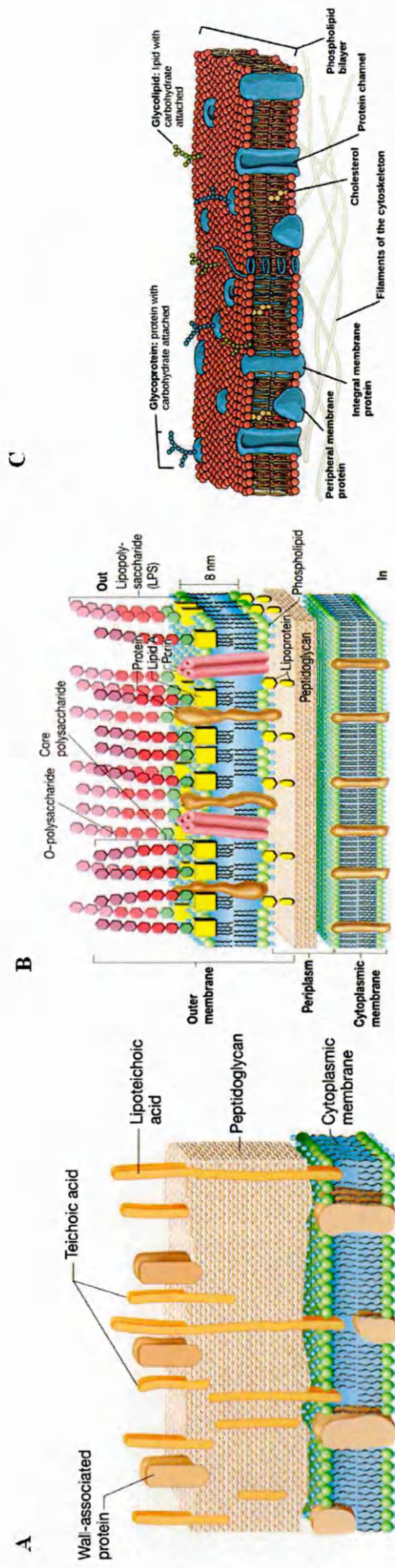


Figure 1.3: The major prototypical characteristics of both prokaryotic and eukaryotic membranes (A) Gram positive membrane characteristics-the cytoplasmic lipid membrane is surrounded by a thick layer of peptidoglycan with teichoic acid connecting both the cytoplasmic membrane to the peptidoglycan cell wall. (B) Gram negative membrane characteristics-the peptidoglycan cell wall is sandwiched between a cytoplasmic membrane and a thicker outer membrane comprising of both phospholipids and LPS. (C) A eukaryotic membrane-no cell wall or out lipid membrane is present with the membrane comprised of both phospholipids, cholesterol and a large number of proteins. Adapted from Madigen *et al.*, 2011.

Differences in phospholipid composition influence membrane charge and curvature, essential parameters when considering a peptide's ability to be electrostatically attracted and undergo incursion into the membrane. Prokaryotic membranes have a higher content of the negatively charged hydroxylated phospholipids phosphatidylglycerol (PG), phosphatidylserine (PS) and cardiolipin (CL), whilst eukaryotic membranes consist of more neutrally charged phospholipids such as phosphatidylcholine (PC), phosphatidylethanolamine (PE), sphingomyelin (SM) and sterols such as cholesterol and ergosterol (Teixeria *et al.*, 2012). Along with charge, shape is an important factor to consider as it has a direct influence on membrane curvature. The zwitterionic lipid PE has an inverted cone geometry thus promoting negative curvature of the membrane, which is thought to impede the activity of peptides that exhibit a carpet mechanism whilst PC and PG are far more cylindrical and do not cause any curvature (Bodone *et al.*, 2012) (see figure 1.3). Along with head group charge and shape, acyl chain bulk and length has a significant effect, longer chains inhibit shorter pore forming peptides, in contrast bulkier chains cause steric hindrance within the membrane causing membrane thinning; the presence of cholesterol and ergosterol inhibits pore formation by ordering the membrane and causing lipid packing (Teixeria *et al.*, 2012).

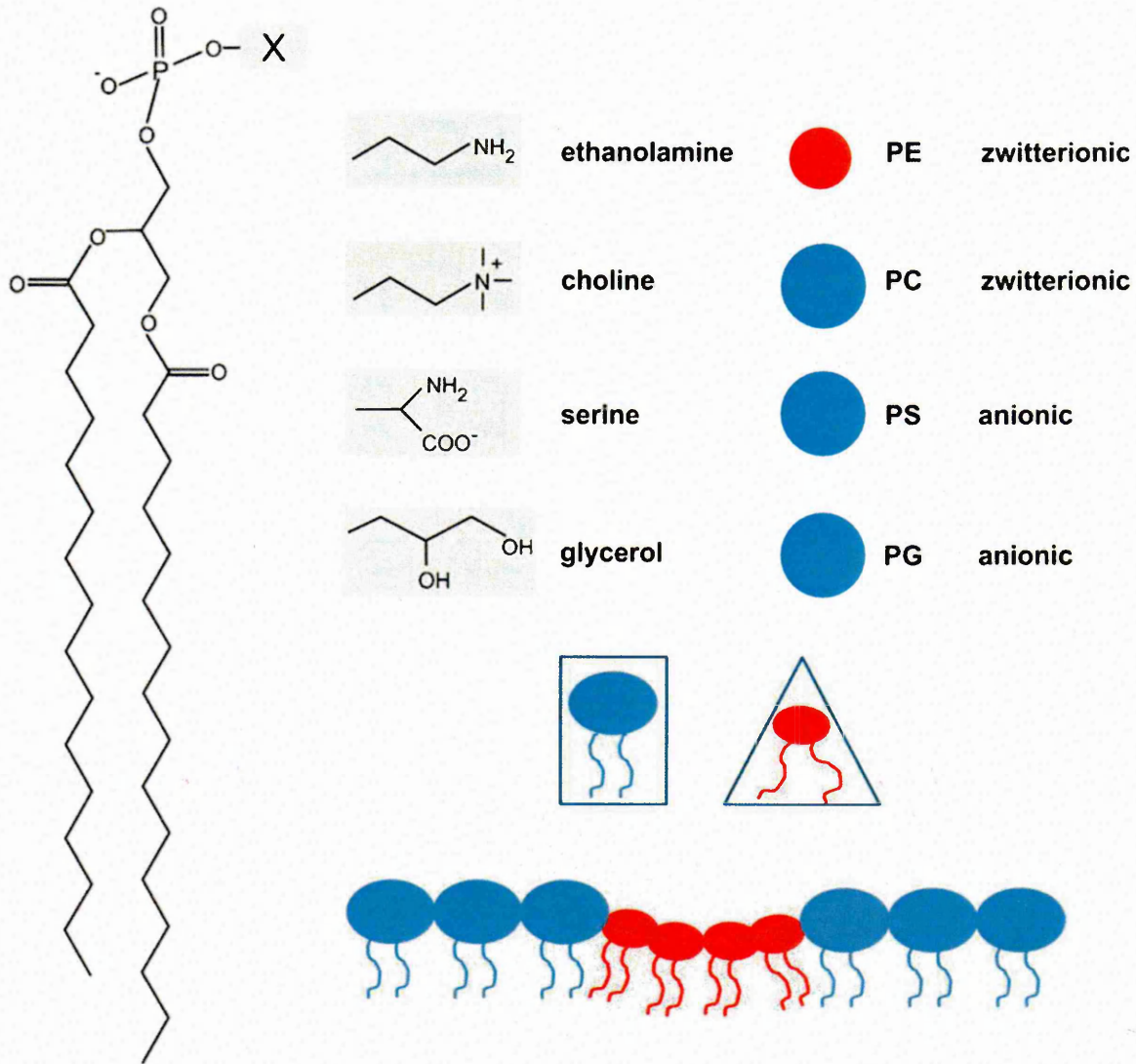


Figure 1.4: Differences of phospholipid geometry and the effect of lipid packing-lipids with a headgroup that has a smaller cross sectional area than the acyl chains such as PE will cause negative curvature when in a bilayer with lipids that have an equal cross sectional area such as PC, PG and PS. Adapted from Fromm & Hargrove 2012

The asymmetry of prokaryotic membranes compared with eukaryotic membranes leads to a more negative charge, with the relative small amounts of negatively charged phospholipids within eukaryotic membranes oriented towards the cytoplasm (Yeaman *et al.*, 2003). Transmembrane potential between eukaryotic and prokaryotic membranes is also very different with the potential in normal mammalian cells resting between -90 to -110 mV whereas typical bacterial membrane potential in logarithmic growth phase sits between -130 to -150 mV. This difference is due to different rates of proton flux across the membrane (Hancock *et al.*, 1997).

The presence of lipopolysaccharides (LPS) and teichoic acids in Gram negative and Gram positive bacteria increase overall negative charge and have been proposed to be of fundamental importance in the initial stages of AMP attack (Hancock *et al.*, 1997, Peschel *et al.*, 1999).

1.8 Natural resistance towards AMPs

Whilst the hypothesis for AMP drug development states that pathogens have little natural resistance towards AMPs, discrepancies in MIC values between different pathogens clearly point towards natural resistance mechanisms that have evolved to combat attack. A number of studies have highlighted possible mechanisms; Basselin *et al.* (1998) and Pershal *et al.* (2001) showed the reduction of net negative charge due to decreases in PG and CL content. Similarly Dorrer *et al.* (1977) had previously showed an increase in the cationic ornithine-amide lipid composition confers resistance to polymyxin B in *Pseudomonas fluorescens*. Modification of both phospholipids and cell wall constituents have also been noted as a mechanism of decreasing charge, for example, the modification of PG by lysine addition in *S.aureus* (Pershal *et al.*, 2001) and the addition of positively charged D-alanine residues to teichoic acid in the cell wall of *S. agalactiae* (Abachin *et al.*, 2002). In Gram negative organisms, changes in

LPS have also been noted through modification of the lipid A molecule including acylation and palmitate and 4-amino-4-deoxy-L-arabionse derivitisation (Ernst *et al.*, 2001) as well as increased LPS content of the zwitterionic PC (Lysenko *et al.*, 2000).

Other strategies involved in AMP evasion include the synthesis of a polysaccharide capsule that is typically negatively charged and so binds the AMPs rendering them ineffective (Friedrich *et al.*, 1999). Reduction in transmembrane potential (Yeaman *et al.*, 1998) has also been shown to render some AMPs inactive, along with the release of proteases (Ulvatne *et al.*, 2002). Mechanisms usually associated with conventional antibiotic resistance such as efflux pumps to decrease the concentration of intracellular AMPs have also been observed in a number of pathogens including *Neisseria gonorrhoeae* (Shafer *et al.*, 1998), *S. aureus* (Kupferwasser *et al.*, 1999) and *Vibrio cholerae* (Bina *et al.*, 2008).

Although resistance mechanisms have been discovered and can be induced for example Perron *et al.* (2006) who successfully induced AMP resistance over 600-700 generations in *E. coli* and *P. fluorescens in vitro*, it should also be considered that the interplay between AMP based innate immunity and pathogen challenge has been on going on for millions of years and, as of yet, the selective pressures that has seen widespread resistance to conventional antibiotics in little over 70 years has not occurred.

1.9 Strategies for AMP production

If AMPs are to progress towards clinical use one major aspect that needs to be overcome is their large scale production as isolation from natural sources is an expensive and time consuming process (Li. 2011). Due to their very nature, soluble recombinant expression of AMPs in bacteria has proven difficult therefore chemical synthesis has been the standard procedure in AMP production however this is expensive

and only feasible for mg amounts (Nair *et al.*, 2007). However in recent years the expression of AMPs in bacteria has been successfully achieved by fusion of the AMP to a number of different carrier proteins (Li. 2011). These carrier proteins fall into two major categories, firstly, soluble-enhancing carriers such as thioredoxin and glutathione transferase (GST) both of which have proven extremely successful especially in *E.coli*. As examples

Another soluble carrier is small ubiquitin-related modifier (SUMO) and a worldwide patent has been granted to researchers within the US to produce a numbers of AMPs (Bommarius *et al.*, 2008). The production of tagged AMPs in insoluble inclusion bodies has also been successfully in *E.coli* using the carriers PurF (Lee *et al.*, 2000), ketosteroid isomerase (Majerle *et al.*, 2000) PaP3.30 (Rao *et al.*, 2004) and TAF12 histone fold domain (Vidovic *et al.*, 2009) and is thought to be more efficient than soluble expression as it offers more protection to the host cell. A similar strategy (Jang *et al.*, 2009) involved the co-expression of AMPs with an anionic protein prone to aggregation which would form a electrostatically driven complex with the cationic peptides forming inclusion bodies. Along with removing the need to cleave the AMP from its carrier after treatment with 8M urea approximately 100mg of peptide was recovered from just 1L of bacterial culture. As with most recombinant expression strategies *E.coli* is the most extensively utilised expression host, however AMPs have been expressed in other organisms that are not susceptible to a particular AMPs effects. As examples, a cathelicidin from *Bungarus fasciatus* (banded Krait snake) intein fusion peptide in *Bacillus subtilis* (He *et al.*, 2015), NK-Lysin has been expressed in the yeast *Pichia pastoris* (Fan *et al.*, 2014) similarly NZ17074 isolated from the lugworm (*Arenicola marina*) was expressed in same organism (Wang *et al.*, 2014), CecropinXJ isolated form *Bombyx mori* larvae has been expressed in *Saccharomyces cerevisiae*

(Xia et al., 2013) and expression in higher eukaryotes such as *Arabidopsis* sp. as also been achieved (Wu et al., 2013).

These strategies offer the potential for a diverse range of AMPs to be expressed and high yields to be recovered which will be required if they are to be used in modern medicine.

1.10 AMP mechanism of action

As stated, the mechanism of action of AMPs is thought to be through membrane disruption (Zasloff., 2002). What is less clear is the precise molecular mechanism of AMPs. The evidence suggest that the key factor for membrane disruption is the initial electrostatic attraction of the peptide to the negatively charged bacterial membrane surface, with numerous studies revealing loss of biological activity upon either reduction of peptide positive charge or decrease in membrane negative charge (Huang., 2000, Shin *et al.*, 2001, Glukhov *et al.*, 2005). After initial electrostatic attraction, a threshold concentration is required before membrane disruption can occur which is critical for all mechanisms described (Huang. 2000, Melo *et al.*, 2009). During this process at low peptide to lipid ratios the peptide is organised and lies parallel to the acyl chains at the interface between the chains and the head groups (Ludtke *et al.*, 1994 & Heller *et al.*, 1997), as this peptide-lipid ratio increases these peptides begin to ‘tilt’ and start to align perpendicularly to the acyl chains at which point interaction with the membrane hydrophobic core can occur (Strandberg *et al.*, 2006). A number of factors govern this threshold concentration and initial membrane incursion is both peptide and membrane dependent. These factors include the ability of a membrane to self associate and physical factors including charge, electrochemical gradient, fluidity and curvature (Lee *et al.*, 2005, Mason *et al.*, 2007, Bechinger *et al.*, 2009).

A number of mechanisms have been postulated to succeed this attraction. These have been depicted in figure 1.5. In the barrel stave mechanism a central pore lumen occurs with the pore characterised by peptide-peptide interactions (Eisenburg *et al.*, 1973). Peptides associated with this mechanism such as alamethicin (Richards *et al.*, 1982), are hydrophobic in nature with the hydrophobic faces of the peptides interacting with the acyl chains, the peptides bind as monomer, adopting an α helical secondary structure/conformation which induces localised membrane thinning by sitting at the phospholipid chain/head group interface, upon the threshold concentration being reached the hydrophobic face inserts into the membrane core and the peptides begin to self associate (Hancock *et al.*, 1999). However, these pores are not static and continued interaction of the monomeric peptide to the membrane leads to further expansion (Hancock *et al.*, 1999, Rakowski *et al.*, 2013). Continued research on alamethicin further supports the view of barrel stave pore formation as a mechanism of AMP mechanism of action. Assessing the thermodynamic probability of pore formation Rahaman and Lazaridis (2014) used molecular simulations to show the formation of stable barrel stave pores of varying size. The trimer and the tetramer formed 6Å pores that were closed while the larger oligomers formed open pores at with the hexamer forming an 8Å pore and the octamer in an 11Å pore. Their results are consistent with barrel-stave model with N terminal portion of the molecule exhibiting a smaller tilt with respect to the membrane than the C terminal portion, resulting in a pore shape that is a hybrid between a funnel and an hourglass. Direct visualisation of alamethicin pores have also been captured using electrochemical scanning tunneling microscopy (ECSTM) in a phospholipid matrix. Each channel consists of six molecules and had a diameter of 19 Å (± 1 Å), three or four of these molecules have the hydrophilic group oriented toward the centre of a water filled channel (Pieta *et al.*, 2012).

In the toroidal mechanism the pore lumen is lined by both peptide and lipid head group interactions and is characterised by the induction of membrane curvature due to interaction of the hydrophilic face of the peptide with polar head groups, this causes bending of the head groups in a continuous fashion to connect the outer and inner membrane leaflet due to the thermodynamically unfavourable interaction between the acyl chain and the aqueous environment (Park *et al.*, 2005). Further examination of this model with molecular simulation studies on magainin and melittin (Sengupta *et al.*, 2008, Leontiadou *et al.*, 2006) showed that the pore contained far more lipid head groups than peptide with only 2-3 peptides associated with each pore and not all the peptides maintained their secondary structure (Nguyen *et al.*, 2011), this refined model has been termed the disordered toroidal model. More recent studies on the precise nature of melittin pore formation support a toroidal mechanism. Zhou *et al.*, (2014) carried out liposome leakage assays on DMPC/cholesterol mixed liposomes with calcien dyes of varying size and determined a lag time of dye release proportional to an increase in dye size suggestive of initial nucleation, pore formation and increasing pore size over time. Whole cell patch clamp studies on the Chinese hamster ovary cell line CHO-K1 using a melittin analogue also supports the notion of a toroidal expanding pore (Fasoli *et al.*, 2014). Both a barrel stave pore and a toroidal pore have been shown to exist with alamethicin and novicidin using ^{31}P solid-state NMR spectroscopy respectively in planer lipid bilayers (Bertelsen *et al.*, 2012). Interestingly, with both peptides, the majority of the lipid remained in a planar conformation but a number of lipids were involved in peptide however more lipid remained in a planer conformation with alamethicin suggesting a transmembrane pore without significant disturbance of the surrounding lipids, whilst novicidin forms toroidal pores at high concentrations leading to more extensive membrane disturbance.

In the carpet model (Shai *et al.*, 1999, Yamaguchi *et al.*, 2001) the peptides cover the membrane surface and upon the critical concentration being reached form transient pores allowing peptide access to the inner leaflet leading to peptide 'carpet formation' on each membrane surface, peptides can then span the transmembrane bilayer causing curvature of the membrane to protect the acyl chains which leads to the disintegration of the bilayer due to micelle formation (Teixeria *et al.*, 2012). However, it has been argued by Nguyen *et al.*, (2011) and Brogden (2005) that the carpet model is an experimental artefact only *seen n vitro* at high a peptide-lipid ratio therefore is an experimental artefact although recent high resolution atomic force microscopy and quartz crystal microbalance-dissipation studies on aurein 1.2 (Fernandez *et al.*, 2012) contradicted this view with a carpet model observed. More recent studies by Roversi *et al.*, (2014) on live *Escherichia coli* cells determined that membrane lyses only occurred when bound peptides completely saturated bacterial membranes (10(6)-10(7) bound peptides per cell), indicating that the "carpet" model for the perturbation of artificial bilayers is representative of what happens in real bacteria.

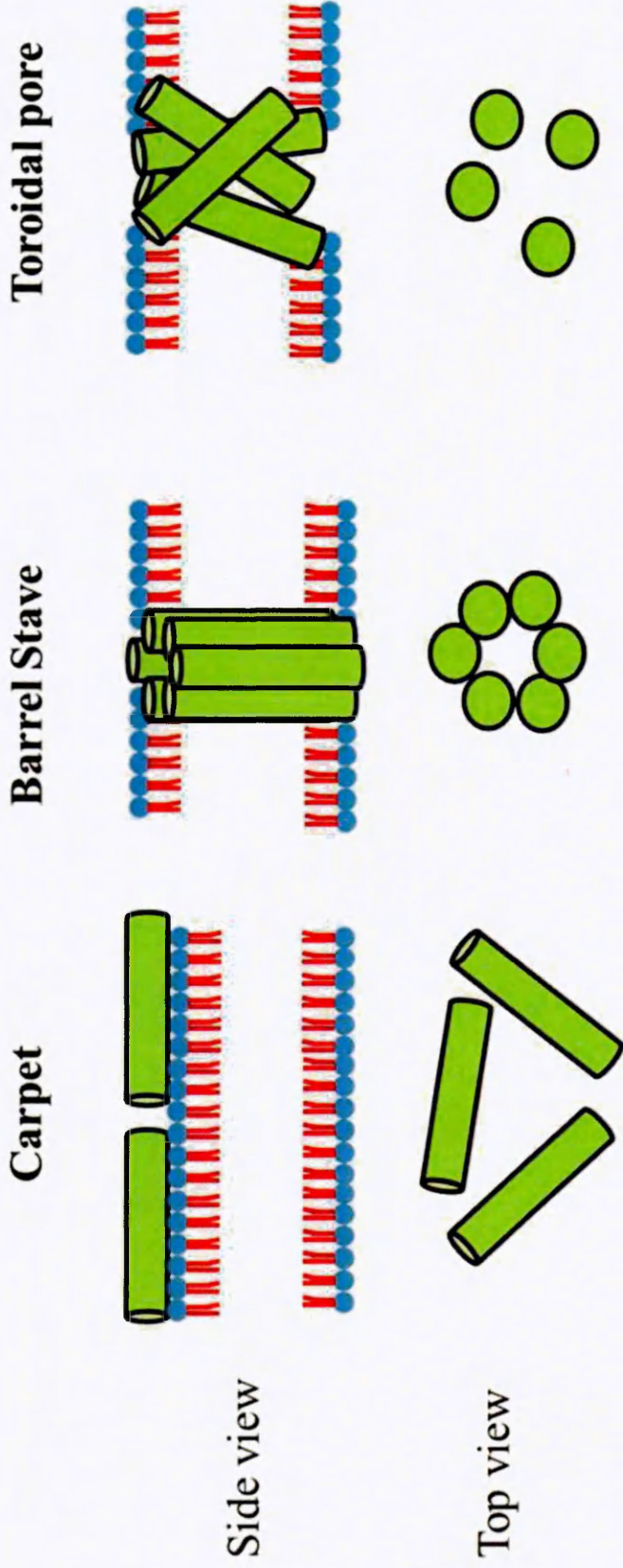


Figure 1.5: Postulated mechanism of action of AMPs.- The mechanism of action of AMPs is postulated to occur in a number of stages (Zaslouff, 2002): (1) Electrostatic interaction onto the membrane surface; (2) a peptide threshold concentration is reached before membrane disruption can occur after which a number of models have been proposed. In the Carpet model, peptides remain parallel to the bilayer causing a detergent like effect. In the Barrel stave pore model peptides insert perpendicularly into the bilayer and self-association occurs forming a pore containing peptide-peptide interactions. The more recent Toroidal indicates a pore forming mechanism in which the pore lumen is lined with both peptides and phospholipid in a less rigid association.

Whilst there is a clear evidence for each of these models a number of other models have been proposed for different peptides.

The interfacial model (Figure 1.5) (Wimley. 2011), postulates that shorter chain AMPs are not sufficient to transverse the membrane therefore a classical pore forming mechanism is not possible. Sequence analysis of a large number of these shorter chain peptides revealed the presence of a 'polar pocket' within the hydrophobic region of the peptide, usually 1 or 2 highly charged residues. This "imperfect amphipathicity" is fundamental to this model, when the peptide is driven into the bilayer and the hydrophobic portion of the peptide interacts the with membrane core, this 'polar pocket' interacts with the phosphate head groups within the inner leaflet causing negative curvature. The importance of this model has been described by Bodone et al. (2012) who questioned the reliability of liposome leakage assays as a method of mechanism determination. Using alamethicin and mastoparan-X, previously determined to act via a pore and carpet mechanism (Richards et al., 1982, Matsuzaki et al., 1997), they showed that these peptides behaved in unexpected ways depending on membrane composition with mastoparan-X being inhibited by increasing membrane thickness. However, alamethicin was not affected. Both peptides were also inhibited when PE was included in the membrane. Taken in this into context previous conceptions of AMP mechanism should be re-examined, especially when considering the interfacial model, which suggests that these two peptides act via singular mechanism. After Wimley's analysis of the imperfect amphipathicity of a number of AMPs (Wimely 2011)Indeed, AMPs that intentionally exhibit an imperfect amphipathic helical structure have been successfully designed by Zhu *et al.*, (2015) with an AMP termed PRW4 having preferential activity.

Along with the interfacial model a number of other researchers have put forward theories that contrast with the three conventional models which highlight how further refinement of these models is leading to new ones. This is exemplified by the ‘leaky slit’ mechanism postulated by Zhao *et al.*, 2004 in which the AMPs form fibril like structures classically associated with neurodegenerative peptides such as α -Synuclein. Peptides align with their hydrophobic side facing the lipids whilst the hydrophilic facet allows for further peptide aggregation through hydrogen bonding; lipids that are in contact with the hydrophilic face undergo dramatic curvature to protect the acyl chains thus allowing for a “slit” to occur along this surface where cellular metabolites can leak out. This mechanism is thought to be a refinement of the carpet and toroidal models and has been shown experimentally using the peptide plantaricin A by imaging liposome leakage assays (Zhao *et al.*, 2006). Further studies on the bacteriocin AS-48, a 70 residue cyclical peptide with 5 helices using coarse grain molecular simulations indicated a ‘leaky slit’ mechanism of action (Cruz *et al.*, 2013). These results showed the peptide formed dimeric structures within the membrane with two types of pores observed.. firstly a small pore with a 1 nm radius and secondly a larger toroidal pore of variable dimension formed by dragging of phosphate lipid groups towards the bilayer interior due to interactions with charged protein residues which the authors postulated to be in agreement with the “leaky slit” model.

Other models include the aggregate channel model, the molecular electroporation model, the sinking-raft model and the peptide-induced lipid segregation model which are depicted in figure 1.6.

In the aggregate channel model (Hancock *et al.*, 1999) peptides insert into the bilayer, however unlike in pore forming mechanisms, large aggregates of unstructured peptides

form that have water molecules adhered to the surface and consequently allow a small amount of leakage through the bilayer. However these structures are not able to cause membrane depolarisation (Wu *et al.*, 1999), act transiently and do not cause significant membrane disruption, thus is thought to be a mechanism for cell entry to other targets.

In the molecular electroporation model, originally proposed for the apoptotic protein Annexin V (Karshikov *et al.*, 1992), the presence of the highly charged peptide in close proximity to the membrane creates an electric field due to the charge density with the relatively long time periods it occurs under (0.1mS) enough to trigger pore formation (Miteva *et al.*, 1999).

The more recent sinking-raft model (Pokorny *et al.*, 2002, 2004) is caused by the mass imbalance within different lipid domains on the outer layer of the membrane caused by the preferential binding of the peptide to a certain lipids. This causes localised membrane strain which is relieved as the peptides sink into the membrane and translocate to the inner leaflet causing membrane leakage in the process (Pokorny *et al.*, 2004).

Preferential peptide-lipid binding also underpins the peptide induced lipid segregation model (Teixeria *et al.*, 2010) in which lateral lipid segregation is observed upon AMP interaction. This mass 'de-mixing' of lipids causes defects within the membrane (Fernandez-Rayes *et al.*, 2010) allowing intracellular constituents to leak out. Interestingly, Epland *et al.* (2008) suggested that this mechanism could provide a rational explanation as to why there is such disparity of MIC values between different bacteria. Using the peptide OAK C12 K-7 α 8 against both *S. aureus* and *B. cereus*, the latter had a far lower MIC which was postulated to be due to the higher concentration of zwitterionic lipids found within its membrane compared to the former which has predominately anionic lipids, Epland's have also examined the anionic lipid segregating

potential of a number of AMPs and cell penetrating peptides (Wadhvani *et al.*, 2012). Among the peptides studied, six AMPs and four CPPs showed strong anionic lipid clustering activity with these peptides also had bacteriostatic activity against *E.coli* that are sensitive to lipid clustering agents whilst AMPs and CPPs that did not cluster anionic lipids were not toxic to *E. coli*. Whilst this mechanism has been seen with AMPs it has mostly been observed with CPPs including snake elapid cardiotoxins (Dubovski *et al.*, 2003), and crostamine, a myotoxin with antimicrobial properties from *Crotalus durissus terrificus* (South American rattlesnake) (Costa *et al.*, 2014).

As is seen with some of the models described not all membrane interaction leads to disruption. Brogden (2005) and Nicholas (2009) examined the possibility of intracellular targeting. Both highlighted this possibility on the basis of a number of issues; (A) our lack of understanding of the physicochemical properties that give such disparity between MIC values, raising the possibility that a site specific intracellular or cell wall target is critical for activity, (B) discrepancies between membrane activity determined by biophysical means and actual bacterial cell death (C) *in vitro* studies have shown AMPs can recognise and inactivate a range of intracellular targets and (D) sequence homology between AMPs and a number of other peptides that transverse the membrane in a non lethal fashion.

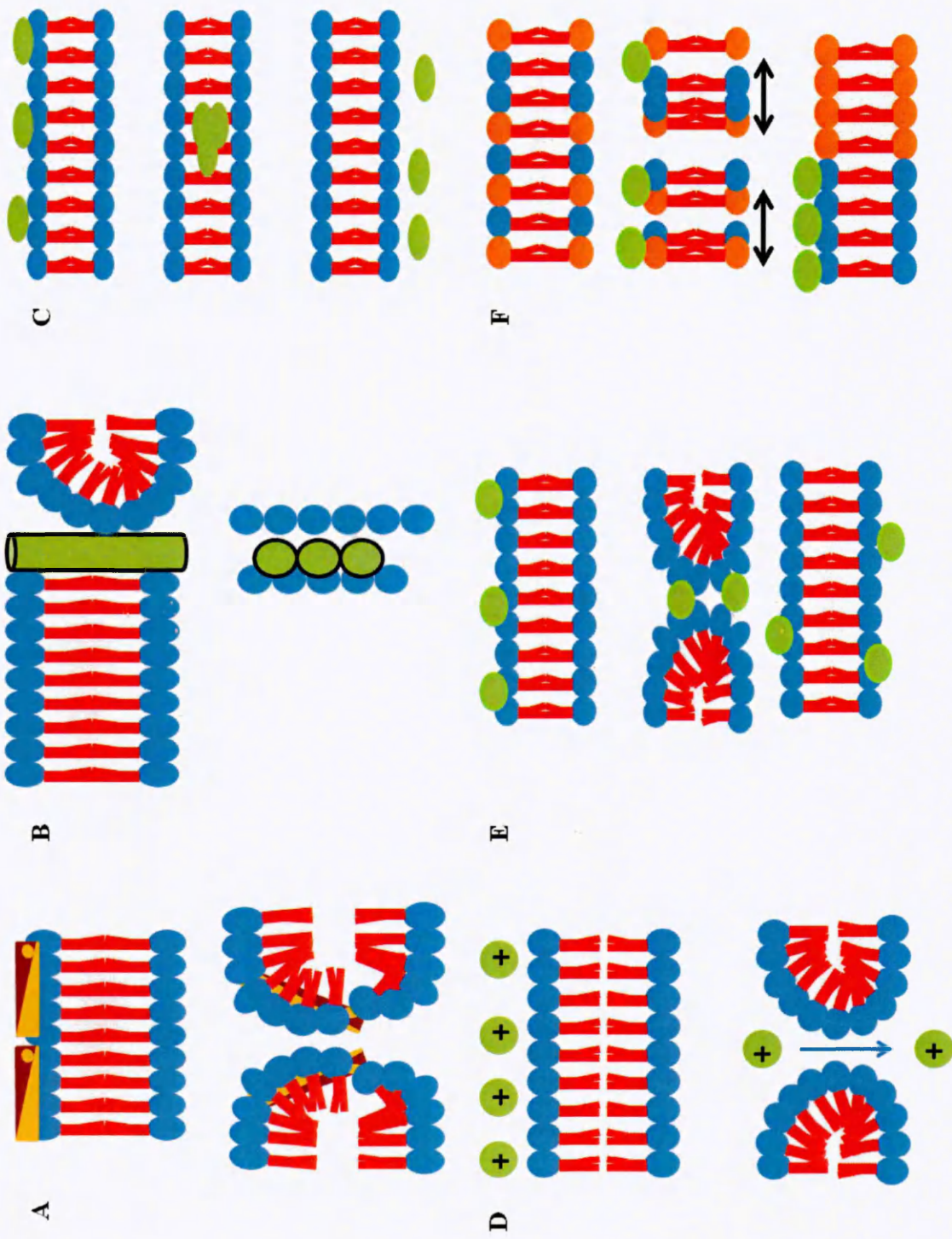


Figure 1.6: Alternative models of AMP mechanism of action-(A) Interfacial model (Wimley, 2011) (B) Leaky slit model (Zhou et al., 2004)(C) Aggregate model (Hancock et al., 1999) (D) Electroporation model (Karshikov et al., 1992) (E) Sinking raft model (Pokorny 2002) and (F) lipid aggregate model (Fernandez-Rayes et al., 2010)

Whilst in high concentration, overwhelming evidence suggests loss of membrane integrity as the fatal mechanism, a number of peptides have, at much lower concentrations, been shown to interact with a variety of targets. For example histatin, a 24 residue helical peptide isolated from human saliva has been shown to kill *Candida* by accumulating in the cell mitochondria and inhibiting F1F0-ATPase involved in ATP synthesis (Edgerton *et al.*, 2000). Interestingly the peptide has a non-lytic mechanism and instead binds to the cell surface bound heat shock protein HSP-70 before being transported across the membrane by a membrane permease. Indolicidin causes pore formation at the MIC however does not cause cell lysis, rather the peptide is thought to bind to DNA and has shown to induce filamentation in *E. coli* (Subbalakshmi *et al.*, 1998). Similarly *in vitro* studies have demonstrated the DNA binding potential of the cyclical β -sheet peptide tachyplesin (Yonezawa *et al.*, 1992). Also Diaz *et al.* (2009) implicated the blocking of bacterial sodium channels as the mechanism of action by the scorpion AMP bacteridine 1. Other peptides highlight these discrepancies for example an analogue of tritrypticin (termed TWF) a cathelicidin derived peptide, shows good activity against both *S. aureus* and *E. coli* however no evidence of membrane disruption or membrane polarisation are observed (Chan *et al.*, 2006). Similarly both dermaseptin B2 and its truncated analogue are highly effective in calcien dye release assays however the latter has no antimicrobial activity (Noinville *et al.*, 2003). These studies highlight that whilst there is clear evidence for AMP mechanism at the level of the membrane, whether this is the primary target needs further clarification and far more extensive studies on intracellular targeting needs to be undertaken. As seen with the discovery of bacteridine 1 the possibility of novel targets perhaps not conventionally thought of as antimicrobial targets need to be assessed.

Whilst AMPs have increasingly become of interest as alternatives to classic antibiotics, factors including toxicity towards mammalian cells and expensive production costs

have hampered development. A subcategory of AMPs that lacks this drawback is the bacteriocins which are small ribosomally synthesized peptides secreted by bacteria to inhibit the growth of evolutionary related species (Allen *et al.*, 2014). Bacteriocins are produced throughout the major lineages of bacteria; with an estimated 99% of all bacteria producing at least one bacteriocin, consequently, there is vast diversity among these compounds, which potentially could be exploited for therapeutic purposes (Snyder and Worobo 2014). Bacteriocins can be categorised into 5 major classes based on a number of different factors including bacterial production strain, common resistance mechanisms, and mechanism of action however this naming system is becoming ever more confusing as more peptides are discovered with wider ranges of activity than previously recognised (Cotter *et al.*, 2006). The class I bacteriocins are commonly known as the lantibiotics and contain the unusual polycyclic thioether amino acids lanthionine or methyllanthionine, as well as the unsaturated amino acids dehydroalanine and 2-aminoisobutyric acid. This class of bacteriocins has already been utilised on a commercial scale with nisin, a 34 residue peptide produced by *Lactococcus lactis*, been used in food preservation for nearly half a century. These class I peptides are produced by Gram positive organisms to target other Gram positives and function by binding to lipid II, a cell wall precursor lipid which disrupts cell wall production (Yang *et al.*, 2014). Class II bacteriocins are a large group of AMPs, below 10 kDa in size, which exerts their antimicrobial activity through membrane permeabilisation and can further be subdivided into 5 groups (Drider *et al.*, 2006). Group IIa bacteriocins are the largest subgroup and contain an N-terminal consensus sequence YGNGVXaaC with the variable C-terminal responsible for species-specific activity (Drider *et al.*, 2006). Group IIb peptides require two different unmodified peptides, both of which must be present in about equal amounts in order for these bacteriocins to exert optimal antimicrobial activity (Oppegård *et al.*, 2007) whilst the group IIc bacteriocins are cyclical in nature

(Hécharad and Sahl 2002) and group IId are post-translationally unmodified but do not contain the conserved N terminal domain found in group IIa (Netz *et al.*, 2002). Finally group IIe peptides require 3-4 peptides to be expressed from a single operon which subsequently form a larger protein with all peptide components required for activity (Netz *et al.*, 2002). Class III bacteriocins are classified as over 10KDa and can be further sub divided into IIIa (membrane lytic) and IIIb (intracellular targeting) (Bastos *et al.*, 2010). The newest group, the class IV bacteriocins are made up of peptides with additional carbohydrate or lipid groups (Stepper *et al.*, 2011).

Because of their targeted activity they are a highly attractive class of AMPs in which to focus on both in their discovery and elucidating their mechanism of action, however the remainder of this thesis will focus on the identifying and furthering our understanding of AMPs from both snake and scorpion venoms.

1.11 AMPs from venom

Venom is a complex mix of proteins and peptides that have evolved over millions of years of to effectively paralyse and kill prey. Dependent on which venom you consider it will be comprised of proteins and peptides whose targets are ion channels, neurotransmitters, coagulation cascades, red blood cells and a whole host of other targets (de Lima *et al.*, 2009).

Envenomation is a traumatic event with the possibility of the fangs/telons being damaged and broken off in the process which may lead to microbial infection, therefore from an evolutionary point of view it is rational to assume that venom contains antimicrobial components that will sterilise this process (de Lima *et al.*, 2009). The percentage component of antimicrobial constituents within venom varies between

species, with wide intra-species variation noted in many organisms with variation dependent on age, sex, geography and climate (Calvete. 2013); indeed up to 25% of the venom of *Lychas mucronatus* has been described as AMPs in particularly challenging conditions (Rumming *et al.*, 2010). Therefore venom presents a wealth of bioactive molecules ready to be mined with a large array of AMPs, particularly from scorpion venoms already characterised (Harrison *et al.*, 2014).

1.11.1 AMPs from snake venom

Whilst AMPs have been isolated from a range of venoms, the isolation of AMPs from snake venom remains, at present, a relatively underexploited source although a whole host of other proteins have been isolated that confer antimicrobial activity including phospholipase A2, C-type lectins and L-amino oxidases (de Oliveira *et al.*, 2013). Table 1.2 details the sequences of selected snake derived AMPs discussed within this thesis.

A 2008 transcriptomic study by Zhou *et al.* found a number of novel α -helical cathelicidin AMP's from the venom glands of *Naja atra* (Chinese cobra), *B. fasciatus* and *Ophiophagus hannah* (king cobra); two full cathelicidin encoding cDNA sequences and a partial cDNA sequence were isolated respectively. Each of these sequences showed a highly conserved amino acid sequence suggesting evolutionary conservation of the cathelicidin peptides throughout the elapid family.

The cathelicidins are an evolutionary diverse family of AMPs made up of a conserved cathelin domain at the N-terminal connected to a hyper variable AMP region at the C-terminal which, after cleavage, produces a diverse range of structural conformations (Ramanathan *et al.*, 2002).

From the predicted amino acid sequences, the *O. hannah* deduced peptide was chemically synthesised resulting in a 34 residue peptide (Zhou *et al.*, 2008). Against a range of clinical isolates (*Enterobacter cloacae*, *Pseudomonas aeruginosa* and *Enterobacter aerogenes*), MIC values of 1-2 µg/ml were observed. Interestingly, the peptide showed only 10.8% haemolytic activity at concentrations of 200 µg/ml. Further studies truncated the peptide at the N-terminus to produce analogues with even lower haemolytic potency (0.69%) at 200 µg/ml when the first 4 residues were omitted whilst retaining its antimicrobial activity (Zhang *et al.*, 2010).

Wang *et al.* (2008) isolated the 30 residue peptide, rich in both lysine (9) and phenylalanine (5), with a molecular weight of 3637.5 from *B. fasciatus*. The peptide showed preferential antimicrobial activity towards Gram negative organisms (*E. coli* <2 µg/ml, *P. aeruginosa* 2.3-18.7 µg/ml and *Klebsiella pneumoniae* 0.3-9.4 µg/ml). Against Gram positive organisms an MICs of between 1.2-9.4 µg/ml was recorded against a range of *Bacillus* species however against *S. aureus* no MIC below 100 µg/ml was recorded. The peptide also showed strong activity against fungal species with *C. albicans* and *P. pastoris* both having MICs of below 5 µg/ml.

An active truncated peptide has also been designed from a cathelicidin from *Naja atra* (Indian cobra) (Latour *et al.*, 2010). From the 34 residue peptide (Mw 4175.2) which had a charge of +15, a peptides was designed was from the N-terminus, (KR(F/A)KKFFKK(L/P)K), which each carried a charge of +6. EC₅₀ values against *Aggregatibacter actinomycetemcomitans* and *E. coli* were comparable (<1.0 µM) for the native peptide and ATRA-1 (KRFKKFFKLLK) however in haemolytic analysis ATRA-1 lysed only 0.9% erythrocytes at 0.67 µM compared with the same percentage at 0.23 µM for the native peptide.

A waprin protein, omwaprin (5602 Da) was identified by LC-MS from *Oxyuranus microlepidotus* (inland taipan) (Nair *et al.*, 2007). The 50 amino acid recombinant peptide showed minor antimicrobial activity against *Bacillus megaterium* (560.2 µg/ml) and *Staphylococcus warneri* (1700 µg/ml), but did not show any effect on *Bacillus thuringiensis*, *S.aureus* and *Streptomyces clavuligerus* or the Gram negative *E.coli* and *Agrobacterium tumefaciens* bacteria with concentrations of 5600 µg/ml. SEM studies on the susceptible *B. megaterium* and *S. warneri* indicated a membrane disruptive mode of action. Alkylation and reduction of the disulphide bridges negated the peptides antimicrobial activity against *B. megaterium*; suggesting a disulphide bond-constrained tertiary structure is necessary for activity. A three dimensional model showed the peptide is likely to consist of a spiral backbone with two circular segments connected by the 4 disulphide bridges with protruding N and C-terminals. The N-terminal consists of 9 residues, 4 being positive (KDRPKKPGL). N-terminal deletion mutation analysis showed this sequence to be vital for antimicrobial activity, indicating the cationic nature of the peptides activity.

An antifungal peptide has also been isolated from *Bothrops jararaca* (jararaca) (Gomes *et al.*, 2005). This 1370 Dalton peptide, termed pep5B, shows high level inhibitory effects against *Fusarium oxysporum*, *Colletotrichum lindemuthianum* & *S. cerevisiae* at 25 µg/ml. Effects of pep5B on the fungal plasma membrane were also tested by monitoring the glucose stimulated acidification of the growth medium by *S. cerevisiae*; 60% inhibition of the process was seen indicating either inhibition of the H⁺ ATPase on the plasma membrane or increase H⁺ permeability. SYNTAX green fluorescence permeabilisation into the cytosol of *F. oxysprum* supported membrane interactive lethal effects.

Possibly a new approach for antimicrobial peptide discovery from snake venom is highlighted by the recent discovery of the antimicrobial effect of crotamine (Yount *et al.*, 2009), a well characterised 42 residue toxin from *C. durissus terrificus*, whose primary structure has been determined for decades (Laure *et al.*, 1975).

Table 1.2: Table of selected AMPs isolated from snake venoms with known sequence

Name (UniProtKB)	Sequence	Length (A)/ molecular weight (Da)	Scorpion species (Family)	Reference
BF-cathlicidin (CAMP_BUNFA)	KFFRKLKKSVMKRAKEFFKKPRVIGVSIPF	30/ 3637; 0DSBs	<i>B.fasciatus</i> (Elapid)	Zhao <i>et al.</i> , 2008
NA-cathlicidin (CAMP_NAJAT)	KRFKFFFKLKNMVKKRAKKFFKKPKVIG VTFF	34/4175; 0DSBs	<i>N.atra</i> (Elapid)	Zhao <i>et al.</i> , 2008
OH-cathlicidin (CAMP_OPHHA)	KRFKFFFKLKNMVKKRAKKFFKKPKRVIG VSIPF	34/ 4155; 0DSBs	<i>O. hannah</i> (Elapid)	Zhao <i>et al.</i> , 2008
Omwaprin (WAPA_OXYMI)	KDRPKKPGLCPPRPQKPCVKECKNDSDCP GQQKCCNYGCK DECRDPIFVG	50/ 5611; 3DSBs	<i>O. microlepidotus</i> (Elapid)	Nair <i>et al.</i> , 2007
Crotamine (MYXC2_CRODM)	YKRCHIKGGHCFPKKELICPPSSDIGKMD CPWKRKCKCKRS	42/ 4905; 3DSBs	<i>C.terifficus</i> (Crotalid)	Coronado <i>et al.</i> , 2004
Neurotoxin II (3S11_NAJOX)	LECHNQSSQPPTTKTCSGETNCKYKKW WSDHRGTIIERGCGCPKVKPGVNLNCCR TDRCNN	61/6885; 3DSBs	<i>N.oxina</i> (Elapid)	Lesovoy <i>et al.</i> , 2009

1.11.2 AMPs from scorpion venom

The noted similarity between insect defensins and scorpion toxins (Bontems *et al.*, 1991) led to the isolation of the first scorpion defensin from the haemolymph of the North African scorpion *Leiurus quinquestriatus* (deathstalker scorpion). This 4.3 KDa peptide contained 38 residues, with the characteristic 6 cysteines of many ion channel scorpion toxins and showed a high degree of homology to insect defensins within the order *Odonata*. This peptide was active against Gram positive *M. luteus* but inactive against Gram negative *E. coli* (Cociancich *et al.*, 1993). The first cysteine-constrained AMP from scorpion venom (scorpine) was isolated by Possani and colleagues (Conde *et al.*, 2000) from the venom of the African scorpion *Pandinus imperator* (emperor scorpion) Scorpine (8.3 KDa, 75 residues, 3 disulphide bridges) has a unique structure, with N-terminal similarity to some insect cecropins and C-terminal similarity to some scorpion defensins. The sequence information of these peptides along with all other scorpion derived AMPs discussed are detailed in Table 1.3.

Scorpine was active (MIC 1-10 μM) against both Gram positive (*B. subtilis*) and Gram negative (*K. pneumoniae*) bacteria and had anti-malarial properties against the causative parasite *Plasmodium berghei* (ED_{50} 0.7 μM and 10 μM against ookinete and gamete stages, respectively). A second putative peptide (BmTXKS2) was also identified. The full length cDNA clone isolated from the venom gland of the Chinese scorpion, *Buthus martensii* Karsch (Zhu *et al.*, 2000). BmTXKS2 was predicted to have 39 residues including 6 cysteines and have similarity to haemolymph defensins. However there have been no subsequent reports of the translated peptide (either native, recombinant or synthesised) being investigated and no biological data is available. In subsequent years

two more members of the scorpine family members have been identified, opiscorpine from *Opisthoptalmus carinatus* (Robust borrowing scorpion) (Zhu and Tytgat. 2004) and heteroscorpine-1 from *Heterometrus laoticus* (Asian Forest Scorpion) (Uawonggul *et al.*, 2007).

Six peptides have been isolated from the venom of *Tityus discrepans* (thick tailed scorpion) termed the bactridines (Bacts) (Diaz *et al.*, 2009), which unlike the scorpine family contain 4 disulphide bridges. Bacts 1 and 2 have been characterised more extensively with Edman degradation and *in silico* analysis revealing charged peptides containing 61 and 64 residues respectively.

Bacts 1 showed an MIC range of 22-77 μM whilst Bacts 2 had an MIC range of 27-65 μM . In haemolytic assays, Bacts 1 showed only 0.2% at 90 μM and 1.1% at 180 μM with Bacts 2 showing 7.6 and 21% at the same concentrations, respectively. Whilst these peptides do not have potent antimicrobial activity, their mechanism of action is interesting. Using the pathogen *Yersinia enterocolitica* loaded with 1 μM of the Na^+ fluorescent indicator CoroNaTM red the efflux of sodium ions was observed upon Bacts 1 and 2 interactions. Furthermore this could be blocked in the presence of the sodium channel blockers amiloride (10 μM) and mibefradil (25 μM) although no inhibition was observed in the presence of 30 μM tetrodotoxin; these interactions were shown to be Na^+ channel specific with no interactions observed with K^+ or Ca^{2+} channels.

Bacts 1 showed no toxicity towards mice (0.4 $\mu\text{M}/\text{g}$) however was toxic to cockroaches (2.8 μM) induced sialorrhoea in crabs at 0.1 $\mu\text{M}/\text{g}$ and death in 3 out of 7 crabs at 0.2 $\mu\text{M}/\text{g}$. Bacts 2 however was toxic to mice at the same concentration suggesting specificity towards different classes of sodium channels. Peigneur *et al.* (2012) showed

no modulation of the mammalian sodium channels Na_v1.2-Na_v1.8 with Bacts 1, however no modulation of the insect DmNa_v1 or the bacterial sodium channel (NaChBac) was seen either suggesting further research needs to be carried out. Bacts 2 showed modulation of Na_v1.2, Na_v1.4 and Na_v1.6. Bacts 1 shares 78% homology to ardiscretin (D'suze *et al.*, 2004) which is an insect sodium channel blocker from the same venom whilst Bacts 2 shares 98 % homology to the first 60 residues of Tz1 and Td4 from *Tityus zulianus* and *Tityus discrepans* (thick tailed scorpions) respectively (Borges *et al.*, 2004). Structural modelling of the two peptides suggested a classical α - β -motif in which the peptides have an alpha helical region and conserved cysteine constrained beta sheet structure.

Bacts 1 represents a novel basis for an AMP although further work is required before a sodium channel specific mechanism of action can be truly revealed, however it would be of interest to the field of venom antimicrobials if these questions were answered and more bacteridine like AMPs were isolated (Kuhn-Nentwig, 2003; Zeng *et al.*, 2005).

Whereas the original antimicrobial peptides isolated from scorpion venoms contained cysteine residues, various non-disulphide bridged peptides have subsequently been isolated and these are now in the majority (e.g. Kuhn-Nentwig, 2003, Zeng *et al.*, 2005, Gao *et al.*, 2010, Zeng *et al.*, 2013).

1.11.2.1 Long chain helical peptides

Parabutoporin, isolated from the venom of the South African scorpion *Parabuidethus schlechteri* is a highly basic peptide (45 amino acids, overall charge of +7). A structurally similar, basic molecule (charge +4), existing as two isoforms, opistoporin 1

and 2 was isolated from another South African scorpion *Opisthoptalmus carinatus* (African yellow leg scorpion) (Moerman *et al.*, 2002). These two isoforms (44 amino acids) differ at position 34 where a phenylalanine replaces a leucine. Parabutopirin was predicted to have an α -helical structure between amino acids 3-35 in comparison to opistoporin 1 and 2 with two α -helical regions between residues 3-14 and 20-39 which are connected by a short random coil WNSEP (Moerman *et al.*, 2002). Circular dichroism (CD) spectra of parabutopirin in 40% 2,2,2-trifluoroethanol (TFE), dimyristoylglycerophosphocholine showed the peptide adopts an α -helical structure in membrane mimicking conditions. Under the same solvent conditions, opistoporin reorganises from an unordered state into a continuous α -helical structure (Moerman *et al.*, 2002). The amphipathic natures of both parabutopirin and opistoporin 1 were also predicted with α -helical wheel projections, which clearly show distinct hydrophobic and hydrophilic regions within each peptide, although comparison of these projections clearly shows that parabutopirin has a larger polar surface.

Antimicrobial assays for parabutopirin showed growth inhibition of all Gram-negative organisms assayed with MICs generally varying from 1-6 μ M. The peptide showed less activity towards Gram-positive organisms with MICs generally greater than 25 μ M. Interestingly, a decrease in growth inhibition was observed in the presence of Mg^{2+} ions (Moerman *et al.*, 2002). Opistoporin 1 showed less inhibitory activity against Gram-negative organisms (MIC values generally ranging from 6-50 μ M) than parabutopirin. On the other hand, differences between the effects of opistoporin and parabutopirin on Gram-positive organisms were less marked, although Gram-positive bacteria did appear slightly more sensitive to the former. In antifungal studies, both parabutopirin and opistoporin inhibited growth of a range of fungi (*Botrytis cinerea*, *Fusarium culmorum* and *S. cerevisiae*) at similar concentrations (50% growth inhibition between 0.3-3.5

μM). Parabutopirin was more than twice as effective as opistopirin in disrupting eukaryotic cell membranes. Using human erythrocytes, parabutopirin induced 50% haemolysis at 37 μM ; in comparison, opistopirin 1 induced only 30 % haemolysis at 100 μM .

Hadrurin is the prototype of another cysteine-free AMP family purified from the venom of the Mexican scorpion *Hadrurus aztecus*. Hadrurin (4436 Da, 41 amino acids), carries an overall positive charge at physiological pH and has the same structural profile as opistopirin, namely two α -helical regions connected by an undefined region between amino acid residues 12-16 (Torres-Larios *et al.*, 2000). The plot of an α -helical wheel shows opposite hydrophobic and hydrophilic regions and these two distinct regions allow the peptide to adopt an amphipathic conformation, as the carboxyl-terminal helix can rotate 100° with respect to the amino-terminal helix. In antimicrobial activity studies with Gram-negative organisms, several *E. coli* strains were very sensitive with MICs less than 10 μM ; in comparison, *Pseudomona* strains required 50 μM for full inhibition (Torres-Larios *et al.*, 2000). Haemolytic activity was observed at 30 μM . Studies with synthetic analogues have demonstrated that the (unnatural) D-isomer of hadrurin has a different activity profile from the native L-isomer, suggesting activity is a consequence of membrane disruption (Torres-Larios *et al.*, 2000).

Studies on two antimicrobial peptides isolated from *P. imperator* (Corzo *et al.*, 2001) have shed further light on the contribution of the two α -helical regions, to biological function. Pin1 has two α -helical regions between residues 3-18 and 20-39, separated by a random coil region containing a proline-19 kink. In contrast, NMR analysis of Pin 2 in a 60% TFE solvent containing DPC micelles, showed that this second peptide had a singular helical structure between residues 2-18 with no significant kink at the

equivalent proline residue (Pro-14) (Nomura *et al.*, 2005). The structural differences found between these two peptides are significant. While the antimicrobial activity of Pin 1 and Pin 2 against a range of Gram-positive and Gram-negative organisms was broadly similar, it is the haemolytic studies on eukaryotic membranes that are of most interest. Pin 2 lysed 51% of sheep erythrocytes at 22 μ M whilst Pin 1 only lysed 1.4% at the same concentration (Corzo *et al.*, 2001). The authors suggest that the ability of Pin 2 to lyse both eukaryotic and prokaryotic membranes may be related more to the venom toxicity, in a similar manner to the bee venom peptide melittin, than a specific antimicrobial action. In contrast, the activity of Pin1 is more in keeping with magainin 1, the prototype AMP isolated from the skin of the South American toad, *Xenopus*.

A flexible hinge region is also important in successful AMP design. Replacing proline-14 in Pin 2 with a more flexible Gly-Val-Gly tripeptide reduces the haemolytic activity of Pin 2 without altering its antimicrobial activity (Rodriguez *et al.*, 2011). This substitution creates a more flexible region while retaining the essential amphipathic nature of Pin 2 which is more in tune with the dual helical structure of magainin 2 (Zasloff, 1987).

With such contrasting effects on prokaryotic and eukaryotic membranes, a comparison of the mechanisms of action of these two peptides is of particular interest. On examination of the effects of Pin 2 on PC lipid vesicles using a calcien dye release assay, it was seen that the dose response curve for dye efflux was sigmoidal, suggesting pore formation during the time course of the experiment (Belokoneva *et al.*, 2004). When PE, known to promote negative membrane curvature (Matsuzaki *et al.*, 1998), was incorporated into the PC vesicles, no change in Pin 2 activity was observed, supporting the hypothesis of a barrel-stave mechanism of pore formation. Dextran-loaded liposome assays also showed great variability in the size (1.8-5 nm) of the

membrane pores generated by Pin 2, dependent on peptide: phospholipid ratios (Belokoneva *et al.*, 2004). Based on NMR studies of Pin 2, Nomura and colleagues (2004) proposed a pore forming mechanism of action, as a consequence of Pin 2 inducing clustering of hydrophobic residues which allows further incursion into the membrane hydrophobic core and interaction with the inner membrane. This process can be conveniently visualized in a step-wise fashion as shown in figure 1.6. Pin 2 inserts into the membrane at a 45° angle however is seen to be only at a 25° angle around the leucine 12 residue. This causes a slight kink in the peptide when in the membrane, and is a phenomenon seen in other pore forming AMPs, and is postulated to be essential for activity. After insertion, oligomerisation occurs between the Pin 2 monomers and then pore oligomerisation is seen leading to membrane being trapped between these pores to be “pinched off”. Thus, Pin 2 induces a 2 fold attack on the target with loss of intracellular constituents through the pore lumen and loss of membrane through pore association.

In contrast, NMR studies with Pin1 showed a radically different mode of action, with a detergent-like effect due to the formation of cubic phase structures. It was suggested that Pin1 sits within the interface of the membrane between the hydrophobic core and the polar phospholipid head groups (Nomura *et al.*, 2005). This can also be conveniently visualised (Fig. 1.7). The Pin1 N-terminal helices are tilted at a 30° angle with respect to the horizontal bilayer plane and the C-terminal helices. Interactions between tryptophan residues at position 4, 6 and 15 on the tilted helices and the polar head groups cause the membrane disruption and the formation of cubic phase structures. The N-terminal helices rotates around the average helical axis.

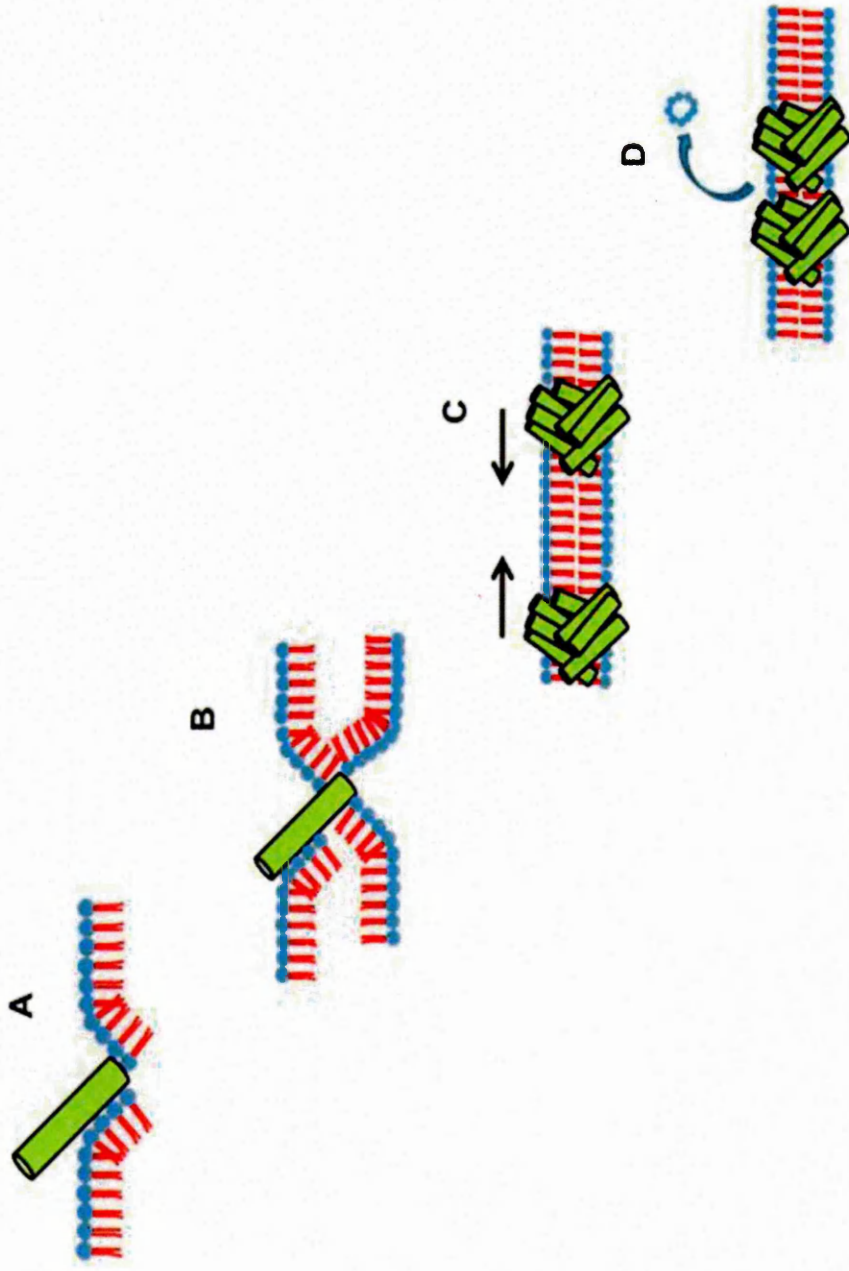


Figure 1.7: Mechanism of action of Pandinin 2 Pin2 interaction causes negative membrane curvature and insertion of the peptide at a 45° angle (A) Electrostatic attraction of the inner leaflet allows negative membrane curvature and formation of a transmembrane helices (B). Oligomerisation of the peptide occurs within the membrane allowing formation of the a barrel stave pore. The pores are further attracted to each other (C), causing pinching off of the membrane between pores (D). This mechanism causes a twofold attack; loss of membrane through pore attraction and loss of intracellular contents through the pores.

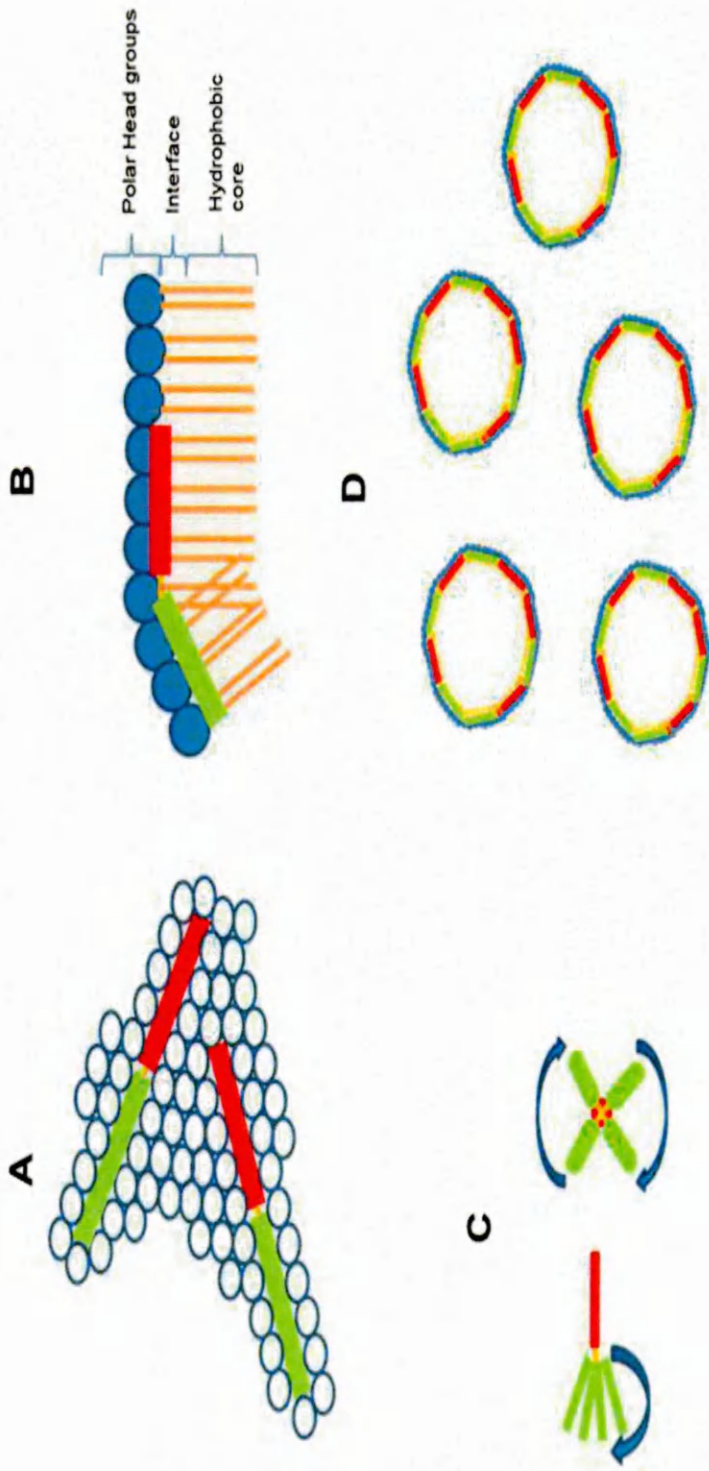


Figure 1.8: Mechanism of action of Pandinin 1-Pin1 interacts with phospholipid head groups. Pin1 sits between the head groups (A) within the interface between the head groups and HC core (B). Interactions between pin1 1-18 (green) and the head groups causes negative membrane curvature (B) as pin1 1-18 is at a 30° tilt with respect to pin1 20-44 (red) due to the presence of a proline at position 19. Membrane disruption accrues when pin1 1-18 rotates around the average helical axis, which is parallel to the lipid long axis (C) causing membrane disruption and dispersion of the lipid into the cubic phase (D).

Using primers originally designed to detect a bradykinin-potentiating peptide (K-12), Zeng and colleagues have identified a full length cDNA encoding a putative AMP (BmKbpp) from the venom glands of the Chinese scorpion, *Buthus martensii* Karsch. BmKbpp (NDBP-3.3 family) is predicted to encode a 47 amino acid mature peptide, the C-terminal region showing 57% homology to peptide K-12 (Zeng *et al.*, 2000). BLAST analysis of BmKbpp revealed high homology with a number of scorpion toxins such as NDB9.6 (98%) from *Lychas murconatus* (Chinese Swimming Scorpion), Tx297 (96%) from *Buthus occintanus israelis* (Gravid deathstalker scorpion) and parabutopirin (68%), suggesting a novel family of AMPs (Zeng *et al.*, 2012).

Secondary structure predictions of BmKbpp show a similar structure as Pin 1, with two α -helical regions (between residues 3-35 and 39-47) separated by a random coil region. Also, α -helical wheel projections reveal a highly amphipathic molecule. As with Pin 1 low haemolytic activity is seen with only 39.9% lysis of human red blood cells at a concentration of 50 μ M. Antimicrobial assays of BmKbpp in liquid cultures showed preferential activity against Gram-negative organisms (MIC's typically in the range 2-5 μ M) in comparison to Gram-positive organisms (MIC's typically > 20 μ M). Using a bioassay-guided fractionation strategy, Miyashita *et al.* (2010) isolated Im-1 (6.3 kDa, 56 amino acids) from the venom of *Isometrus maculatus* (Lesser Brown Scorpion). Im-1 belongs to the Bpp family and showed 43% homology toward parabutopirin, especially at the N-terminus. Secondary structure analysis indicated an α -helical structure between residues 3-40 which was confirmed by CD spectra in 50% TFE. Synthetic Im-1 had potent antimicrobial effects in liquid culture assays against both Gram-negative and Gram-positive bacteria (typical MIC values 0.4-0.8 μ M and 0.8-1.6 μ M, respectively) (Miyashita *et al.*, 2010).

Another long chain peptide, vejovine (4.8 kDa, 47 amino acids), has been isolated from the venom of *Vaejovis mexicanus* (Eastern plain scorpion) (Hernandez-Aponte *et al.*, 2011), with 52% homology to hadrurin. In antimicrobial assays performed in liquid broth cultures, both native and synthetic vejovine showed preferential activity towards Gram-negative organisms (*E. coli* MIC values 4.4-20 μM) with no activity towards Gram-positive *S. aureus*. Vejovine gradually breaks down when freshly milked venom is stored, producing a truncated derivative (Vm36), lacking the first eight N-terminal amino acids of vejovine. In comparison with vejovine, Vm36 showed no antimicrobial activity, demonstrating the importance of the N-terminal region of this and presumably other AMPs with similar structure. In CD studies, vejovine adopted an α -helical secondary structure in 60% TFE although it remained unordered in aqueous solution. In contrast, Vm36 peptide adopted an α -helical structure in aqueous solution which may indicate that the increased flexibility of vejovine is a key factor in promoting antimicrobial activity. Vejovine (50 μM) induced 40% haemolysis of human erythrocytes in eukaryotic cytotoxicity studies.

Using a cDNA cloning strategy, three peptides have been identified from the venom gland of *Heterometrus spinifer* (Giant Forest Scorpion) termed Heterin-1, Heterin-2 and spiniferin (Wu *et al.*, 2014). Heterin-1 is 43 residues in length and shares 73% homology with the opistoporins and 68% with pandinin 1 with secondary structure prediction indicative of a mono-helical structure between residues 3-38 flanked by two random coil regions, however, unlike these other peptides Heterin-1 has an amidated C-terminal. In antimicrobial assays it had good activity against the Gram positive pathogens of *B. megaterium* and *Micrococcus luteus* (4.0 μM) whilst its potency against *S. aureus* and a range of Gram-negative organisms was less so (15.0-42.0 μM) in cytotoxicity assays 54% haemolysis was seen at 10.0 μM .

1.11.2.2 Intermediate chain peptides

A completely new class of scorpion AMPs has been reported from the venom gland of the Asian scorpion *H. spinifer* (Nie *et al.*, 2012). Clones encoding four highly homologous peptides were characterised and one peptide (HsAp) was synthesized by solid state methods. HsAp (29 amino acids) showed no significant homology to any other class of scorpion AMPs. It has broad spectrum antibacterial activity against both Gram-positive (MICs typically 11-50 μM) and Gram-negative organisms (MICs typically 25-50 μM), without clear target-cell specificity as well as anti-fungal activity (MIC approx. 50 μM). HsAp was postulated to have an α -helical structure (residues 7-24) with coiled N and C terminals. It has classical amphipathic characteristics although its hydrophobic face is disrupted by two hydrophilic residues (serine and glutamic acid). Nie and colleagues indicated that HsAp is a bacterial infection-responsive peptide because the genomic sequence of its gene is intronless. At present HsAp has limited therapeutic potential because of its potent haemolytic activity against human erythrocytes (95% haemolysis at 3.2 μM)

Heterin-2 from the scorpion *H. spinifer* is a 24 residue C-terminally amidated peptide which shares 92% homology to pandinin 2. Secondary structure predictions revealed a single helical domain between residues 2-21 flanked by two random coil regions and is amphipathic in nature. Moderate antimicrobial potency was observed against Gram-positive pathogens (5.6-30.0 μM) and it was broadly less potent against Gram-negative organisms (15.8->45.0 μM), it also exhibited high cytotoxicity with 6.4 μM causing over 90% haemolysis. Interestingly when the C-terminal random coil region is removed (KKD) the therapeutic index is improved with a halving of the haemolytic potential and

an overall increase in the MIC against Gram-positive organisms; however a reduction is seen against Gram-negative pathogens (Wu *et al.*, 2014).

1.11.2.3 Short chain peptides

The first short chain AMPs were isolated from the venom of the African scorpion *Opisthacanthus madagascariensis* (Madagascan scorpion) IsCT and IsCT2 (Dai *et al.*, 2001 and 2002) share 78% homology (both approx. 1.5 kDa, 13 amino acids), have the same net charge (+2) and are both amidated at the C-terminus. The precursor of each peptide consists of a signal peptide and a C-terminal pro-sequence which contains the typical C-terminal processing signals Gly-Arg-Arg or Gly-Lys-Arg. Both peptides showed a broad spectrum profile against most Gram-positive and Gram-negative bacteria on solid agar plates (MICs typically 0.6-16 μ M) although Gram-negative *Pseudomonas* strains were unusually resistant (MICs typically > 66 μ M). Both peptides were weakly haemolytic (10% lysis of sheep erythrocytes at 100 μ M) (Dai *et al.*, 2002) although IsCT (approx. 3 μ M) was extremely effective, in comparison to mastoparan, at degranulating rat peritoneal mast cells, as measured by a histamine release assay (Dai *et al.*, 2001). A pore-forming mechanism of action was postulated (Dai *et al.*, 2002) due to the threshold concentration kinetics during antimicrobial assays and calcien release assays with synthetic membranes. The latter revealed a membrane disruptive mechanism for both peptides. At low peptide concentrations a preferential affinity towards phosphatidic acid (PA) compared with PC was noticed; however this selectivity was not seen with high concentrations of peptides.

Extensive structure-function analysis has been carried out on IsCT and IsCT2 (Dai *et al.*, 2001, 2002; Lee *et al.*, 2004). CD spectra and helical wheel predictions of both peptides revealed an α -helical organisation in membrane-mimicking environments (40

and 70% TFE) which adopted a classical amphipathic structure. A sequence comparison between the two peptides shows differences at Phenylalanine-2 (leucine), Alanine-4 (lysine) and Asparagine-7 (glutamine) (IsCT2 residues in brackets). Helical wheel analysis demonstrates that these differences cause changes within the hydrophilic face of IsCT2, although there is no overall change in charge; this suggests that both overall ionic charge and amphipathic nature, as distinct from specific amino acid residues, are critical for AMP function. Mutation studies on IsCT (Lee *et al.*, 2004) showed the importance of the hydrophobic residue at position 6. Substitution of Tryptophan 6 for Alanine 6 resulted in a remarkable decrease in both antimicrobial and haemolytic activities. Dai and colleagues (Dai *et al.*, 2002) also identified two other peptides in the crude venom, analogous to IsCT and IsCT2 (IsCTf and IsCT2f, respectively). These latter two peptides are thought to be proteolytic products of the parent molecules devoid of the two penultimate amino acids (leucine and phenylalanine-NH₂). IsCTf and IsCT2f have no antimicrobial activity and have no α -helical structure as evidenced by CD spectral analysis, implicating these two C-terminal residues as critical for function.

Two AMPs, BmKb1 and BmKn2, have been identified from the venom gland cDNA library of *B. martensii* (Zeng *et al.*, 2004). These peptides are both basic (BmKb1, charge +1; BmKn2, charge +2) and like the IsCT peptides discussed earlier, also have amidated C-terminals. BmKb1 has a 52 amino acid pre-pro sequence containing a 22 amino acid signal sequence, which after post translational modification gives an 18 amino acid mature peptide. In comparison, BmKn2 has a 47 amino acid pre-pro sequence containing a 23 amino acid signal sequence, finally resulting in a 13 amino acid mature peptide. Secondary structure predictions suggest that both BmKb1 and BmKn2 have α -helical regions (amino acids 2-16 and 2-11 respectively) flanked by two

random coils; helical wheel projections demonstrate their amphipathic natures. The shorter and more highly charged BmKn2 is considerably more active than BmKb1 (MICs for Gram-positive organisms were typically 0.4-6 μ M for BmKn2 as compared with 9-45 μ M for BmKb1; MICs for Gram-negative organisms were typically 1-15 μ M for BmKn2, as compared with 10-50 μ M for BmKb1). The activity of BmKn2 against 18 strains of multidrug resistant *N. gonorrhoeae* has recently been analysed via an MTT assay with these strains having an MIC₅₀ value of between 6.9-27.6 μ M (Arpornsuwan *et al*, 2014). This study also noted the C-terminally amidated residue was critical for function with a dramatic decrease in activity observed upon deletion.

Based on these findings, PCR primer sets were designed to detect BmK1 homologues in other venoms, for example mucroporin from *Lychas mucronatus* (ornate black scorpion) (Dai *et al.*, 2008) and imcroporin from *I. maculates* (Zhao *et al.*, 2009). Mucroporin shows 51 % homology with BmKb1 and consists of a 35-amino acid pre-pro peptide which gives rise to a 17 residue mature peptide amidated at the C-terminal. Mucroporin (charge +1) and a mucroporin-M1 analogue (charge +5) were both active against Gram-positive bacteria (MIC values 3-29 μ M), although the difference in charge did not have a consistent effect on bacterial susceptibility. In contrast, both peptides had much weaker activity against Gram-negative bacteria, with MIC values greater 50 μ M (Dai *et al.*, 2008).

Because *S. aureus* was particularly sensitive to mucroporin M1, this peptide was further tested against clinically important isolates of this particular bacteria. The data revealed that mucroporin-M1 can inhibit a range of antibiotic-resistant pathogens of both methicillin- and penicillin- resistant strains (4-10 μ M), as well as penicillin- sensitive strains (4-20 μ M). Scanning electron microscopy (SEM) studies showed rapid lysis of

bacterial cells after mucroporin or mucroporin-M1 treatment, suggesting a membrane disruptive mechanism. Mucroporin M1 has been shown to specifically inhibit RNA viruses, including SARS-corona virus, influenza and measles viruses, presumably by targeting the viral membrane (Li *et al.*, 2011). DNA viruses were not inhibited. The same groups have more recently shown (Zhao *et al.*, 2012) that the peptide inhibits hepatitis B virus replication, both *in vitro* and *in vivo*, by activating the mitogen-activated protein kinase (MAPK) pathway, which resulted in the down-regulation of the nuclear hormone transcription factor, HNF4 α .

Imcroporin, the second peptide identified as a BmKb1 homologue through a PCR screen, has the same number of amino acids and charge, as mucroporin. Secondary structure prediction and helical wheel analysis suggested that imcroporin has a highly amphipathic nature with a 100% alpha-helical conformation (Zhao *et al.*, 2009). The antimicrobial activity profile of imcroporin was very similar to mucroporin; growth of Gram-negative organisms was weakly inhibited (MICs typically >57 μ M) whereas Gram-positive organisms, including methicillin- and penicillin- resistant strains of clinical isolates of *S. aureus* were more sensitive to the peptide (MICs typically 11-30 μ M). For comparison, the MICs of all clinical isolates against vancomycin were 3 μ M. Imcroporin was also tested in an *in vivo* mouse model (Zhao *et al.*, 2009). The peptide (single dose, 60 μ g/g, given one hour after intraperitoneal infection with *S. aureus*) was as effective as vancomycin (60 μ g/g) in curing mice; all mice survived, seven days after treatment. However imcroporin also exhibited significant cytolytic properties against mammalian cell lines and red blood cells, as evidenced by MTT assays and haemolysis assays respectively. Imcroporin (57 μ M) killed between 25-100% of kidney and hepatoma cells and haemolysed 70% of human erythrocytes. Kill kinetics and enzyme

activity assays of cell supernatants revealed, as with mucroporin, a rapid membrane disruptive mechanism of action.

The great majority of scorpions are considered harmless and probably as a consequence, the characterisation of peptides found in their venom glands has been very limited. The Asian scorpion, *Scorpiops tibetanus* (higher mountain scorpion) is one such example and Cao, Li and colleagues (Yuan *et al.*, 2010) have cloned a new antimicrobial peptide gene (StCT1) from *S. tibetanus* by screening a venom gland cDNA library with IsCT primers. The precursor of StCT1 is characterized by a signal peptide (24 amino acids) followed by a putative mature peptide of 14 residues and finally, an unusual 37-amino acid acidic propeptide at the C-terminus, suggesting that the mature peptide is C-terminally amidated. A synthetic amidated peptide corresponding to the putative mature peptide of StCT1 showed preferential activity towards *S. aureus* with weak activity towards Gram-negative organisms, in a similar manner to mucroporin and imcroporin. MIC values against MRSA strains ranged between 85-135 μM whilst penicillin-resistant strains were more sensitive (MIC 34 μM). It is interesting to note that although the amidated StC1 peptide has approx 40% homology with IsCT, the latter peptide (in contrast to StC1) has activity against both Gram-positive and Gram-negative organisms. Using the same approach, a StCT2 gene has also been cloned (Cao *et al.*, 2012). A synthetic, amidated 14 amino acid StCT2 peptide, corresponding to the predicted mature peptide, also showed potent activity against *S. aureus* and methicillin resistant *S. aureus* (MICs values 3- 13 μM). Both StCT1 and StC2 peptides belong to the NDBP -5 family.

Two structurally divergent peptides (meucin-18; meucin-13) have been isolated from a venom gland library of the Asian scorpion *Mesobuthus eupeus* (lesser Asian scorpion)

by a random sequencing strategy (Gao *et al.*, 2009). Based on MIC values, most Gram-positive organisms were 3-4 fold more susceptible to meucin-18 than meucin-13, while Gram-negative organisms were 2-5 fold more susceptible to the longer peptide. Meucin-18 was also 2-14 fold more potent than meucin-13 against a range of fungi and yeast.

Both meucin-18 and meucin-13 were cytotoxic toward rabbit erythrocytes; however meucin-18 (6.25 μ M) was twice as haemolytic as meucin-13 at the same concentration (74 vs 38% haemolysis, respectively). Whole cell patch clamp experiments identified a sharp decrease in ion currents followed by a rapid, partial recovery, when rat dorsal root ganglion (DRG) cells were exposed to either peptide. These electrophysiological experiments were supported by morphological studies, when the surface of DRG cells was transformed from a smooth to a rough state after incubation with peptides. Evidence for the peptides causing membrane permeabilization in microbial cells (bacteria, yeast and fungi) was obtained with the fluorescent DNA-binding dye, propidium iodide. Taken together, these studies suggest that meucins cause permanent cell damage.

Gao and colleagues (2009) have then gone on to try and rationalize their biological data in terms of structural differences between meucin-13 and meucin-18. Meucin-13 has an amidated C-terminal in contrast to meucin-18 which does not. Extensive structural studies have been carried out on both peptides using CD spectroscopy and NMR spectrometry. The CD spectrum of meucin-13 in 50% TFE characterized the peptide as being primarily α -helical. This was confirmed by NMR, which identified an α -helical structure between residues 5-13 with an unordered N-terminus. Meucin-18 showed similar results to meucin-13, although NMR revealed a more ordered N-terminal structure. This is thought to be due to the presence of alanine at position 6 (meucin-13)

instead of phenylalanine (meucin-18). A structurally ordered N-terminus is postulated to be important for biological activity. Gao and colleagues have also suggested that differences in biological potency might be related to differences in the hydrophilic/hydrophobic balance between the two meucins due to the more balanced amphipathicity of meucin-18. The C-terminal extension of meucin-18 with a free (charged) carboxy terminus means that overall, meucin-13 is more hydrophobic. This relative increase in hydrophobicity may reduce the biological activity of the latter due to its increased self-association in aqueous solution (Jiang *et al.*, 2008). Gao and colleagues also noted that meucin-18 has a positively-charged region (adjacent lysine-6 and lysine-11 residues) that could prove crucial for increased interaction with negatively-charged prokaryotic membranes.

The pattern of α -helical peptides from scorpion venoms showing preferential activity towards Gram-positive organisms has continued with the cloning of Ctriporin by the random screening of a large number of clones from the venom gland cDNA library of *Chaerilus tricostatus* (big Charles scorpion) (Fan *et al.*, 2011). Ctriporin is a 19 amino acid peptide (net charge: +2) with, like many other previously described peptides, an amidated C-terminus that is produced by the post translational cleavage of a 34-residue acidic propeptide. Secondary structure analysis and CD spectra of the peptide in 30 and 70% TFE revealed an amphipathic α -helical structure. However, the ambiguity still remains as to whether the peptide is completely α -helical or contains a random coil region, due to the presence of glycine-4, glycine-7 and proline-8, residues known to disrupt α -helical structures. MIC values (Gram-positive organisms) ranged from 3-5 μ M whereas Gram-negative organisms had MICs >49 μ M). All clinical isolates of MRSA strains gave MIC values of 5 μ M (c.f. vancomycin 3-6 μ M). Similarly the penicillin-resistant strain of *Staphylococcus epidermidis* had an MIC of 5 μ M,

analogous to vancomycin. Ctriporin also had antifungal activity against *Candida* (MIC 10 μM) and *in vivo* studies with mice demonstrated that topical applications of the peptide were more effective than currently established topical treatments, pexiganan and omiganan pentahydrochloride in treating fungal and *S. aureus* infections. Time kill kinetics and SEM studies suggested that ctriporin caused a rapid disruption of cell membranes, analogous to other α -helical peptides.

Two further short AMPs (AamAP1 and AamAP2) have been isolated from the venom of the North African scorpion *Androctonus amoreuxi* (big tailed scorpion) (Almaaytah *et al.*, 2012) and the precursor-encoding cDNAs have been cloned, using a shot-gun approach. They both have 18 amino acids and are amidated at their C-termini. AamAP1 and 2 differ by only 2 residues with leucine being replaced by proline at position 2 and phenylalanine being replaced by isoleucine at position 17. Secondary structure prediction suggested that AamAP2 has a far greater random coil region than AamAP1. However these structural differences did not manifest themselves in changes in biological activity. Although neither peptide was particularly active (MICs 20-150 μM) AamAP1 was slightly more active against Gram-negative organisms while the reverse was true for Gram-positive organisms. Both were equally effective against yeast and caused a significant haemolysis of red blood cells in the same concentration range.

Using a size-selective screening strategy, three new antimicrobial peptides (Pantinin-1, -2 and -3) were characterized from a venom gland cDNA library of the African scorpion *P. imperator* (Zeng *et al.*, 2013). All three were predicted to be mature peptides of 13-14 amino acid residues with precursor peptides indicating the now-characteristic C-terminal post-translational processing, resulting in C-terminal amidation. Peptides were cationic and secondary structure prediction suggested that pantinins are α -helical,

amphipathic structures. Amino acid sequence homology revealed that these peptides belong to the ever-growing 5th family of NDBPs. Pantinins are relatively potent against Gram-positive bacteria (MICs 4-48 μM), including vancomycin- and methicillin-resistant bacteria but are much weaker against Gram-negative bacteria (MICs 36- >87 μM). In addition to their antimicrobial activities, the three peptides showed haemolytic activity on human RBCs in a dose-dependent manner.

Two C-terminal amidated peptides (TsAP-1 and -2) have been isolated from the venom of *T serrulatus* by shot gun cloning and LC-MS identification (Guo *et al.*, 2013). Each peptide contained 17 residues with a net charge of +2. TsAP-1 had very weak antimicrobial activity against yeast and both Gram-positive and Gram-negative organisms (MICs typically 120-160 μM) and showed very little haemolytic activity. TsAP-2 had no effect against Gram-negative organisms at the highest concentrations tested but was surprisingly effective in inhibiting the growth of both yeast and Gram-positive organisms (MICs 5-10 μM). TsAP-2 had weak haemolytic activity (18%) at four times the MIC for Gram-positive bacteria. The α -helical content (76% TsAP-2 vs. 59 % TsAP-1) and hydrophobicity (0.51 hydrophobic moment TsAP-2 vs. 0.43 TsAP-1) has been suggested for the divergence in biological activities of these two peptides.

As part of this study the biophysical characterisation of the mechanism of action of AMPs will be examined, in part, on hydrated lipid bilayers using both atomic force microscopy (AFM) and quartz crystal microbalance-dissipation (QCM-D). Below is an explanation of these techniques.

Table 1.3: Table of selected scorpion derived AMPs with known sequence

Name (UniProtKB)	Sequence	Length (A) / molecular weight (Da)	Scorpion species (Family)	Reference
<i>A. Cysteine containing AMPs</i>				
Scorpine or Panscorpine (KBX3_PANIM)	GWINEEKIQKKIDERMGNTVLGGMAKAV HKMAKNEFOCMANMDMLGNCEKHCQT SGEKGYCHGTKCKCGVPLSY	75/8350; 3DSBs	<i>P. imperator</i> (Scorpionidae)	Conde et al., 2000
Opiscorpine-1 (KBX31_OPICA)	KWFNEKSIQNKIDEKIGKNFLGGMAKAV VHKLAKNEFMCVANVDMTKSCDTHCQ KASGEKGYCHGTKCKCGVPLSY	76/8428; 3DSBs	<i>O. carinatus</i> (Scorpionidae)	Zhu and Tytgat, 2004
Opiscorpine-2 (KBX32_OPICA)	KWLNKSIQNKIDEKIGKNFLGGMAKAV VHKLAKNEFMCMANMDPTGSCETHCQK ASGEKGYCHGTKCKCGVPLSY	76/8367; 3DSBs	<i>O. carinatus</i> (Scorpionidae)	Zhu and Tytgat, 2004
Opiscorpine-3 (KBX33_OPICA)	KWLNKSIQNKIDEKIGKNFLGGMAKAV VHKLAKNEFMCVANVDMTKSCDTHCQK ASGEKGYCHGTKCKCGVPLSY	76/8394; 3DSBs	<i>O. carinatus</i> (Scorpionidae)	Zhu and Tytgat, 2004
Opiscorpine-4 (KBX34_OPICA)	KWLNKSIQNKIDEKIGKNFLGGMAKAV VHKLAKNEFMCVANIDMTKSCDTHCQK ASGEKGYCHGTKCKCGVPLSY	76/8408; 3DSBs	<i>O. carinatus</i> (Scorpionidae)	Zhu and Tytgat, 2004
Heteroscorpine (KBX3_HETLA)	GWINEEKIQKKIDEKIGNNILGGMAKAV VHKLAKGEFQCVANIDTMGNCEETHCQK	76/8293; 3DSBs	<i>H. laoticus</i> (Scorpionidae)	Uawonggul et al., 2007

	TSGEKGFCHGTKCKCGKPLSY				
HgeScplp1 (KBX3_HADGE)	GWMSEKVVQGILDKKLP EGIIRNAAKAIV HKMAKNQFGCFANVDVKGDCKRHCKA EDKEGICHGTKCKCGVPISYL	76/8370; 3DSBs	<i>H. gertschi</i> (Caraboctonidae)	Diego-Garcia et al., 2007	
HgeβKTx (KBX2_HADGE)	KSTVGQKLKKKLNQAVDKVKEVLNKSEV MCPVVSSFCKQH CARLGKSGQCDLLECIC	58/6427; 3DSBs	<i>H. gertschi</i> (Caraboctonidae)	Diego-Garcia et al., 2007	
HgeScplp2 (KBX32_HADGE)	GILREKYAHKAIDVLT PMIGVPVVS KIVNN AAKQLVHKIAKNQQLCMFNKDVAGWCE KSCQQSAHQKGYCHGTKCKCGIPLNYK	84/9326; 3DSBs	<i>H. gertschi</i> (Caraboctonidae)	Schwartz et al., 2007	
Bactridin-1 (AMP1_TITDI)	KDGYIIEHRGCKYSCFFGTNSWCNTECT LKKGSSGYCAWPAWCYGLPDNVKIFD SNNLKC	61/6928; 4DSBs	<i>T. discrepans</i> (Buthidae)	Diaz et al., 2009	
Bactridine-2 (AMP2_TITDI)	KDGYLVGNDGCKYSCFFRPGTYCANEC RVKGDGYCYAWMACYCYSMPNWVKT WNRATNRCCR	64/7374; 4DSBs	<i>T. discrepans</i> (Buthidae)	Diaz et al., 2009	
B. Long chain non-cysteine containing AMPs					
Opistoparin-1 (OPO1_OPICA)	GKVVDWIK STAKKLWNSE PVKELKNTA LNAAKNLVAEK IGATPS	44/4836	<i>O. carinatus</i> (Scorpionidae)	Moerman et al., 2002	
Opistoparin-2 (OPO2_OPICA)	GKVVDWIK STAKKLWNSEPVKELKNTA LNAAKNFVAEKIGATPS	44/4870	<i>O. carinatus</i> (Scorpionidae)	Moerman et al., 2002	
Hadurin (HADR_HADAZ)	GILDTIKSIASKVWNSKTVQDLKRRGINW VANKLGVSPQAA	41/4436	<i>H. aztecus</i> (Iuroidea)	Torres-Larios et al., 2000	

Pandinin-1 (PAN1_PANIM)	GKVVDWIKSAAKKIWSSEPVSQLKGQV LNAAKNYVAEKIGATPT	44/4800	<i>P. imperator</i> (Scorpionidae)	Corzo et al., 2001
Parabutoparin (PBPO_PARSC)	FKLGSFLKKA WSKLAKKLRKAKGKEML KDYAKGLLEGGSE EIVPGQ	45/5030.3	<i>P. schlechteri</i> (Buthidae)	Moerman et al., 2002
Vejovine (F1AWB0_9SCOR)	GIWSSIKN LASKA WNSDI GQSLRNKAAG AINKFVADKIGVTPSQAAASM TLDEIVDA MYVD	47/4873	<i>V. mexicanus</i> (Vaejovidae)	Hernandez- Aponte et al., 2011
BmKbpb (BPK3_MESMA)	FRFGFLKVVWKSCLKAKKLRKSKGKQLLK DYANKVNLNGPEEEAAPAE	47/5321	<i>M. martensii</i> (Buthidae)	Zeng et al., 2000
Im-1 (BPP_ISOMC)	FSFKRLKGFACKLWNSKLARKIRTKGLKY VKNFADMLSEGEAAPAAEPPVEAPQ	56/6344.5	<i>I. maculatus</i> (Buthidae)	Miyashita et al., 2010
Heterin-1	GVVDWLKKTAKNVVNSDIVKQKGGKAI NAAKNYVAEKIGATPS-NH2	43/4742.54	<i>H. spinifer</i> (Scorpionidae)	Wu et al., In press
C. Intermediate chain non-cysteine containing AMPs				
Meucin-24 (KBX2_MESEU)	GRGREFMSNLKEKLSGVKEKMKNS	24/2753.95	<i>M. eupeus</i> (Buthidae)	Gao et al., 2010
Meucin-25 (M25_MESEU)	VKLIQIRIWIQYVTVLQMFMSMKTQK	25/3095.56	<i>M. eupeus</i> (Buthidae)	Gao et al., 2010
HsAp (JX311701)	SGTSEKERESGRLLGVVKRLIVCFR SPFP-NH2	29/3246	<i>H. spinifer</i> (Scorpionidae)	Nie et al., 2012
Pandinin-2	FWGALAKGALKLIPSLFSSFSKDD	24/2612	<i>P. imperator</i> (Scorpionidae)	Corzo et al., 2001

(PAN2_PANIM)	FWGALAKGALKLIPSLVSSFTKKD-NH2	24/2576.47	<i>H. spinifer</i> (Scorpiomidae)	Wu et al., In press
<i>D-Short cytotoxic AMPs</i>				
Heterin-2				
IsCT (NDB52_OPIMA)	ILGKIWEGIKSLF-NH2	13/1502	<i>O. madagascariensis</i> (Hemiscorpiidae)	Dai et al., 2001
IsCT2 (NDB53_OPIMA)	IFGAIWNGIKSLF-NH2	13/1463.92	<i>O. madagascariensis</i> (Hemiscorpiidae)	Dai et al., 2002
BmKb1 (KB1_MESMA)	FLFSLIPSAISGLISAFK-NH2	18/1910	<i>M. martensii</i> (Buthidae)	Zeng et al., 2004
Meucin-13 (NDB5Y_MESEU)	IFGAIAGLLKNIF-NH2	13/1375.82	<i>M. eupeus</i> (Buthidae)	Gao et al., 2009
VmCT1 (NDB5D_VAEMS)	FLGALWNVAKSVF-NH2	13/1450.8	<i>V. mexicanus</i> (Vaejovidae)	Ramirez-Carretero et al., 2012
VmCT2 (NDB5E_VAEMS)	FLSTLWNAAKSIF-NH2	13/1496.8	<i>V. mexicanus</i> (Vaejovidae)	Ramirez-Carretero et al., 2012
Mucroporin (MUCR_LYCMC)	LFGLIPSLIGGLVSFAFK-NH2	17/1731	<i>L. mucronatus</i> (Buthidae)	Dai et al., 2008
AamAP1 (VAP1_ANDAM)	FLFSLIPHAIGGLISAFK-NH2	18/1931.94	<i>A. amoreuxi</i> (Buthidae)	Almaaytah et al., 2012
AamAP2 (VAP2_ANDAM)	FPFSLIPHAIGGLISAIK-NH2	18/1880.93	<i>A. amoreuxi</i> (Buthidae)	Almaaytah et al., 2012

Imcroporin (IMCR_ISOMC)	FFSLPGLIGGLVSAIK-NH2	17/1761	<i>I. maculatus</i> (Buthidae)	Zhao et al., 2009
SICT1 (NDB5X_SCOTI)	GFWGSLWEGVKSVV-NH2	14/1549.79	<i>S. tibetanus</i> (Euscorpidae)	Yuan et al., 2010
SICT2 (NDB5Y_SCOTI)	GFWGKLWEGVKSAI-NH2	14/1576.84	<i>S. tibetanus</i> (Euscorpidae)	Cao et al., 2012
Meucin-18 (NDB59_MESEU)	FFGHILFKLATKIIPSLFQ	18/2106	<i>M. eupeus</i> (Buthidae)	Gao et al., 2009
Ctriporin (VAP_CHATC)	FLWGLIPGAIASVTSLIKK-NH2	19/ 2015.2	<i>C. tricostratus</i> (Chaeriloidea)	Fan et al., 2011
Hp1090 (NDB59_HEITPE)	IFKAIWSGIKSLF-NH2	13/1508.88	<i>H. petersii</i> (Scorpionidae)	Yan et al., 2011
Pantinin-1 (KC538864)	GILGKLWEGFKSIV-NH2	13/1545.90	<i>P. imperator</i> (Scorpionidae)	Zeng et al., 2013
Pantinin-2 (KC538865)	IFGAIWKGISSLL-NH2	14/1403.71	<i>P. imperator</i> (Scorpionidae)	Zeng et al., 2013
Pantinin-3 (KC538866)	FLSTW NGIKSLL-NH2	14/1490.80	<i>P. imperator</i> (Scorpionidae)	Zeng et al., 2013
TsAP-1 (HF677516)	FLSLIPSLVGGISAFK-NH2	17/1733.32	<i>T. serrulatus</i> (Buthidae)	Guo et al., 2013

TsAP-2 (HF677517)	FLGMIPGLIGGLISAFK-NH2	17/1735.20	<i>T. serrulatus</i> (Buthidae)	Guo et al., 2013
----------------------	-----------------------	------------	------------------------------------	------------------

1.12 Atomic force microscopy

The utilisation of atomic force microscopy (AFM) in the field of materials science has proved useful in obtaining molecular scale images within the materials native environment (El Kirat *et al.*, 2010). It provides three-dimensional images with nanometre scale resolution and can provide crucial information regarding the physical properties of the surface such as surface topology, hardness and elasticity. AFM has traditionally been used within the physical sciences, however, more recently the ability to image biomaterials in a pseudo native state, not possible in other high resolution techniques such as SEM and transmission electron microscopy (TEM), has been explored (Medalia *et al.*, 2001).

AFM functions by moving a fine cantilevered tip over the samples surface in a raster fashion with electrostatic interactions, typically Van der Waals forces, between the surface and the tip causing the tip to deflect which in turn is detected and recorded by the machine. As seen in figure 1.8 an AFM system consists of a cantilevered probe containing a sharp tip, typically silicon nitride with a diameter of 5-20 nm, which is mounted to a piezoelectric actuator and photo sensitive diode. The PZT scanner itself is capable of moving the sample in the x, y & z direction (Binnig *et al.*, 1986)

The principle of AFM is to shine a laser beam on to the top surface of the cantilever whilst the tip is scanning a surface, this beam is re played back to the photo electric diode through a feedback loop which allows the PZT to change position and thus keep a

constant force/constant height between sample and tip. By maintaining these constants through repositioning of the scanners it is possible to attain topological information of the sample. There are 3 modes in which an AFM system is operated in (Binnig *et al.*, 1986): (I) contact mode (II) non- contact mode and (III) tapping mode. In each mode it is possible to attain topological information as well as changes in electrostatic, magnetic and atomic forces with the sample.

1.12.1 Operation characteristics of AFM

- Contact mode

In contact mode the tip is constantly touching the sample surface, whilst the tip scans physiochemical information is determined mainly via repulsion of interatomic electron clouds between the tip and surface due to the extremely small distances between them. Contact mode can be operated in both constant height and constant force mode. In constant height mode the PZT scanner only moves in the x & y direction and keeps the z direction constant accurately measuring topology. In constant force mode, upon initial interaction between tip and sample, a constant force required to keep the tip at a specific deflection (due to atomic repulsion) is set and this required force is maintained via the feedback mechanisms described previously. One advantage of contact mode is the speed at which the sample can be scanned. However, due to constant contact between tip and sample damage can occur with soft sample material and, therefore, is seldom used for biological applications (Morita *et al.*, 2009)

- Non-contact mode

In non-contact mode the tip is oscillated and remains a distance of between 50-150 Å above the sample surface, this oscillation is required for the detection of electrostatic

interactions between tip and sample due to the distance between them. When the tip is oscillating in free air a set amplitude can be determined, however, upon closer electrostatic interaction between sample and tip, energy will be dissipated and a change in amplitude will be detected which is then relayed back through the feedback system to readjust the position of the PZT scanner. Because of the lack of tip-sample interaction non-contact mode yields higher resolution images than contact mode and does not suffer from sample degradation of soft material, thus is applicable for biological samples. One of the major drawbacks of non-contact mode is interaction with the tip and fluid layers that build up upon the sample surface which results in a loss of resolution as electrostatic interactions tend to occur between the tip and this contaminant layer instead of the actual surface (Morita *et al.*, 2009).

- Tapping mode

Tapping is essentially a cross between contact and non-contact mode where the tip gently taps the surface as it scans. In this mode the tip is oscillated at near its resonance frequency in free air with amplitudes between 20-100 nm. The tip is then lowered towards the surface until interaction occurs. As the sample is scanned the oscillating tip taps the surface at a set frequency and as with non-contact mode dissipation of energy occurs due to an increase of electrostatic forces. The PZT scanner then adjusts to maintain a set amplitude. By maintaining this set amplitude the samples topology can be mapped as a depression in the surface with relayed an amplitude signal near to the free air signal conversely any elevation will result a decrease in amplitude. Because of the high resolution and soft approach of tapping mode it is routinely used for biological samples (Morita *et al.*, 2009).

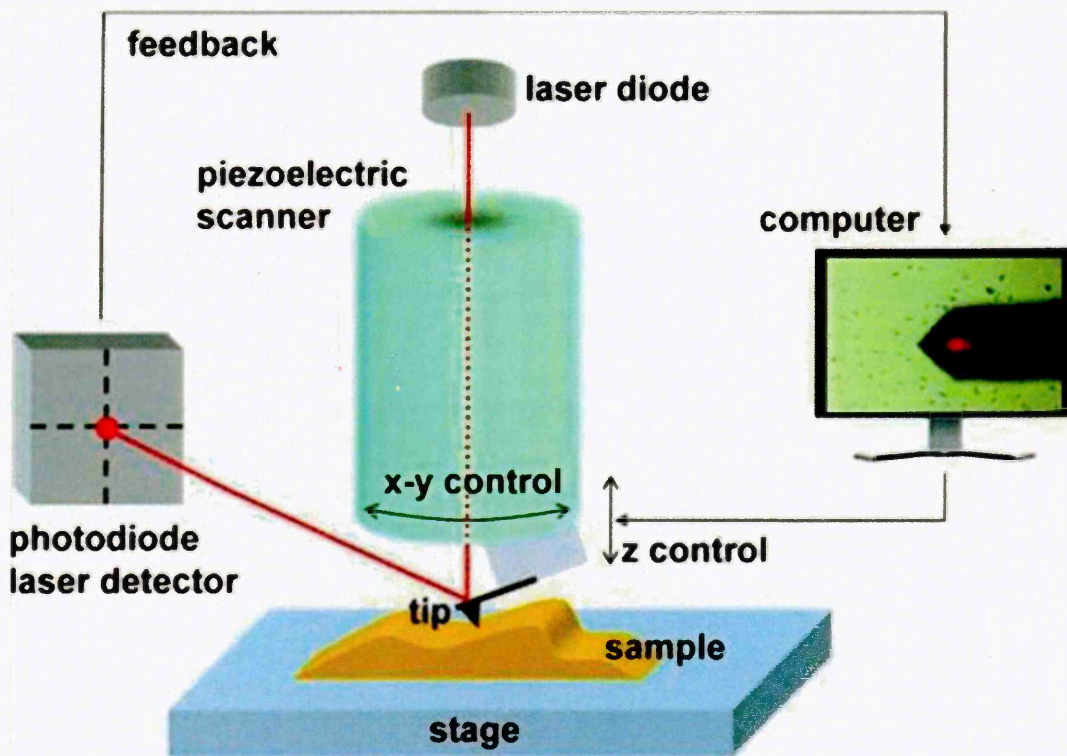


Figure 1.9: Schematic illustration of a scanned tip AFM system. (Trache and Meininger. 2005). A flexible cantilever with a tip at the end is rigidly connected with a xyz piezoelectric element. The optical lever consists of a laser diode beam that is focused on the back of the cantilever and bounces off reaching the photodetector. The photodetector is connected via a feedback loop to the z controller to alter the height of the cantilever to the original set point therefore mapping the features of a surface with respect to its height (Tsargorodska. 2007).

1.12.2 Force volume curves

As well as obtaining crucial information regarding the topological and physicochemical properties of a surface, AFM can also be used to determine the 'stiffness' of the sample by using atomic force spectroscopy (AFS) to generate a force curve (Fig. 1.9).

AFS is carried out in contact mode and is the point wise analysis of the sample by determining the deflection of the cantilever as the z distance decreases with respect to tip sample-distance. Thus, as the z distance decreases, the progression of the cantilever deflection is recorded. Due to the initial tip-sample distance being a function of the reading, AFS spectra is a relative reading (Polyakov *et al.*, 2011).

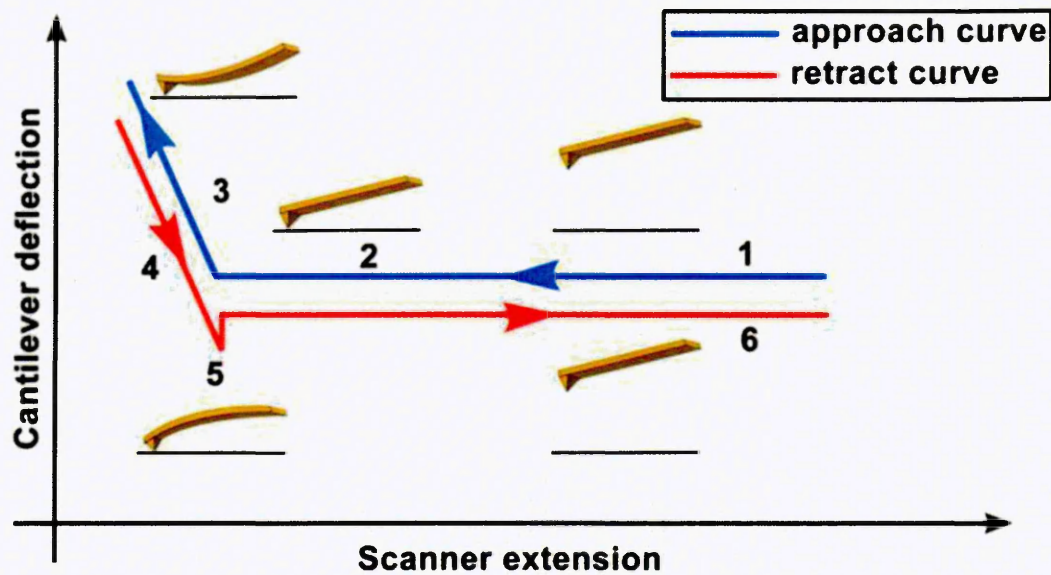


Figure 1.10: Schematic of a force spectroscopy curve (Fuentes-Perez *et al.*, 2013). (1). The electrostatic interactions between the tip and sample are seen and the cantilever tip is pulled towards the surface (2). As the tip and surface physically touch mechanical properties come into play and the tip cantilever is bent upwards (3). When undertaking AFS with deformable materials such as lipid bilayers, the puncturing of the bilayer is seen as the mechanical force increases and it is a good way of measuring the stiffness of a bilayer and after initial bilayer formation after lipid rupture if a double bilayer has been formed. The red line represents the retraction of tip from the surface (4) hence the force is decreasing as the mechanical stress between the tip and surface are relieved. However as can be seen a deviation between the approaching and retraction line occurs which is due to the electrostatic attraction occurring between tip and surface; at (5) the remaining adherence between tip and sample are being disrupted thus the force increases as more energy is required to pull away from the surface (Polyakov *et al.*, 2011).

1.13 Quartz crystal microbalance-dissipation (QCM-D)

As with AFM, QCM-D was initially developed for use within materials science and electrochemistry (Rodhal *et al.*, 1997), however in recent years it has been adapted to biological science (Dixon., 2008). QCM-D is based on the inherent piezoelectric effect of a quartz crystal, when an alternating current (AC) is applied the crystal will oscillate in shear mode (side to side) close to the resonant frequency (f_R) due to continued expansion and contraction of the crystal lattice structure which generates acoustic waves. The crystal has a very high quality factor (Q factor) which is a ratio of the frequency and bandwidth with the frequency partially dependent on the thickness of the crystal therefore any change in thickness is related in a linear fashion to a decrease in the frequency if all the other variables remain constant. The dissipation reading is a determines the loss of energy from the crystal surface to the environment and is a measurement of the viscoelastic properties of the crystal associated film after the AC is turned off, essentially the “wobbliness” of the crystal as the shear oscillation begins to stop, this is achieved by measuring the decay of the crystals oscillation after rapid excitation close to the f_R . Thus when a phospholipid membrane is adhered tightly to the crystal surface a high frequency and low dissipation is observed, however as peptide adheres and begins to disrupt the membrane the frequency will decrease as the thickness of the crystal increases and as the peptide disrupts the packing order of the membrane the dissipation reading will increase as the membrane begins to disassociate from the crystal surface and interact with the liquid environment (Rodhal *et al.*, 1995, Piantavigna *et al.*, 2011, Rydberg *et al.*, 2014). This is depicted in figure 1.10.

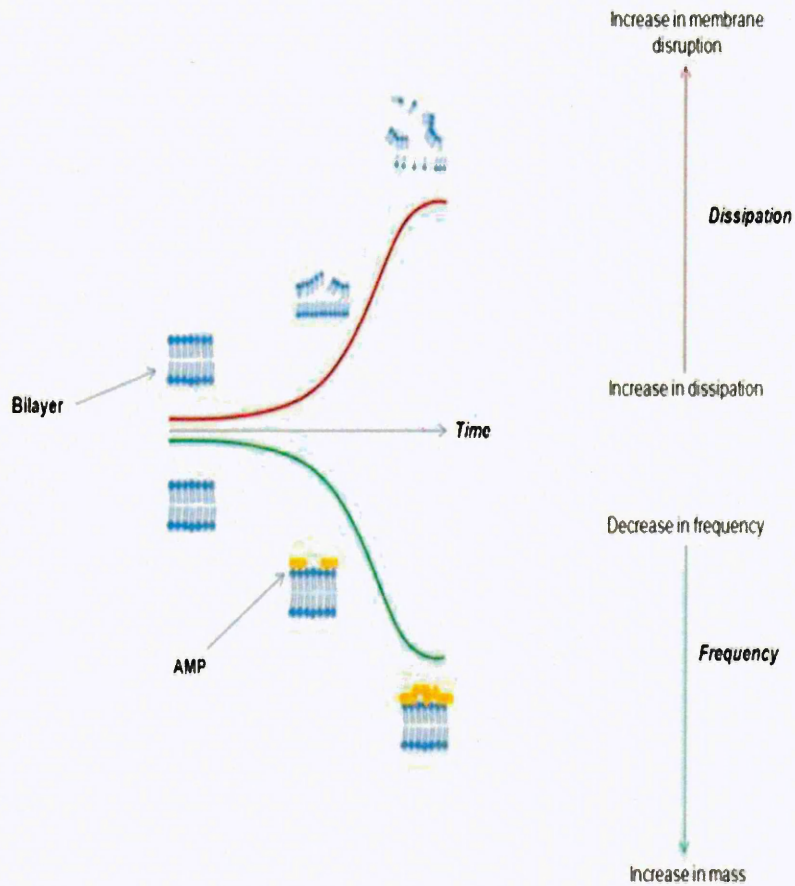


Figure 1.11: Explanation of the QCM-D reading upon peptide attack-before peptide interaction the bilayer is tightly bound to the crystal surface resulting in steady dissipation and frequency readings (flat red and green lines). As AMPs begin to accumulate and attack the surface the frequency decreases as more mass is on the crystal surface whilst an increase in dissipation is observed due to peptide disruption of the bilayer and increased interaction between the crystal surface and the fluid mobile phase (Piantavigna et al., 2011).

1.14 Scope of the present study

This present study aims to mine the relatively unexplored resource of snake venoms for novel antimicrobial peptides using an empirical strategy (protein purification) to maximise our chances of finding novel antimicrobial compound scaffolds. It also aims to further our understanding of scorpion AMP mechanism of action which, in turn, will have wider implications for the study of AMP mechanism of action as a whole. Such an understanding will be critical if this promising research area is to progress into the clinical setting.

The objectives were to:

- Identify novel AMPs from snake venoms of both vipridae and elapidae origin and from distinct geographical regions to minimise degeneracy
- Characterise the interactions of these peptides with bacterial cells identified previously through the genomic analysis of the North African scorpion *Scorpio maurus palmatus*
- Ascertain the mechanism of action of these peptides on whole cells. Including insights into the possibility of intracellular targets
- Investigate the mechanism of interaction of these peptides with synthetic model membrane systems using a variety of biophysical techniques

2 CHAPTER
MATERIALS AND METHODS

2.1 Purification and characterisation

2.1.1 Venom

Table 2.1 details the snake venoms used within this study, the family they belong to and the geographical region of the snakes natural habitat. Venoms were either purchased from Sigma (UK), Latoxan (France) or gifted by Mohamed Abdel-Rahman from the Institute of Zoology, Suez Canal University, Ismailia, Egypt. Venoms were chosen from both elapidae and viperidae families from a variety of geographically distinct regions to both maximise the chances of identifying novel AMP scaffolds and to minimise the chance of degeneracy.

Table 2.1: Venoms used within this study

Species	Family	Geographical location
<i>Bitis arietans</i>	viperidae	Sub-Saharan Africa
<i>Cerastes cerastes</i>	viperidae	North Africa
<i>Crotalus adamanteus</i>	viperidae	North America
<i>Dendroaspis polylepis</i>	elapidae	Eastern Africa
<i>Naja heje</i>	elapidae	North Africa
<i>Nochetis scutatus</i>	elapidae	Australia

2.2 Purification of venom constituents

Venom was initially separated by being subjected to one round of gel filtration and then further purification on ion exchange. The quantity of venom purified was dependent on supply and is individually listed within chapter 3. For the gel filtration, Superdex 200 prep grade matrix (Sigma, UK) was packed into a HiLoad® 26/60 column (GE Healthcare, Sweden) according to the manufacturer's instructions to give a bed volume of 400 ml. The buffer used was 50 mM sodium acetate containing 20 mM sodium chloride (NaCl) at pH 4.3 (Buffer A), NaCl was included to inhibit electrostatic interaction between the venom and the matrix. The venom was resuspended in 2.5 ml of degassed buffer A and subjected to 10 mins centrifugation at 10,000 G on a bench top centrifuge (Eppendorf, UK) to remove any insoluble particulates, loaded onto the column via a manual injection loop and 1.5 column volumes (CV) of Buffer A was passed through the column at a flow rate of 0.5 ml/min. Protein concentration was monitored at 280 nm and 3 ml fractions were collected. Fractions were pooled, tested for their antimicrobial activity and the pooled fraction concentration determined at 280 nm on a Nanodrop ND-1000 (Thermo scientific, UK). Active fractions were then subjected to ion exchange.

A HiLoad® 16/20 column was packed with SP sepharose high performance matrix according to the manufacturer's instructions. The column was equilibrated with buffer A and then the active fraction loaded, 5 CV of buffer A was then passed through to wash out any unbound protein. The column was then subjected to a gradient of 0-100% B over 20 CV (buffer B-50 mM sodium acetate containing 1M NaCl at pH 4.3) at a flow rate of 0.5 ml/min, with protein concentration measured at 280 nm, 3 ml fractions were collected and individual peaks pooled. The antimicrobial activity of each fraction was determined.

2.2.1 Peptide synthesis

Smp13, Smp24, Smp24GVG, Smp24T, Smp43 & Pin2 were synthesised by ProImmune, Oxford, UK.

Table 2.2 Peptides used within the study.

Peptide name	Sequence	Charge	% Hydrophobicity
<i>Smp13</i>	ILQDIWNGIKNLF-NH ₂	0	53
<i>Smp24</i>	IWSFLIKAAATKLLPSLFGGGKKD	+3	47
<i>Smp24GVG</i>	IWSFLIKAAATKLLGVGSLFGGGKKD	+3	48
<i>Smp24T</i>	IWSFLIKAAATKLLPSLFGG	+2	57
<i>Smp43</i>	GVWDWIKKTAGKIWNSEPVKALKSQALNAAKNFVAEKIGATPS	+4	44
<i>Pin 2</i>	FWGALAKGALKLIPSLFSSFSKDD	+3	50

2.2.2 MALDI-TOF analysis

MALDI-TOF spectrometry profiling was carried out on a Voyager-DE STR (Applied Biosystems, UK) in positive linear mode equipped with a 355 nm NDYAG solid state laser operated at 60 Hz. The analysis of samples was performed using a variable mass range depending on sample and a total of 400 shots were acquired per spectrum with a delay of 750 ns and a grid of 93%. Calibration of the instrument was performed using ion signals from a peptide/protein mixture (5000–17,000 Da), consisting of Insulin, Cytochrome C, Apomyoglobin and Human haemoglobin. Alpha cyno-4-hydroxycinnamic acid (CHCA) was used as the proton donor matrix. CHCA was dissolved at 10mg/ml in a 70:30 ethanol/acetonitrile solution and mixed with equal concentrations of sample (3 µl). These samples were then spotted (0.5 µl) on fresh aluminium sheets recently cleaned with acetone and allowed to dry before being attached to the target plate using double sided conductive carbon tape (TAAB, Berkshire UK) which prevented cross contamination from previous samples.

2.3 Biological Characterisation

2.3.1 Antimicrobial assay

The following microbes were used throughout this study and are listed below:

Escherichia coli JM109, *Pseudomonas aeruginosa* NCIMB 8295, *Bacillus subtilis* NCIMB 8024, *Staphylococcus aureus* SH1000, *Klebsiella pneumoniae* NCTC 13439, *Staphylococcus epidermidis* ATCC12228 & *Candida albicans* ATCC10231

Antibiotic resistant strains of *S. aureus* used were as follows: methicillin-resistant *S. aureus* (MRSA) ATCC 33591, epidemic methicillin-resistant *S. aureus* (EMRSA) 15 and EMRSA-16, clinical isolate MRSA *mecA mupA* positive, along with the

vancomycin intermediate resistant *S. aureus* (VISA) Mu50, VISA 1235 and VISA 1697. All clinical isolates were from K.miller (SHU) personal collection.

All antimicrobial assays were carried out by the microplate dilution method described by Andrews. (2001) and performed on a Tecan CENios Plus (Tecan, ,Switzerland) Synthetic AMPs were examined at a concentration range of 0-512 µg/ml whilst purified snake venom compounds were assayed, in the first instance at 50, 25 and 12.5 µg/ml. All samples were tested in duplicate on two separate occasions.

2.3.2 Haemolysis assay

Haemolytic activity was determined on sheep erythrocytes as described by Corzo *et al.*, (2001). Synthetic AMPs were examined at a concentration range of 0-512µg/ml whilst purified snake venom compounds were assayed at 50, 25 and 12.5 µg/ml. Haemolysis was determined on a Tecan Infinite M200 (Tecan, Switzerland) at 570nm. 10% Triton X was used as a positive control with deionised water used as negative control. All samples were tested in triplicate.

2.3.3 Cytotoxicity assay

An ATP release assay (Sigma, UK) was used to determine the cytotoxic potential of peptides against HepG2 liver cells in accordance with the manufacturer's protocol. The HepG2 cells were grown in Dulbecco modified Eagle's minimal essential medium (DMEM) glutamate max medium contain 1 g/l D-glucose, 10% foetal calf serum (Batch processed) and pen-step. Cells were grown at 37°C with 5% carbon dioxide until 80% confluence was reached. Cells were then trypsinised, washed in 1 x phosphate buffered saline (PBS) and resuspended at the desired concentration to be plated to a final density of 110,000 cells/well. Cells were incubated for 24 hrs (hours), washed with PBS and then peptide samples were added and incubated for 15 mins. Synthetic peptides were

incubated at a concentration of 0.5-512 $\mu\text{g/ml}$ whilst purified snake peptides were incubated at 50, 25 and 12.5 $\mu\text{g/ml}$ for 1 hr. All assays were performed in triplicate. 10% Triton X was used as a positive control and deionised water used as a negative control. Luminescence was determined on a Wallac Victor2 1420 multi-label counter (Perkin Elmer, Llantrisant, UK).

2.3.4 Membrane integrity assay (BacLight)

Bacterial membrane integrity following antimicrobial peptide attack was determined by the BacLight method described below and adapted from Hillard *et al.* (1999). Bacterial membrane integrity was determined for both Gram positive (*S. aureus* SH100) and Gram negative (*E. coli* JM109) organisms using the live/dead BacLight kit (Invitrogen UK). Overnight cultures were diluted with Muller-Hinton broth to an optical density of between 0.5-0.6 at 600 nm, 500 μl of culture was pelleted at 10,000 G for 15 mins for each sample to be tested and subsequently washed with PBS. The pellet was resuspended in 475 μl of deionised water and 25 μl of peptide added at 4x MIC (for the snake purified fractions 50 $\mu\text{g/ml}$ was used) and incubated at room temperature for 10 mins on a rocking platform. Each sample was then centrifuged at 10,000 G for 10 mins and resuspended in 500 μl of deionised water. The optical density was adjusted to 0.5 OD_{600} before 1.2 μl of BacLight reagent was added according to the manufactures instructions and incubated for 15 mins in the dark at room temperature. Fluorescence was measured at both 645 nm and 530 nm to determine both intact (green) and damaged (red) cells respectively. The excitation wavelength was 485 nm for both. 100% loss of membrane integrity was determined by the addition of 10% triton X whilst deionised water was added as a negative control. All samples were performed in triplicate.

2.3.5 Intracellular bio-reporter gene assay

To determine if any of the peptides had intracellular targets a *B. subtilis* reporter gene assay was performed as described by Urban et al. (2007). In the study, a set of five *B. subtilis* promoters were fused to the firefly luciferase reporter gene, enabling a comprehensive high-throughput detection system of antibiotic interference in the major biosynthetic pathways of bacteria: the biosynthesis of DNA by the *yorB* promoter, of RNA by the *yvgS* promoter, of proteins by the *yheI* promoter, of the cell wall by the *ypuA* promoter were all used which had previously been identified by microarray to be consistently overexpressed when cells were under attack antibiotic agents known to target these pathways. These reporters were validated using 14,000 pure natural products, representing a source of highly diverse chemical entities, many of them with antibiotic activity (6% with anti-*B. subtilis* activity of $\leq 25 \mu\text{g/ml}$). In the assay all samples were exposed to 50% the MIC (Smp24 2 $\mu\text{g/ml}$, Smp24GVG 4 $\mu\text{g/ml}$, Smp24T 4 $\mu\text{g/ml}$, Smp43 4 $\mu\text{g/ml}$, Pin 2 4 $\mu\text{g/ml}$) of each peptide in triplicate and with luminescence determined on a Wallac Victor2 1420 multi-label counter (Perkin Elmer, Llantrisant, UK) using the luciferin/luciferase assay according to the manufacturer's instructions (Promega, UK). Responses were determined by calculating the % increase from the negative control.

2.4 Biophysical determination of mechanism of action

2.4.1 Lipids used within study

All lipids used in the study were purchased from Sigma (UK) and are listed in table 2.4 along with their charge state, propensity to cause curvature and lipid packing.

Table 2.3: Lipids used within this study

Lipid name	Charge state (pH 7)	Notes
1,2-Dioleoyl- <i>sn</i> -glycero-3-phosphocholine (DOPC)	Neutral	
1,2-Dioleoyl- <i>sn</i> -glycero-3-phospho- <i>rac</i> -(1-glycerol) (DOPG)	Negatively charged	
1,2-Dioleoyl- <i>sn</i> -glycero-3-phosphoethanolamine (DOPE)	Neutral	Induces negative curvature
Cholesterol	Negatively charge hydroxyl (OH) group that interacts with the aqueous phase	Induces lipid packing and membrane thickening
Cardiolipin	Negatively charged	Commonly found with bacterial membranes
Sphingomyelin	Neutral	Induces the presence of lipid rafts due to its higher melting point compared with other lipids

2.4.2 Bilayer preparation

Supported lipid bilayers were produced by vesicle rupture (Heath *et al.*, 2013). Briefly, lipids were resuspended in chloroform, mixed and dried under nitrogen. The lipids were then resuspended in milli Q-Water (Millipore, Billerica, MA) to a final concentration of 0.2mg/ml and tip sonicated for 10 mins.

2.4.3 AFM imaging of hydrated lipid bilayers

Supported planer lipid bilayers were produced on a freshly cleaved mica surface by vesicle rupture. 200 μ l of vesicles were placed onto the mica surface and incubated in the presence of 2 mM magnesium chloride for 15 mins at room temperature; after which 8 washes with 100 μ l of milli Q were performed to remove unruptured vesicles. The presence of a uniform bilayer was confirmed by lateral scanning in tapping mode over a 8 μ m² area and the presence of multiple bilayers was ruled out by a statistically significant (nine) number of force spectroscopy curves.

Observations of the attack of Smp42 were performed using either a Nanoscope IIIa Multimode atomic force microscope (Digital instruments Santa Barbara CA) or a Zeiss Axiovert 100 M (Zeiss MicroImaging GmbH, Germany). To observe the membrane disruptive mechanism of Smp43 a Dimension FastScan® Bio™ (Bruker, UK) was used. For all experiments oxide sharpened silicon nitride tips with a typical spring constant of 0.32 N m⁻¹ were used.

2.4.4 QCM-D protocol

Silicon dioxide sensor crystals (5 MHz) were used for the QCM-D experiments (Q-Sense AB, Gothenburg, Sweden). QCM-D sensor crystals were cleaned by sonication for 15 mins in 0.4% (w/v) SDS followed by thorough rinsing in ultrapure water, before

a further 15 mins sonication and thorough rinsing in ultrapure water and finally dried under oxygen free nitrogen. The substrates were then further treated for 30 mins with UV/ozone (UV/ozone cleaning system, low pressure quartz mercury vapour lamp emitting 254 and 185 nm UV, UVOCS, Montgomeryville) followed by rinsing in ultrapure water and dried under oxygen free nitrogen. QCM-D experiments were performed on the Q-Sense E4 (Q-Sense AB, Gothenburg Sweden). Experiments were performed using silicon dioxide sensor crystals (Q Sense AB, Gothenburg, Sweden) at 22 °C. Changes in the dissipation, D , and normalised frequency, f , ($f = f_n/n$ where n is the number of the overtone, i.e. $n = 3, 5, 7$ etc.) of the 5th overtone ($n = 5, 25$ MHz) are presented in this work. Vesicles and buffer used were degassed under vacuum and incubated at the appropriate temperature in a block heater (Grant Instruments, Cambridge) before being introduced to the system. Bilayer formation occurred as follows. Initially milli-Q water was injected into the system at 40 $\mu\text{L}/\text{min}$ to determine the resonant frequencies of the overtone after which the vesicle solution was injected at the same flow rate at a concentration of 0.2 mg/ml. Both frequency and dissipation were monitored until vesicle absorption and rupture occurred and a planar lipid bilayer formed. After the dissipation reading had stabilised the bilayer was rinsed to remove excess vesicles. Successive peptide concentrations were then injected at a flow rate of 50 $\mu\text{L}/\text{min}$ with changes in dissipation and normalised frequency being monitored for a period of 20 mins before the next injection. Changes in the dissipation, D , and normalised frequency, f , ($f = f_n/n$ where n is the number of the overtone, i.e. $n = 3, 5, 7$ etc.) of the 5th overtone ($n = 5, 25$ MHz) are presented in this work.

2.4.5 Liposome leakage assay

Liposomes for leakage assays were made differently from those of AFM and QCM-D with the lipid extruder method employed modified from Xue *et al.*, (2009). Differences in lipid preparation were due to the need for a uniform intact liposome preparation in this assay compared with the eventual rupture and bilayer formation observed in AFM and QCM-D.

Liposome compositions were mixed and dissolved in chloroform and the solvent evaporated under a stream of nitrogen gas. The lipids were resuspended in 1 ml of carboxyfluorescein (CF) Buffer (50 mM sodium phosphate, 10mM NaCl and 1 mM of ethylenediaminetetraacetic acid (EDTA) pH 7.4) saturated with CF and then sonicated for 60 mins in a sonicating bath. The lipid preparation subsequently underwent 5 rounds of freeze thawing using liquid nitrogen after which the preparation was extruded using an Avanti lipid extruder (Avanti lipids, USA) with a membrane containing a 100 nm molecular cut off. Unencapsulated CF was removed by 3 centrifugation washes using a Beckman TLA-120.2 Rotor on the Beckman Optima TLX (Beckman, UK) at 100,000 rpm for 30 mins. The liposomes were then resuspended in 1 mL of CF liposome buffer and stored at 4°C in the dark overnight for the liposome dye release assay. The liposome dye release assay was then performed as follows: 20 µL of sample, 10 µL of liposomes and 170 µL of CF liposome buffer were inoculated into wells of a black 96 well plate to give the final volume of 200 µL. The well contents were mixed during plate inoculation and incubated in the dark for 15-25 min. CF fluorescence was measured on the Tecan infinite M200 plate reader (Tecan, Switzerland). Fluorescence excitation was optimised to 480 nm and emission was optimised at 520 nm. Blank CF liposome buffer and 10 µL of liposomes were used as a negative control to normalise results. 10% Triton-X was used as a positive control to measure complete dye release.

The rate of CF leakage is expressed as a percentage dye release of the total encapsulated carboxyfluorescein and then normalised against the blank buffer signal. All samples were run in triplicate.

**IDENTIFICATION AND CHARACTERISATION OF
ANTIMICROBIAL PEPTIDES FROM SNAKE VENOMS**

3.1 Background and Aims

A number of antimicrobial peptides have previously been identified in snake venoms. However, this rich source of bioactive compounds is relatively unexplored compared with other venoms and other natural product reservoirs (de Oliveria *et al.*, 2013). Whilst a number of other proteins have been identified as having antimicrobial activity within snake venom such as phospholipase A2 (PLA2), L-amino oxidase and C-type lectins (Radis-Baptista *et al.*, 2006, Samy *et al.*, 2011), only a small number of venoms have been examined, therefore, exploring a wider range of venoms to isolate their antimicrobial components and characterise them biologically as well as determining their mechanism of action by determining their membrane destructive effects is attractive. This chapter examines a number of different venoms of elapid and viper origin and examines their potential as antimicrobial compounds in terms of antimicrobial activity and cytotoxic effects. Their membrane damaging effects are also assessed to determine a possible mechanism of action. The chapter then moves on to assess possible future steps to be taken to create clinically relevant antimicrobial compounds from these peptides and suggests how a generalised strategy could be applied to structurally divergent snake peptides that could dramatically increase the prospects of developing antimicrobial peptides from this rich source of bio active peptides.

3.2 Method Summary

Snake venoms were purified as described in 2.1.1. Fractions were pooled into individual peaks, the protein concentration and antimicrobial activity determined against Gram positive (*S. aureus* SH1000) and Gram negative (*E. coli* JM109) bacteria. Active fractions were further purified, peaks pooled and the protein concentration and antimicrobial activity re-examined. Individual active peaks were characterised via

MALDI-TOF mass spectrometry to determine size and purity. Once activity and purity had been determined antimicrobial activity, haemolytic and cytotoxic potential was determined at 50, 25 & 12.5 $\mu\text{g/ml}$. The effect of purified proteins on bacterial cell membrane integrity was also examined at 50 $\mu\text{g/ml}$ (if bacteria were susceptible).

3.3 Results

Purified venom proteins are listed in Table 3.1 along with their molecular weights as determined by MALDI-TOF mass spectrometry, their antimicrobial activities and membrane damaging effects determined by the Baclight assay.

Table 3.1: Molecular weight, antimicrobial activity and membrane damaging effect against *E.coli* and *S.aureus* of all the peptides isolated in this study

Peptide venom origin	Molecular weight	MIC against <i>E.coli</i> ($\mu\text{g/ml}$)	MIC against <i>S.aureus</i> ($\mu\text{g/ml}$)	Membrane damage <i>E.coli</i> (%)	Membrane damage <i>S.aureus</i> (%)
<i>Bitis arietans</i>	13450	25.0	25.0	102.4 (± 7.7)	101.3 (± 4.9)
<i>Cerastes cerastes</i>	13827/18354	25.0	25.0	98.2 (± 6.2)	91.3 (± 1.6)
<i>Crotalus adamanteus</i>	13673	25.0	50.0 (Partial)	79.9 (± 1.6)	104.5 (± 4.2)
<i>Dendroaspis polylepis</i>	6600	50.0	Not Susceptible	73.5 (± 4.2)	Not susceptible
<i>Naja haje</i>	13807	25.0	Not Susceptible	96.3 (± 5.6)	Not susceptible
<i>Notechis scutatus</i>	6943	25.0	25.0	106.6 (± 0.77)	103.0 (± 2.9)

3.3.1 Isolation and characterisation of an antimicrobial component of *Bitis arietans* venom

Figure 3.1 (a & b) detail the purification of 50 mg of *Bitis arietans* (puff adder) venom, the active fraction was eluted mid way through the run on a Superdex 200 gel filtration column suggesting that the protein was above 10 KDa, roughly 30% of the total protein concentration loaded onto the column was eluted in this fraction (14.28 mg). Further purification using cation exchange yielded 8 peaks with the major peak having activity (peak 4) eluted after 25% of the salt gradient suggesting a basic protein it also represented a major protein within the venom accounting for 13% (6.59 mg) of total protein. Mass analysis was undertaken by MALDI-TOF and is seen in figure 3.1c. There is a major peak at 6889.31 with a smaller peak at 13451.07 with a repeating pattern of peaks decreasing in size. As there is no peak below 6889.31 it would suggest that this is the fragment carrying a double charge therefore the peak at 13451.07 is the actual protein (calculated mass of 13450). Based on its molecular weight it is most likely a phospholipase A2 (PLA2) protein. The repeat pattern can be explained by calculating the ratios of the possible aggregates with the peak at 20218.87 being the double ion of the trimer (ratio of 1.990), the peaks at 33520.07 and 47130.24 can be assigned as the double charged ions of the quintuplet and septuplet aggregates. In biological assays it had broad spectrum antimicrobial activity with full inhibition of both *E. coli* and *S. aureus* at 25 µg/ml and partial activity seen at 12.5 µg/ml. In cytotoxicity assays 89.3% (± 4.9), 49.6% (± 1.7) and 7.9% (± 2.0) haemolysis (figure 3.2a) was observed with the decreasing concentrations. 71.6% (± 6.7) cell damage against was seen HepG2 cells at 50 µg/ml with 28.7% (± 4.1) and 9.4% (± 0.2) damage detected at the lower concentrations (Fig. 3.3a) As would be expected from such a potent broad spectrum peptide, maximum membrane damage was detected in the

backlight assay against both organisms with readings over 100% obtained in both cases (Table 3.1). The readings over 100% may be done to slight optical discrepancies between the two dyes with propidium iodide being more prominent (Invitrogen BacLight data sheet. 214).

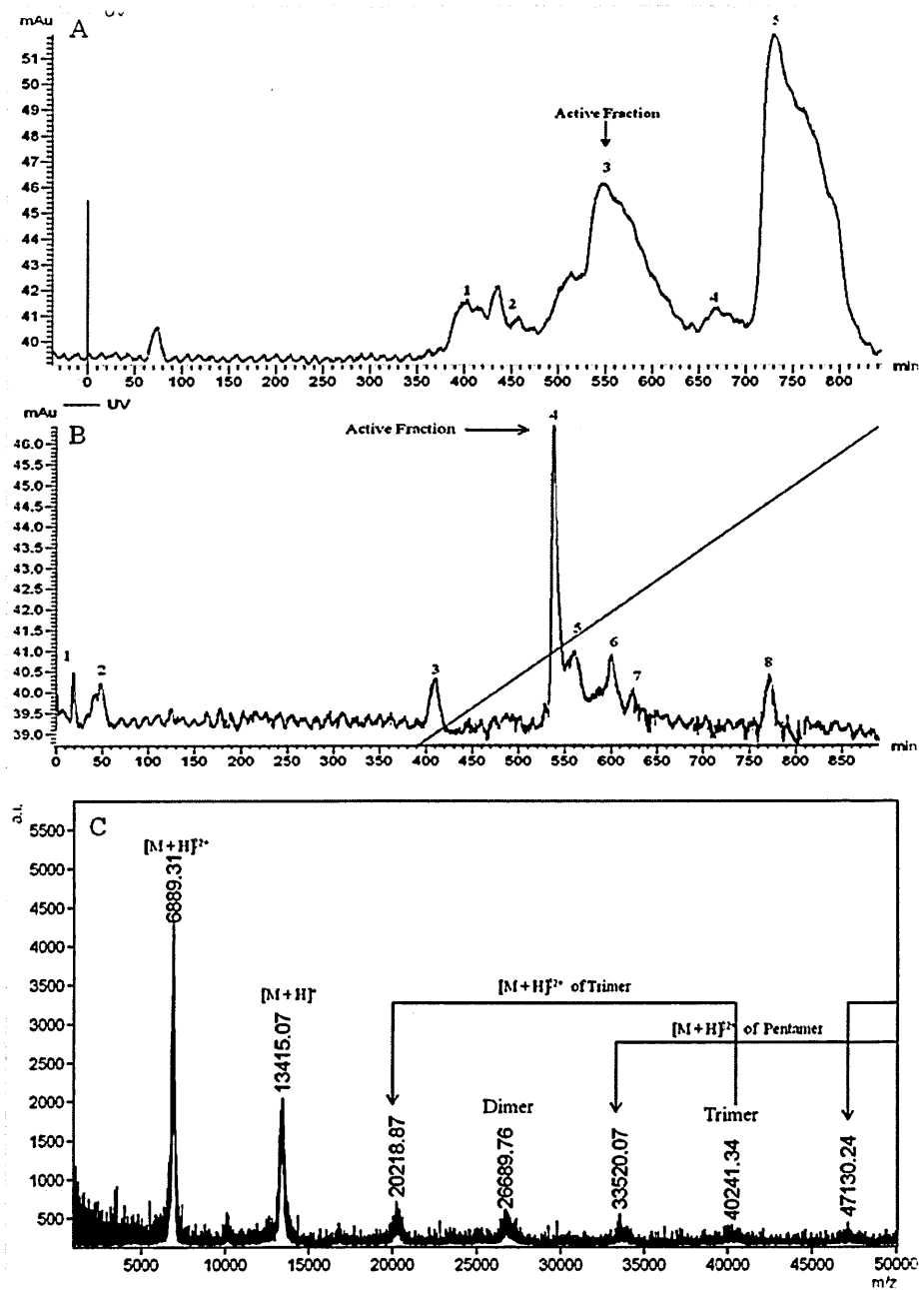


Figure 3.1: Isolation and characterisation of a potential PLA2 antimicrobial protein from *Bitis arietans* venom (A) Superdex 200 profile with active fraction eluted after 550 ml (B) SP ion exchange of fraction 3 from GF, elution occurred at the beginning of the salt gradient reflective of a weak cationic nature. (C) MALDI-TOF analysis revealed a peak at 13415.07 with a number of oligomeric structures detected

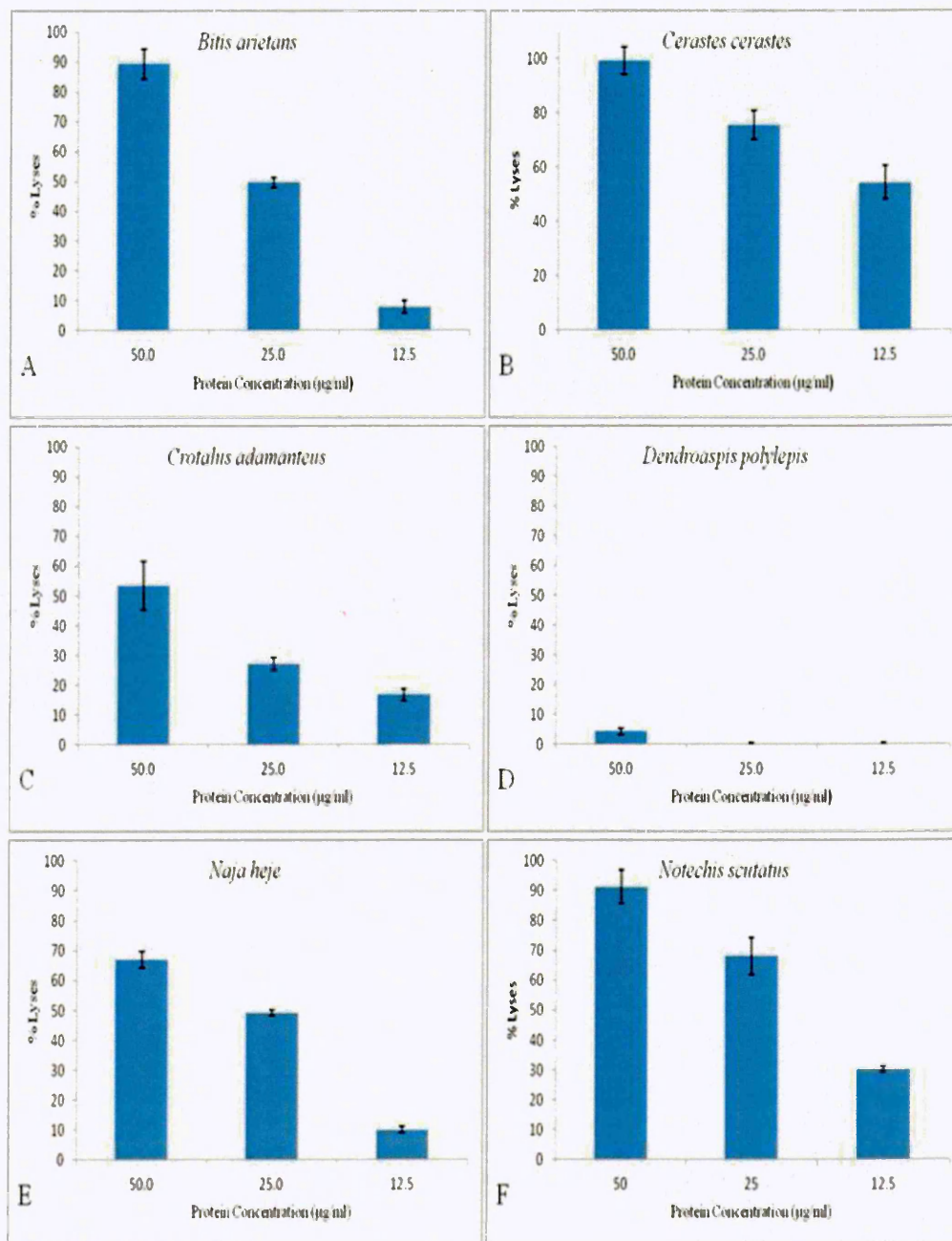


Figure 3.2: Haemolytic effects of antimicrobial snake proteins against sheep erythrocytes. The peptide isolated from *Dendroaspis polylepis* (D) exhibited very low haemolytic activity even at the highest concentration of 50 µg/ml

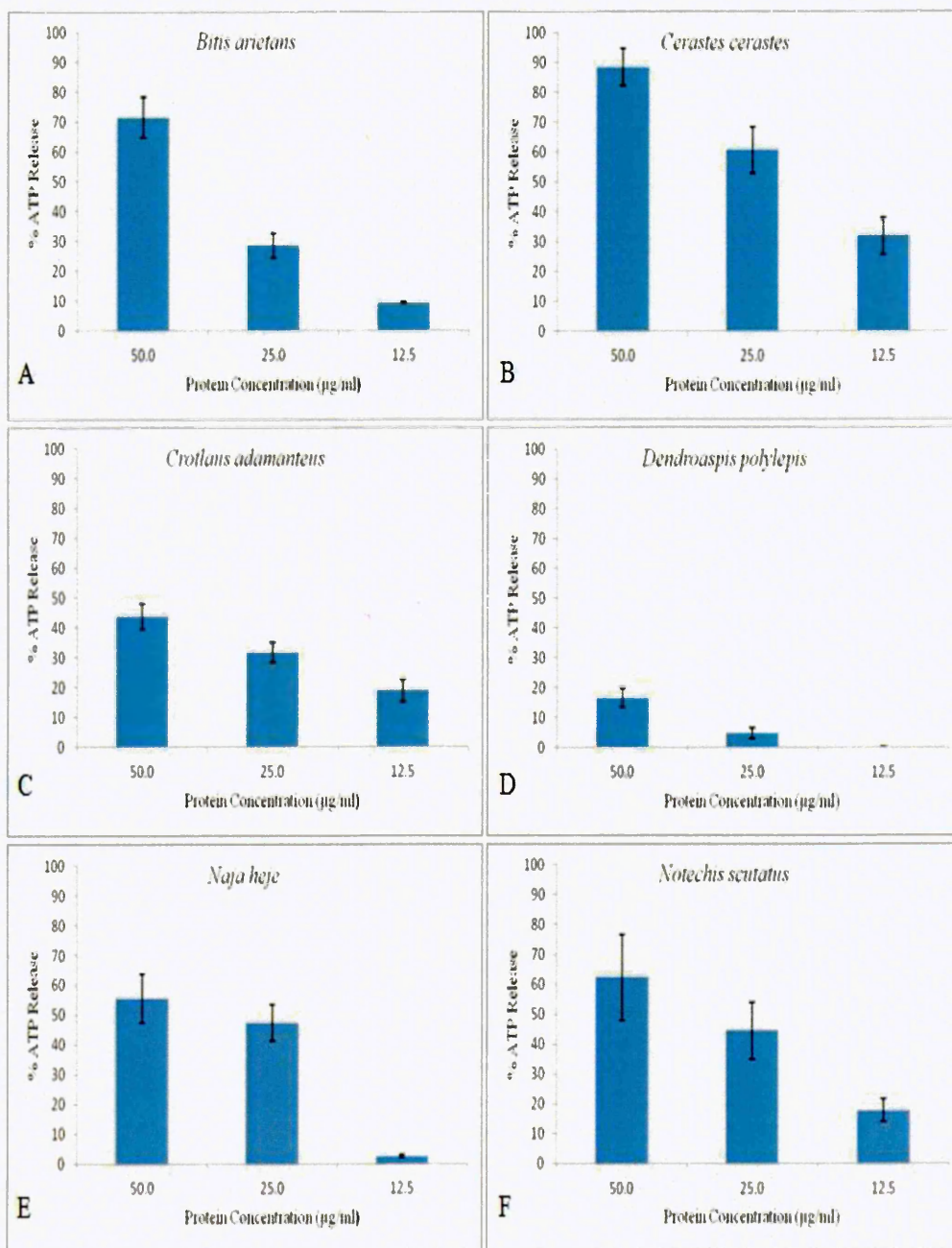


Figure 3.3: Membrane damaging effects of snake proteins against the eukaryotic cell line HepG2 determined by release of ATP. The peptide isolated from *Dendroaspis polylepis* (D) exhibited low toxicity against this cell line even at the highest concentration of 50 µg/ml.

3.3.2 Isolation and characterisation of an antimicrobial component of *Crotalus adamanteus* venom

A second potential PLA₂ has been purified from *Crotalus adamanteus* (Eastern diamondback rattlesnake) (Fig. 3.4a-c) 120 mg of venom was applied to the gel filtration column (Fig. 3.4a) with the active fraction been in relatively small abundance compared with the other peaks representing 9.24 mg of total protein content. The active fraction from the ion exchange column (Fig. 3.4b) shows a resolved peak with baseline resolution; it is also seen that the protein carries either a neutral or acidic charge as it is eluted within the wash on a cationic column with 860 µg being obtained. MALDI-TOF analysis (Fig. 3.4c) revealed the presence of only two peaks, a major peak at 13674.51 and a smaller peak at 6645.03. No peak approximately half that of 6645.03 is observed therefore the major peak can be assigned a mass to charge ratio (m/z) of +1 whilst the minor peak has an m/z of +2 thus the protein has a calculated mass of 13673.51. This minor peak is not exactly half the mass of the major one however the machine of analysis (Voegyler DSTR) has a mass accuracy of between 0.2-0.3 percent therefore this slight discrepancy can be accounted for. In antimicrobial activity full inhibition was seen at 25 µg/ml against *S. aureus* with partial activity is seen at 12.5 µg/ml, in contrast against *E. coli* only partial activity at 50 µg/ml is observed (Table 3.1). In cytotoxicity assays the protein showed moderate toxicity with 53.4% (\pm 8.2) haemolysis at 50 µg/ml with 27.2 (\pm 2.1) and 16.7% (\pm 1.9) lyses seen at the lower concentrations of 25 and 12.5 µg/ml respectively (Fig. 3.2c) whilst against HepG2 cells 43.8% (\pm 4.2) ATP release was observed at 50 µg/ml with 31.7 (\pm 3.4) an 19.0% (\pm 3.8) cell damage seen at 25 and 12.5 µg/ml (Fig. 3.3c). The membrane disruptive nature of the protein was also determined with maximum membrane damage observed against *S. aureus* (readings over 100% determined as maximum) in the backlight assay whilst against *E. coli* only

79.9% (± 1.6) cell damage was observed however at this concentration only partial inhibition was detected (Table 3.1).

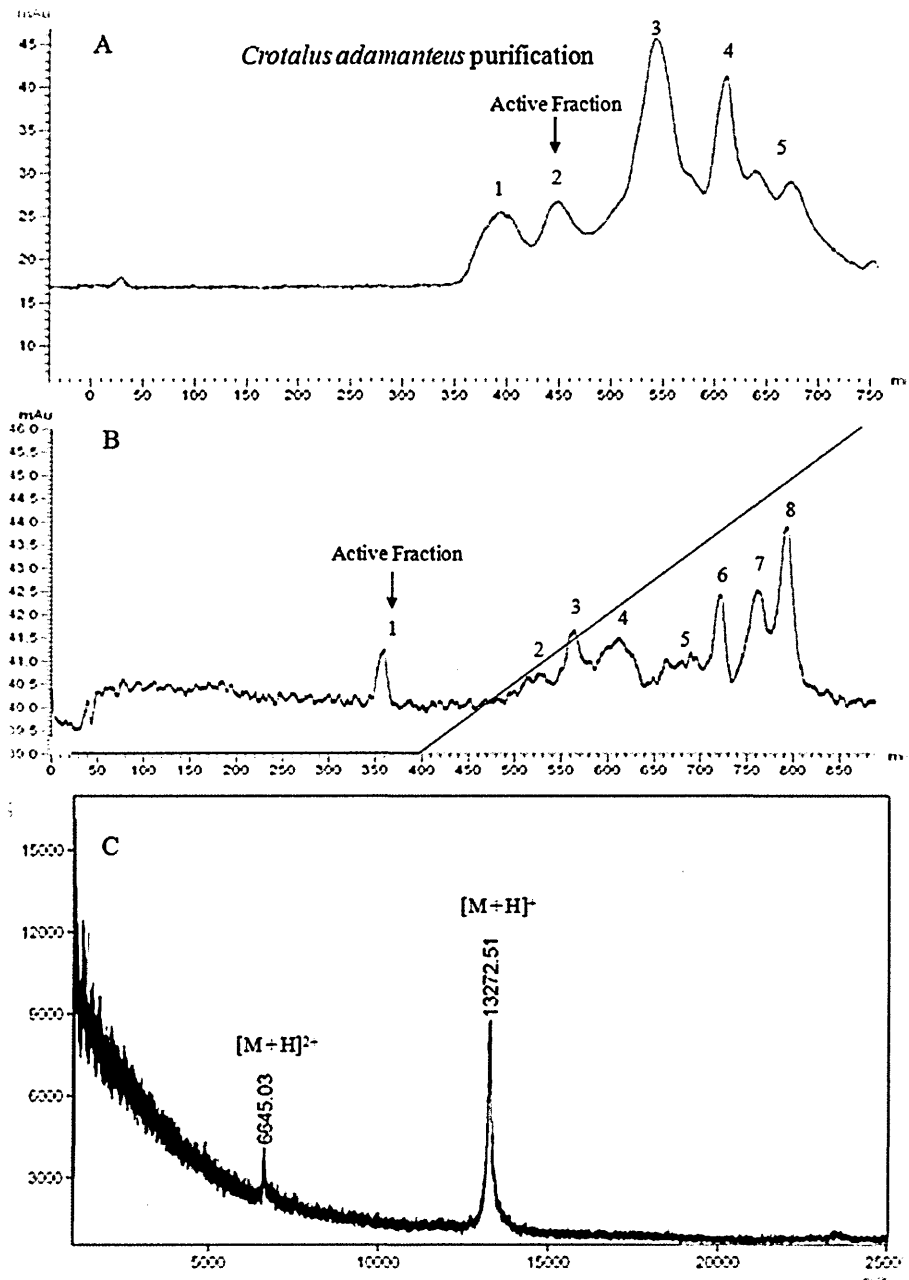


Figure 3.4: Purification of a potential PLA2 protein from *Crotalus adamanteus* venom (A) Superdex 200 profile with active fraction eluted early in the run (B) SP ion exchange of fraction 2 from GF, elution occurred before NaCl gradient reflecting the neutral/acidic nature of the protein. (C) MALDI-TOF analysis revealed a peak at 13272.51

3.3.3 Isolation and characterisation of an antimicrobial component of *Naja haje* venom

A third potential PLA2 antimicrobial protein has been isolated from the venom of the elapid *Naja haje* (Egyptian cobra). 50 mg of venom was applied to the gel filtration column and as can be seen (Fig.3.5a) the majority of the venom did not show any activity with fraction 3 (2.8 mg) showing activity. When applied to an ion exchange column, unlike the *C. adamanteus* potential PLA2, elution was not observed until the middle of the salt gradient reflecting the basic nature of the protein (Fig. 3.5b). As with the *C. adamanteus* protein it is of low abundance within the venom with the final ion exchange peak having a concentration of 212 µg. MALDI-TOF analysis revealed a minor peak at 13808.32 Da with the major peak at 6891.24 with no peak observed at half this value, therefore 6891.24 has been assigned an m/z of 2 leaving the minor peak with an m/z of 1, thus the protein had a calculated mass of 13807.32 (Fig. 3.5c). Again these figures are within the boundaries of mass accuracy. Interestingly no antimicrobial activity is observed against *S. aureus* at the highest concentration of 50 µg/ml however against *E. coli* full inhibition is seen at 25 µg/ml with only partial inhibition detectable at 12.5 µg/ml. In cytotoxic assays 67.0% (± 2.8) haemolysis was observed at 50 µg/ml with 49.2% (± 1.0) and 10.0% (± 1.0) erythrocyte damage at the lower concentrations (fig. 3.2e). Against HepG2 cells 55.6% (± 8.1) cell damage was observed at 50 µg/ml whilst at 25 and 12.5 µg/ml 47.4% (± 6.0) and 2.6% (± 0.5) cell damage was seen respectively (Fig. 3.3e). BacLight analysis showed a membrane damaging effect against *E. coli* with 96.3% (±5.6) cell damage observed and due to lack of susceptibility *S. aureus* was not assayed (Table 3.1)

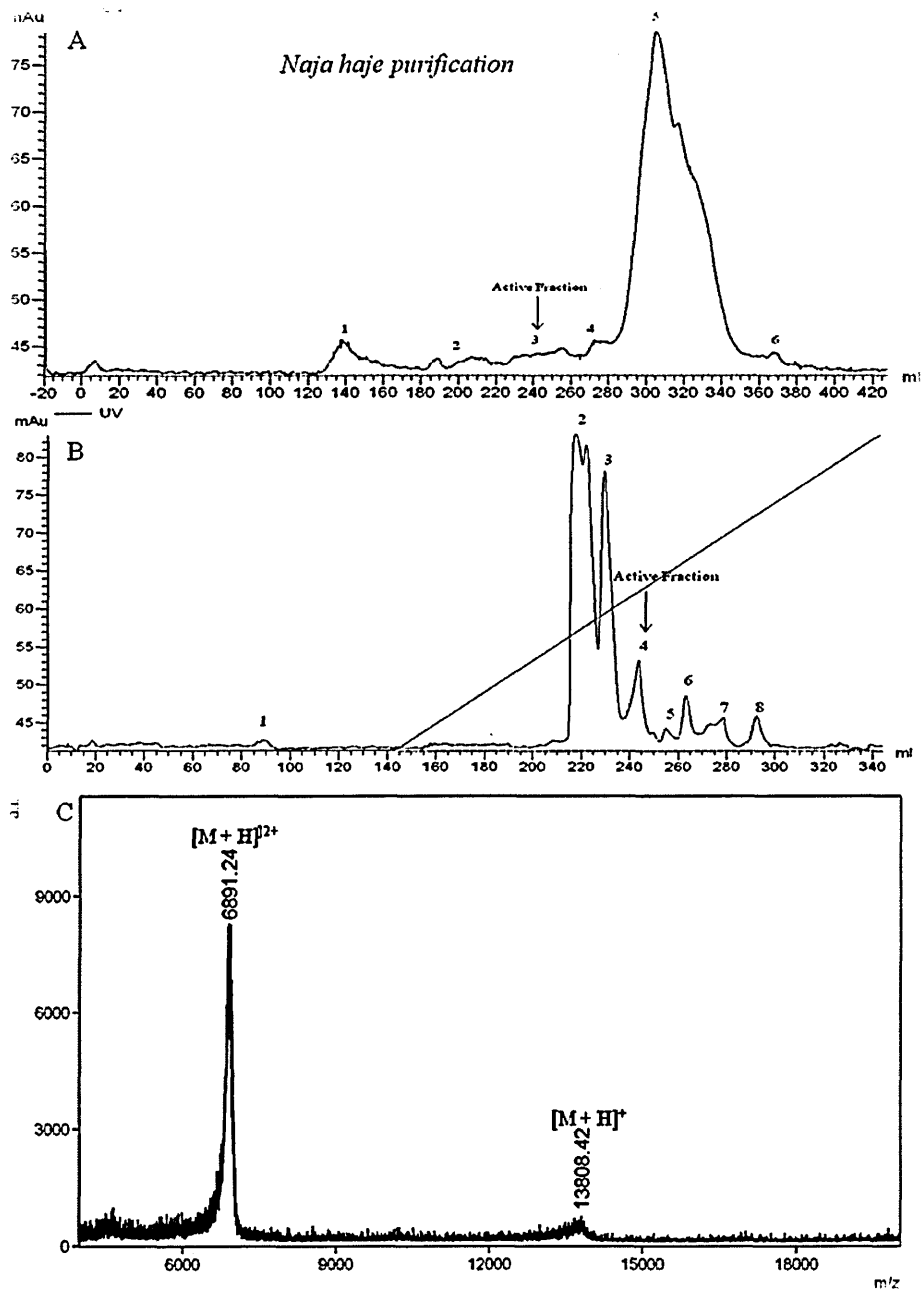


Figure 3.5: Purification of a possible PLA2 protein from *Naja haje* venom (A) Superdex 200 profile with active fraction eluted mid way through the run (B) SP ion exchange of fraction 3 from GF, elution occurred after approximately 500 mM of NaCl, reflecting the cationic nature of the protein. (C) MALDI-TOF analysis revealed a peak at 13808.41

3.3.4 Isolation and characterisation of an antimicrobial component of *Dendroaspis polylepis* venom

50 mg of the African elapid *Dendroaspis polylepis* (black mamba) was purified, the active gel filtration peak made up a small proportion of the total venom loaded containing only 2.7 mg (5.4%) (Fig.3.6a) and from the cation exchange a highly basic peptide has been identified that account for only 0.8% of the venom (407 μ g) (Fig. 3.6b). The peptide had a calculated mass of 6600 (Fig. 3.6c) with a number of peaks observed in the mass spectra which can be rationalised by calculating the dimer and trimer molecular masses and their expected m/z ratios. Biologically it is only active against *E.coli* with full activity at 50 μ g/ml and partial activity at both 25 and 12.5 μ g/ml with only 4.3% (\pm 1.1) haemolysis observed at 50 μ g/ml respectively (Fig. 3.2d). Against HepG2 cells, no damage was detected at 12.5 μ g/ml with only 3.2% (\pm 1.7) and 16.7% (\pm 3.2) damage at 25 and 50 μ g/ml (Fig.3.3d). In the membrane susceptibility assay only 73% (\pm 4.2) membrane damage was observed against *E. coli*, due to lack of susceptibility *S. aureus* was not tested (Table 3.1).

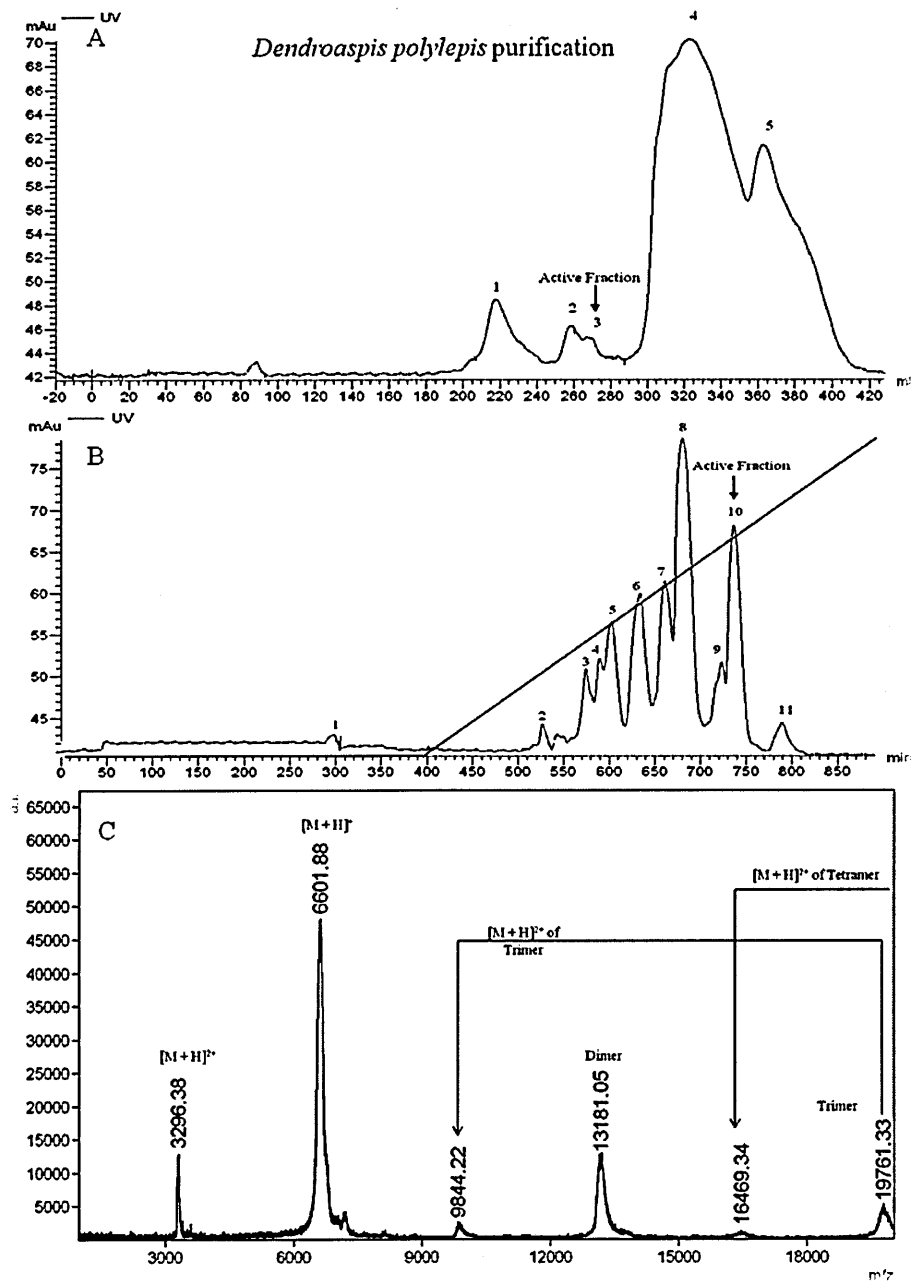


Figure 3.6: Isolation of an antimicrobial protein from *Dendroaspis polylepis* venom (A) Superdex 200 profile with active fraction eluted mid way through the run (B) SP ion exchange of fraction 2 from GF revealed a highly cationic protein. (C) MALDI-TOF analysis revealed a peak at 6601.88

3.3.5 Isolation and characterisation of an antimicrobial component of *Notechis scutatus* venom

The only Australian snake examined in this study was from *Notechis scutatus* (mainland tiger snake). The starting protein concentration was 50 mg with the active fraction after gel filtration accounting for 12.3 mg (24%) (Fig.3.7a). As is seen from figure 3.7b the active fraction is either acidic or negatively charged with no interaction observed during cation exchange and had a protein concentration of 5.1 mg, thus being a large proportion of the venom (10%). MALDI-TOF analysis (Fig.3.7c) revealed a peptide with a molecular weight of 6943. Biologically the peptide was fully active against *E. coli* and *S. aureus* at 25 µg/ml and showed partial activity at 12.5 µg/ml however it was also highly haemolytic with 91.2% (\pm 5.6) lyses at 50 µg/ml, at the lower concentrations 68.1% (\pm 6.2) and 30.2% (\pm 1.1) lyses was observed respectively (Fig.3.2f). Against HepG2 cells 62.4% (\pm 14.4) cell damage at 50 µg/ml, at 25 and 12.5 µg/ml 44.5% (\pm 9.6) and 17.7% (\pm 3.7) damage were observed was observed (Fig.3.3f). BacLight analysis revealed maximum membrane damage against both organisms (both readings above 100% therefore taken as maximum) (Table 3.1)

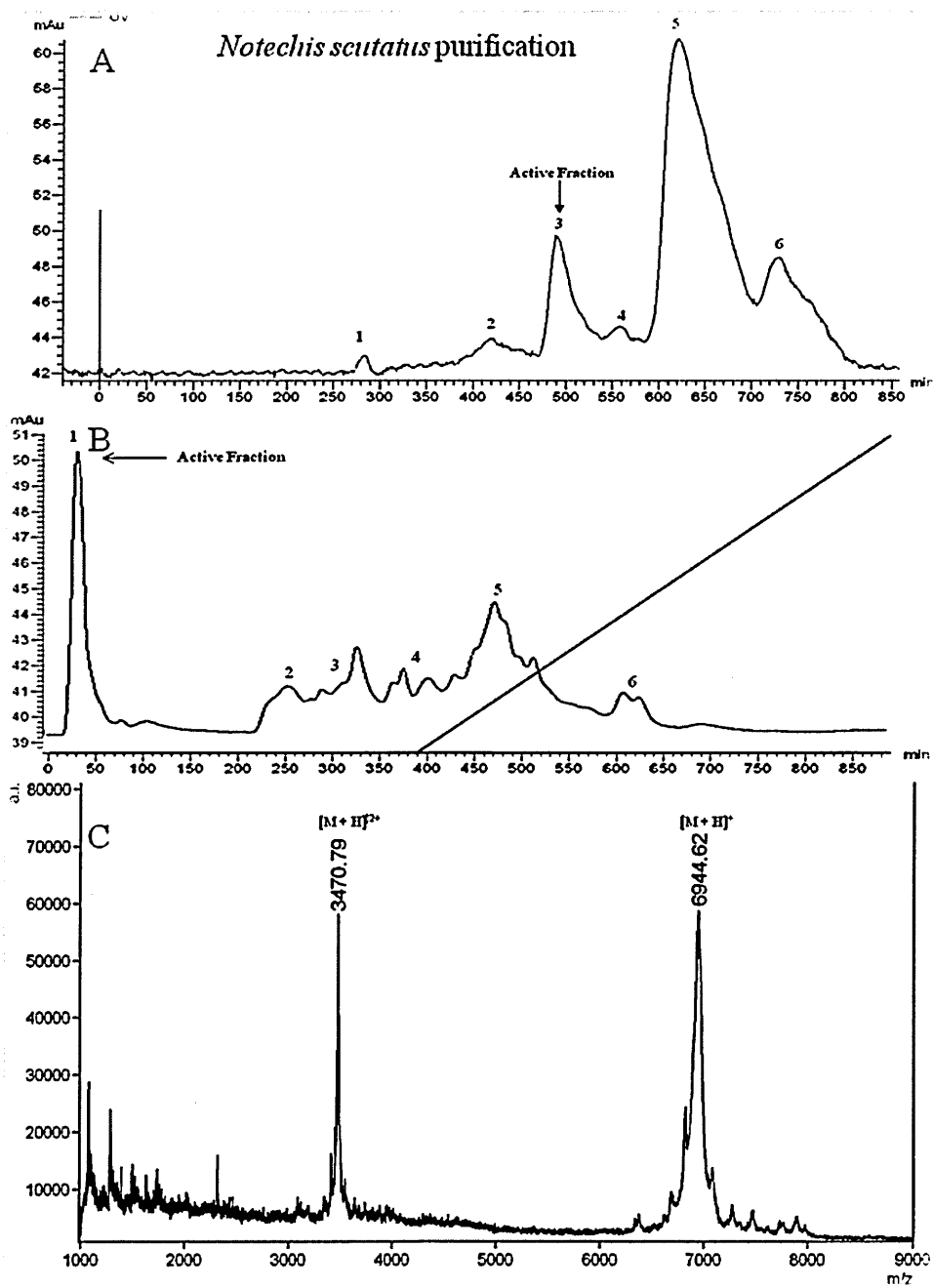


Figure 3.7: Purification of an AMP from *Notechis scutatus* venom (A) Superdex 200 profile with active fraction eluted mid way through the run (B) SP ion exchange of fraction 3 from GF, elution occurred before NaCl gradient reflecting the neutral/acidic nature of the protein. (C) MALDI-TOF analysis revealed a peak at 6944.62

3.3.6 Isolation and characterisation of an antimicrobial component of *Cerastes cerastes* venom

35 mg of the North African viper venom *Cerastes cerastes* (horned desert viper) was purified. The gel filtration active fraction contained 6.4 mg (18%) (Fig. 3.9a) subsequent ion exchange produced 9 peaks with peak 8 been active; its elution near the end of the salt gradient near the end of the salt gradient suggests a highly basic nature which only accounted for a small proportion of the total venom with 914 µg protein purified (2.6%) (Fig.3.9b). MALDI-TOF analysis determined that the peak was not pure with 2 proteins present, one at 13827 and the other at 18354 (Fig.3.9c). In antimicrobial testing it showed full activity against both *E. coli* and *S. aureus* at 25 µg/ml with partial activity observed at 12.5 µg/ml. However, 75.6% (± 5.4) haemolysis was observed at 25 µg/ml (99.2% (± 4.9) at 50 µg/ml and 54.3% (± 6.1) at 12.5 µg/ml) (Fig.3.2b). Against HepG2 cells 88.4% (± 6.3) damage was observed at 50 µg/ml with 60.7% (± 7.7) and 31.9% (± 6.2) observed at the lower concentrations (Fig. 3.3b). 98.2 (± 6.2) and 91.3% (± 1.6) bacterial membrane damage was also observed against *E. coli* and *S. aureus* respectively (Table 3.1). Because of its unfavourable biological profile and that both proteins present were of a significant size it was decided not to carry on purification.

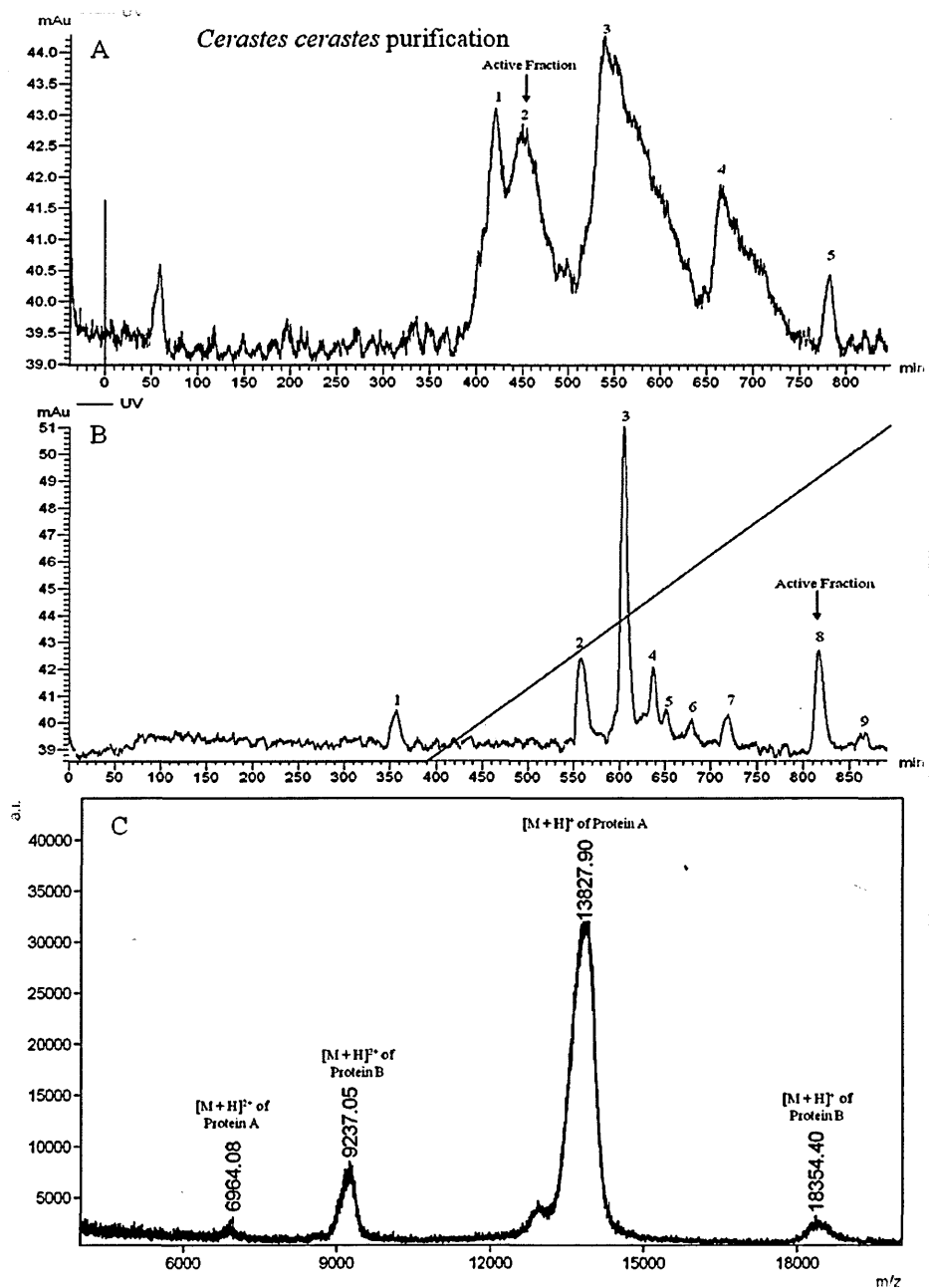


Figure 3.8: Isolation of a potential antimicrobial protein from *Cerastes cerastes* venom (A) Superdex 200 profile with active fraction being eluted mid way through the run (B) SP ion exchange of fraction 2 revealing a highly basic peak (C) MALDI-TOF analysis revealed two proteins because of their size and toxicity it was decided to end further purification

3.4 Discussion

Unlike most venomous creatures such as arthropods and other insects whose antimicrobial content is typically peptides between 1-5KDa, snake antimicrobial content is radically different. With the exceptions of the cathelicidin family detected by transcriptomic analysis of the elapids *B. fasciatus* (bandad krait), *N. atra* and *O. Hannah* (Zhao *et al.*, 2008) and more recently in the viper family (Falcao *et al.*, 2014) no peptide has been isolated below 5 KDa with antibacterial activity, although an anti-fungal peptide has been isolated from the viper *Bothrops jararaca* (Brazilian jararaca) (at 1.3KDa (Gomes *et al.*, 2005). Indeed, as the present study further highlights antimicrobial defence in snake venom is elicited mainly through larger proteins such as PLA2s or peptides above 5 KDa.

In the present study potential PLA2 proteins have been isolated from both viper (*Bitis arietans* (puff adder) & *Crotalus adamanteus* (Eastern diamondback rattlesnake)) and elapid venom (*Naja haje* (Indian cobra)).

Whilst the MALDI-TOF spectra for these proteins have been interpreted to be around 13,000 Daltons (and thus PLA2s) this is ambiguous with further experiments needed to be to determine if the proteins are the correct size and not dimers of smaller peptides. One such experiment to determine the presence of smaller monomeric peptide, dimeric structures or one larger protein would be to carry out an alternative MS technique such as electrospray ionisation (ESI) mass spectrometry which favours the production of multiply charged species allowing for greater structural elucidation. By analysing multiply charged species it would be possible to identify the molecular ion through mathematical deconvolution (Bhardwaj and Hanley 2014). Another experiment would be to incubate the protein with a strong denaturing agent such as 8M urea which would disrupt any inter-molecular bonding that may exist and determine if the protein is in fact

a dimeric structure which could be then be detected by MALDI-TOF as a single smaller or by changes in the band size on an native acrylamide gel.

There has been a significant number of similar size proteins characterised from snake venoms as PLA2s that exhibit antimicrobial activity, including recently from *C. adamanteus* itself (Samy *et al.*, 2014) which has a molecular mass of 13272 Da. Whilst there is a discrepancy between this figure and the MALDI-TOF analysis of the potential PLA2 in this study they both show preferential activity towards *S. aureus*, however the transcriptomic analysis of *C. adamanteus* venom revealed the presence of 7 PLA2 proteins which maintain a high degree of homology throughout them (Rokyta *et al.*, 2012) therefore it is possible that this could be an isoform with the addition of a few amino acids or a post translational modification.

B. arietans venom is a relatively unexplored although a PLA2 has recently been purified, however it has a molecular weight of 27.4 KDa, contains 14 cysteine residues and has been shown to block nicotinic acetylcholine receptors (nAChRs) with no antimicrobial activity described (Fulfius *et al.*, 2011). PLA2 proteins have been identified in other *Bitis* species of similar size to the protein purified in this study including from *Bitis gabonica* (Gaboon viper) at 13376 (Brottes *et al.*, 1986), *Bitis caudalis* (horned viper) at 13363 (Viljoen *et al.*, 1982) and *Bitis nasicornis* (Rhinceros viper) at 13665 (Joubert *et al.*, 1983). Therefore the isolation of a potential PLA2 of 13414 Daltons represents a novel addition to the *Bitis* PLA2 family and the first to be described to have antimicrobial activity.

Similarly the potential PLA2 from *N. haje* represents a new member of the *Naja* PLA2 family with no such protein isolated from that venom, although a PLA2 has been isolated from other another *Naja* species (*N. naja oxiana* (Caspian cobra)) that does have antimicrobial activity (Samel *et al.*, 2013).

PLA2s are a well known component of many snake venoms, typically they are between 13-15 KDa and are members of a larger super family of PLA's consisting of 11 groups arranged on the basis of size, structural homology, amino acid sequence and disulphide bridge pattern. Each group can then be further sub divided; all snake venom phospholipases are group 2 (PLA2) which are then further subdivided into group IA isolated from the elapids and group IIA from the vipers (de Oliveira *et al.*, 2013). This latter group is further subdivided on the basis of the amino acid at position 49; one having a negatively charged aspartic acid residue and the other having a positively charged lysine residue. This is important regarding the binding of Ca^{2+} ions to the molecule, with the latter inhibiting PLA2/ Ca^{2+} interaction; this substitution confers Asp49 homologues with catalytic activity whilst Lys49 are catalytically inactive.

Both PLA2-I and PLA2-II have been characterised as having antimicrobial activity, and have been shown to exert their antimicrobial activity by both a membrane damaging mechanism of action as well as the production of hydrogen peroxide (Kini. 2003).

Whilst none of the potential PLA2 proteins isolated in this study are useful in their current form one strategy to develop their clinical applications would be to determine truncated sequences with antimicrobial activity which has previously been applied for PLA2 proteins.

Santamaria *et al.* (2005) examined the activity of 8 previously identified PLA2-II proteins from *Bothrops asper* (terciopelo viper) (I-IV), *Bothriechis schlegeli* (eyelash viper) (I), *Cerrophidion godmani* (Godman's pit viper) (I & II) & *Atropoides nummifer* (Mexican jumping pitviper) (I) (Angulo *et al.*, 1997, Diaz *et al.*, 1992 & 1995, Gutierrez *et al.*, 1984 & 1986, Kaiser *et al.*, 1990, Lomonte *et al.*, 1989) which contained both Asp49 & Lys49 variants. The C terminal (KKYRYYLKPLCKK) of *B. asper* PLA2-II (115-129) had previously been tested for its activity showing near 100%

inhibition of *E. coli* & *V. cholerae* at 30 μ M with a membrane damaging mechanism (Paramo *et al.*, 1998). In the more recent study this peptide was used as a scaffold for amino acid substitution, with 10 variants synthesised resulting in the identification of the peptide pEM-2 (KKWRWWLKALAKK) which retained antimicrobial activity, however, its cytotoxic effects were significantly reduced and comparable to the clinically used antibiotic polymyxin B (Santamaria *et al.*, 2005).

Clearly such truncation studies could be applied to the current potential PLA2 proteins isolated in this study to produce peptide scaffolds in which rational design techniques could be applied. Along with Paramo *et al.* (1998) and Santamaria *et al.* (2005) the idea of the C-terminal being responsible for the antimicrobial activity of PLA2 proteins has been further supported by Diz Filho *et al.* (2009) in which a Ca^{2+} dependent PLA2 from *Crotalus durissus ruruima* (South American rattlesnake) was shown to have antimicrobial activity. However whilst this C-terminal activity seems sufficient for antimicrobial activity in some PLA2's, in others this is not the case. For example an isoform termed F17 isolated from *Crotalus durissus terrificus* (tropical rattlesnake) requires catalytic function for antimicrobial activity (Toyama *et al.*, 2003).

Along with the potential PLA2 proteins isolated two peptides below 10 KDa have also been identified from, *Dendroaspis polylepis* (black mamba) and *Notechis scutatus* (tiger snake) which have molecular weights of 6600 & 6943 Da respectively. All these peptides have been isolated from elapid venom which contains a high proportion of cysteine containing peptides typically involved neuro- and cardiotoxic activities (Doley *et al.*, 2009), therefore based on their size and origin it would be expected that they are cysteine containing peptides.

The peptide isolated from *D. polylepis* has a molecular weight and biological activity in line with the three fingered toxin F-VIII isolated from the closely related *Dendroaspis*

angusticeps (Eastern green mamba) which had a molecular weight of 6597.8 (Conlon *et al.*, 2014) and showed similar low biological activity, however this peptide also showed no activity against *E. coli* whilst the peptide isolated in this study shows weak activity. This could be down to either differences in *E. coli* strain susceptibility or slight changes in the amino acid sequence between species. Toxin F-VIII is a member of the three fingered toxin super family therefore it would be reasonable to assume that this peptide is also a three fingered toxin. Although this peptide has only moderate activity its low cytotoxic activity makes it an ideal candidate for the future development, especially when considering the possible modification strategy described below.

Three fingered peptides have typically been characterised as being crucial for venom toxicity, they have a common structure of three β -stranded loops extending from a central core containing all four conserved disulphide bonds (Fig. 3.10a). However despite the common scaffold, they bind to different receptors/acceptors and exhibit a wide variety of biological effects. Members of this family include α -neurotoxins, which bind to muscle acetylcholine receptors (nAChR) (Chang *et al.*, 1979) k-bungarotoxins, which bind neuronal nicotinic receptors (Grant *et al.*, 1985), muscarinic toxins with selectivity towards muscarinic receptors (Jerusalinsky *et al.*, 1994), fasciculins that inhibit acetylcholinesterase (Cervenansky *et al.*, 1991), calciseptine that blocks the L-type calcium channels (de Weille *et al.*, 1991), cardiotoxins that are pore forming peptides (Bilwes *et al.*, 1994), dendroaspins, involved in disrupting cell-adhesion processes (McDowell *et al.*, 1992) and b-cardiotoxins, which bind to b1- and b2-adrenergic receptors (Rajagopalan *et al.*, 2007).

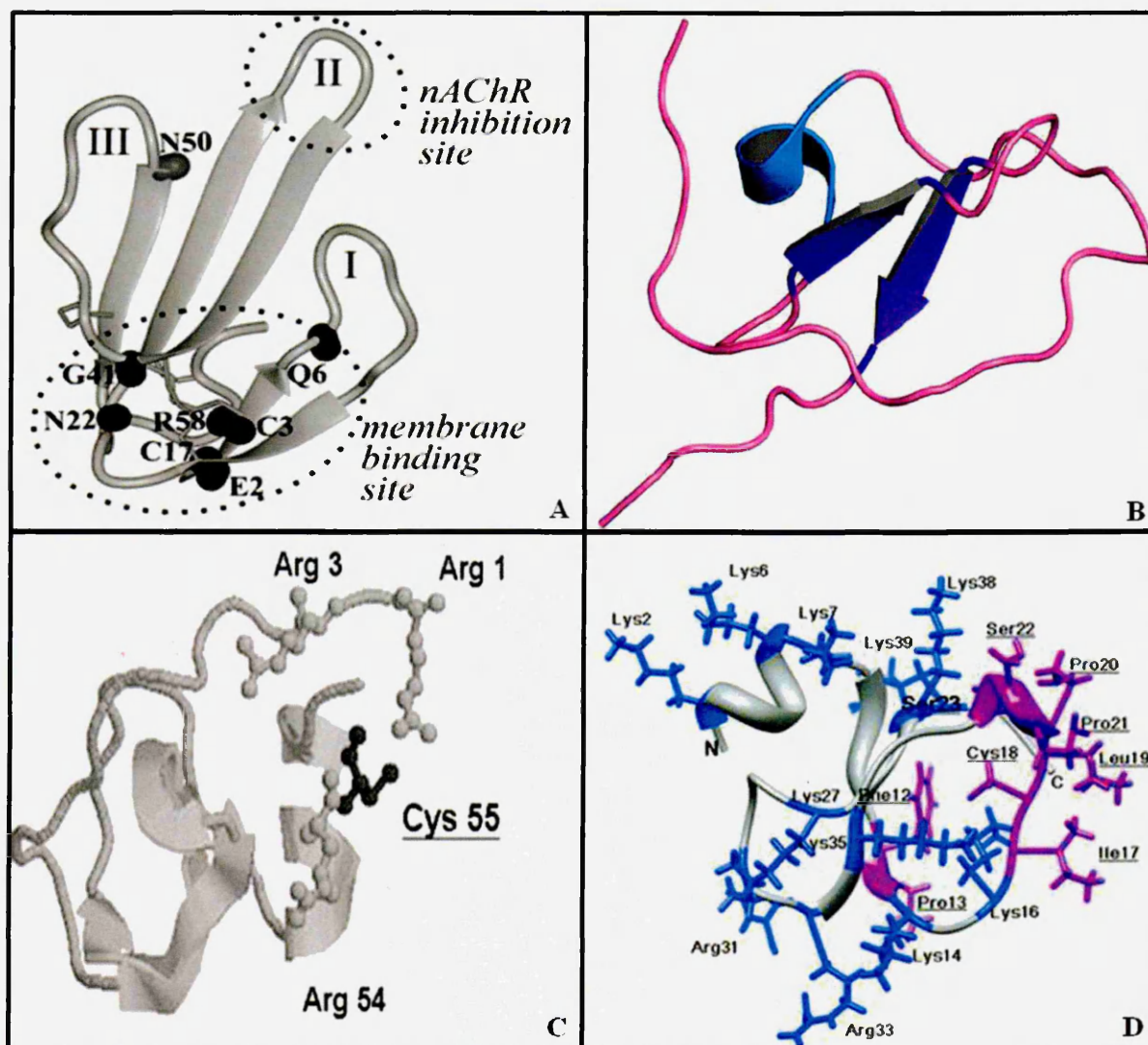


Figure 3.9: Structural motifs of snake venoms that could be used as AMPs. Possible modification could be made to number snake motifs as examples (A) three fingered toxins. Neurotoxin II isolated from the venom of *N. oxiana* (Lesovoy et al., 2009) interacts with membranes at the base of the molecule with mAChR binding site at the opposite end of the molecule, importantly this peptide has been recombinantly expressed (B) Waprin proteins such as omwaprin (Nair et al., 2007) have been chemical synthesised despite cysteine bonding therefore modification is possible (C) The antimicrobial B chain of β -bungarotoxin has been recombinantly expressed (Wen et al., 2013) along with (D) crotoamine (Coronado et al., 2004).

Recently certain three fingered toxins have been shown to exhibit antimicrobial activity. Kao *et al.* (2011) examined the antimicrobial properties of γ toxin, a cardiotoxin isolated from the elapids *Naja nigricollis* (black necked spitting cobra) and cardiotoxin 3 from *N. atra* which have been postulated to disrupt mammalian cell membranes by binding to the anionic lipid of component and is therefore cytotoxic and haemolytic. It is the same mechanism of action that allows them to have antimicrobial function therefore in its current form it has little use as a therapeutic, however NMR studies of the interaction between γ toxin and dodecylphosphocholine liposomes revealed the peptide remains structurally unchained during binding which is facilitated by the hydrophobic face of the peptide (Dauplais *et al.*, 1995). Increased hydrophobicity is well known to increase the cytotoxic effects of AMPs (See intro) therefore it could be postulated that a site directed mutagenesis study that lowers the hydrophobic content of the binding face could lower its cytotoxic effects whilst retaining its antimicrobial effects. Successful recombinant expression of snake three fingered toxins has already been achieved by Lesovoy *et al.* (2009) who expressed the α -neurotoxin II (NTII) from *N. oxiana* in *E. coli*. This 61 chain residue peptide is known for binding to nAChR receptors however Lesovoy also showed the binding of the peptide to DOPC/DOPS/Chol liposomes, this secondary function was postulated to assist in the modulation of the primary nAChR receptor binding. Interestingly however, residues implicated in membrane binding are at the opposite end of the peptide to the nAChR receptor binding site which is located within the loop section of the middle finger whilst residues implicated in membrane binding are located at the base of the peptide in a non-consecutive flat plane (Fig. 3.10a).

Whilst no published data is available to ascertain the antimicrobial effects of this peptide it never the less offers an intriguing possibility. Firstly the nAChR receptor binding site could be “knocked out” by sequence scrambling or alanine scanning which

would not be expected to not cause any major structural changes within the peptide due to its position within the loop region. Once 'safe' mutation studies could then be carried upon the residues implicated in membrane binding. Thus it may be possible to re-engineer the peptide whilst maintaining the evolutionary advantages that has allowed it to be effective within a mammalian prey's bloodstream, i.e. its stability from protease degradation. If successful, the engineering of the three finger toxins could give us a wealth of new molecules to examine with nearly 350 known peptides of this family already characterised at the protein level (Source: Uniprot) and no doubt many more identified by transcriptomics.

Similar modification could be applied to other snake peptides such as the antimicrobial peptides waprins and peptides with previously known function which have recently been identified to have antimicrobial activity such β -bungarotoxin from *B. fasciatus* or the viper myotoxin crotamine.

Waprin peptides contain the whey acidic protein disulphide bridged core (WAFC) domain characterised by four disulphide bridges which is found in a variety of proteins from both vertebrates and invertebrates (Smith *et al.*, 2011) (Fig. 3.10b). Along with nawaprin and omwarpin described previously, a number transcriptomic studies have detailed the presence of potential waprin AMPs in other venoms including *Liophis poecilogyrus* (yellow-bellied Liophis), *Pseudoferania polylepis* (Macleay's water snake), *Rhabdophis tigrinus tigrinus* (tiger keelback), *Thrasops jacksonii* (black tree snake), *Philodryas olfersii* (Lichtenstein's green racer) and *N. scutatus* (Fry *et al.*, 2008, St pierre *et al.*, 2008).

The B chain of β -bungarotoxin is a 7 KDa peptide thought to be responsible for the blockage of voltage-gated K^+ channel of the larger PLA2 hetero-dimer chain A (14 KDa) and chain B (7 KDa) and has recently been shown to have antimicrobial activity

via a membrane disruptive mechanism (Wen *et al.*, 2012 & 2013). Interestingly residues implicated in membrane disruption are located around the cysteine residue that usually forms a bridge to the A chain which would suggest that the residues implicated in K⁺ channel modulation are not responsible for membrane disruption therefore as with the nAChR receptor binding site these residues could be 'knocked out' whilst maintaining membrane disruption (Fig. 3.10c)

Crotamine is a 42 residue basic peptides first isolated in the 1940's from the venom of *C. durissus* (Gonçalves *et al.*, 1947). It has recently been shown to have antimicrobial activity against *E. coli* at 25-100 µg/ml however has no activity against other Gram negative or Gram positive organisms at the 200 µg/ml and showed no haemolytic activity at these high concentrations (Oiquiura *et al.*, 2011). Structurally crotamine is evolutionary related to the β-defensins found with vertebrates with three disulphide bridges and whilst sequence homology is low their structural arrangement consists of a three-stranded-sheet core and a framework of loops stabilized by six disulfide-linked cysteines (Coronado *et al.*, 2013).

Evidence of membrane permeability is abundant, Costa *et al.* (2014) observed the propensity of crotamine to disrupt liposomes containing negatively charged phospholipids whilst Siebur *et al.* (2014) detailed its pore forming ability on planer lipid bilayers in which the peptide forms oligomers in solution that insert into the membrane. However, recently, its ability to interact with DNA has also been observed (Chen *et al.*, 2012) raising the possibility of intracellular targets. Further support for this is shown by Hayashi *et al.*(2008) who determine the mechanism of cell penetration in eukaryotic cells occurs through liposomal endocytosis.

As is seen from the high resolution structure of crotamine (Coronado *et al.*, 2004) it is a highly amphipathic peptide with clear definition between the hydrophobic (purple) and

hydrophilic (blue) residues (Fig. 3.10d) therefore manipulation of these areas could yield a more effective AMP, for example the addition of a polar residue within the hydrophobic core to create an imperfect amphipathic peptide as described by Wimley. (2011) that could increase antimicrobial activity. Importantly the hydrophobic residues are located around a loop region of the peptide and not in the evolutionary conserved β -sheet domain therefore the effects of residue modification of structure would be expected to be minimal. Whilst crostamine does have advantageous antimicrobial properties with low haemolytic potential it never the less is still a toxic peptide which causes irreversible membrane depolarization, and spontaneous repetitive firings of mammalian skeletal muscle (Chang *et al.*, 1978, Rizzi *et al.*, 2007). However recent electrophysiology data conducted by Jan Tytgat's group (Peigneur *et al.*, 2012) determined this was caused by the peptides ability to modulate potassium channels and suggested four residues involved in this process (Arg31-Trp32 and Tyr1-Lys2) which again could be substituted without compromising the hydrophobic region of the peptide-nessesery for membrane core interaction.

Taken in context, whilst the proteins that have been isolated in this chapter are either too large for drug development in their current form and at present, have undesirable biological activities they offer a starting scaffold in which either specific sections of the peptide can re-engineered or truncated motifs synthesised from larger proteins. Future work on these peptides should be undertaken firstly to ascertain their full length sequences to determine if any short truncated helical peptides could be synthesised as described by Santamaria *et al.* (2005).

Secondly transcriptomic analysis of the venom glands of these snakes, particularly those where sub 10 KDa peptides have been isolated, should be undertaken so that recombinant peptides can be constructed and a site directed mutagenesis study designed.

Successful recombinant expression has been achieved with the three fingered toxins (Lesvoy *et al.*, 2009), B chain β -bungarotoxin and crotamine (commercially available through recombinant expression) whilst successful chemical synthesis has been achieved with the waprin fold (Bannigan *et al.*, 2010) therefore the chance of correct protein folding is relatively high.

A large number of venom glands have previously undergone both proteomic and transcriptomic analyses which will no doubt be indispensable if either of these strategies is to be taken forward. However precedent should not be given to these technologies compared with the purification strategy described in this chapter. The present study should be widened to examine more snake venoms from the other two venomous snake families *Atractaspididae* and *Colubridae* which could provide us with novel peptide sequences and structures. The re-examination of previously known snake peptides for their antimicrobial activity should also be undertaken after the success of β -bungarotoxin and crotamine.

Ultimately, the larger number of structural motifs identified that exhibit antimicrobial activity the greater the chance of developing new classes of antibiotics.

4 CHAPTER 4
CHARACTERISATION OF ANTIMICROBIAL PEPTIDES FROM
SCORPION VENOM

4.1 Background and aims

A large array of scorpion AMPs have already been identified, with over 40 peptides biologically characterised (Harrison *et al.*, 2014) some of which exhibit strong antimicrobial activity and low toxicity and thus provide good scaffolds for the future development of AMPs. However, a large number of genomic studies have identified more scorpion AMPs but their biological activities remain unknown (Silva *et al.*, 2009, Schwartz *et al.*, 2008, Zhu *et al.*, 2000). One such study (Abdel-Rahman *et al.*, 2013) used both proteomic and genomic approaches to identify four AMPs from the venom gland of the North African scorpion *Scorpio maurus palmatus* (Chactoid scorpion). These peptides span all the major classes of scorpion AMPs previously identified including α -helical peptides of short, mid and long chain length and a scorpine like cysteine constrained peptide.

This chapter aims to characterise their biological activity as well as providing evidence of their mechanism of action by elucidating any membrane destructive properties and intracellular targets.

Due to cost issues only the three helical peptides were synthesised and characterised. Sequence and physical properties are detailed in Table 2.1.

Structural modifications were also undertaken on one of the peptides (Smp24) to try and improve its biological profile, these were termed Smp24GVG and Smp24T (Table 2.1). These alterations were based on structural modifications that had a beneficial effect on the biological activity of the evolutionary related Pin 2 (Rodriguez *et al.*, 2011 & 2014). In the first modification, the central proline residue was substituted for a glycine-valine-glycine motif and secondly the C-terminal was truncated by four residues.

The chapter also aims to investigate the mechanism of action of these peptides based on homology comparison with other scorpion AMPs that have previously been identified and makes recommendations on how further modification can increase the potential for these peptides to be developed in the clinical setting.

4.2 Method Summary

Six scorpion peptides were assayed in the study as detailed in Table 4.1. All peptides were assayed for their antimicrobial activity by the micro dilution method from a concentration of 0.5-512 µg/ml. A range of Gram positive and Gram negative organisms were used, some of which displayed antibiotic resistance and a fungal strain was also included in the study. Peptides that displayed antimicrobial activity were assayed for their haemolytic and cytotoxic effects against sheep erythrocytes and by an ATP release assay against human liver derived HepG2 cells at the same concentration range as in the antimicrobial assays. Evidence of membrane damage and interaction with the possible intracellular processes of DNA, RNA and protein synthesis has also been explored to provide evidence of mechanism of action against live bacterial cells.

4.3 Results

4.3.1 Antimicrobial activity of AMPs from the *Scorpio maurus palmatus*

The antimicrobial activities of Smp13, Smp24, Smp43 along with the Smp24 derivatives are listed in Table 4.1. Pin 2 was also assayed for comparison.

Table 4.1: Antimicrobial activity of AMPs (MIC) isolated from *Scorpio maurus palmatus*, Smp24 derivatives and Pin 2 from *P. imperator*

Bacteria strain	MIC (µg/ml)						
	Smp 13	Smp 24	Smp 24	Smp 24	Smp 24T	Smp 43	Pin 2
<i>B.subtilis</i> NCIMB 8024	No Activity	4	8	8	8	4	8
<i>S.epidermidis</i> sp.	No Activity	8	16	16	16	64	16
<i>S.aureus</i> SH100	No Activity	8	16	16	16	32	8
<i>E.coli</i> JM109	No Activity	64	64	64	128	128	64
<i>K.pneumoniae</i> NCTC 13439	No Activity	128	128	128	128	64	256
<i>P. aeruginosa</i>	No Activity	256	256	256	256	64	256
<i>C.albicans</i> sp.	No Activity	32	128	128	128	128	32

Table 4.2: Effect of Smp24 on a range of *S. aureus* strains

<i>S.aureus</i> strain	MIC (µg/ml)
hVISA (isolate)	64
MRSA mecA mupA +ve	16
MSSA (isolate)	32
EMRSA-15	16
<i>S.aureus</i> ATCC 25923	32
MRSA ATCC 33591	512 (Partial)
EMRSA-16	512 (Partial)
VISA MU50	32

No activity is seen with the shorter Smp13 whilst the mid and longer chain Smp24 and Smp43 exhibit preferential activity towards Gram positive organisms with no considerable difference seen when compared with the modified Smp24 peptides. Gram positive organisms are overwhelmingly more susceptible to *S. maurus palmatus* derived AMP attack than their Gram negative counterpart with Smp43 exhibiting the highest activity against this class of organisms. Because of the strong activity observed with Smp24 towards *S. aureus* SH1000 the peptide was assayed against a wider range of *S. aureus* strains some which were classified as having resistance towards meticillin as well as showing intermediate resistance towards vancomycin. A wide of MIC values were observed between strains, particularly between EMRSA-15 and EMRSA-16 which had MICs of 16 µg/ml and 512 µg/ml respectively highlighting the possibility of resistance to be acquired either through plasmid acquisition, mutation or phenotypic routes against AMPs.

4.3.2 Haemolytic activity of AMPs from *Scorpio maurus palmatus*

In haemolytic assays (Fig. 4.1) Smp43 showed very low toxicity with only 1.2% (± 0.5) lyses observed at the highest concentration of 512 µg/ml however 89.6% (± 5.6) lysis was observed at the same concentration with Smp24. Indeed, significant disruption is observed between 64 µg/ml (14.5% ± 2.0) and 128 µg/ml (52.8% ± 4.2) with an increase of 38.3% lysis observed. Maximum disruption is observed with Pin 2 at the highest concentration (98.9% ± 4.0) whilst lysis was higher at the lower concentrations of 64 and 128 µg/ml compared with Smp24 (34.0% ± 1.7 & 71.6 % ± 6.6 respectively). The modifications of Smp24 had contrasting effects. The addition of a flexible glycine-valine-glycine hinge region unexpectedly caused an increase in haemolysis, for example at 64 µg/ml 22.6% (± 2.9) lysis occurred whilst at 128 µg/ml 67.4% (± 5.3) was detected. However, the truncated Smp24 derivative showed a decrease in haemolysis with only

50.8% (± 2.9) seen at the highest concentration whilst at 64 and 128 $\mu\text{g/ml}$ only 6.9% (± 0.8) and 14.3% (± 3.2) observed representing a decrease in haemolysis from the native Smp24 of 7.6 and 38.5% respectively.

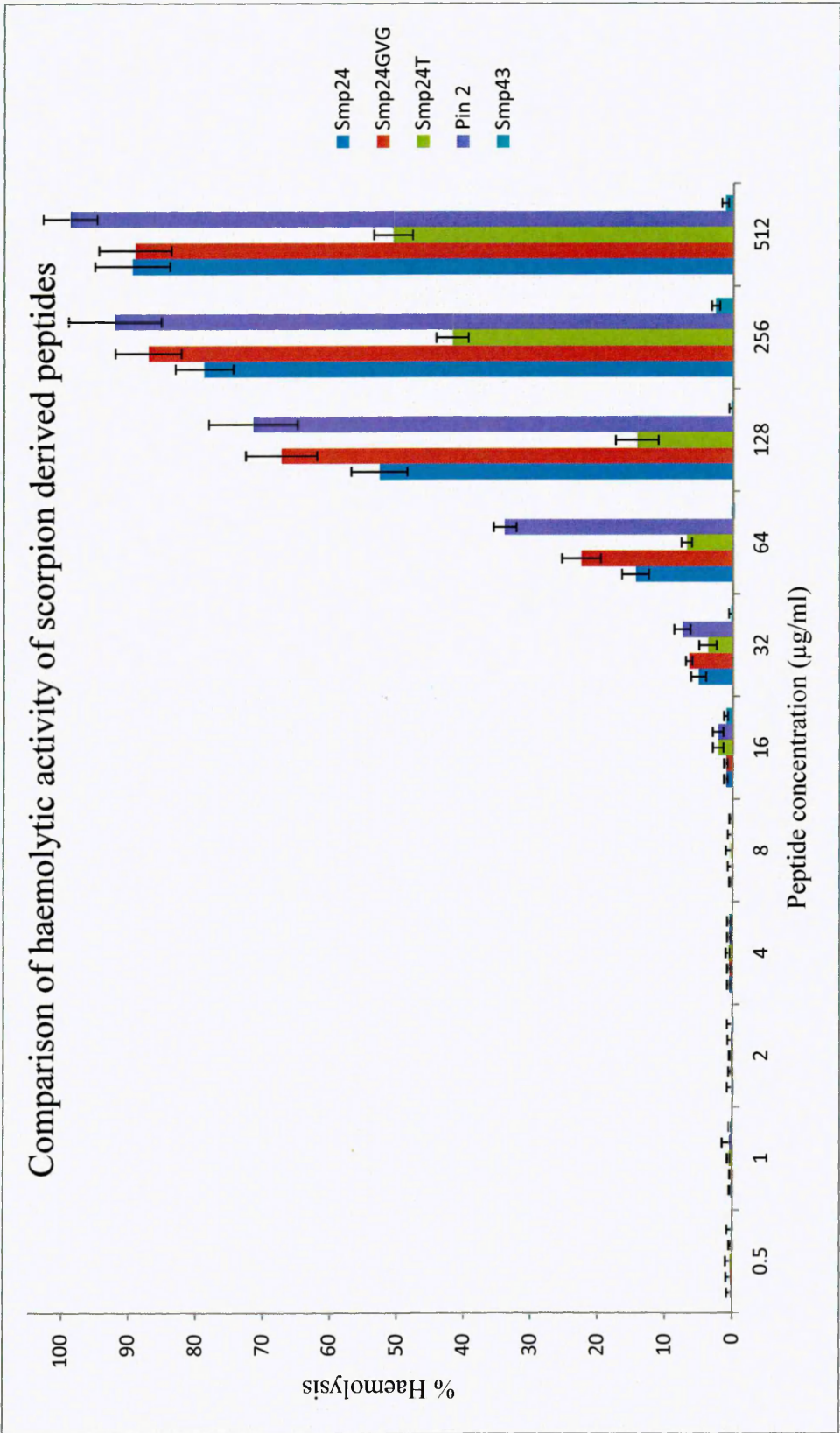


Figure 4.1: Haemolytic activities of peptides used within this study-Smp43 shows very low haemolytic activity at the highest concentration of 512 µg/ml. The native Smp24 and Pin 2 are highly haemolytic whilst addition of a GVG into Smp24 had a negative effect on haemolysis however the truncated SMn24 did show lower toxicity

4.3.3 Cytotoxic activity of AMPs from *Scorpio maurus palmatus*

Cytotoxicity testing was carried out on HepG2 liver cells (Fig.4.2) using an ATP release assay. Because all systemic drugs would go through the liver and a large proportion of modification reactions happen in the organ a hepatic cell line was chosen to determine toxicity against this important organ.

As observed in haemolysis assay, significant cell damage occurs in a concentration dependent fashion with a noted increase in ATP release seen at 32 $\mu\text{g/ml}$ with all five peptides used in this study. For example at 16 $\mu\text{g/ml}$ no peptide causes no more than 2% cell damage however a doubling of the concentration causes 14.6% (± 4.3) ATP release with Smp43 whilst Smp24 and its truncated derivative showed similar increases with 15.9% (± 1.3) and 11.8% (± 4.0) release detected respectively. The addition of a hinge region caused a significant increase in cell disruption with 32.7% (± 4.0) ATP release noted and a similar level was seen with Pin 2 which caused 27.0% (± 5.0) release. As seen in haemolysis assays, the truncated peptide was overall less cytotoxic than the native and hinged peptide as demonstrated at the higher concentration of 64 $\mu\text{g/ml}$ with only 26.8% (± 2.1) damage observed whilst 39.0% (± 6.2) and 56.8% (6.5) is seen with Smp24 and Smp24GVG respectively. Surprisingly, when considering the low toxicity displayed with Smp43 against red blood cells, the peptide causes significant damage above 32 $\mu\text{g/ml}$ which is consistent with the other peptides used within this study clearly highlighting the differences in eukaryotic cell membrane architecture and the need for a range of diverse mammalian cell types to be assayed during cytotoxic testing.

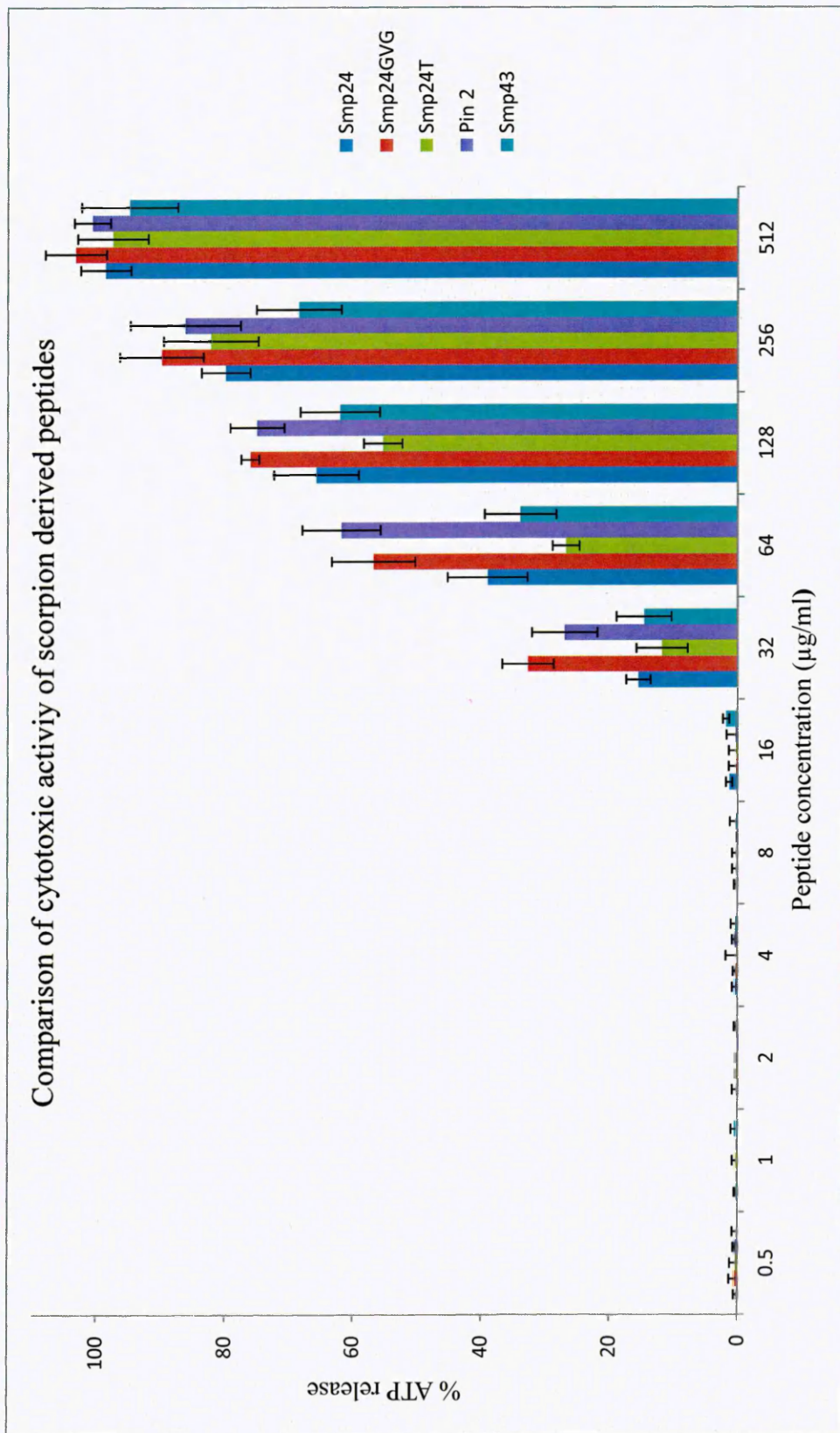


Figure 4.2: Cytotoxic activities of peptides used within this study. All the peptides begin to show moderate cytotoxic activity at 32 µg/ml. However unlike in haemolytic assays Smp43 does not exhibit low toxicity at high peptide concentrations.

4.3.4 Membrane disruptive potential of scorpion AMPs

As with the snake peptides isolated in Chapter three, prokaryotic membrane disruption was determined by the BacLight assay. As examined in Table 4.3 all the peptides assayed caused maximum disruption against both Gram positive and Gram negative organisms at a concentration of 4 times MIC clearly indicating the membrane disruptive activity of these peptides.

Table 4.3: Effect of scorpion AMPs on Gram positive and Gram negative membranes

% Membrane damage					
	Smp24	Smp24GVG	Smp24T	Smp43	Pin 2
<i>E.coli</i> JM109	110.5 (\pm 3.9)	97.2 (\pm 1.2)	99.5 (\pm 3.5)	105.4 (\pm 1.8)	108.6 (\pm 4.1)
<i>S.aureus</i> SH1000	101.2 (\pm 4.8)	105.3 (\pm 4.5)	11.6 (\pm 2.9)	103.2 (\pm 5.1)	103 (\pm 2.9)

4.3.5 Elucidation of intracellular targets of scorpion AMPs using the *B. subtilis* whole cell assay

Further evidence of membrane interaction is observed with the stress responses observed in the *B. subtilis* whole cell assay (Fig. 4.3) where each peptide induced a near 1500% increase in the cell envelope stress response compared to a no peptide control after 1 hr incubation. This stress response decreases over a 4 hr period, however at this time point, a significant stress is still present upon the cell envelope with between 130-190% induction still present suggesting a rapid peptide attack within the first hour and then a decrease in attack as the peptide is depleted over time.

The stress responses that would be elicited after an attack on DNA, RNA and protein synthesis have also been assayed. Interestingly all four shorter peptides caused a significant induction of response against the *yorB* (DNA) stress response after 3 hr incubation with Smp24GVG showing the greatest increase (288.4% \pm 14.2) with Smp24 and the truncated peptide showing 228.1% (\pm 12.1) and 162.3% (\pm 6.4) respectively whilst Pin 2 caused a 192.4% (\pm 13.1) increase in luminescence against the same stress response, however Smp43 showed no such induction with only a 4.8% (\pm 1.9) increase recorded.

Whilst after 1 hr a DNA stress response is observed with Smp24, Smp24GVG, Smp24T and Pin 2 (65-120%) it is interesting that the maximum response is noted after 3 hrs in contrast to cell envelope stress, however conceivably it is logical that a maximum stress response after interaction with an intracellular target is elicited after incursion through the cell envelope.

For the RNA and protein synthesis assays no stress response was induced above a 20% increase for any of the five peptides with a large amount of variation and no trends seen

in any of the data. Therefore, it was concluded that no real interaction is taking place between these two intracellular targets and any of the peptides.

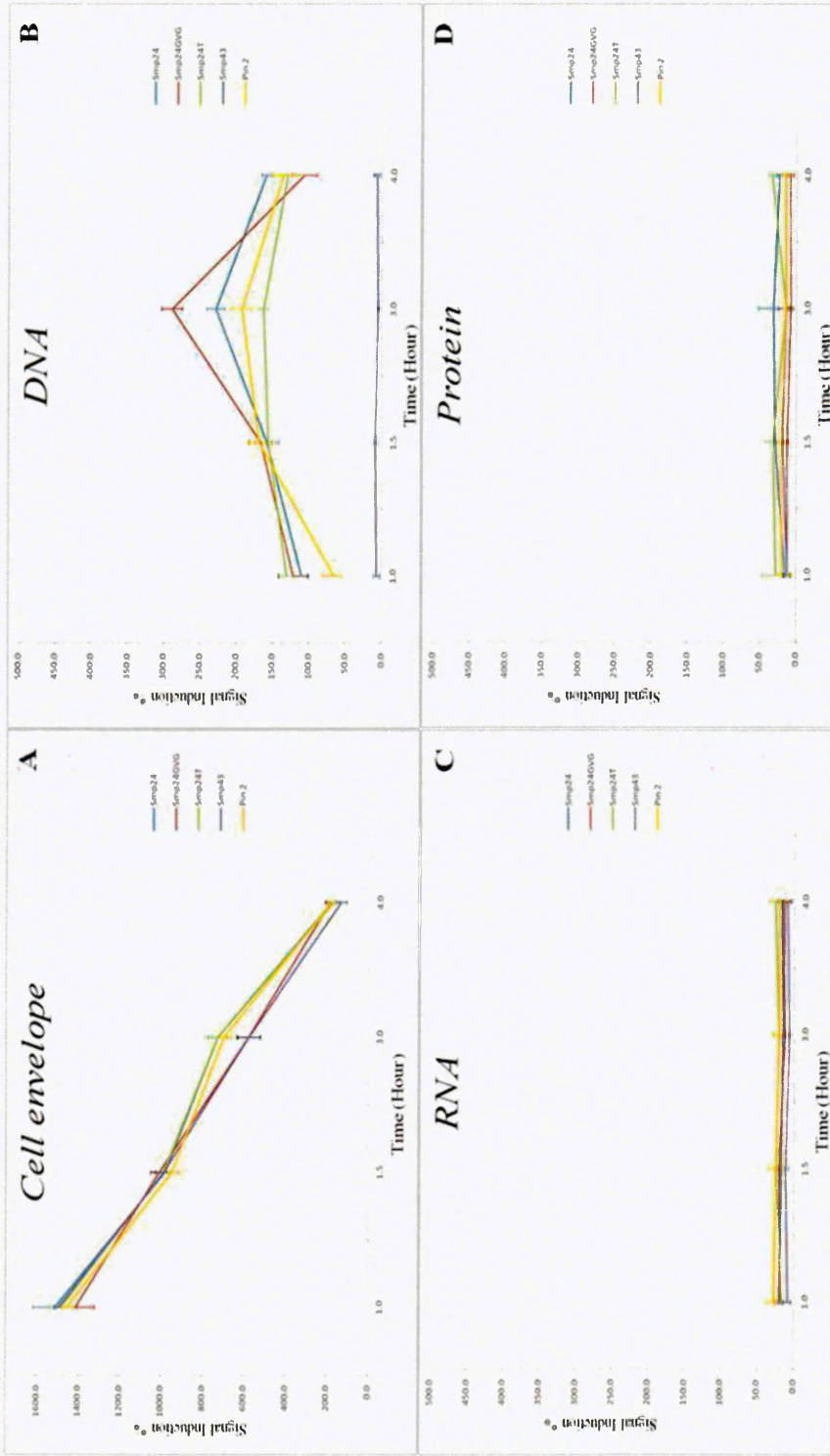


Figure 4.3: Stress response of *B. subtilis* elucidated after incubation with scorpion AMPs using the luciferase/luciferin assay. (A) The cell envelope stress response signal is high within the first 1 hour of peptide interaction with every peptide reflecting peptide/membrane interaction is critical for function. However the constant fall over the 4 hour period with each peptide indicates a short peptide activity time or interaction with intracellular targets after membrane interaction. (B) Possible interaction with DNA pathways with a maximum signal after 3 hours with Smp24 and Smp24GVG. (C) and (D) no interaction with RNA or protein synthesis was observed with any peptide

4.4 Discussion

A large number of scorpion AMPs have been characterised due to their size (<5 KDa) and diverse biological activities. However, an array of scorpion AMPs have been not characterised biologically. This study aimed to follow on from previous research undertaken by our collaborators Mohamed Abdel Rahman and Lourival Possani (Abdel Rahman *et al.*, 2013) and biologically characterise three of the four AMPs detected in the venom of *S. maurus palmatus*.

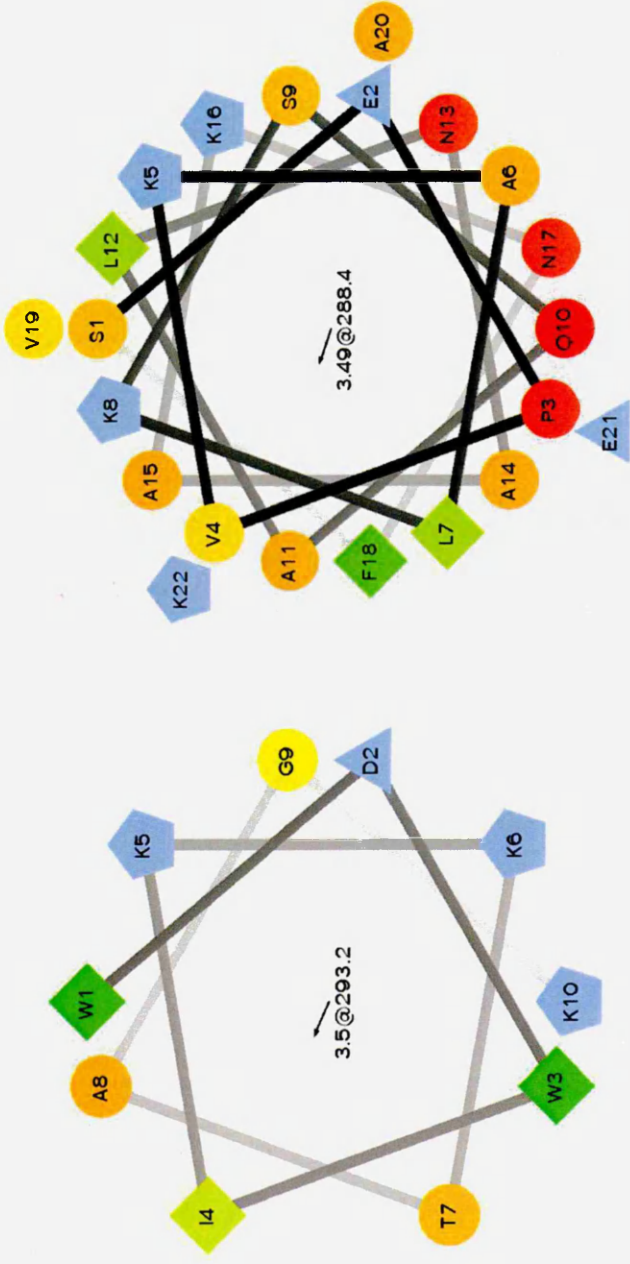
This scorpion belongs to the family *Scorpionidae*, with BLAST analysis revealing Smp43 shares high homology with the scorpion AMPs opistoporin 1 & 2 and Pin 1 sharing 86, 83 & 76% homology respectively (Fig. 4.4).

Opistoporin 1 & Pin 1 both have been shown to have helix-hinge-helix structures (Moerman *et al.*, 2002, Corzo *et al.*, 2001). Pin 1 is far more extensively studied with an NMR derived structure and characterised mechanism of action.

Similarly Smp24 shares 54% homology with Pin 2 (Fig. 4.5b) and contains structural motifs evolutionary conserved within shorter (17-20 residue) chain scorpion AMPs. Most notably the LIPS motif found within the core of the sequence of BmKb1, ctriporin, imcroporin, meucin-18, mucroporin as well as Pin 2. As with Pin 1, Pin 2 is the only peptide within the mid chain class that has been studied beyond basic biological characterisation.

Structurally, Pin 1 has two helices (3-18 and 26-37) linked by a random coil region, with coil regions at the N and C terminals. Alignment of Pin 1 and Smp43 reveal there is high conservation within these helical regions, also secondary structure prediction using the Jpred 3 server (Cole *et al.*, 2008) predicted a di helical structure for Smp43 between residues 3-12 and 16-36 (red residues) (Fig. 4.5a). When the regions corresponding to the coil regions in Smp43 are analysed using helical wheel projection software (Fig. 4.6) both regions form amphipathic helical wheels therefore it would be reasonable to assume that like Pin 1 and the opisthoporins Smp43 has a di-helical structure. Similar structural predictions of Smp24 determined an N-terminal extending to residue 15. Pin 2 has been deduced by NMR to be helical at the N-terminal up to residue 18 and alignment of the two peptides (Fig. 4.5b) reveals that their helical regions share high homology including 10 identical residues and two highly conserved substitutions within the first 18 residues, three residues are also identical (KKD) at the C-terminal which is associated with the cytotoxic nature of Pin 2 (Rodriguez *et al.*, 2011).

The shorter Smp13 belongs to the family of cytotoxic peptides such as the IsCT peptides (Dai *et al.*, 2002), however unlike other peptides within this family the Smp13 carries no charge therefore it is not surprising it has no antimicrobial activity, and its actual function within the venom remains to be elucidated.



3-12

16-36

Figure 4.6: Helical wheel analysis of the predicted helical regions of Smp43 using the rzlab software from the University of California (WWW.rzlab.ucr.edu). Hydrophilic (circles), hydrophobic (diamonds), potentially negatively charged (triangles), potentially positively charged (pentagons). Most Hydrophobic (green) and the amount of green decreasing proportionally with zero hydrophobicity yellow. Hydrophilic residues are coded red with pure red being the most hydrophilic (uncharged) residue, and the amount of red decreasing proportionally to the hydrophilicity. The potentially charged residues are light blue.

The biological activity of Pin 1 and 2 are broadly similar to Smp43 & Smp24. Both exhibit broad spectrum antimicrobial activity. Pin 1 shares low haemolytic activity with Smp43 whilst Smp24 and Pin 2 are haemolytic. Biophysical characterisation has determined the mechanism of action of these two peptides. Briefly, Pin 2 exerts its effect through pore formation (Fig. 1.6, Page 40) whilst Pin 1 has a more generalised carpet mechanism (Figure 1.7, Page 41) (Nomura *et al.*, 2004 & 2005).

A helical-hinge-helical topology seen within Pin 1 and postulated to exist in Smp43 is present in a number of AMPs with a high therapeutic index. As examples, cecropin A, a 37 residue peptide isolated from the silk moth *Hyalophora cecropia* which has two helical regions extending from residues 5 to 21 and from residues 24 to 37 (Holak *et al.*, 1988), and dermaseptin B2, a 33 residue peptide isolated from the Amazonian tree frog *Phyllomedusa bicolor* has a highly helical structure interrupted by a valine and glycine at positions 9 and 10. Interestingly, NMR data also pointed towards a carpet model mechanism of action rather than pore formation as seen with Pin 1 (Galanth *et al.*, 2009). Hybrid peptides using residues 1-8 of cecropin A and 1-12 of magainin 2 linked by a Gly-Ile-Gly motif showed broad spectrum antimicrobial and low haemolytic activity (Shin *et al.*, 2000).

The proline residue found within the helical region of Pin 2 is predicted to be at the end of this region in Smp24 therefore would not be expected to cause any significant helical kink as it does in Pin 2.

The effect of proline within AMPs is ambiguous. For example, some AMPs such as melittin and pardaxin that contain a proline residue in the central region of their sequence have high antimicrobial and haemolytic potential and removal of this further increases toxicity (Dempsey *et al.*, 1991). This view is supported by Bodone *et al.* (2013) who suggested that this kink is required for selectivity for prokaryotic

membranes over eukaryotic membranes as removal will increase toxicity due to increased helical structure. This increases the hydrophobic face and its propensity to bind to neutrally charged bilayers is greater, whereas more compact proline containing peptides will be less attracted to these surfaces but will still retain electrostatic attraction to negatively charged bilayers. In contrast to this view, a number of proline deficient peptides such as magainin 2 showed low toxicity (Zasloff., 1987) and previous efforts to decrease the haemolytic effect of Pin 2 by substitution of the proline residue for a flexible glycine-valine-glycine hinge region proved successful, based on the structural motifs found within the oxypinins from the wolf spider and ponerins G1 from the ponerin ant (Rodriguez *et al.*, 2011).

A similar strategy was employed with Smp24 however as is seen in figures 4.1 & 4.2 this modification decreases the therapeutic index supporting the notion of increased toxicity. Analysis of the predicted helical region of Smp24 and Smp24GVG would suggest that a more compact helix is observed in Smp24 with the N-terminal helical region stretching to residue 12 (red residues) with an extended helix up to residue 15 (green) (Fig. 4.7). Furthermore the prediction of buried residues shows nine residues buried in Smp24 and 12 in Smp24GVG however this included the lysine residue at position seven which may have an effect by increasing the hydrophobic face within that section of that peptide. This view is supported by calculating the hydrophobic moment (HM) of the peptides (Reißer *et al.*, 2014). In the case of Smp24 and Smp24GVG, the native sequence has a HM of 127° whilst Smp24GVG has an increased HM of 133.18° . This increase in the HM is known to increase both antimicrobial and haemolytic activity (Kondejewski *et al.*, 2002). However the decrease in haemolytic activity noted with Pin 2GVG is striking as the increase in HM is far greater than noted with Smp24 (114.8° to 139.9°), therefore increased HM is not a prerequisite to an increased haemolytic effect.

Secondly, whilst inclusion of a glycine-valine-glycine motif into each peptide increases the hydrophobic content by the same amount, Smp24 is more hydrophobic than Pin 2 from the outset due to phenylalanine at residue four in place of an alanine, an isoleucine at six instead of alanine and an isoleucine is replaced by leucine at fifteen. As described by Chen *et al.* (2007) increasing hydrophobic content past a certain threshold is associated with an increased toxicity, therefore hydrophobic content of Smp24 may have been pushed beyond a critical threshold.

Finally any addition of residues within the middle of a peptide will have an impact on the spatial distribution of residues downstream and may have implications for membrane binding.

Addition of the glycine-valine-glycine motif to Smp24 effects spatial distribution of the polar (blue) and non-polar (red) residues within the peptide and is a good example of this phenomenon (Fig. 4.8 and Fig. 4.9) Interestingly, the two extruding polar surfaces seen at the C-terminal of Smp24 are on the opposite side of the helix in Smp24GVG whilst the effect of the GVG motif on Pin 2 shows these extruding polar surfaces present at the C-terminal however their position matches that of Smp24GVG (Fig. 4.10), thus it is possible that the spatial distribution of these two extruding polar surfaces has an effect on biological activity due to the orientation of peptide-lipid interaction.

Smp24 IWSFLIKAATKLLPSLFGGGKKDS
-----B-BB--BBBBBB-----

Smp24GVG IWSFLIKAATKLLGVGSLFGGGKKDS
-----BBB---BBBBBB-----

Figure 4.7: Comparison of the predicted helical regions of Smp24 and Smp24GVG using the Jpred 3 server (Cole et al., 2008). Residues in red are predicted to form an helical structure with residues in black predicted to be unstructured. Residues that are predicted to be buried and not expected to interact with a bilayer are indicated with B

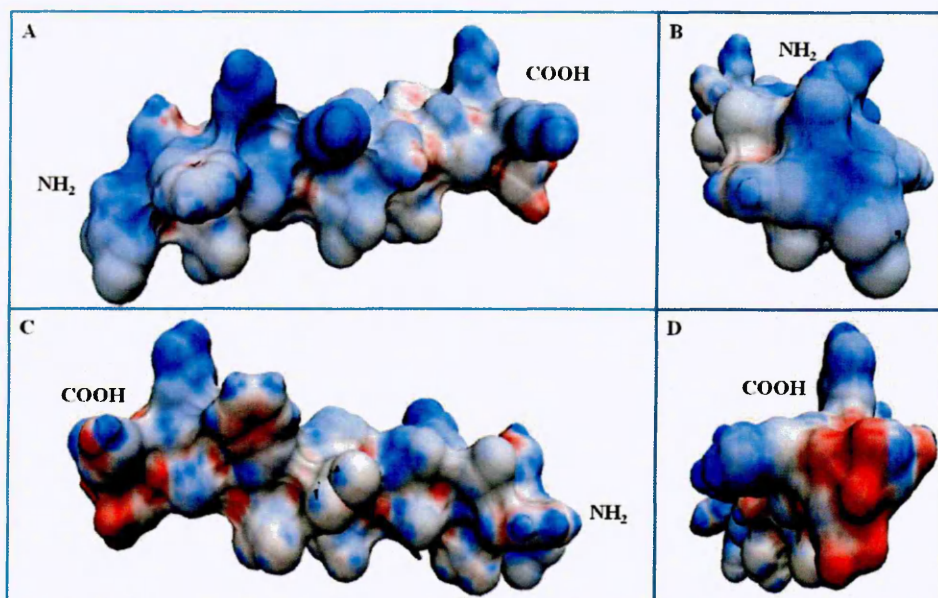


Figure 4.8: Spatial distribution of Smp24 modelled using the 3D Hydrophobic Moment Vector Calculator (Reißer et al., 2014). Polar facets are highlighted in blue and non-polar facets highlighted in red. Large proportion of the peptide surface are polar reflecting the importance of an AMPs electrostatic attraction to the prokaryotic membrane surface.

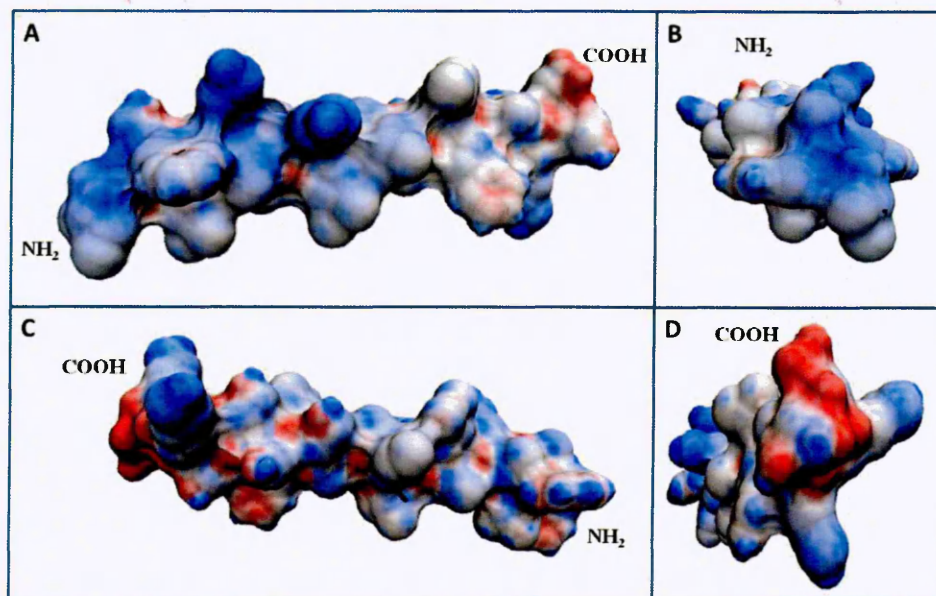


Figure 4.9: Spatial distribution of Smp24GVG modelled using the 3D Hydrophobic Moment Vector Calculator (Reißer et al., 2014). Polar facets are highlighted in blue and non-polar facets highlighted in red. Compared with Smp24 (Fig. 4.8) the modified Smp24GVG peptide is less polar at the N-terminal whilst the polar extrusions at the C-terminal are in the opposite orientation.

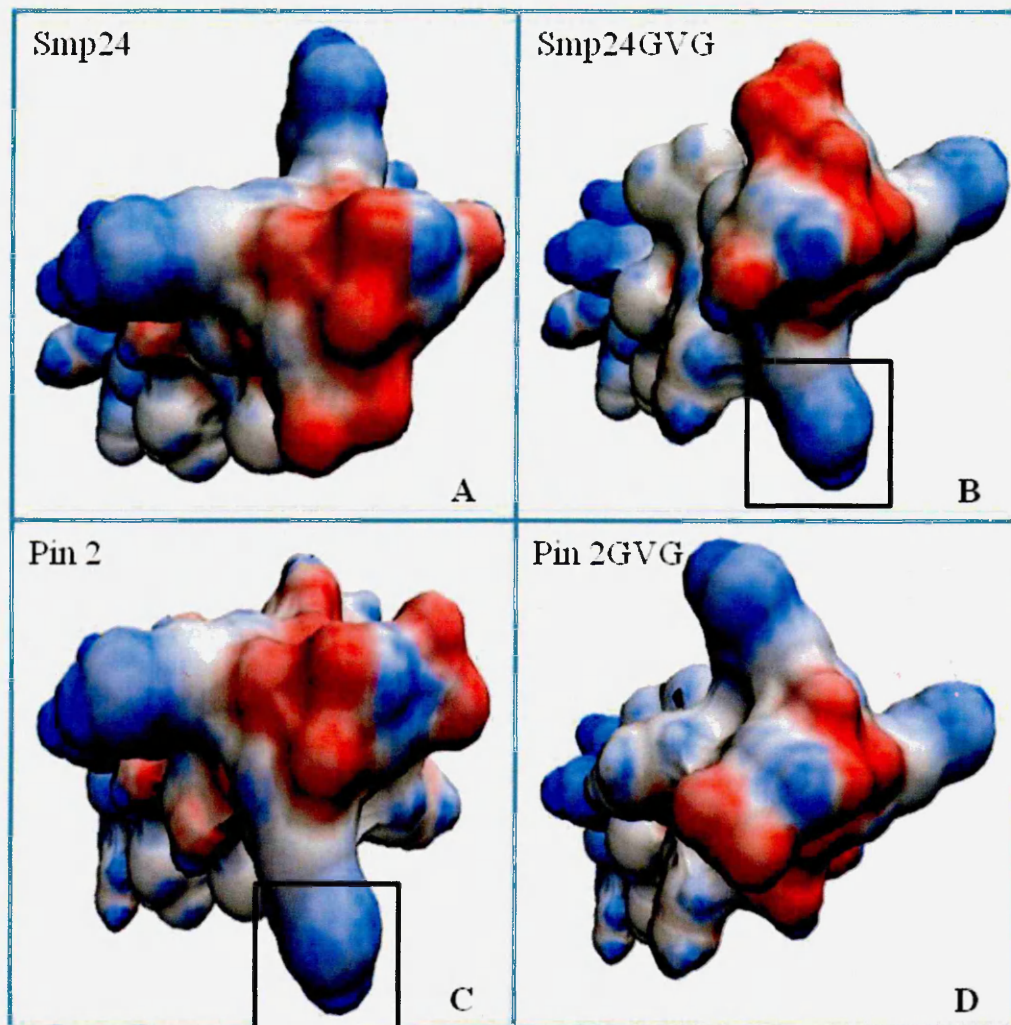


Figure 4.10: C-terminal analysis of the effect of the GVG motif insertion in to both Smp24 and Pin 2 modelled using the 3D Hydrophobic Moment Vector Calculator (Reißer et al., 2014). Polar facets are highlighted in blue and non-polar facets highlighted in red. Smp24 and Pin2 GVG (A & D) both have comparatively low cytotoxic effects than Smp24GVG and Pin2 (B & C). Interestingly, the two extruding polar facets are on one side of the peptide in Smp24 and Pin2GVG and on the other In Pin2 and Smp24GVG indicating a critical role of spatial distribution on AMP activity.

Similarly to Pin 2 (Rodriguez *et al.*, 2014), reducing the length of the C-terminal of Smp24 by the removal of the last 4 residues increased the therapeutic index. Likewise, shortening of the random coil region in Pin 2 had the same effect even though both peptides suffered a reduction in charge, although the electrostatic attraction is not as important towards eukaryotic membranes due to their zwitterionic nature (Jiang *et al.*, 2008). The reduction in haemolysis seen in Pin 2 after truncation to 14 and 17 residue peptides is of interest as CD spectra showed a change in structure from a predominantly helical structure to a β -hairpin structure similar to Indolicidin (Rodriguez *et al.*, 2014). The structure of Smp24T needs to be elucidated to determine if this is also the case, however unlike with Smp24T, the membrane disruptive mechanism of action has not been examined with the truncated Pin 2 peptides. Whilst membrane disruption with Pin 2 is well established a number of β -hairpin peptides including Indolicidin and Tachyplesin I are thought to exert their effect through intracellular targeting rather than membrane disruption (Nicholas., 2009).

Two modification strategies have been employed within this study. However future modification could include increasing the net positive charge. A strategy that was successful with mucroporin-M1 (Dai *et al.*, 2008). Another strategy could be to include modified amino acids such as N-methyl glycine which induced a di-helical structure in the 13 residue IsCT1 AMP which also increased the peptides ability to bind to DNA (Lim *et al.*, 2006).

Although Smp43 exhibited low haemolysis it still caused significant ATP release in HepG2 cells suggesting disruption of eukaryotic membranes. However, it is worth noting these are cancer derived cells which have a more negatively charged membrane than normal eukaryotic cells due to an increase in the anionic lipid PS content within the membrane outer leaflet, differential branching and sialic acid content of N-linked

glycans associated with transmembrane proteins and the increase in O-glycosylated mucins (so AMPs are electrostatically attracted to the membrane. Indeed, a number of AMPs have been examined for their anti-cancer effects such as melittin (Gajski and Garaj-Vrhovac., 2013). On this basis it would be useful to assess any toxic effects on primary cells which exhibit normal membrane compositions both to redefine peptide toxicity and determine any beneficial anticancer properties. Even so, whilst peptide modification has focussed on Smp24, due to its size and previous modifications to similar peptides no such modifications were examined with Smp43. One strategy employed on similar long chain scorpion AMPs hadrurin and vejovine was the creation of hybrid peptides 18 residues in length which increased therapeutic index (Sanchez Vasquez *et al.*, 2013).

Aspects of AMP development that have not been assessed in this study are both the protease stability and immunogenic potential of these peptides. Peptides of α -helical nature have reduced protease stability compared to cysteine containing AMPs (Falciani *et al.*, 2014), so, it would be important to determine this stability and to assess different peptide modifications to reduce degradation. A number of studies have examined this problem. As an example, Carmona *et al.* (2013) have examined the biological activity of the proteolytic-insensitive D-conformer Pin 2. A 30-40% reduction in haemolytic activity was observed with the D-conformer, which retained the antimicrobial profile of the native peptide. Crucially, when incubated with trypsin, elastase, whole human serum or proteases from *P.aeruginosa*, only the D-conformer retained activity, suggesting a feasible strategy for increasing AMP stability. These results are mirrored by previous studies on phylogenetically diverse AMPs including cecropin A (Wade *et al.*, 1990), melittin and paradaxin (Orzen *et al.*, 1997), LL-37 (Dean *et al.*, 2011), magainin (Guell *et al.*, 2011) and mastoparan (Jones and Howl. 2012).

Other strategies employed to increase both peptide stability and plasma half life have focussed on the delivery system, for example using liposome encapsulation (Ahmad *et al.*, 1995) or conjugation to human serum albumin (HAS) as a carrier protein (Hussain and Siligardi. 2010). More recent studies have investigated the potential of inorganic nanostructures for AMP delivery (Brandeli *et al.*, 2012). Interestingly, as well as increasing stability toward proteases, these strategies have also increased the therapeutic index of AMPs *in vivo*.

The reduction of immunogenicity of a protein/peptide is of great importance not just to AMPs but to protein therapeutics as a whole and, consequently, a number of strategies has been proposed to achieve this. Although no studies have been directed toward decreasing the immunogenicity of AMPs in particular, various general strategies have been examined and could provide useful areas for further AMP research. For example PEGylation (De Groot *et al.*, 2007) is an approved non-toxic and non-immunogenic procedure by interfering with antibody and/ or HLA epitope binding. Similarly peptide glycosylation also results in decreased immunogenicity through a similar mechanism (Von Delwig *et al.*, 2006). PEGylation has also been shown to increase the stability of AMPs in the presence of proteases (Falciani *et al.*, 2014) as well as decrease toxicity and increase biocompatibility (Morris *et al.*, 2012). Conjugation of peptides to IgG has also been carried out to successfully evade the adult immune system (Zambidas *et al.*, 1996) and is a strategy employed within clinical practice for the delivery of anti-inflammatory drugs. Finally, modifications of a peptide sequence to delete potential T-cell epitopes have also been examined (De Groot *et al.*, 2007). Therefore while a number of different strategies are available to improve stability and reduce immunogenicity, it is important to emphasise that the central goal of any strategy should be to maintain beneficial biological activity.

Along with the membrane disruptive mechanism that has been determined by the BacLight assay, the *B. subtilis* whole cell bioassay showed a possible interaction with DNA for Smp24, its derivatives and Pin 2. Previously a number of peptides have been shown to interact with intracellular targets including DNA (Yonezawa *et al.*, 1992, Park *et al.*, 1998, Zhang *et al.*, 2014). However, this is the first study that provides evidence of interaction between scorpion AMPs with intracellular targets, although the IsCT derivative described earlier has been postulated to do so (Lim *et al.*, 2006).

The classical example of AMP/DNA targeting is that of buforin II. As with the shorter chain peptides in this study buforin II contains a proline residue within the central core of its sequence (Park *et al.*, 1998). Its mechanism of action consists of penetrating the membrane without causing permeabilisation and accumulating in the cytosol before binding strongly with DNA, in contrast, the proline deficient magainin 2, causes membrane permeabilisation and stays bound to the lipid bilayer with a low propensity for DNA binding (Kobayashi *et al.*, 2004). Structural comparison between magainin 2 and buforin II using NMR (Bechinger *et al.*, 1993, Yi *et al.*, 1996) determined that magainin 2 is a highly helical structure between residues 2-20 whilst buforin II does not maintain a definitive structure in 50% TFE suggesting a variable structure with a kinked helical conformation. Residues 12-21 at the C terminal are compact and helical with an unordered structure at 1-4 and an extended helix between 5-10 at the N terminal, these two straight helical regions are separated by a proline at position 11 (Park *et al.*, 2000). Both of these peptides have been shown to form toroidal pores within the membrane; however the half life of a buforin II transient pore is significantly shorter than that of magainin 2 allowing the peptide to disassociate from the membrane and accumulate before membrane leakage occurs, in contrast magainin 2 forms transient pores have a longer half live that remain tightly bound to the membrane (Park *et al.*, 2000). This transient pore collapse is electrostatically driven with repulsive forces within the helical

portion of the peptide driving the process. For example buforin II has 5 positively charged residues within the 17 residues that form the helix whilst magainin 2 has the same charge spread over 23 residues so the electrostatic repulsion between the pore forming helices is greater in buforin II. Similarly, in the presence of pure PG, liposome permeabilisation is seen with buforin II due to the attractive electrostatic forces stabilising the pore. However, in PE:PG membranes the pores collapse faster. The kink effect of the Proline is also thought to have a destabilising effect on pore half life with substitution of proline to alanine increasing peptide half life to resemble that of magainin 2 (Kobayashi *et al.*, 2004). Further evidence for the destabilising effect proline can have is found with the pore forming peptide alamethicin where substitution of alanine for proline is known to destabilise the pore (Kaduk *et al.*, 1998)

Sequence analysis for the peptides in this study shows a charge of +2 over the predicted helical section of Smp24 and Pin 2. Coupled with the destabilising proline residue it could be hypothesised that these peptides represent a “half way house” between buforin II and magainin 2 in which both longer pore half lives are noted compared with buforin II due to reduced charge but the peptide can still disassociate from the membrane and interact with DNA due to Pro destabilisation. This may account for the peptides membrane permeable effect seen within the Baclight assay and possible interaction with DNA.

The precise structural conformation that is driving DNA binding seems to be hard to elucidate with sequence analysis between intracellular targeting peptides low and a range of structures being able to bind to DNA, therefore trying to predict and rationalise this phenomena into rational AMP design will be difficult and further research on AMP intracellular interaction needs to be undertaken (Nicholas, 2009). However it was noted by Park *et al.* (2000) that removal of the N terminal disordered region negated buforin

II's antimicrobial properties and, whilst peptides that showed DNA binding in this study are predicted to be helical at the N-terminal, significant disorder is predicted at the C-terminal which could facilitate nucleic acid interaction. It would be of interest to substitute the proline residue within Smp 24 & Pin 2 for an alanine as seen in buforin II to determine if DNA interaction still occurs.

Whilst the prevailing consensus is that membrane disruption is the primary mechanism of AMP activity, it is worth remembering the role of these peptides *in vivo* especially in scorpion venom. The total amount of venom produced per scorpion through artificial electrical stimulation of the venom gland is around 0.5mg and it would not be expected that a scorpion would inject such a large quantity of venom naturally (Oukkache *et al.*, 2013). Thus the concentration of AMP excreted will be at a very low concentration (low μg or ng) therefore it is possible that *in vivo* the AMP exerts its effect through intracellular targeting or through a synergistic effect with other venom peptides.

The intracellular stress responses of Smp43 are limited to the cell wall/membrane. Considering the high homology between the peptides within the present study and the Pandinin peptides it is worth again considering the mechanism of action of the latter two.

The localised pore formation seen with Pin 2 highlights the possibility of membrane interaction being a prelude for the peptide to cross the membrane into the cytosol and interact with the intended target. In contrast Pin 1 generalised degradation causes massive disruption of membrane integrity. Therefore, it could be rationalised that if Smp24 had a localised pore forming mechanism, intracellular targeting could follow, whilst the generalised membrane disruptive effect of Smp43 would not necessitate intracellular targeting.

As is seen in antimicrobial assays of the five biologically active peptides there are wide differences in MIC values, especially between Gram negative and Gram positive organisms, with all peptides showing preferential activity towards Gram positive bacteria-in keeping with α -helical peptides from scorpion venom.

The decreased susceptibility of Gram negative organisms to AMPs has been noted previously with a variety of mechanisms proposed. A number of studies have shown AMP resistance to be mediated via two component signalling pathways that are directly responsible for AMP sensing. For example in *Enterobacteriaceae*, after outer membrane peptide uptake the cationic peptides bind to the anionic face of the PhoQ sensor kinase found within the periplasmic space leading to the activation of genes associated with the PhoPQ system (Bader *et al.*, 2003). Activation of this two component systems have a profound effect on the outer membrane has been shown to be responsible for reducing average O-antigen chain-length, acylating, deacylating, and hydroxylating lipid A, lipid A and LPS core phosphate modification with cationic groups, palmitoylation of outer membrane PG and increase in cardiolipin levels, and the expression of basic outer membrane proteins which alter membrane architecture making AMP penetration less favourable in a number of bacteria.

Similar systems in *P. aeruginosa* has been discovered termed CprRS and ParRS which act independent to each other (Fernandez *et al.*, 2010) whilst in *Salmonella Typhimurium* the RcsFCDB phosphorelay system is responsible for an increase in resistance via the lipoprotein RcsF, which is located in the inner leaflet of the outer membrane, that, after sensing, activates the system in an as yet undefined fashion. This ultimately leads to the expression of capsule genes and production of colanic acid, which is a precursor of 4-amino-4-deoxy-L-Arabinose (L-Ara4N) and is responsible for polymyxin B resistance due to lipid A modification (Farris *et al.*, 2010).

Proteolytic degradation, capsule production, membrane modification and both efflux and influx pumps has also been identified in Gram negative organisms. Degradation of AMPs has been associated with outer membrane proteases, for example the evolutionary conserved omptin family found within the *Enterobacteriaceae* of which OmT from *E.coli* is a classical example (Hritonenko *et al.*, 2007). Another omptin protease from *Citrobacter rodentium*, a rare cause of urinary tract infection, termed CroP causes AMP degradation with these proteolytic fragments then transversing the outer membrane and activating PhoPQ thus further decreasing susceptibility (Le Sage *et al.*, 2012).

The ability of certain organisms to limit the amount of peptide reaching the outer and inner membranes via encapsulation is also a well recognised strategy for AMP resistance. For example the presence of capsule polysaccharides (CPS) around *K. pneumoniae* is known to protect against AMPs. Typically, these structures are anionic presumably to facilitate cationic peptide binding (Llobet *et al.*, 2008). The formation of biofilms, which renders a large number of antibiotics ineffective compared with planktonic culture, are also noted as a mechanism for AMP resistance. Typically the extracellular matrix of biofilms is largely composed of exopolysaccharides which are anionic in nature and function by the same electrostatically driven deactivation method as CPS capsules (Sutherland., 2001), for example *P. aeruginosa* has been shown to inactivate the human cathelicidin LL-37 via production of a b-D-manuronate and a-L-guluronate containing polymer alginate (Herasimenka *et al.*, 2005).

Changes in outer membrane structure have also been shown to be a major factor in AMP resistance especially modification of LPS which can be achieved through modification *in situ* or during synthesis after activation via a two component pathway and reduces the overall negative charge of the LPS molecule thus reducing electrostatic

attraction (Gunn *et al.*, 2000). Such modifications have been noted in a number of species including *E. coli*, *P. aeruginosa*, *S. typhimurium* and *Neisseria spp.* (Richards *et al.*, 2012).

The presence of membrane transporter systems is a highly effective strategy to remove antibiotic agents from the periplasmic and cytoplasmic space and is seen in a number of resistance mechanisms especially against antimicrobial agents with intracellular targets (Otto. 2009). Both efflux pumps and influx pumps are associated with AMP resistance, for example the Sap ABC importer system in *S. Typhimurium* transports AMPs from the periplasmic space to the cytoplasm following binding to the SapA periplasmic protein where they are then degraded and used as a nutrient source (Parra-Lopez *et al.*, 1993). Conversely, efflux pumps have been associated with resistance in a number of species including *K. pneumoniae* and *N. gonorrhoeae*. In *K. pneumoniae* the AcrAB pump is associated with resistance (Padilla *et al.*, 2010) whilst in *N. gonorrhoeae* the MtrCDE pump is required for resistance (Veal *et al.*, 1998).

The present study shows the difficulty in discovering effective antimicrobial agents against Gram negative organisms. This failure to develop new antibiotics against this class of organisms further highlights the need for empirical compound discovery research to widen the cohort of molecules less susceptible to these complex resistance mechanisms (Silver. 2011).

Further studies on a range of *S. aureus* strains revealed wide discrepancies in MIC values especially between EMRSA-15 and EMRSA-16. It is of interest to determine how resistance towards other membrane active peptides has been characterised.

Daptomycin, a 13 residue lipopeptide which has a ring formation within its structure incorporating residues 3-10 linked through an ester bond between a kynurenine and

threonine residues, forms pores in bacterial membranes in a calcium dependent manner in the presence of PG (Straus and Hancock. 2006; Zhang *et al.*, 2014).

Recently decreased susceptibility to Daptomycin has been described in *S. aureus* (Mishra *et al.*, 2014, Tsukimori *et al.*, 2014) along with *B. subtilis* (Hachmann *et al.*, 2011) and a number of *Enterococcus* strains (Saito *et al.*, 2014). These higher MIC values have been associated with infection where a sub therapeutic dose has been administered that has been lower than the concentration required for mutation inhibition (Nannini *et al.*, 2010) according to the mutation selection window concept (Drlica *et al.*, 2007). These mutations have occurred in genes that have caused changes in the architecture of the cell membrane. For example, mutations in *mprF* have resulted in the ability of the bacteria to increase the net surface charge of the membrane by the conversion of PG to lysyl-PG due to the production of lysyl-PG synthase (Friedman *et al.*, 2006), similarly net surface charge is altered by the alanylation of teichoic acid due to the over expression of the *dltABCD* operon (Yang *et al.*, 2009). Other cell membrane associated changes described included a decrease in production of PG in *B. subtilis* via mutations in the *pgsA* allele which encodes the PG synthase gene *pgsA* (Hachmann *et al.*, 2011). However, this mutation only increased the MIC from to 1 to 2 µg/ml over a 5 year period, highlighting the slow evolution of resistance towards this membrane active peptide. The increased presence of cardiolipin within *Enterococcus* strains has caused decreased susceptibility to daptomycin and is conferred by mutations that alter the cell envelope stress response (*liaFSR*) including mutations that increase the activity of cardiolipin synthase (Davlieva *et al.*, 2013). Changes in the cell wall have also been implicated with increase cell wall turnover via mutations in the gene *yycG* that encodes a histidine kinase (Mishra *et al.*, 2012). Also increased thickness of the cell wall associated with decreased vancomycin susceptibility, a glycopeptide that inhibits cell wall synthesis, has also been associated with an increase in daptomycin MIC that has

been postulated to be due to the molecule becoming trapped in the cell wall (Van Hal *et al.*, 2011).

Resistance has also been observed against nisin, a 34 residue peptide produced by *Lactococcus lactis* number of resistance mechanisms have been described including cell wall thickening through increased teichoic acid facilitated by the *dlt* operon (McBride and Sonenshein, 2011), cell membrane biosynthesis and removal of the peptide from the cytoplasm (Kramer *et al.*, 2006) and the production of the nisin resistance protein which causes inactivation of nisin via reduction of the carboxyl alanine (Sun *et al.*, 2009).

Interestingly, these resistance mechanisms are mediated through genomic changes rather than being plasmid mediated (Kramer *et al.*, 2006). Resistance towards membrane active agents, especially in *S. aureus*, have arisen due to mutations within the genome rather than acquired by plasmid uptake. Whilst resistance is observed in the current study by certain *S. aureus* strains this is likely due to an increase resistance to lipopeptides such as vancomycin which has been shown a prerequisite for increased resistance to membrane active agents as a consequence of cell wall thickening and the likelihood of a substantial increase in antimicrobial peptide resistance after repeated exposure remains low (Mishra *et al.*, 2012).

In summary, three scorpion AMPs have been characterised from the venom of *S. maurus palmatus*. Two of these peptides (Smp24 & Smp43) showed broad spectrum antimicrobial activity but different haemolytic effects whilst the third shorter peptide had no biological activity. Modification of Smp24 led to both beneficial and adverse biological effects and highlighted the potential for further manipulation of these peptides as AMP scaffolds. Both show the classical membrane disruptive mechanism of action, however Smp24 and its derivatives along with Pin 2 showed evidence of DNA interaction.

Based on alignment with other scorpion AMPs the longer peptide Smp43 has a helical-hinge-helical structure, allowing for a high therapeutic index and exerts its effects through a carpet model mechanism. The shorter peptide, Smp24 has a lower therapeutic index with a helical region at the N-terminal and unordered structure at the C-terminal with a pore forming mechanism being hypothesised

This study highlights the beneficial effect a helical-hinge-helical conformation has on an AMPs biological activity in line with other previous studies (Galanth *et al.*, 2009) and it is these peptides should be the focus of further AMP development.

5 CHAPTER 5
BIOPHYSICAL CHARACTERISATION OF THE ANTIMICROBIAL
PEPTIDES SMP24 & SMP43 FROM *SCORPIO MAURUS PALMATUS*

5.1 Background and Aims

A central question in AMP research is understanding the mechanism by which peptides interact with a phospholipid bilayer. As described in chapter 1, three main mechanisms have been proposed, the barrel stave, toroidal pore and carpet model, however, more recent models have also been proposed (Teixeria *et al.*, 2012).

The use of atomic force microscopy to image planer lipid bilayers has become a well-established technique (El Kirat *et al.*, 2010), however it has only recently been employed to determine the mechanism of action of AMPs.

Won *et al.*, (2011) examined the effects of anoplin a 10 residue amidated α -helical peptide isolated from the venom of the solitary wasp *Anoplius samariensis*. Using the native peptide and 2 derivatives, a non amidated version (An-OH) and a D-amino acidic (D-AN-OH) version, AFM images collected in air clearly shows the formation of lipid domains of both DPPC & DPPG bilayers upon AN-OH and AN-NH₂ interaction with these domains having a height of approximately 2 nm with varying diameters in the tens to hundreds of nanometre range, however the size of these domains were smaller upon AN-NH₂ interaction compared with the acidic free form. Fernandez *et al.*, (2012) investigated the mechanism of aurein 1.2, a 13 residue amidated peptide isolated from the skin of various Australian frogs using both AFM and QCM-D to determine a carpet model mechanism of action. QCM-D analysis showed a 15% reduction in lipid content with the negatively charged bilayer compared with 5% with the DMPC model. AFM imaging was undertaken on both membrane model systems in vesicle form at 0.67 μ M and 6.7 μ M peptide concentrations. At the lower concentration no effects were observed, however, at the higher concentration the vesicles are destroyed and the formation of smaller collapsed vesicle like structures are seen, reflecting the detergent/carpet like effect of the peptide on both model membranes. In contrast to this

carpet mechanism, Lam *et al.* (2007 & 2012) visualised the effect of the highly positively charged 18 residue peptide protegrin-1 (PG-1) isolated from porcine leukocytes. AFM imaging of a DMPC bilayer showed a concentration dependent effect. At low concentrations (up to 1.5 $\mu\text{g/ml}$) no detectable morphological changes occurred, however the peptide was thought to have bound to the surface of the membrane due to a decrease in perturbation of the soft bilayer during lateral scanning and as the concentration increased up to 2.0 $\mu\text{g/ml}$ morphological changes were observed at the edge of the bilayer with a loss of a smooth edge (line tension). Further increases up to 4.0 $\mu\text{g/ml}$ revealed the development of pores within the bilayer and with further increases in concentration the development of worm like structures which are 9 nm in diameter.

Along with assessing the damage AMPs cause to planer lipid bilayers researchers have also examined their effects on whole bacteria, this offers a number of distinct advantages over SEM, previously utilised to determine whole cell damage, due to the ability of AFM's to be performed in pseudo native conditions and the possibility of introducing the peptide during the time course of the experiment. Lu *et al.*, (2014) examined the effects of two AMPs on *P. aeruginosa* with the loss of membrane integrity determined by efflux of the cytoplasmic contents of the cell and changes in the viscoelastic properties of the cells during force spectroscopy, similarly Li *et al.*, (2007) showed the complete collapse of the cell structure of *E. coli* and *P. aeruginosa* using endotoxin-binding Sushi peptides. Of particular interest is the use of high speed AFM to image the effect of CM15 on an *E.coli* cell in which the peptide is seen binding to the live cell and then once a critical concentration can is reached the cell membrane losing complete integrity and a crumpling effect observed (Fantner *et al.*, 2010). This study represents the first of its kind to capture the dynamic process from start to finish on a living cell. One criticism of using AFM to image whole cell events is that, whilst

providing informative images of membrane damage near physiological conditions the resolution is poor typically in the high nm to low μm range and no individual events such as pore formation are observed as are seen in planar lipid bilayer studies.

In this study we examine the mechanism of action of Smp24 and Smp43 using a variety of biophysical techniques.

5.2 Method Summary

The mechanism of action of the two AMPs Smp24 and Smp43 was examined using a number of biophysical techniques using synthetic membranes which mimic prokaryotic and eukaryotic membranes. Methods included CF release assays, QCM-D and AFM on hydrated planer lipid bilayers. The effect of the incorporation of CR and CL were also examined.

5.3 Results

5.3.1 Analysis of Smp24 using liposome leakage assays

Liposome leakage assays were performed on a number of different liposome compositions. Against a negatively charged lipid membrane (PC:PG (1:1)) significant membrane disruption starts to occur at 1.25 μM Smp24 with 37.7% (± 1.7) CF release, increasing peptide concentration to 2 μM caused a maximum CF release of 70.9% (± 2.6) (Fig. 5.1). The gradual release of CF at increasing concentration is suggestive of pore formation rather than a carpet mechanism as complete membrane collapse is not observed. The electrostatic nature of this attack has also been examined with a decrease in CF release in the presence of 500 mM NaCl, for example at 1.25 μM Smp24 only 6.25% (± 1.0) CF release is observed whilst 53.3% (± 2.19) release is seen at 2.0 μM (Fig. 5.1).

Against a neutrally charged bilayer (PC:PE (1:1)) CF release is less pronounced with only 19.6% (± 1.7) observed at 1.25 μM peptide concentration. As against PC:PG, no membrane collapse is observed with a gradual increase in CF release is seen until a maximal release of 48.7% (± 2.0) (Fig. 5.2). However unlike with PC:PG membrane disruption is not driven by an electrostatic interaction with no difference in lyses observed in the presence of 500 mM NaCl (Fig. 5.2).

The inclusion of cardiolipin (10%), found within some bacterial membranes, increases CF release at Smp24 peptide concentrations above 1.25 μM compared with the PC:PG bilayer with 100% release seen at 1.75 μM and above (Fig. 5.1). Unexpectedly, the inclusion of cholesterol into both PC:PG and PC:PE membranes increased CF release with Smp24 (Fig. 5.1 & 5.2). The possible reasons for this are discussed in the discussion of this chapter. Against PC:PG:CL (45:45:10) complete CF release is observed at 1.0 μM peptide concentration (Fig. 5.1), however against PC:PE:CL CF release increases to 72.4% (± 0.8) at 1.25 μM Smp42 and to a maximum of 89.0% (± 2.8) at 2.0 μM peptide concentration (Fig, 5.2).

Effect of varying concentrations of Smp24 on PCPG bilayers

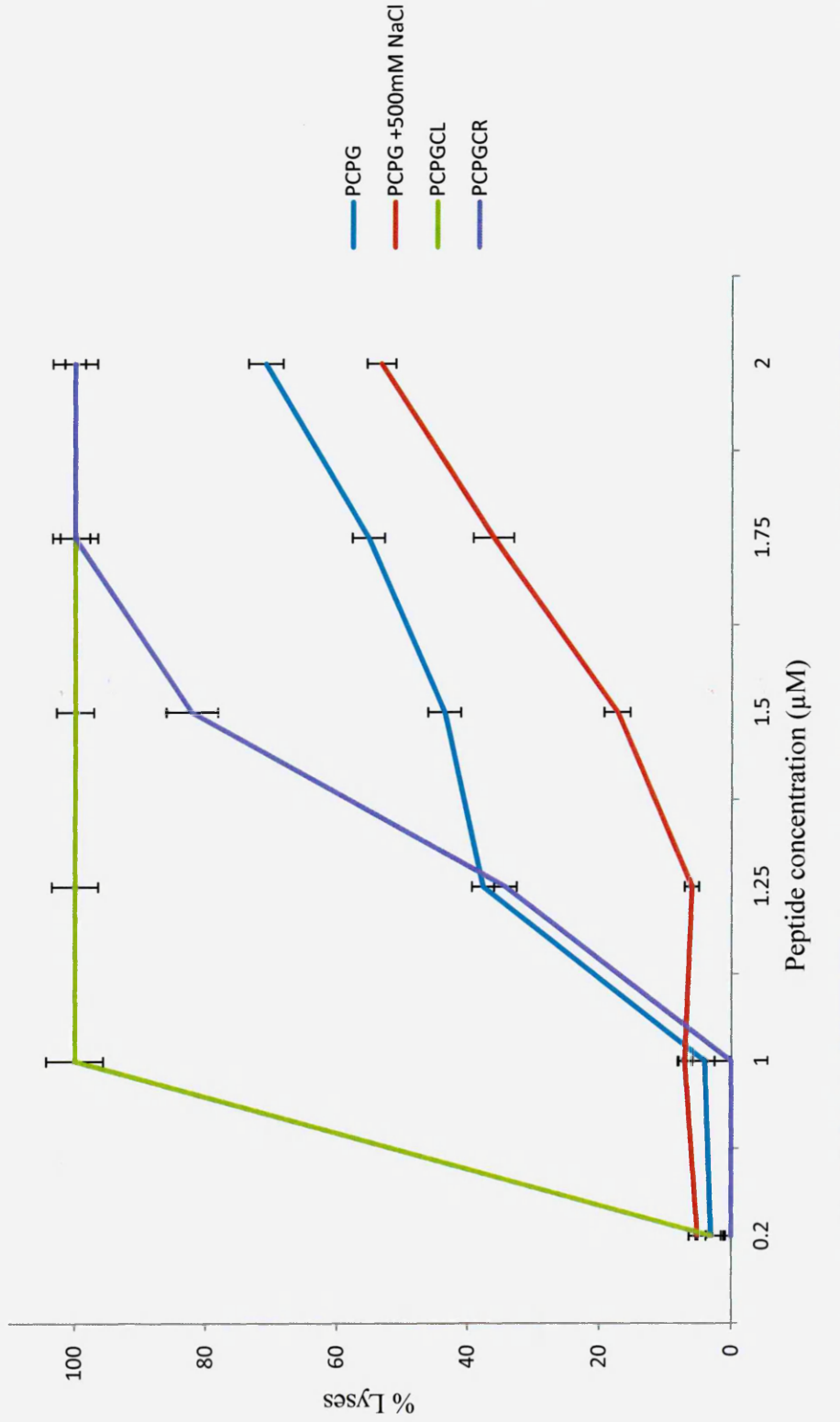


Figure 5.1: Effect of Smp24 against a number of PCPG bilayers at varying concentrations. Blue line- a maximum of 70.9% lysis is observed PCPG at 2μM, however in the presence of 500mM NaCl a significant decrease in lysis is observed at 2μM (53.3%). The inclusion of cholesterol (green) and cardiolipin (purple) increased the lytic activity of Smp24.

Effect of varying concentration of Smp24 on PCPE bilayers

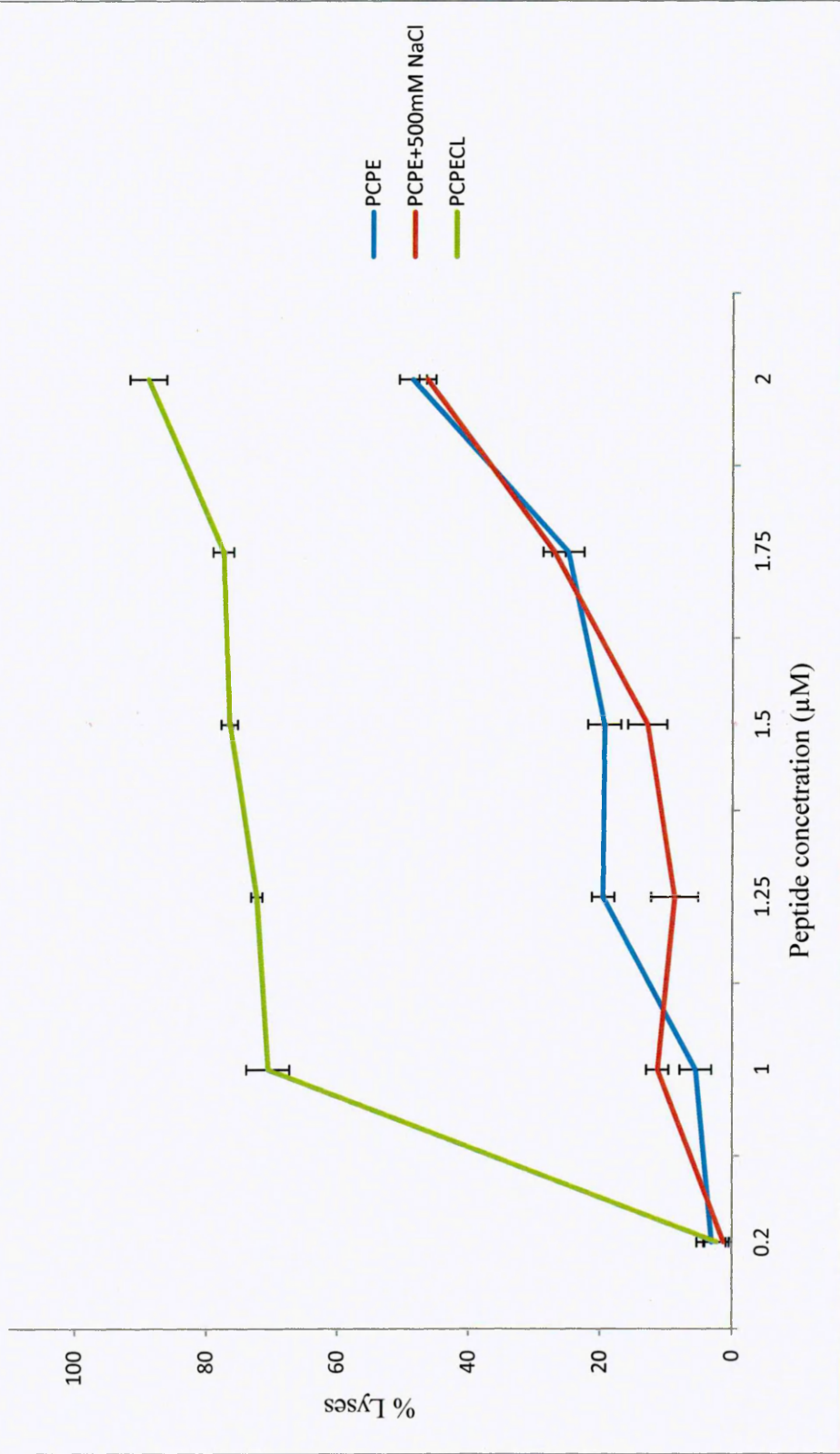


Figure 5.2: Effect of Smp24 against a number of PCPE bilayers at varying concentrations. Blue line- a maximum of 48.7% lysis is observed PCPE at 2μM, however in the presence of 500mM NaCl no significant difference in lysis is observed. The inclusion of cholesterol (green) significantly increased lysis to 72.4% at 2μM.

5.3.2 Analysis of Smp24 attack on hydrated lipid bilayers using AFM

To visualise the membrane disruptive mechanism of Smp24, AFM was undertaken on hydrated lipid bilayers following attack with Smp24 at 1.25 μM and 2.0 μM against the following bilayer compositions; PC:PG, PC:PE, PC:PG:CL along with a bilayer that exhibits phase separation where clear lipid ordered and lipid disordered domains can be observed. This phase separated bilayer had a composition of PC/SM/CL (1:1:0.67) (SM- sphingomyelin).

A smooth bilayer is observed before peptide attack with clear lipid ordered (L_O) and lipid disordered (L_d) seen with the light areas been in the L_O phase (figure 5.3a). After peptide attack at 1.0 μM the smooth appearance of these L_O domains begin to diminish and, whilst pore formation is not observed, the loss of the smooth appearance within the lipid ordered areas has implications for the nature of peptide mechanism of action (Fig. 5.3b-f-consecutive scans 5min/frame). The PC:PG bilayer exhibits a smooth appearance before peptide attack (Fig. 5.4a) however after 5 minutes of incubation vesicles are observed blebbing off the surface (Fig. 5.4b), a further 5 minute incubation led to pore formation as revealed in figure 5.4e & f. These pores vary in size with a number of different pores detected having a diameter between 23.49-39.9 nm (Fig. 5.5). The depth of these pores range between 2-4 nm and so do not represent the removal of a full bilayer. An increase in peptide concentration (Fig. 5.6a & b) to 2.0 μM caused the complete destruction of the bilayer with large vesicle formation and a marked softening of the bilayer seen in lateral scanning, reflecting the dramatic effect slight changes in the peptide: lipid ratio has

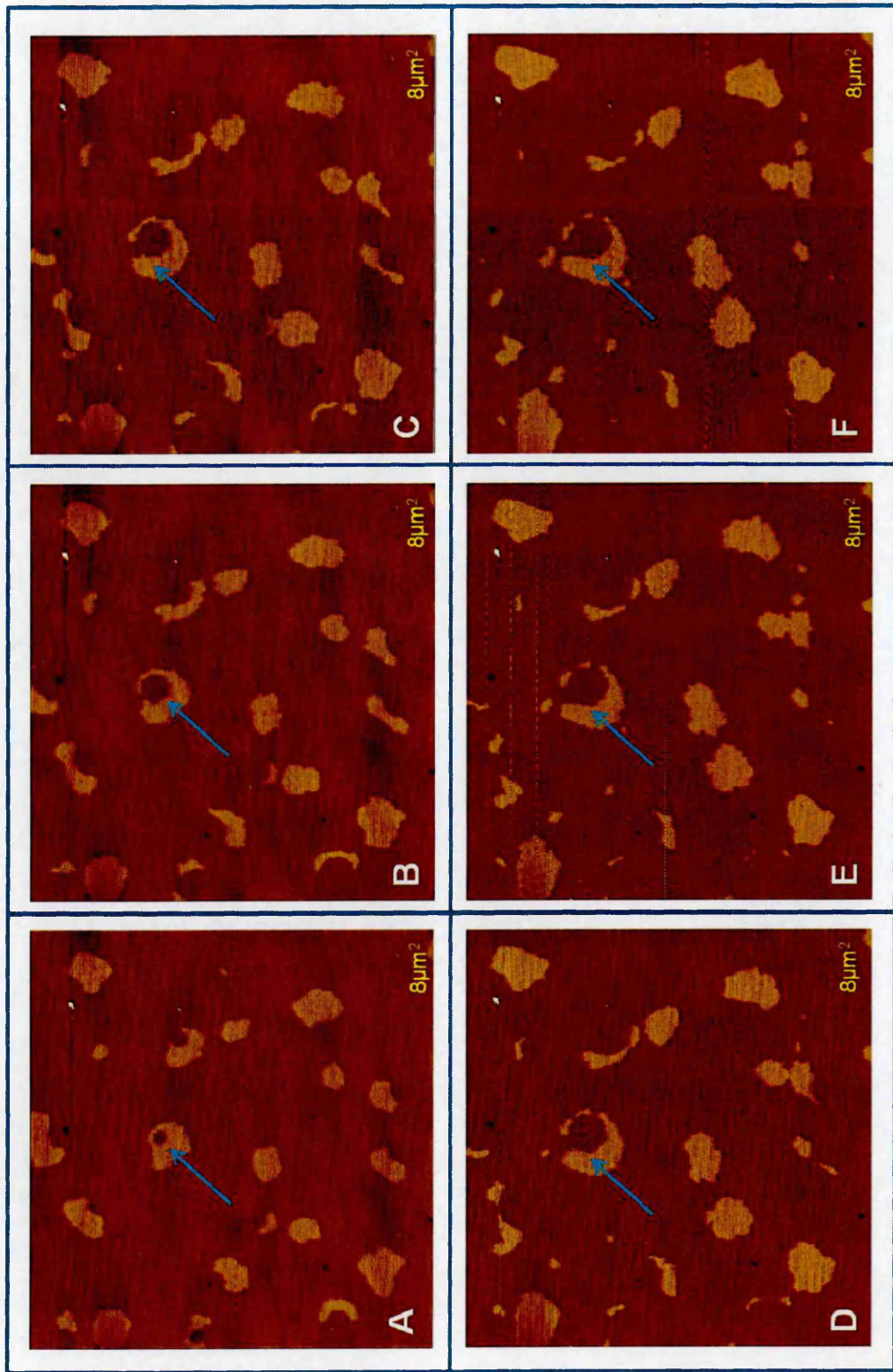


Figure 5.3: The effect of Smp24 on a phase separated bilayer at 1.0 μM determined by AFM. (A) before Smp24 attack (B) After 5 minutes incubation the line tension is beginning to relax with further relaxation of line tension within the lipid order phase of the 30 minute incubation time (B-F)

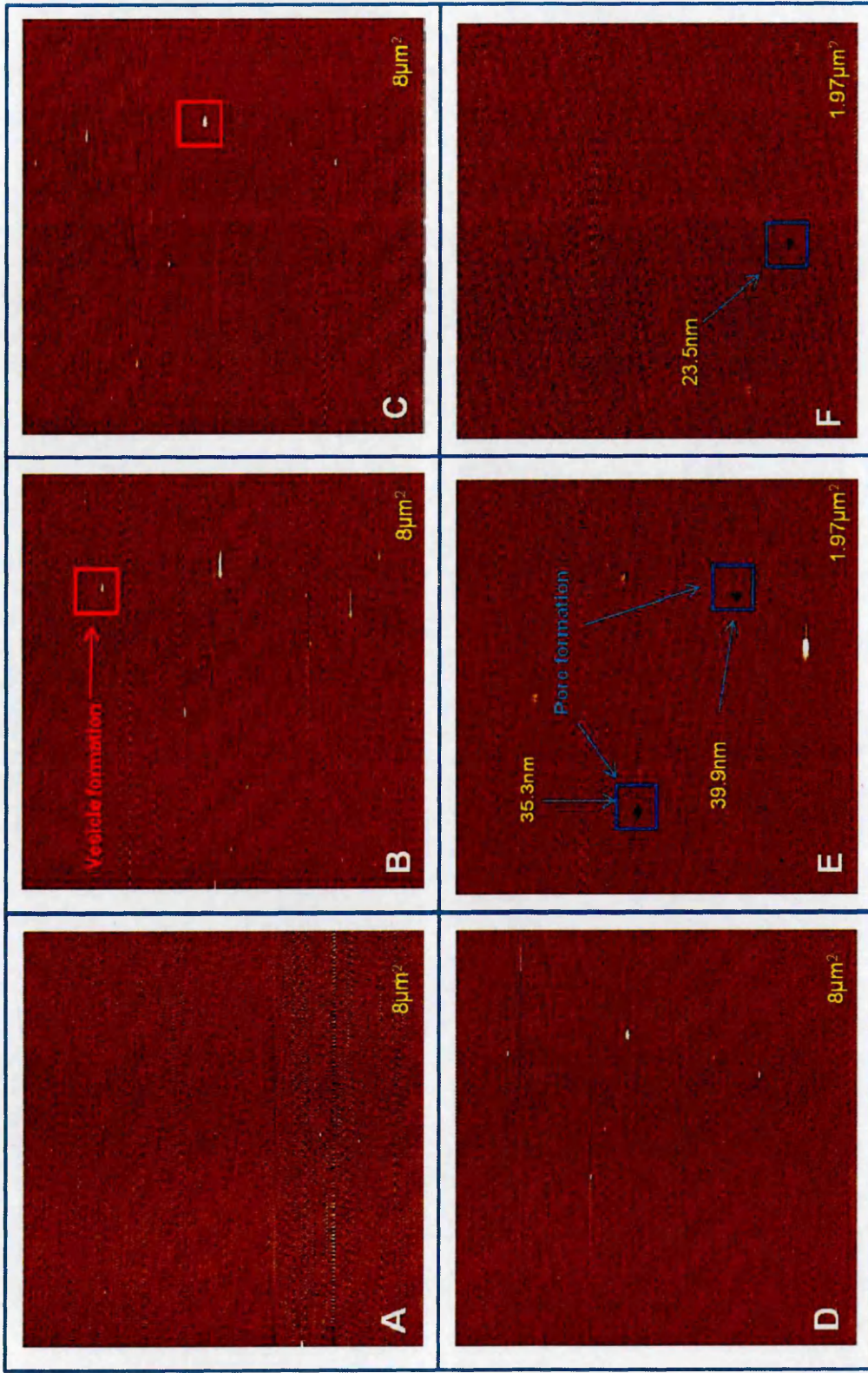


Figure 5.4: The effect of Smp24 attack on a PCPG bilayer at 1.25 μM determined by AFM. (A) Before Smp24 attack a smooth bilayer is observed. (B) after 5 minutes incubation vesicle formation is observed characterised by white patches appearing in the height image (C-D0 further vesicle formation is observed (E-F) pores of varying size observed within the the bilayer.

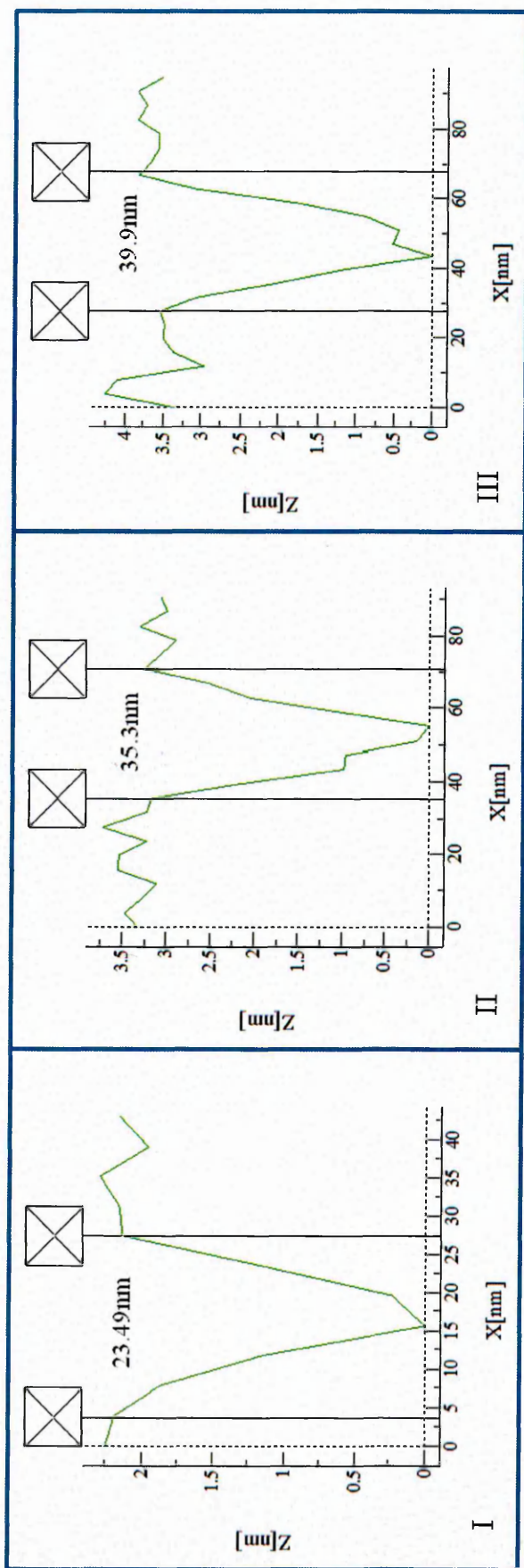


Figure 5.5: Analysis of pore size detected within a PCPG bilayer after 1.25 μM Smp24 attack. Each pore has a varying diameter.

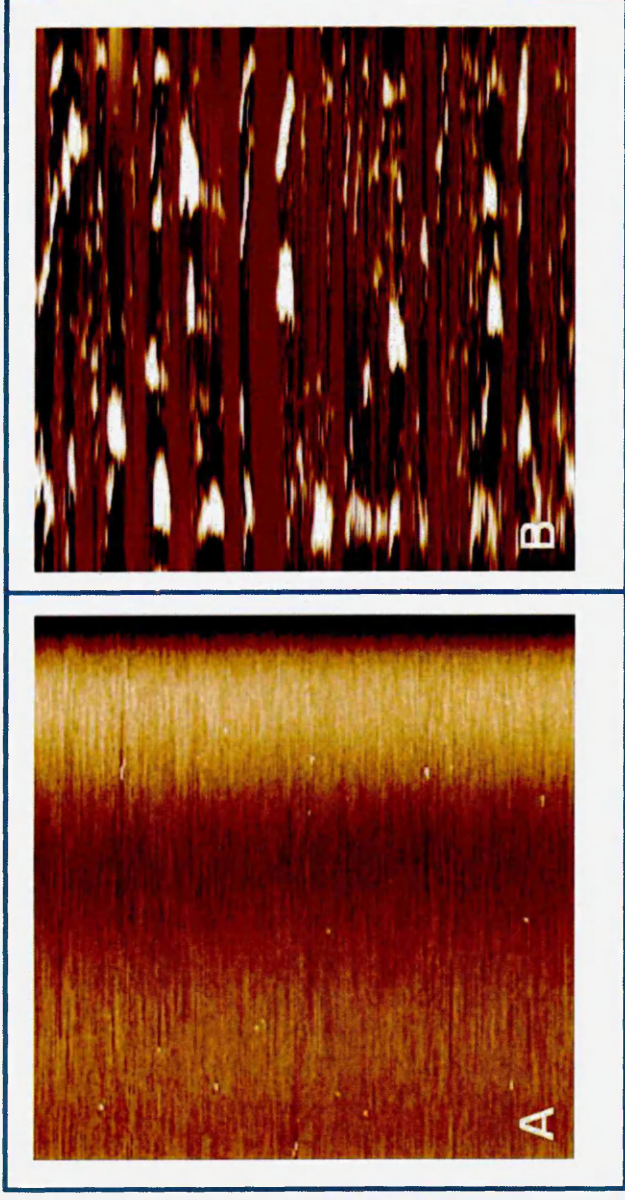


Figure 5.6: The effect of Smp24 attack on a PCPG bilayer at 2 μM determined by AFM (A) a smooth bilayer is observed before Smp24 attack. (B) Complete disruption of the bilayer is observed after only 5 minutes incubation

Figure 5.7 shows the effect of Smp24 at 1.25 μM on a neutrally charged PC:PE bilayer ($8 \mu\text{m}^2$ at 1.97 Hz) with figure 5.11a showing the bilayer before peptide attack. Upon peptide attack (B-D consecutive scans 5 min/frame) vesicle and pore formation are not observed, instead removal of the bilayer in 'stratified lines' is seen (Fig. 5.7f). Analysis of these disrupted areas (Fig. 5.8a) reveals these areas are approximately 200 nm in width and within these areas a varying depth of disruption (i.e. bilayer removal) is seen ranging between 2-4 nm. Increasing the concentration of the peptide to 2.0 μM (Fig. 5.9b-f) increases the destruction of these areas however does not cause complete destruction of the whole bilayer as is seen with PC:PG with an increase in the width of these disrupted areas to approximately 350 nm (Fig. 5.8b) however the varying depth of bilayer removal is still apparent.

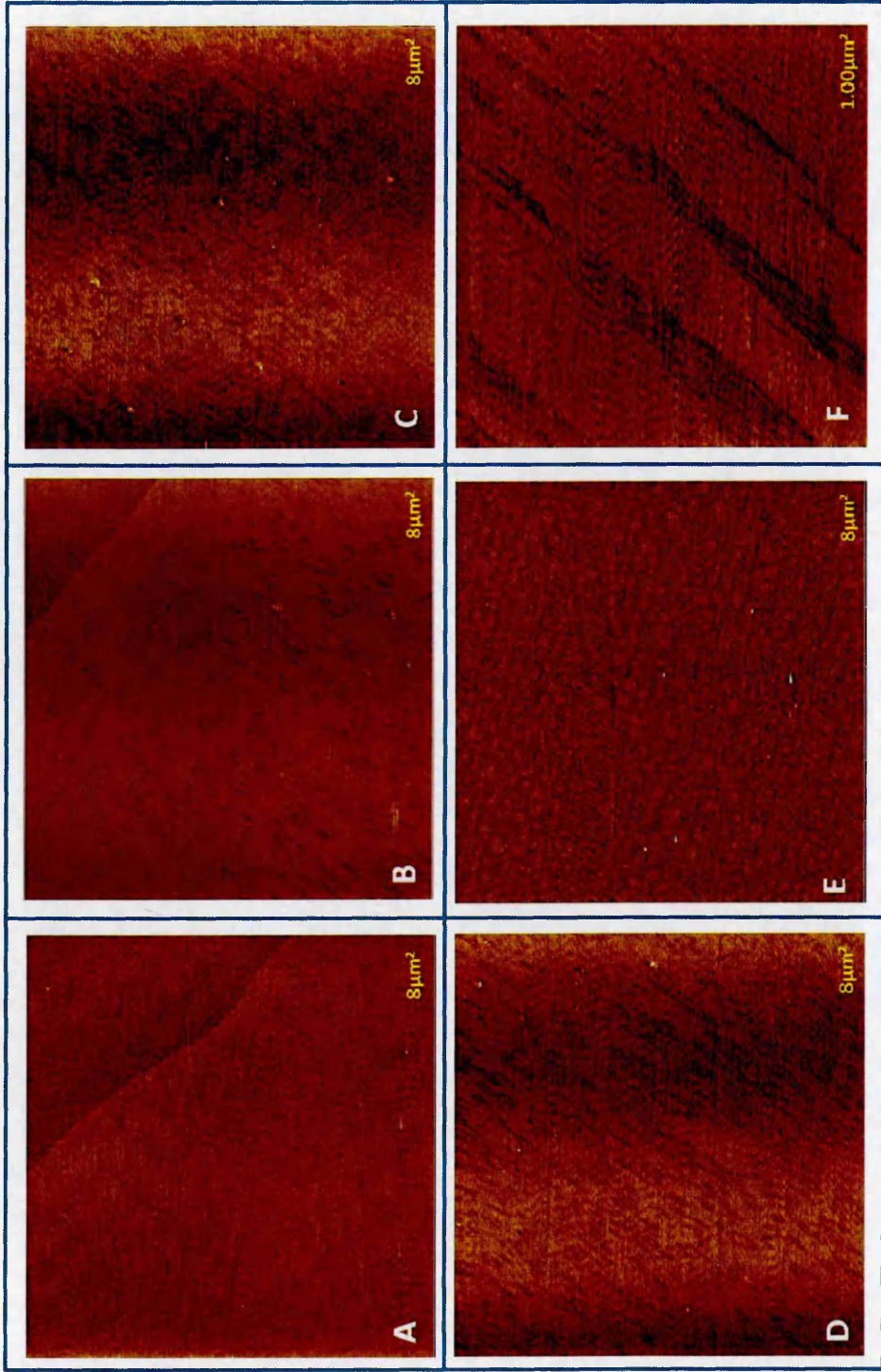


Figure 5.7: The effect of Smp24 on a PCPE bilayer at 1.25 μM determined by AFM (A) a smooth bilayer is observed before peptide attack (B) after 5 minutes incubation localised bilayer disruption is observed. After 10 and 15 minutes (C+D) further disruption is observed however no pore formation is seen.(E) The induction of lipid segregation has also been observed with Smp24 in a PCPE bilayer (F) Zoom in of disrupted areas from (D) shows the formation of 'stratified lines'

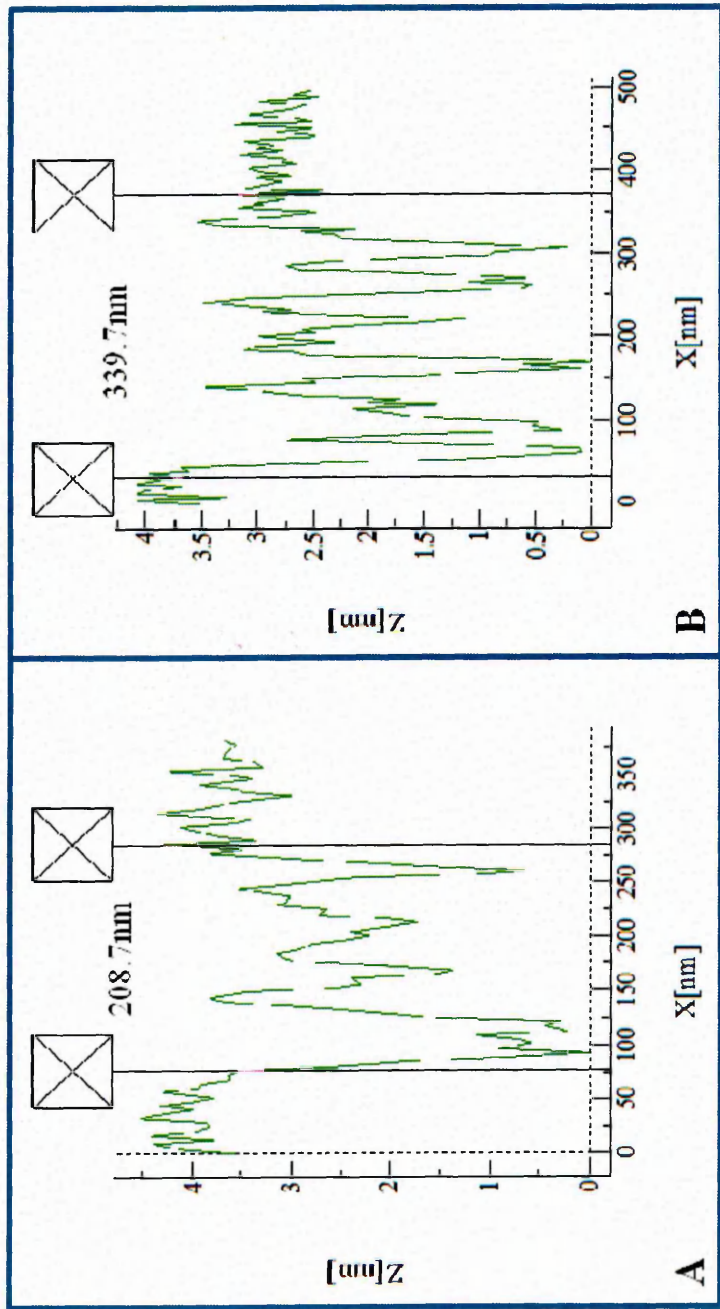


Figure 5.8: The analysis of PCPE bilayer disruption after Smp24 attack at 1.25 and 2.0 μM . height analysis of disrupted areas revealed not all the bilayer is removed within the disrupted areas with these disrupted areas varying in width.

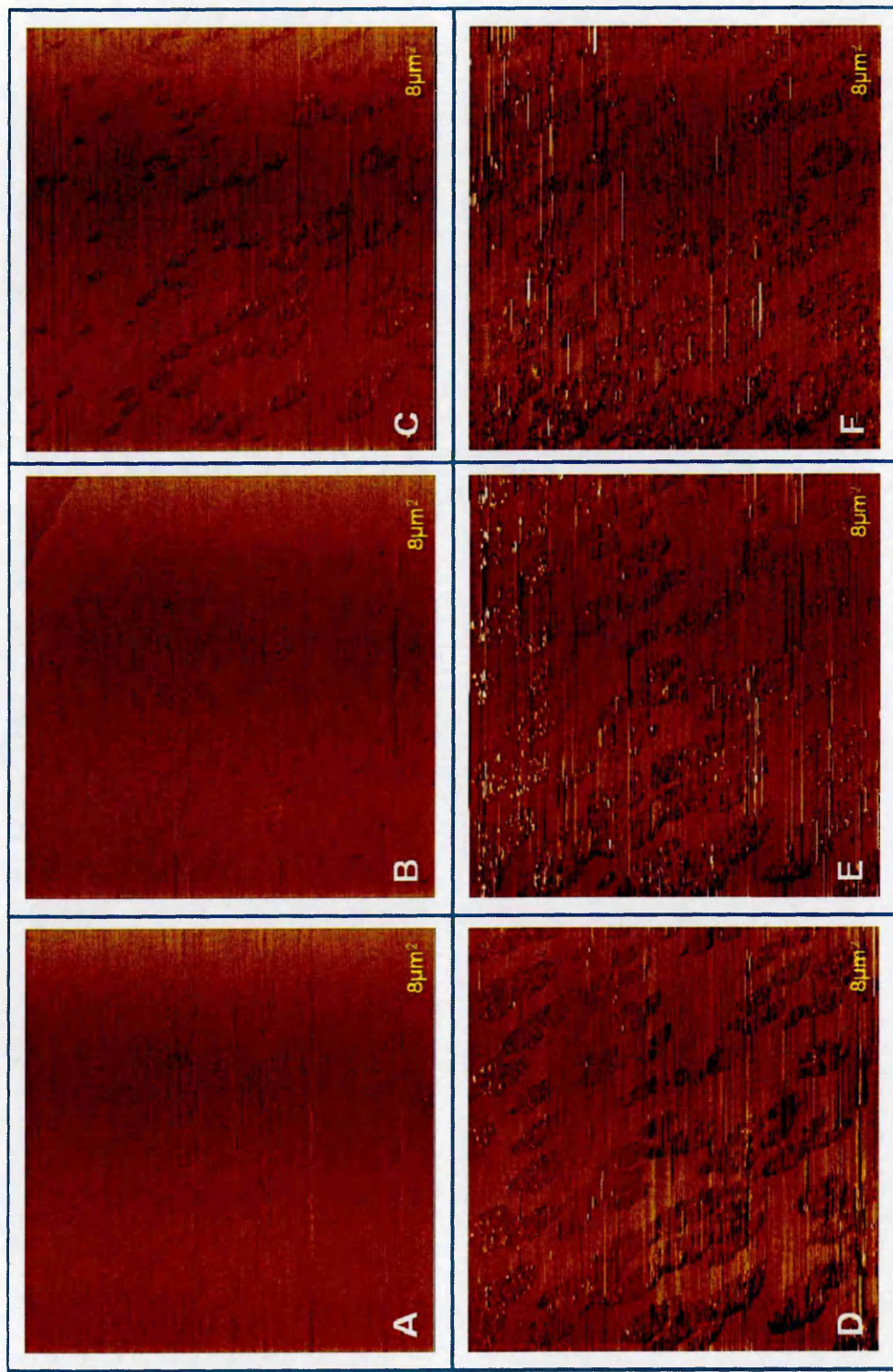


Figure 5.9: The effect of Smp24 on a PC:PE bilayer at 2.0 μM determined by AFM. (A) before Smp24 peptide attack. (B) disruption caused after 5 minutes. (C-F) disruption caused after 10-25 minutes-the areas of disruption are more pronounced than with the lower concentration of 1.25 μM . The presence of vesicle formation (white patches) is also seen in (E) and (F)

The effect of the addition of 10 % CL to a PC:PG bilayer after peptide attack at 1.25 μ M has been determined (Fig. 5.10). Whilst areas of the bilayer before peptide attack contain holes, these holes are still present throughout the attack and do not influence the effect of cholesterol in the membrane. There is a significant difference between the original bilayer and the cholesterol containing bilayer with larger more concentrated areas of membrane disruption occurring rather than discrete pore formation with these areas being similar to the PC:PE bilayer (Fig. 5.10f).

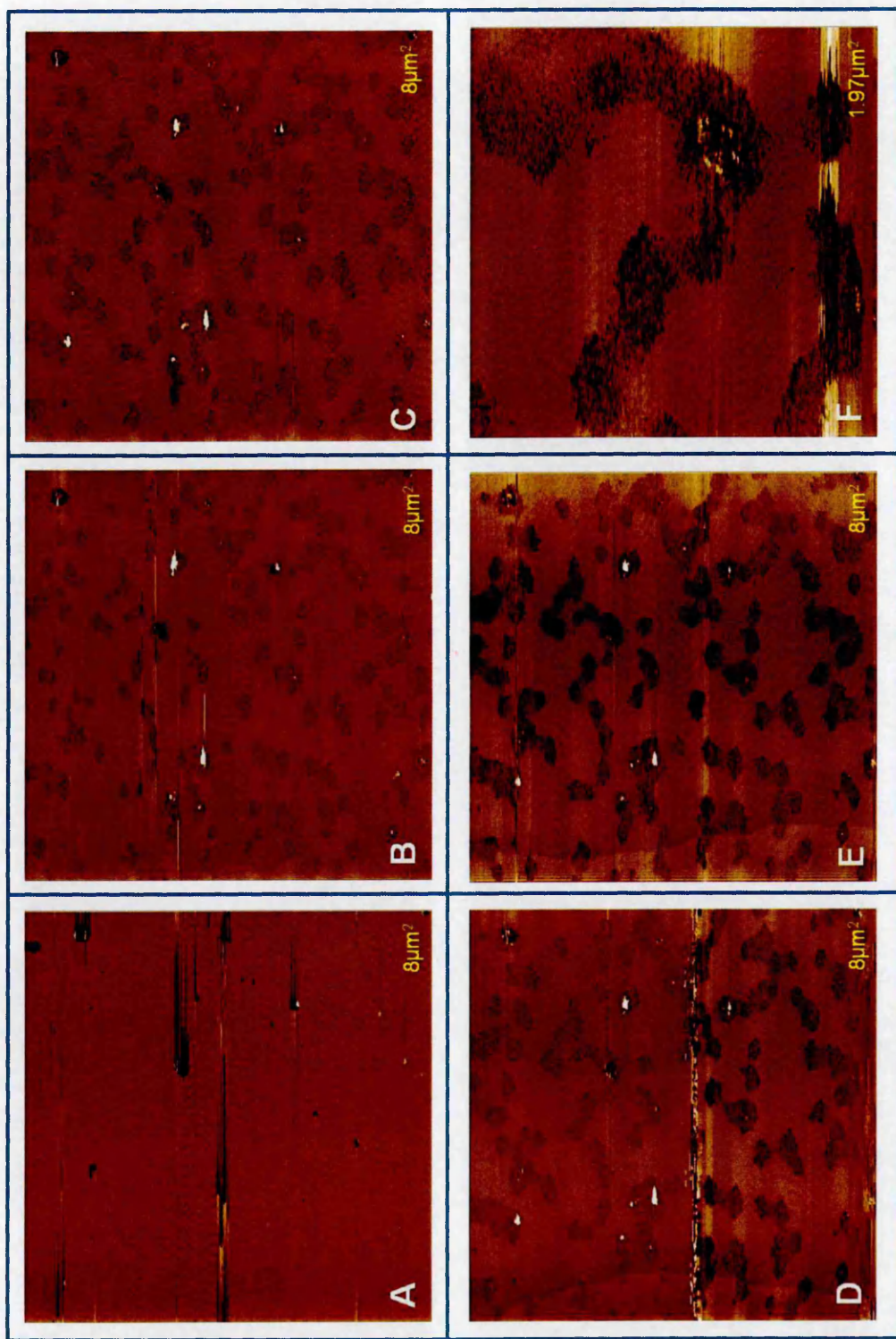


Figure 5.10: The effect of the incorporation of 10 % cholesterol into a PCPG bilayer has on Smp24 attack at 1.25 μM determined by AFM. (A) Before Smp24 attack (B-E) Disruption of the bilayer after 5-20 minutes. (F) Zoom in on disrupted area showing no pore formation with the mechanism more reminiscent of disruption observed in the PCPE bilayer

5.3.3 Analysis of Smp24 attack on hydrated lipid bilayers using QCM-D

Along with liposome leakage assays and AFM the interaction of Smp24 with PC:PG and PC:PE bilayers have also been assessed using QCM-D. QCM-D curves for both bilayers in which the bilayer is attacked with peptide at increasing consecutive concentrations over the same time period are shown in figures 5.11 and 5.12. In each graph the frequency has been inverted, with a decrease in frequency representative of an increase in the peptide upon the surface. The dissipation measurement is a measure of the increased interaction between the crystal surface and fluid environment flowing over the crystal. If the membrane is tightly bound to the surface the dissipation reading will be low, however if after peptide attack the membrane is disrupted and interaction with the fluid environment increases the energy that is lost from the surface of the crystal to the environment increases thus dissipation increases. The frequency and dissipation readings of QCM-D upon interaction with an AMP have been summarised in figure 1.11. For each figure each colour represents the shift in frequency and dissipation over the same time period (20 mins) of different concentrations of Smp24.

Upon Smp24 interaction with the negatively charged bilayer PC:PG at low concentrations (0.1 and 0.2 μM) the frequency decreases from around -24 Hz to -25.5 Hz whilst only a small shift in dissipation from 0.2 to 0.35 is observed. However, at an increase in concentration to 0.75 μM , a marked increase in both peptide accumulation and membrane disruption occurs with the frequency decreasing -25.5 Hz to -37.3 Hz and the dissipation increasing to a maximum of 1.6, this then decreases back down to 1.4. This “swing back” phenomenon could represent the threshold concentration being overcome and incursion of Smp24 into the membrane taking place with a transient stabilisation as peptides lay parallel with the phospholipid chains. A further injection of 0.75 μM Smp24 has little effect with only a small decrease in frequency taking place

down to -39 Hz, however further increases in peptide concentration to 1.25 μM significantly decreases frequency to -45 Hz and increases dissipation to 2.8 reflecting further peptide accumulation and further incursion into the membrane (Fig.5.11).

Whilst large shifts in frequency and dissipation is the over-riding theme of Smp24 attack on the negatively charged model membrane, for the neutrally charged PC:PE bilayer the picture is very different with an increase in frequency from -27.7Hz to -24.4 Hz and a minor decrease in dissipation from 0.66 to 0.44 (Fig. 5.12). The lack of dissipation “swing back” would also suggest that a threshold accumulation and incursion event does not take place. Therefore it is clear both from the QCM-D and AFM images obtained, that a radically different mechanism takes place at the same concentration on different bilayer compositions.

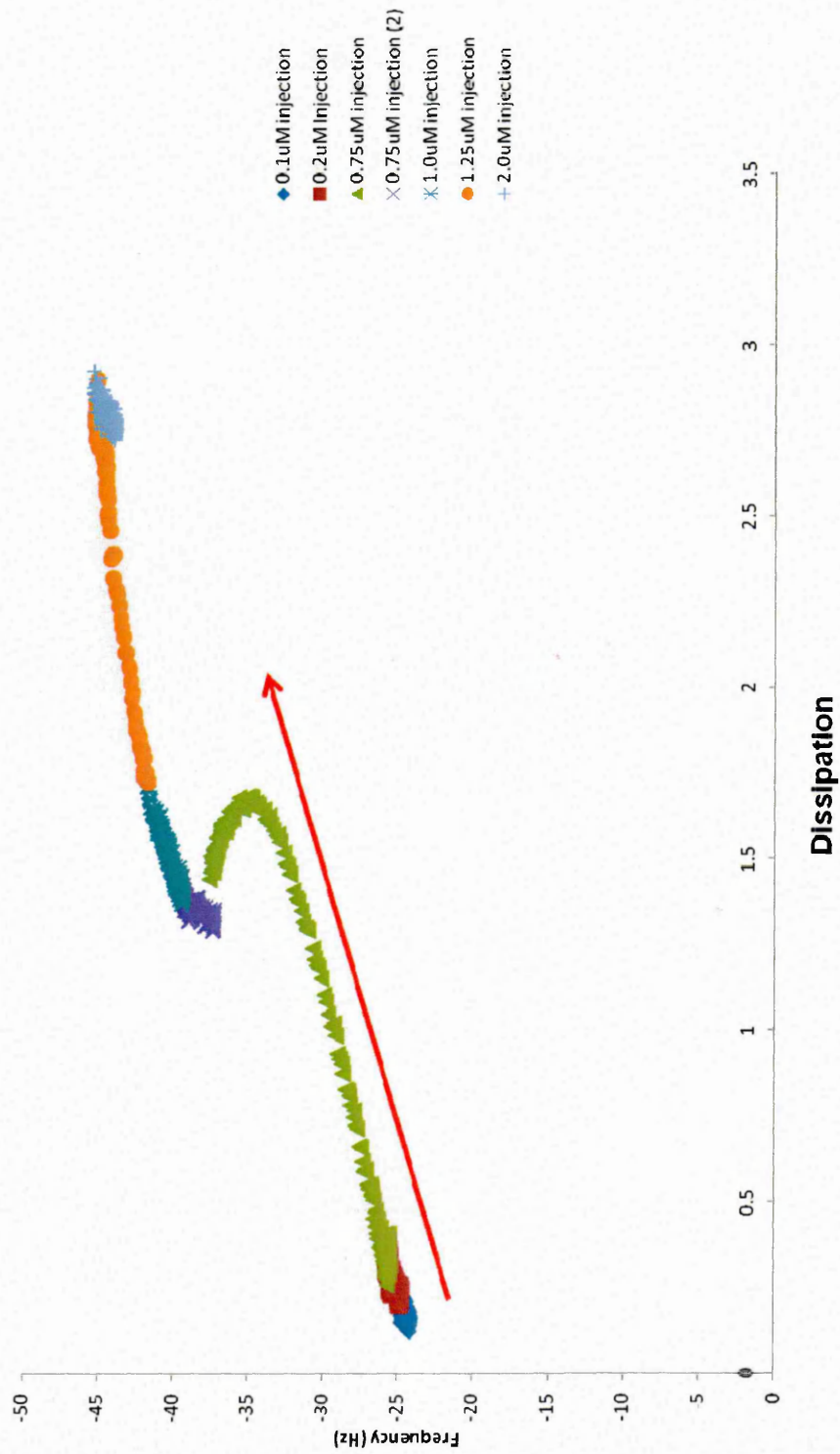


Figure 5.11: QCM-D analysis of Smp24 attack on a PCPG bilayer. The bilayer becomes increasingly fluid throughout the time course of the experiment (increase in dissipation) with an increase in peptide accumulation also observed (decrease in frequency). The red arrow indicates the overall direction of the disruption of the bilayer

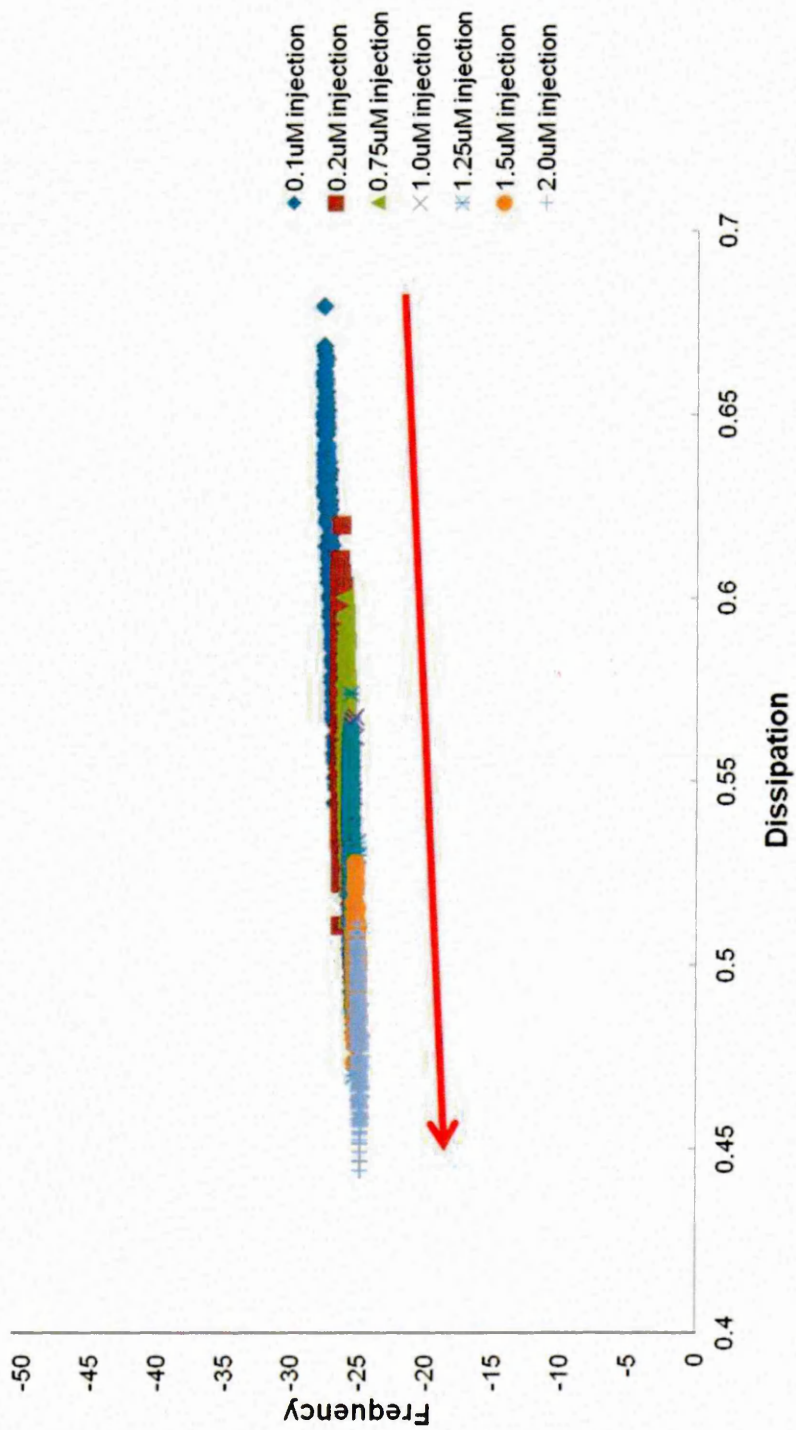


Figure 5.12 QCM-D analysis of Smp24 attack on a PC:PE bilayer. Against a PC:PE bilayer a slight decrease in fluidity is observed throughout the time course of the experiment (decreased dissipation) with only a small amount of peptide accumulation observed (decrease in frequency). The red arrow indicates the overall disruption of the bilayer

5.3.4 Analysis of Smp43 attack on liposomes

Liposome leakage assays have also been undertaken against PC:PG, PC:PE and membranes containing cardiolipin and cholesterol using Smp43. As is seen in figures 5.13 & 5.15 a significant difference in membrane disruption occurs between PC:PG and PC:PE confirming the AFM results. At 1.0 μM Smp24 97.4% (± 4.35) CF release is observed with PC:PG liposomes with maximum release observed at higher concentrations whilst only 9.1% (± 1.8) CF release was detected against a PC:PE composition with Smp43 attack at 1 μM with a maximum CF release of 46.3% (± 2.0) at 2.0 μM . The electrostatic nature of attack was also examined. In the presence of 500 mM NaCl the effect of Smp43 on PC:PG was significantly diminished with only 30.6% (± 4.1) CF release seen at 1.0 μM compared with 86.5% (± 6.8) at the same concentration in the absence of NaCl when tested at a concentration range of 0.2-1.0 μM (Fig. 5.14). In contrast when 500mM NaCl was included with PC:PE no significant difference in CF release was observed with 42.3% (± 1.0) release observed at 2.0 μM compared with 46.3% (± 2.0) with no NaCl (Fig. 5.15).

CL was also incorporated into each membrane composition at a concentration of 10%, and as is seen in figures 5.13 and 5.15 it has contrasting effects on CF release. When incorporated into a PC:PG bilayer a significant decrease in CF release is observed with an almost complete inhibition of membrane disruption at 1.0 μM Smp43 with only 1.1% (± 1.4) detected and a maximum release of 39.9% (± 4.0) at 2.0 μM (Fig. 5.13). However against PC:PE a difference in release is observed at 1.75 μM Smp43 and above with 79.7% (± 3.9) release seen at 2.0 μM (Fig.5.15)The presence of cardiolipin with a PC:PG bilayer caused no significant difference in leakage been highly susceptible to Smp43 at 1.0 μM and above (Fig. 5.13).

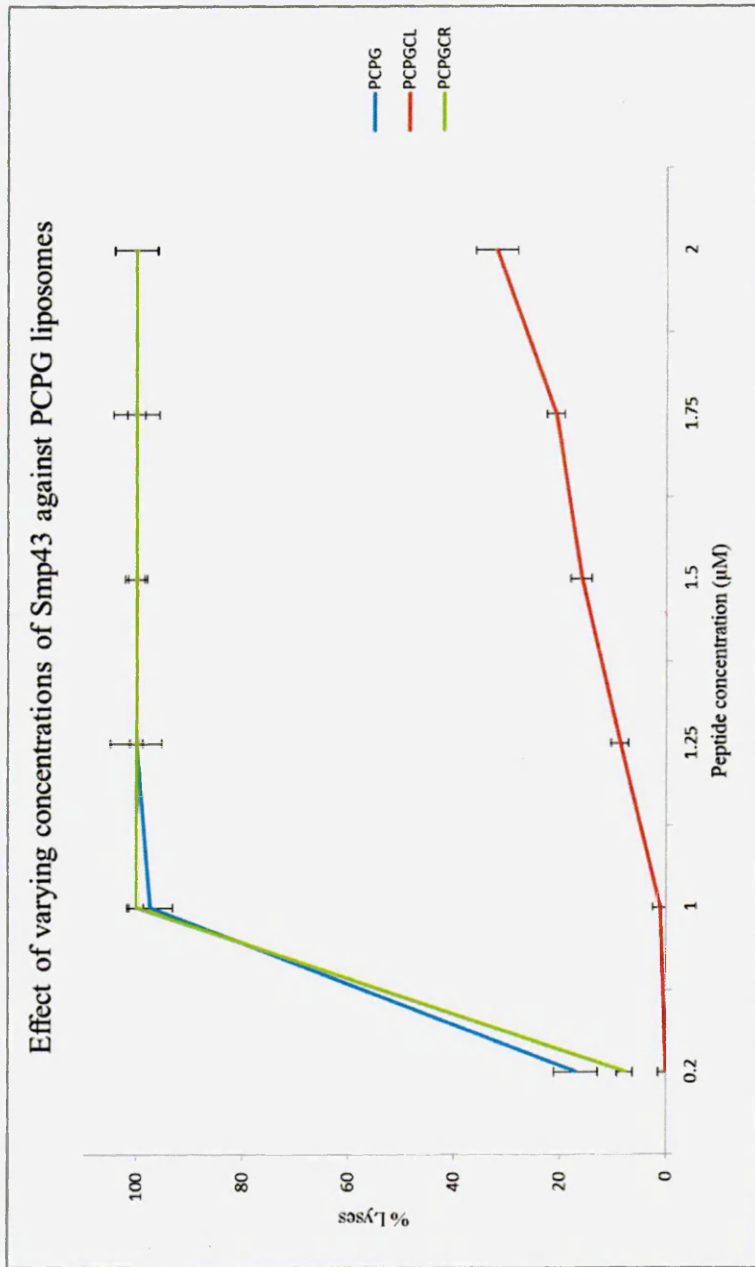


Figure 5.13: Effect of Smp43 against a number of PCPG bilayers at varying concentrations. Blue line- near maximum lysis is observed PCPG at 1 µM. The inclusion of cholesterol (red line) had a significant effect of lysis with only 39.9% lysis detected at 2 µM. The inclusion of cardiolipin had no significant effect on activity compared with the PCPG bilayer (green)

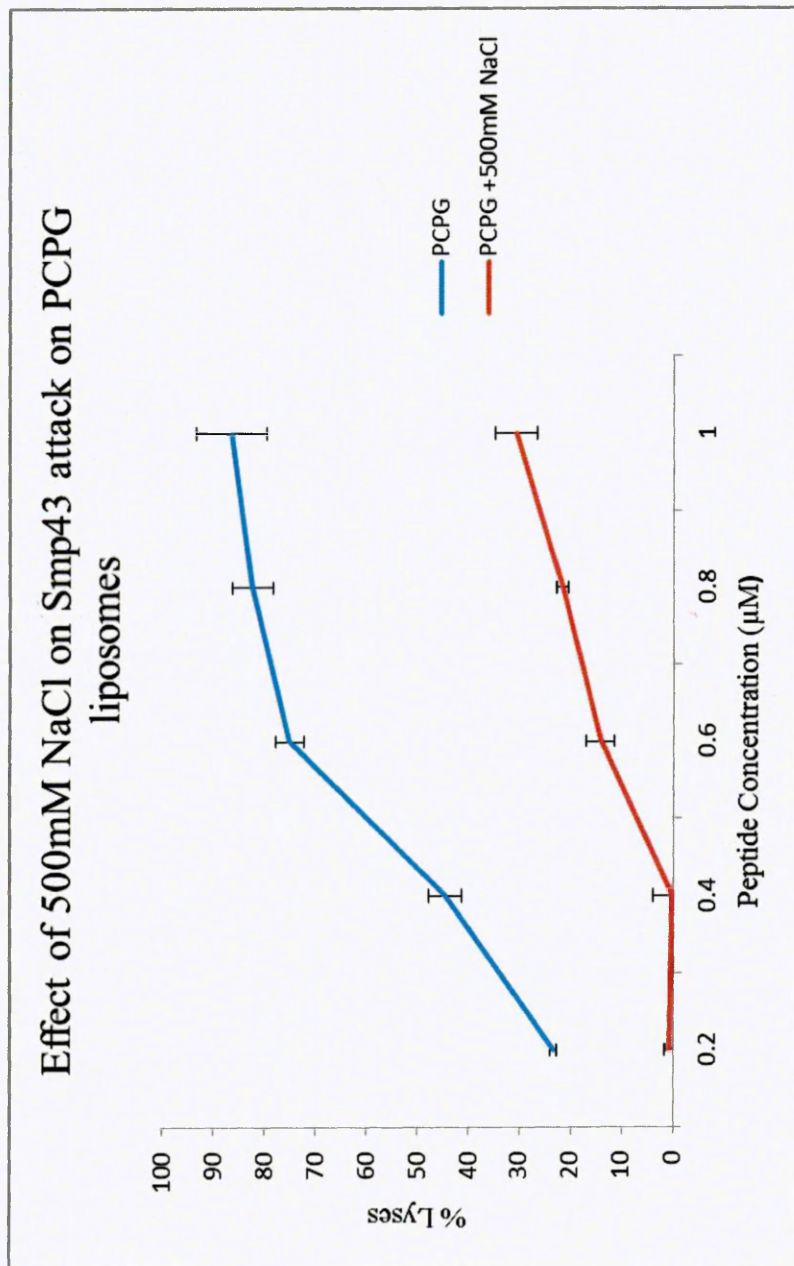


Figure 5.14: Effect of NaCl on Smp43 lyses of PCPG liposomes. The inclusion of salt to disrupt the electrostatic attraction Smp43 to the negatively charged liposome has a significant effect with only 30.6% lysis observed at 1 μM compared with 86.5% when no NaCl was present

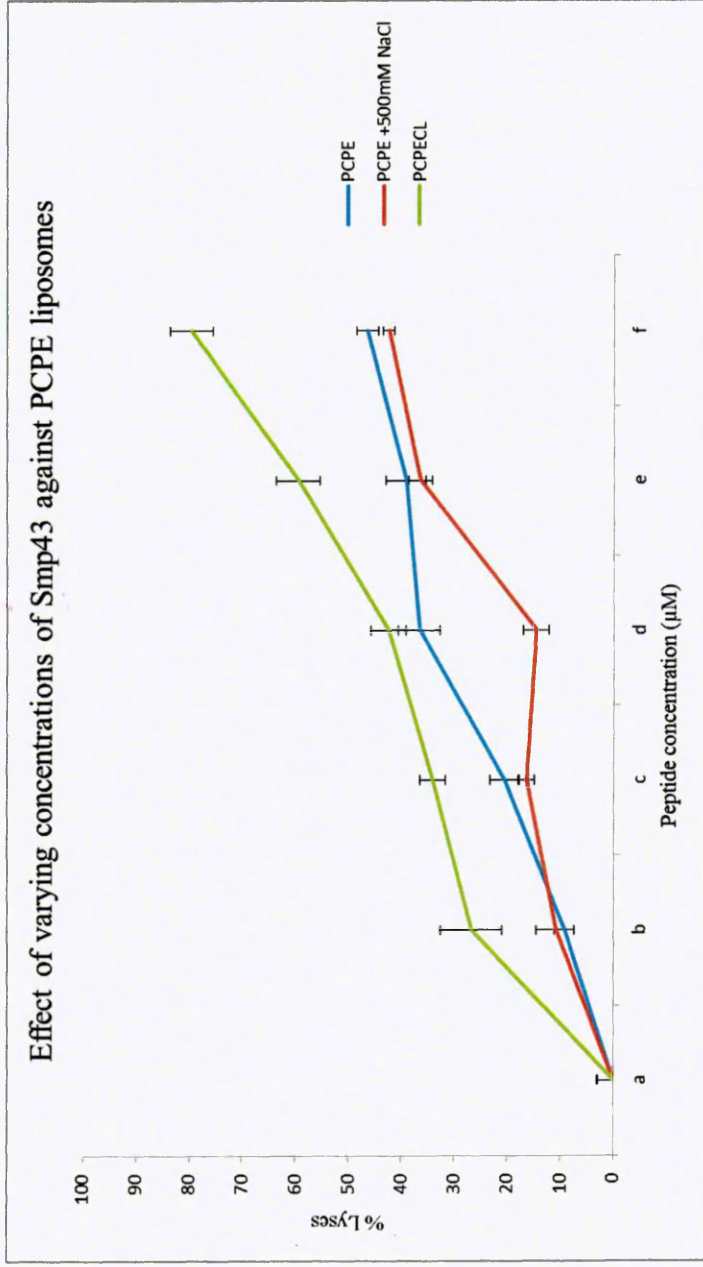


Figure 5.15: Effect of Smp43 against a number of PCPE liposomes at varying concentrations. Blue line- only maximum lysis is observed PCPG at 1 µM. The inclusion of cholesterol (red line) had a significant effect of lysis with only 39.9% lysis detected at 2 µM. The inclusion of cardiopilin had no significant effect on activity compared with the PCPG bilayer (green)

5.3.5 Analysis of the mechanism of action of Smp43 using the Dimension FastScan Bio™ AFM

The mechanism of action of Smp43 has been probed using liposome leakage assays and AFM, however for this peptide a Dimension FastScan Bio™ AFM was used with the potential to scan at up to 125 Hz which allowed the attack of the bilayer to be captured at a much faster rate than previously possible (Heath *et al.*, 2014). For example, the 8 μm^2 scans obtained using Smp24 took 5 mins to generate, however using the fast scan AFM peptide attack was captured at 10 s/frame (1 μm^2 scan). Thus it has been possible to capture AMP attack from initial incubation and give a better understanding of the whole process than previously possible. Both PC:PG and PC:PE bilayers were attacked at 1.0 μM Smp43 using a flow cell the bilayer with imaging taking place for 60s before the peptide was injected. As is seen in video 5.1 (on CD) there is a time lapse of 129 s before initial incubation to visible membrane disruption. Initial disruption occurs at two nucleation sites which have a pore size of 33.0 nm and 19.1 nm and the depths of these pores are between 0.6-1.5nm (Fig.5.16) suggestive of the removal of only one lipid layer as a planer lipid bilayer has a depth of between 4-6 nm (Heath *et al.*, 2013). From these two nucleation sites membrane disruption expands in a seemingly random fashion until a further nucleation site appears after 371 s at the top of the frame. From the beginning of the video no vesicle blebbing is observed during attack. However, as is seen after the formation of the initial nucleation sites, the height differentiation increases, indicated by the increasing light nature of the false colour image representing the remaining bilayer. This increasing in height differentiation is also seen during expansion of the third nucleation site. After approximately 700 s membrane disruption starts to slow down suggesting that the peptide has been used up. A similar mechanism of action is observed against the PC:PE bilayer (video 5.2) (on CD). However, the time

lapse until initial membrane disruption occurs and the speed and scale of disruption is significantly different from the PCPG bilayer. Initial membrane disruption only occurs at a single nucleation site after 367 s with a shallow indentation observed with a width of 27.5 nm and a depth of 0.5 nm (see figure 5.17a-c). A second nucleation site occurs approximately 140 s later. The speed at which disruption occurs is significantly increased against PC:PG as is seen in when comparing the level of destruction 2 mins after initial disruption (figure 5.18). Similarly the difference in the level of disruption after 20 mins incubation is significant with only a small section of the PC:PG bilayer (Fig. 5.19a) still intact whilst nearly all of the PC:PE bilayer remains intact (Fig. 5.19b), even after 40 minutes incubation with the PC:PE bilayer a large proportion of the bilayer remains.

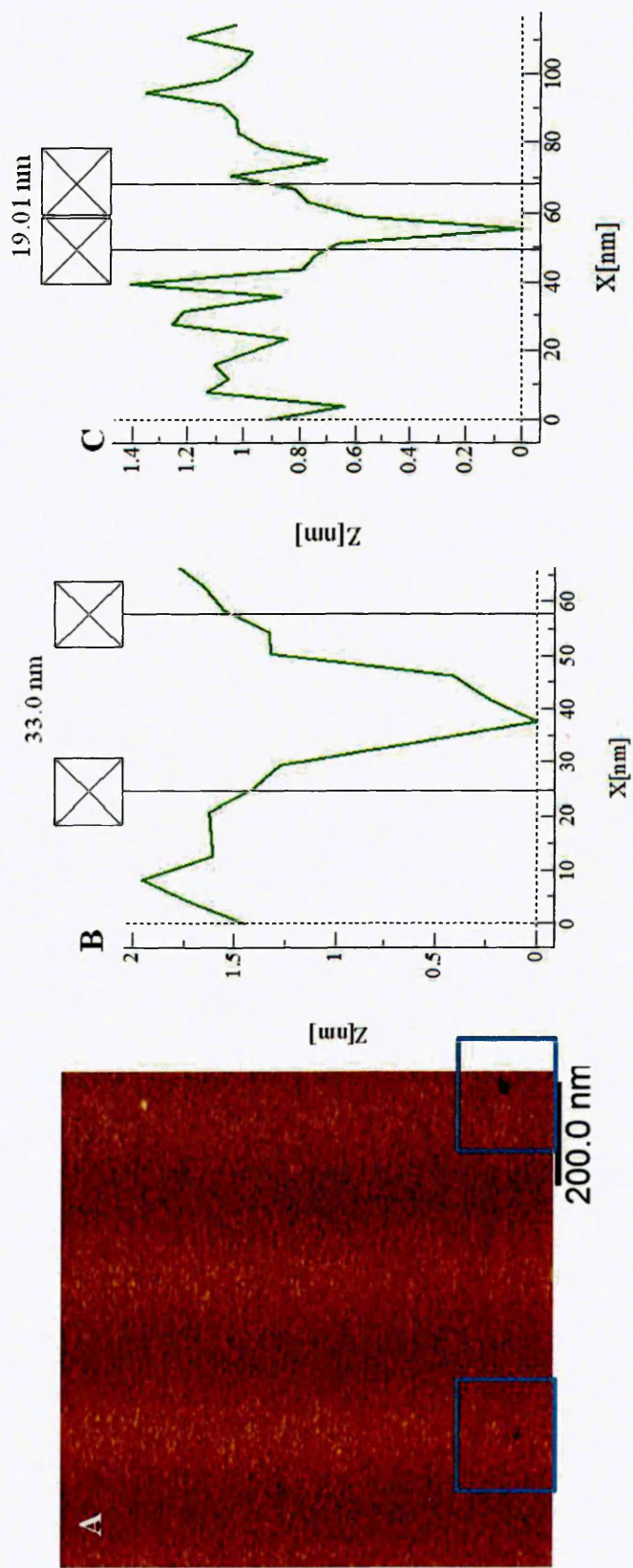


Figure 5.16: Initial nucleation sites of Smp43 attack on a PCPG bilayer as determined by AFM. (A) Nucleation sites observed within the lipid bilayer (B +C) analysis of the nucleation site diameters

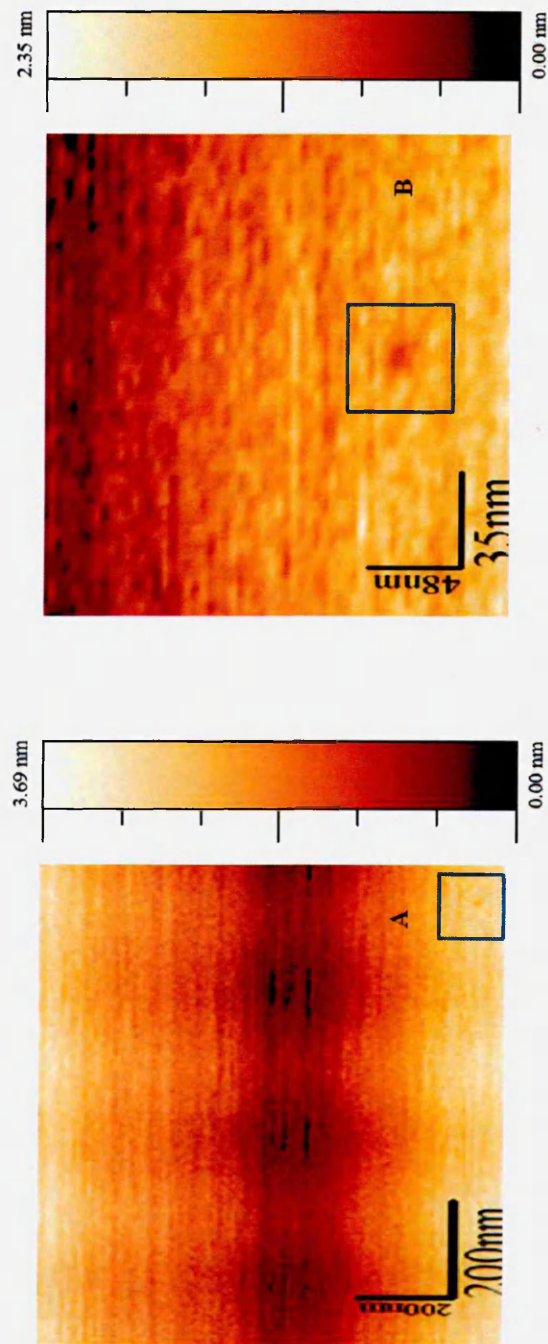


Figure 5.17: Initial nucleation site of Smp43 attack on a PCPE bilayer as determined by AFM. (A) Nucleation sites observed within the lipid bilayer (B) Zoom in of nucleation site detected in (A). (C) analysis of the nucleation site diameters

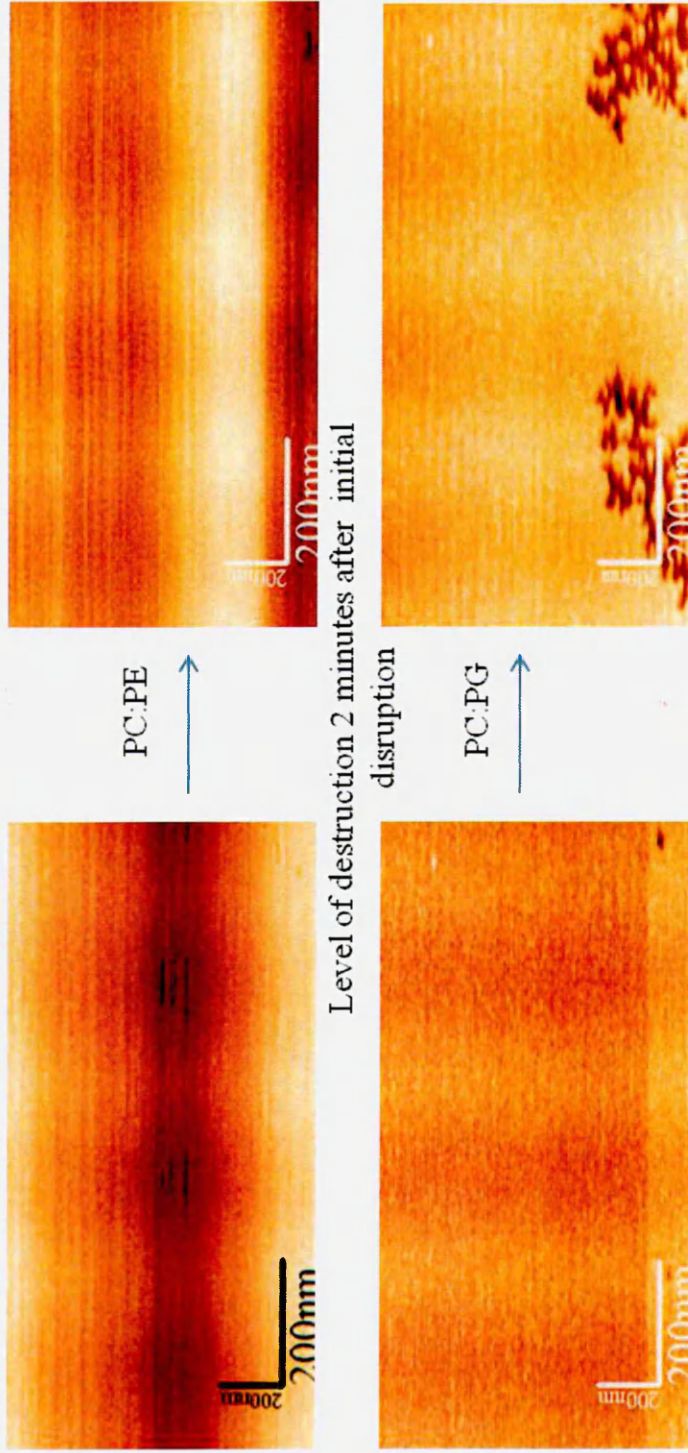


Figure 5.18: The contrasting speed of membrane disruption after Smp43 attack after initial nucleation is observed on both PC:PG and PC:PE bilayers. After a 2 minute time point very little damage is observed within the PCPE bilayer, in contrast, extensive damage is seen 2 minutes after initial nucleation

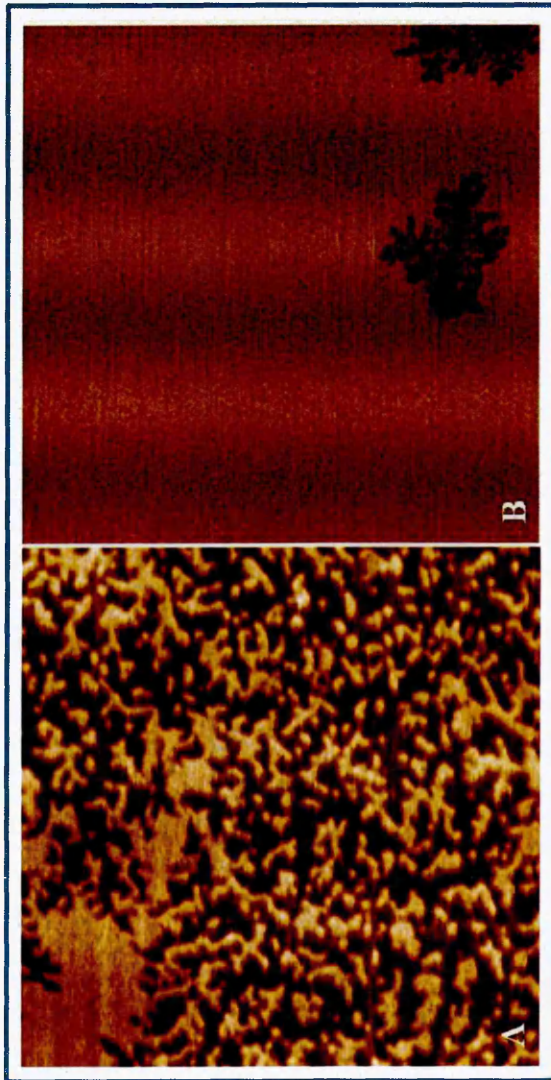


Figure 5.19: The contrasting effects of Smp43 attack on PC:PG and PC:PE bilayers as determined by high speed AFM. As is seen in (A) extensive membrane damage is observed with the PCPG bilayer however against the PCPE bilayer (B) damage is less pronounced even though the mechanism is the same

5.4 Discussion

This study has investigated the effect of both Smp24 and Smp43 using CF release assays, AFM and QCM-D on synthetic membrane systems with the aim of elucidating their mechanism of action.

The membrane composition of prokaryotic membranes makes them more negatively charged than their eukaryotic counterparts, with prokaryotic membranes composed largely of the hydroxylated phospholipids PG, PS and CR, whilst eukaryotic membranes consist of more neutrally charged phospholipids such as PC, PE, SM and sterols such as cholesterol and ergosterol. (Yeaman *et al.*, 2003). Although a number of bacteria do contain PE, for example the outer membrane of *E. coli* is predominantly PE (Ratledge & Wilkinson., 1988), the membrane compositions chosen within this study reflect prototypical prokaryotic and eukaryotic membranes with PC:PG being used to mimic the former and PC:PE chosen as the latter based on its zwitterionic properties.

Whilst both peptides show preferential activity against PC:PG bilayers, Smp43 has a lower attraction towards the PC:PE bilayer than Smp24 which is reflective of the lower cytotoxic nature of the former peptide against erythrocytes seen in biological testing. Furthermore, it shows that these two membrane compositions correlate well with biological activity providing adequate models to investigate AMP action.

The inclusion of cardiolipin into the PC:PG bilayer increased the propensity of lyses in the presence of Smp24. Whilst this would be expected due to its negative charge and high concentration within bacterial membranes it is not necessarily a prerequisite for increased AMP activity. For example, it has recently been demonstrated to inhibit the pore forming abilities of daptomycin in PG liposomes at a concentration of 10 & 20% (Zhang *et al.*, 2014) with genetic studies suggesting a role for cardiolipin in decreased

daptomycin susceptibility in a number of bacteria (Davlieva *et al.*, 2013 & Mishra *et al.*, 2013).

A major driving force of AMP selectivity is the electrostatic attraction to prokaryotic membranes due to both the presence of negatively charged phospholipids along with LPS in Gram negative organisms and teichoic acid in their Gram positive counterparts (Hancock *et al.*, 1997 & Peschel *et al.*, 1999). Both peptides used within this study are positively charged with Smp24 & Smp43 carrying a charge of +3 & +4 respectively. As is seen in figures 5.2 and 5.18 the electrostatic attraction of these positively charged AMPs to negatively charged bilayers is significantly disrupted in the presence of 500 mM NaCl reflecting the importance of this attraction. In contrast no significant decrease in lysis is observed with PC:PE liposomes suggesting that electrostatic interaction is not a factor in membrane disruption with respect to the zwitterionic bilayer. However both peptides do cause CF release and membrane damage is observed using AFM, therefore another factor is driving this disruption.

It is well known that PE induces negative curvature of the bilayer due to the cone shaped nature of the lipid with the head group having a smaller cross sectional area than bulkier lipids such as PC. The presence of such lipids induces packing defects within the bilayer resulting in the negative curvature (Vamparys *et al.*, 2013). A number of peptides have been shown to interact with membranes active through a process of curvature-sensing, of interest, is the neuronal degenerative peptide α -Synuclein composed of a highly conserved sequence (KTKEGV) repeated imperfectly throughout the N-terminal half of the protein that can be displayed as an amphipathic helix upon binding to membranes (Drin & Antony., 2010). In the presence of cone shaped lipids such as PE, increased binding is observed, with significant rearrangement of the bilayer observed to accommodate the peptide, causing bilayer lateral expansion in order to

bridge the spaces between head groups and relieve the negative curvature strain induced by the high PE content in the lamellar phase (Ouberai *et al.*, 2013).

Other peptides containing amphipathic lipid packing sensor (ALPS) motifs such as synapsin 1 (Krabben *et al.*, 2011) and ArfGAP1 (Bigay *et al.*, 2005), recognises lipid-packing defects by a conserved mechanism of peptide partitioning where hydrophobic residues interact into large packing defects within the bilayer. They are 20–40 residues in length and share low sequence homology but similar physicochemical features including hydrophobic residues every three or four residues, typically phenylalanine, leucine, or tryptophan. However, small polar residues between however charged residues are rare and bind to packing defects caused by positive curvature (Bigay *et al.*, 2005, Prin *et al.*, 2007 & Vanni *et al.*, 2013).

Indeed the phenomena of curve sensing is thought to be critical to a number of fundamental cellular functions and allows peptides, typically amphipathic in nature, to identify and aggregate on the correct sub cellular membrane and are critical for a number of transport and signalling pathways (Antony., 2011). Therefore it is perhaps not surprising that peptides characterised as being amphipathic such as AMPs can exploit such fundamental biochemistry.

Whilst electrostatic attraction and lipid defect sensing may be responsible for the initial attraction of these peptides, the AFM images generated for Smp24 reveal radically different effects depending on lipid composition.

Against the PC:PG bilayer the formation of pores within the bilayer is observed (Fig.5.8e & f) each of the pores detected varies in size between 23-40 nm with the pores being around 2-3 nm in depth (Fig 5.9) therefore the pores seen within this study are not

sufficient to span the whole bilayer. This could be due to a number of reasons. Firstly, if the pore is of a toroidal nature the pore edges would be very unstructured, as opposed to a barrel stave pore. Therefore, the pore could be wider at the top than at the bottom and the depth analysis discrepancy is due to the radius of the tip being too large to measure the narrowest point of the pore. Secondly, only the top leaflet has been removed so in fact the peptide is exerting a carpet mechanism like effect and the disruption observed is a highly localised carpet mechanism. Thirdly, a pore has been formed however peptide has subsequently adhered to the exposed mica surface so the tip hits the peptide instead of the mica giving a false depth reading. From the liposome leakage assays, however, it is clear that complete membrane collapse is not taking place with a gradual release of CF suggestive of pore formation rather than a carpet mechanism (Belokoneva *et al.*, 2003). Also the QCM-D seems to suggest pore formation, as an accumulation of peptide occurs represented by a decrease in frequency, this build up along with an increase in the dissipation reading, a measure of the loss of energy from the crystal surface to the aqueous phase due to increased interaction. Interestingly, the dissipation reading undergoes a swing back event where dissipation momentarily decreases which could be hypothesised to be an insertion event taking place as insertion of the peptide into the bilayer would lessen the interaction of peptide with the aqueous phase thus a decrease in dissipation is seen. After this event, and at higher peptide concentrations dissipation increases further, presumably as more peptide accumulates on the bilayer with pore formation leading to the eventual destruction of the bilayer as observed in figure 5.10. Smp24 seems to follow the classical pattern of AMP pore formation, starting with electrostatic attraction, accumulation and subsequent peptide insertion after reaching a critical threshold concentration (Zasloff, 2002).

The mechanism of pore formation could be assumed to be toroidal on the basis of a number of factors. Firstly, pores of varying size, secondly, increasing peptide

concentration leads to complete destruction of the bilayer as opposed to increased pore formation and thirdly as is observed after peptide attack on the phase separated bilayer the peptide is line active.

Line activity is defined by the ability of a peptide to interact with points within the bilayer, typically at the edges, which high a high steric hindrance as depicted in figure 5.20 and is explained in more depth below.

In a planer lipid bilayer system the edges of the bilayer are intrinsically curved as to allow protection of the hydrophobic chains, however this curvature comes at a price as the hydrophobic tails are bent towards each other and in close proximity, therefore it is energetically less favourable for a lipid molecule to stay at the edge of this system instead of being in the bulk (See Fig. 5.20). Because of the high unfavourable energy associated with this phenomenon bilayers have high line energy, in which the edges of the bilayer are shortened so that more lipid remains in the bulk then at the edges, these systems are said to have a high line tension which regulates the length of the lipid/aqueous edge leading to the appearance of smooth short edges when examined by AFM (Garcia Saez *et al.*, 2007). In a phase separated bilayer the smooth edges within the lipid ordered areas seen before peptide attack is due to this high line tension. Previous studies have also examined the effects of AMPs on line tension which have led to insights into the mechanism of action of the peptides.

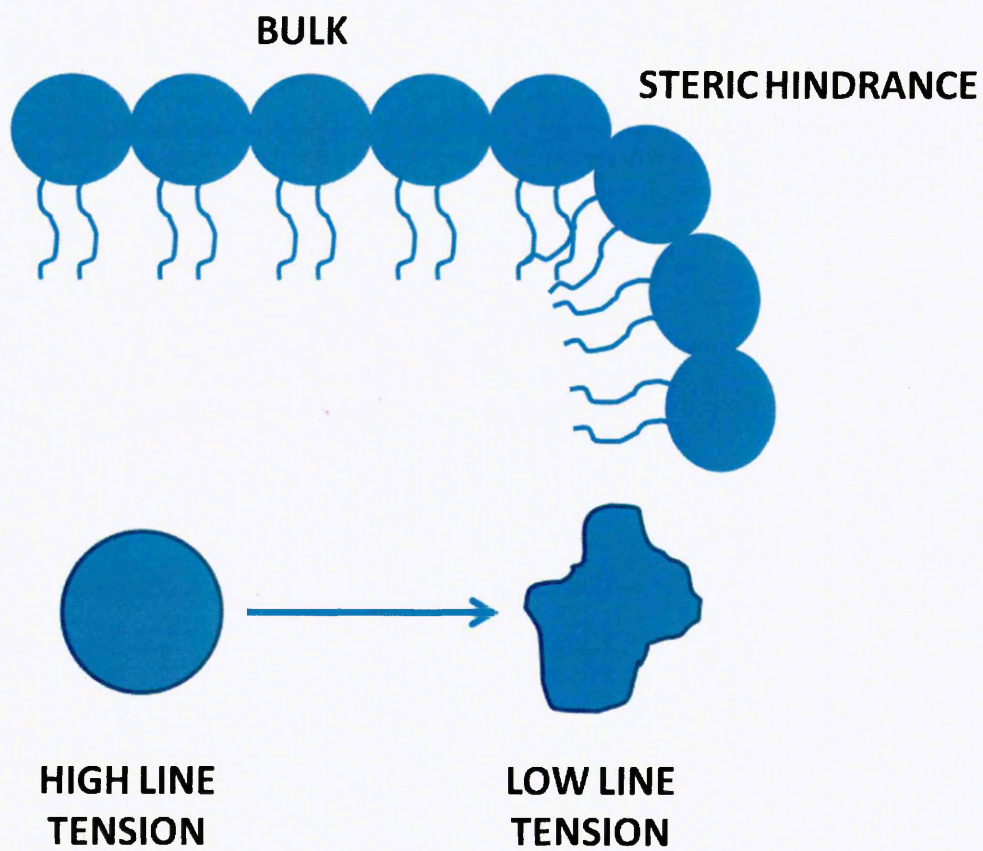


Figure 5.20: At the edges of a bilayer it is energetically unfavourable for an individual phospholipid to be at the edge of the bilayer due to steric hindrance therefore a high line tension is observed as more phospholipids remain in the bulk

Lam *et al.* (2012) examined the effects of PG-1. During binding at low concentrations the peptide interacts with the edges of the bilayer and adopts an extended hair pin shape in which the hydrophilic N-terminal region interacts with the head groups within the bottom leaflet and the central hydrophilic region interacts with the top leaflet flanked by two hydrophobic regions sitting with the phospholipid chains. This peptide interaction has the effect of lowering the overall line energy (thus line tension) of the system and allows for a more rugged and relaxed line edge as is seen with the interaction of Smp24 at the edge of the lipid ordered areas within the phase separated bilayer.

Increasing the concentration of PG-1 causes saturation of the edges of the bilayer at which point the line tension cannot be lowered any further and the peptides start to induce curvature of lipid areas within the bulk of the bilayer, thus increasing steric stress of these phospholipid chains which then allows for incursion of the peptide into the membrane and the formation of open pores within the bulk. The peptide interaction follows the same pattern in the bulk as at the edge and thus is a peptide-lipid interaction reminiscent of a toroidal mechanism of action (Ludkte *et al.*, 1996, Matsuzaki *et al.*, 1996). Further increases in peptide concentration allows the peptides to form dimeric structures which allows the line tension to be reduced so much that worm like structures are formed as it is energetically favourable to have an increased edge (Fig. 5.21).



Figure 5.21: Worm like structures detected by Lam *et al.*, 2012 using atomic force microscopy. (A) Without PG-1, line-tension of a unperturbed liquid lipid bilayer patch maintain a smooth edge contour (B) With the perturbation of PG-1 at low concentration, bilayer contours are extended and stable over time, suggesting line tension is lowered with the incorporation of PG-1 at the edge of the bilayer (C) With further increase of PG-1 content in the bulk, pore formation was observed. While the size of PG-1 molecule is much smaller than the dimension of these pores (~ 9 nm in diameter), the PG-1 molecules are believed to aggregate in order to induce pore formation (D). At higher concentrations of PG-1, wormlike micelle formation was observed transforming the entire bilayer into a structure with characteristics width of ~ 7 nm and a much reduced thickness. The rich morphologies of structural transformation in the lipid/PG-1 mixture are reminiscent of phase behavior of DMPC/DHPC mixture, in which DHPC acts as line-active agent to lower line tension.

Further evidence of line active peptides has been demonstrated by AFM imaging of phase separated bilayers with helix 5 of the bax peptide involved in eukaryotic cell death by pore formation in the mitochondrial cell wall (Garcia Saez *et al.*, 2007). AFM studies previously determined the peptides pore forming abilities in planer lipid bilayers supporting a toroidal model (Epland *et al.*, 2002). In the latter study on phase separated bilayers containing DOPC/SM/Chol (1:1:0.67) smooth L_O areas are clearly visible, however, after 30 minute incubation, the effect on line tension is apparent with a loss of line integrity.

The loss of line tension seen in the current study with Smp24 is compared with previous studies therefore a similar mechanism of action in which membrane disruption occurs through peptide-lipid rather than peptide-peptide interactions is a realistic assumption

Whilst a toroidal pore like mechanism can be hypothesised for the Smp24 attack on the PC:PG bilayer, attack on the neutrally charged bilayer is radically different. As is seen using AFM, no pore formation is observed. However, large areas of disruption occur that result in stratifications without the removal of the complete bilayer in these areas (Fig. 5.7f) Formation of possible domains has also been observed suggesting that phase separation is induced (Fig. 5.7e). Furthermore liposome leakage assays do not show a complete collapse of the bilayer (Fig. 5.1) and less leakage is observed than with the PC:PG bilayer suggesting that a carpet mechanism is not occurring, a hypothesis supported by the QCM-D results which suggest no accumulation event occurring (Fig. 5.12).

A number of AMPs have previously been shown to disrupt membranes by a mechanism termed peptide-mediated non-lamellar formation which has been suggested as a fundamental mechanism of protein-membrane interaction (Henley *et al.*, 2010).

Membrane lipids can self-assemble into numerous different phases, including micellar, lamellar, hexagonal and cubic phases and the ability of membranes to form these structure is governed by lipid structure (Hanley *et al.*, 2010). Membranes that are composed of lipids with a similar headgroup and acyl chain cross sectional area, for example PC and PG, favour the formation of planer lipid bilayers whereas membranes containing the cone shaped PE lipids prefer inverted micelles and inverted hexagonal lipid phases or regions with high negative membrane curvature strain (Tresset., 2009). Therefore, it is important to understand how membrane properties governing membrane dynamics are affected by changes induced by the interaction with AMPs. In the absence of peptides, the stored curvature elastic energy causes the bilayer to expand laterally, this expansion decreases steric hindrance and is thermodynamically favourable. However, expansion can only occur up to a certain threshold as changes in membrane conformation causes increased exposure of the acyl chains to water therefore beyond this threshold it becomes thermodynamically favourable for an inverse phase to occur. Typically with PE, a Hexagonal II phase (H_{II}) tubular structure forms with the head groups orientated to the centre of the cylinder due to its favoured negative curvature (Fig. 5.22). A similar feature was observed for some integral membrane proteins, which may release stored curvature elastic stress locally during insertion into the bilayer by allowing the chains to dislocate more and forces the head groups together, making the peptide-lipid assembly thermodynamically more stable. Lipid lateral stress can be induced by proteins causing membrane structural changes allowing the formation of phases that are highly curved such as hexagonal, cubic or even micellar phases (Heller *et al.*, 1997, Lohner *et al.*, 2001, Pozo *et al.*, 2005 & Epanand *et al.*, 2008). A link between

alterations in lipid structure and the modification of cell signalling events has been suggested (Epan., 1998). For example amphitropic enzymes comprise a class of proteins whose activities are modulated by the reversible translocation to membrane surfaces in response to local fluctuations on membrane dynamics and organisation (Hurley *et al.*, 2000). An example of this process is the enzymatic protein kinase C (PKC) family. PKC enzymes are involved in cell proliferation, differentiation and signalling and activity is influenced by the presence of non-lamellar forming lipids, for example the PKC-catalyzed phosphorylation of histone occurs in the presence of cubic phase structures (Giorgione *et al.*, 1998).

Analysis of the AFM images after 1.25 μM Smp24 attack on PC:PE show elongated stratifications (Fig. 5.7F). These areas of disruption have a width of around 200 nm. However not all the bilayer is removed within them and presumably these represent the elongated stratifications. Further increase in peptide concentration causes a widening of these disrupted areas to around 350 nm but complete bilayer removal is not observed (Fig. 5.8b & 5.9c-f). Based on the propensity of PE containing bilayers to form non-lamellar phases it is conceivable that Smp24 is inducing this process and that the stratifications are elongated structures similar to those described by Tresset. (2009) (Fig. 5.22).

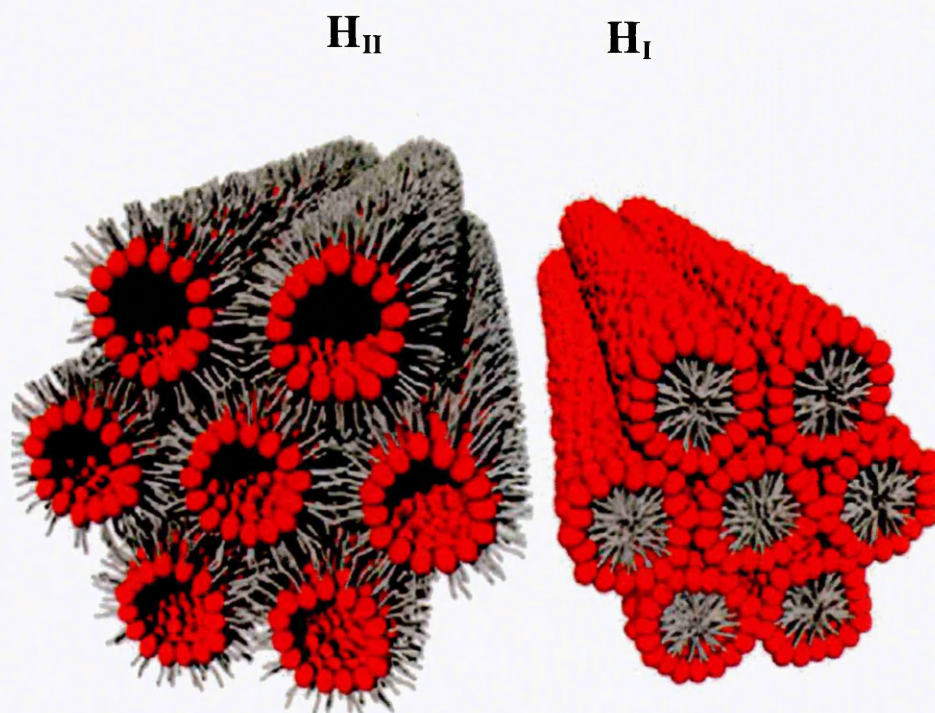


Figure 5.22: Non lamellar structures possibly present after Smp24 attack on PCPE bilayers with the lipid headgroups represented in red and the acyl chains represented in grey. Taken from Tresset (2009).

The formation of non-lamellar phases has been seen with a number of AMPs. gramicidin S (GS) has the ability to form cubic phases in lipid bilayers along with lipid extracts of *E. coli* (Prenner *et al.*, 1997 & 1999). NMR and X-ray diffraction have revealed that the binding of GS membranes solely composed of PC, PS, CL or SM showed no formation of non-lamellar phases, however, in the presence of PE, PG and PC the formation of a cubic phases is observed (Fontell 1990). The detection of non-lamellar phase formation, after attack by human lactoferrin derivatives on *E. coli* total lipid extracts using small-angle X-ray scattering in which two different cubic phases coexisted with the lamellar phase, was also seen (Zweytick *et al.*, 2008).

Furthermore, the AMPs sprotargin-1 and PGLa were able to form cubic phases on pure POPE membranes (Hickel *et al.*, 2008), and nisin caused cubic phases with POPE membranes and alamethicin has also been shown to induce cubic phase structure in PE membranes (Keller *et al.*, 2008). It has been suggested that the insertion of the peptide in the bilayer shifts the amphiphilic balance by increasing the hydrophobic contribution, driving non-lamellar structure formation (El Jastimi *et al.*, 1999)

A comparison of figures 5.7e and 5.7f suggests it is possible that Smp24 induces both non lamellar structures and phase separation upon attack at 1.25 μM . As is seen in 5.11e, after peptide attack the bilayer has both L_o and L_d areas represented by differences in the height differentiation (lighter patches are higher).

Membrane disruption by induction of lipid-peptide domains through lateral phase segregation of zwitterionic from anionic lipids and has been seen along with the induction of non-lamellar phases in various studies (Arouri *et al.*, 2008, Epland & Epland., 2009, Teixeira *et al.*, 2010). For example, linear and cyclic arginine- and tryptophan-rich AMPs have been shown to induce de-mixing of a DPPG/DPPE bilayer

in to separate domains (Arouri *et al.*, 2008) and it was recently postulated that AMPs with a high positive net charge, conformational flexibility and sufficient hydrophobicity facilitate preferential interaction with anionic lipids and the promotion of lipid lateral segregation (Epland & Epland *et al.*, 2009). This mechanism has also been suggested to be responsible for a peptide's ability to affect certain bacteria and not others. For example, a study on the peptide OAK C12 K-7a8 using *Bacillus cereus* and *S. aureus* showed the former was far more susceptible with the authors suggesting the high concentration of PE in the bilayer was responsible for this as *S. aureus* has a much lower PE content therefore lipid segregation is inhibited (Epland *et al.*, 2008). Also, LL-37 derivatives induced lipid phase segregation of anionic lipids away from zwitterionic lipids (Epland *et al.*, 2009). Overall, these studies suggest that some antimicrobial peptides are able to induce lipid segregation on species with membranes composed of zwitterionic and anionic lipids.

In figure 5.23 there is a striking resemblance between the bilayer attack and patterns produced during diffuse limited aggregation (DLA) (Witten and Sander., 1981, Mandelbrot *et al.*, 1995). DLA is characteristic of systems in which molecules that undergo Brownian motion form irreversible aggregate clusters on a surface. In the process a seed particle attaches to the surface and then other particles attach to this particle. The rate-limiting step in aggregation is often the diffusion of the particles to the surface of the aggregate. Similar growth processes occur when a chemical species precipitates from a supersaturated matrix or when crystals grow from a super cooled melt. In these cases diffusion of the species toward the surface (or heat away from it) can be the rate-limiting process. The aggregates formed in all of these cases have extremely complicated multi-branched forms familiar in the case of dust balls, agglomerated soot, and dendrites (Witten and Sander., 1983).

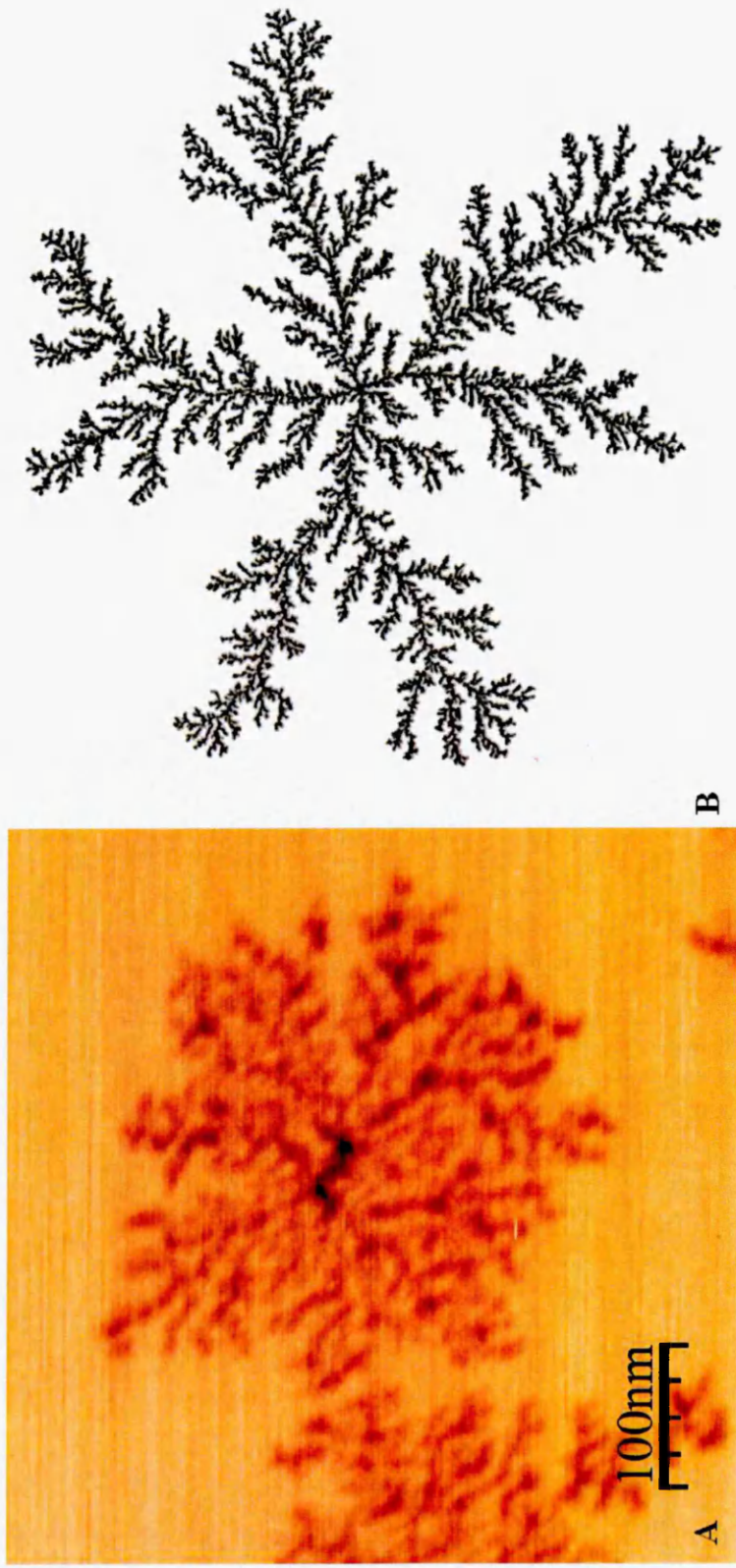


Figure 5.23: The comparison of DLA type patterns seen with Smp43 attack and a typical DLA structure. A nucleation point occurs and then growth of the structure occurs from this point (DLA image taken from <http://classes.yale.edu/fractals/panorama/physics/dla/dla.html>)

A number of proteins have been shown to self-organise into DLA patterns. For example, Meier *et al.* (2014) examined the aggregation morphology of high molecular weight polypeptides after modification with polyethelene oxide using AFM this modification leads to DLA-type formations with a similar morphology to the areas of membrane damage seen in the present study. The aggregation of amyloid- β using three dimensional Monte Carlo simulations of DLA acting linear polymers in a confined space, representing the endoplasmic reticulum, has been examined (Budrikis *et al.*, 2014). In this simulation the authors altered the rates of protein production and degradation and show that the system undergoes a non-equilibrium phase transition from a physiological phase with little or no polymer accumulation to a pathological phase characterized by persistent polymerization. A number of elastomeric proteins such as elastin, resilin, abductin and wheat gluten have been theoretically examined for their DLA properties (Song *et al.*, 2012). These DLA protein events may have implications not just for a number of clinically relevant protein diseases but also in the rational design of proteins for bioengineering.

The DLA mechanism of action would be driven principally by the aggregation of protein on to the lipid surface and then the further attraction of protein until membrane destruction occurs. It is worthwhile considering other examples of lipid protein aggregation events notably fibril formation seen within protein misfolding diseases, such as Alzheimer's, Parkinson's and prion disease, in which a range of proteins from globular to unstructured proteins form aggregates causing massive disruption of cellular membranes, for example in neuronal cells (Eichner and Radford., 2011). The precise nature of amyloid fibril formation is currently unknown (Jahn and Radford., 2008), However, the protein being in an unfolded state, within an hydrophobic environment

and neutralisation of the peptides charge, are important for aggregation to occur (Rochet *et al.*, 2000) Zhao *et al.* (2004) on examining fibril formation with a number of different proteins including lysozyme, insulin, GAPDH, myoglobin, cytochrome C, histone H1 & α -lactalbumin determined that the presence of acidic phospholipids within liposome such as PG:PS, promoted fibril formation in each of these proteins. However, no fibril formation was observed in the presence of a simple PC bilayer. The authors again postulated that this was due to the neutralisation of cationic charge on the protein by acidic lipids which allowed protein aggregation to occur as there would be a reduction in repulsive electrostatic forces between the monomers, thus, lipid mediated protein aggregation occurs. A similar mechanism has been determined for amyloid proteins such as A β , α -synuclein and prions (Terzi *et al.*, 1994, McLaurin *et al.*, 1998) and it has been suggested that due to the wide variety of proteins shown to exhibit these properties that acidic lipid mediated fibril formation may be a generic mechanism of electrostatically attracted proteins (Zhao *et al.*, 2004). The same group have also demonstrated fibril formation with a number of AMPs, including plantaricin A, as shown by the staining of protein aggregates with Congo red (Zhao *et al.*, 2006). Also, AMPs classically thought to form toroidal pores such as magainin 2, LL-37, melittin, temporin L and the non permeabilising peptide Indolicidin have all been shown to form acidic lipid mediated fibrils (Zhao *et al.*, 2001 & 2002). Based on these findings the “leaky slit” mechanism briefly discussed in chapter 1 was hypothesised (Zhao *et al.*, 2006) The amphipathic peptides bind to the acidic lipids neutralising charge, whilst the hydrophobic face of the peptide is arranged perpendicular to the lipid bilayer with toxicity caused by curvature of the membrane to allow protection of the bilayer hydrophobic core from the hydrophilic face of the peptide. This allows a slit to form in the membrane due to the high positive curvature of the protecting head groups.

In relation to the membrane destructive effects of Smp43 it could be hypothesised that membrane disruption is a consequence of protein aggregation driven by the same fundamental processes observed in fibril formation and as is observed with fibril aggregating AMPs. In the PC:PG bilayer the rapid and far reaching membrane disruption observed could be a consequence of PG mediated charge neutralisation which easily facilitates increased protein aggregation. In contrast, the more protracted destruction observed upon PC:PE interaction can be easily rationalised as the net anionic charge of this bilayer is far lower, therefore, aggregation occurs at a much slower rate. However, in both videos the formation of actual mature fibrils is not observed. Therefore the actual mechanism of peptide orientation within the bilayer still remains to be elucidated. The presence of unstructured aggregates that cause membrane disruption by inducing increased positive curvature on the top leaflet of the bilayer formed in the carpet mechanism could be one conclusion. The complete collapse of PC:PG liposomes upon Smp43 attack would be suggestive of such a mechanism instead of a “leaky slit” which would be expected to allow far more gradual CF release to occur. One possible explanation for reduced disruption of the PC:PE bilayer is that, due to the intrinsic negative curvature PE containing bilayers adopt, they have an inhibiting effect on carpet model peptides as they cancel out the positive curvature caused by attack which is supportive of an aggregate carpet model (Shai *et al.*, 1999).

However, although evidence for protein aggregate formation/membrane disruption is apparent the DLA-type patterns seen upon attack could conceivably be driven by another process in which, similar to toroidal pore formation where monomer peptide-lipid interaction occurs, it is the release of consecutive steric hindrance events caused by peptide insertion that drive the process forward allowing for dialectical destruction of the bilayer.

In this hypothesis, initial peptide attack on the PC:PG bilayer would be driven by electrostatic attraction with a membrane nucleation event occurring as peptide accumulation passes a critical point and insertion occurs. Upon peptide insertion the steric hindrance would occur as the lipid head groups lining the peptide-lipid pore undergo increased positive curvature to protect the acyl chains from the aqueous environment (Matsuzaki *et al.*, 1996). As is seen in a number of studies using AFM (Lam *et al.*, 2012, Garcia-saez *et al.*, 2007), and with Smp24 in this study, upon attack of phase separated bilayers, at the edges of bilayers or at phase separation boundaries a high line tension is observed. Similarly a toroidal pore lumen would have a high line tension as lipid head groups undergo positive curvature to protect the acyl chains which could easily be exploited by peptides allowing for insertion and decrease in steric hindrance (Garcia Saez *et al.*, 2007). This phenomenon has previously been described by Rakowski *et al.* (2013) in which an ever expanding pore mechanism (Fig. 5.24) was observed using nano-secondary ion mass spectrometry (nano-SIMS) and AFM until complete destruction of the bilayer is observed. Peptide accumulates on the bilayer (S-state), insert to form a pore (I state) and then further pore expansion is seen (E state). Smp43 could be hypothesised to be acting in such a way where, after nucleation, peptides insert to relieve the strain caused by the insertion of a previous peptide and expand out in a random pattern.

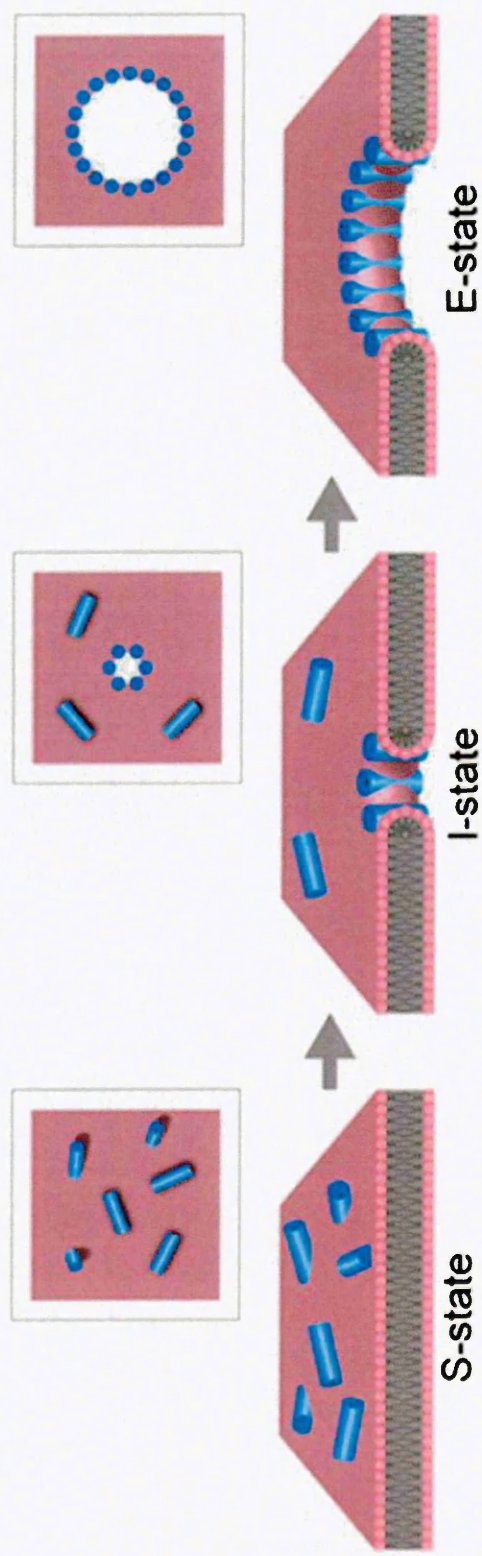


Figure 5.24: Expanding pore mechanism for amphipathic AMPs proposed by Rakowski *et al.*, 2013. In the S state peptides bind to the surface causing weakening of the membrane and after a critical point the I state is then possible where peptides insert perpendicular to the lipid heagroups to form a torodial pore. Due to steric hindrance peptides can then insert around the edges of the pore allowing for pore expansion (E state)

An analogy to this is the destructive effect of tectonic plate shift in earthquakes. Pressure builds up between two plates leading to a slip relieving pressure. However, in turn, further pressure build up along the plate until another slip occurs. This process continually repeats itself along the plate boundary until all the pressure is released and the system is at its lowest energy state. A classical example of this is the North Anatolian fault line that crosses Northern Turkey from East to West and has suffered earthquakes moving westwards each time as the sequence of pressure build up, release and subsequent build up occurs (Stewart., 2005).

Furthermore, as found in a classical toroidal pore mechanism (Matsuzaki *et al.*, 2006), the insertion of peptide could cause lipid “flip flop” between peptides where negatively charged peptides would be promoted to the top leaflet causing further electrostatic attraction to the bilayer in a self promoting attack. In this model whilst nucleation on negatively charged lipid bilayers would be electrostatically driven, on PC:PE initial nucleation could be driven by another process such as curve sensing (Antony., 2011), although PC does carry a small net anionic charge so electrostatic attraction cannot be ruled out (Zhao *et al.*, 2004). Once integrated, the process of steric hindrance relief would be the same. One criticism of this model is that PE is not known for inhibition of pore forming peptides (Matsuzaki *et al.*, 1998). However, there are clear differences seen between the two bilayers, so what is causing inhibition after nucleation? The assumption of pore formation being independent of PE concentration has recently been called into question with the unexpected inhibition of alamethicin attack on PE containing liposomes (Bodone *et al.*, 2012). This blurred the lines between a carpet mechanism and a toroidal pore in favour of the interfacial model where electrostatic attraction of the bottom leaflet to the peptide, upon peptide insertion into the membrane,

causes membrane disruption intrinsically driven by polar pockets within the hydrophobic segments of AMPs (Wimely *et al.*, 2011). From one viewpoint, the presence of PE and retardation of Smp43 attack could be seen as supportive evidence for a carpet mechanism of aggregation. Toroidal like mechanism of consecutive steric hindrance relief cannot be ruled out, although on the basis of the DLA like patterns observed as opposed to the uniform expansion described in by the expanding pore model, aggregation and carpet mechanism could be considered more likely.

Further experiments need to be undertaken to determine if this DLA pattern is a consequence of protein aggregation or a toroidal pore like model. For example tandem AFM-fluorescent microscopy where the peptide has been labelled to determine peptide localisation on the bilayer. Similarly, FRET analysis, where two populations of the same peptide have been labelled, one with a fluorescent tag and the other with a quencher to determine peptide-peptide aggregation could be utilised. Other imaging techniques could be employed such as Nano-SIMS (Rakowski *et al.*, 2013) or Laser-scanning coherent anti-Stokes Raman scattering (CARS) microscopy (Li and Cheng., 2008).

Addition of CL to both PC:PG and PC:PE bilayers has a significant effect on the activity of both peptides, increasing CF release against all bilayers, except for the attack of Smp43 on PC:PG which showed a decrease in release. This increase in membrane disruption is in contrast to a number of studies which have all reported decreases in membrane damage after cholesterol addition (McHenry *et al.*, 2012). One possible reason for this unexpected effect is increased electrostatic attraction due to CL induced domain formation.

As revealed by AFM, there is a significant difference observed between the PC:PG and PC:PG:CL bilayer after Smp24 attack with larger more concentrated areas of membrane

disruption occurring rather than discrete pore formation with disruption similar to the possible induced non-lamellar peptide mediated structures seen within AFM. The reason for this unexpected effect needs to be further examined however a number of reasons could be possible. Firstly the effect of CL ordering is not homogenous throughout the bilayer with some areas being within the lipid ordered phase (L_0) phase, where lipid packing is increased, however others may be in the lipid disordered phase (L_d), where lipid packing is decreased, therefore the lateral expansion of these areas due to decreased lipid packing could promote non-lamellar phase structures due to increased interaction between the acyl chains and the aqueous phase allowing the peptide to interact more readily with the bilayer. Secondly, CL could be inducing electrostatic imbalance in the membrane due to L_0 phase domain formation. Using both AFM and Frequency Modulated-Kelvin Probe Force Microscopy (FM-KPFM), Drolle *et al.* (2012) determined CL induces slight thickening of the bilayer and domain formation. However, these domains were shown to be electrostatic in nature. The same study examined the effects of amyloid β proteins on a DOPC bilayer with and without 20% CL. A clear increase in peptide binding was observed in the former with the authors pointing towards the electrostatic effects of cholesterol. An increased lysis of PC:PE membranes due to an increase in electrostatic attraction to these domains is plausible especially when considering the propensity of PE containing membranes for segregation (Hanley *et al.*, 2010). With both peptides, however, the decrease in CF release seen with Smp43 against PC:PG is more in keeping with previously held assumptions of CL inhibition and highlights the varying mechanism of action between the two peptides.

In conclusion, the mechanism of action of two AMPs with radically different biological activity has been examined. The mechanism of the shorter cytotoxic peptide was revealed to be dependent on lipid composition with a toroidal pore like forming mechanism indicated in prokaryotic mimicking membranes whilst in eukaryotic

mimicking membranes possible induction of peptide-mediated non-lamellar phase formation mechanism and/or lipid segregation. The mechanism of action of the longer chain peptide is radically different from the former with DLA like patterns, possibly induced by a process of anionic lipid mediated aggregation, seen against the negatively charged bilayer. Whilst in a neutrally charged bilayer, a significant retardation of the same fundamental process seems to be occurring. Overall, this chapter highlights the potential of using AFM to understand AMP mechanism of action and how the technology, especially high resolution Fast Scan AFM can change previous assumptions on the subject matter.

6 CHAPTER 6
CONCLUSIONS AND FUTURE WORK

The purpose of this study was to identify novel antimicrobial agents from both snake and scorpion venom and to biologically characterise these agents and elucidate mechanisms of action.

An empirical approach towards drug discovery was taken with snake venom and yielded a both AMPs as well as larger cytotoxic proteins. Elapid venoms yielded a number of AMPs of which a promising peptide from *Dendroopsis polylepsis* was identified. Whilst it only exhibited moderate antimicrobial activity it had little cytotoxic effect, therefore has the potential to be developed into a novel antimicrobial agent. As described in chapter 3, a number of structural motifs within snake venoms, especially elapid venoms, have been either recombinantly expressed or chemically synthesised. It therefore is highly possibly that after sequence and structural characterisation has taken place that this peptide can undergo modification to improve its antimicrobial properties. Considering the size of this peptide and its origin, it is most likely a cysteine constrained three fingered toxin or waprin peptide which has evolved resistance to its prays mammalian degradation mechanisms therefore is an ideal candidate for future systemic applications, although its stability against bacterial degradation needs to be assessed. Elapid venom is predominantly composed of such cysteine constrained medium chain peptides and every effort should be made to investigate their biological properties in terms of AMP research and for other disease states.

From viper venom a number of potential PLA2 proteins which, whilst having good antimicrobial activity, were also cytotoxic. Therefore in terms of their size and biological profile they have limited potential as future antimicrobials. Whilst studies have shown that truncating these proteins to short linear helical peptides has resulted in peptides with favourable biological activity (Santamaria *et al.*, 2005), the failure of

large scale peptide library studies to find suitable AMPs of similar size and physiochemical properties is a cautionary tale (Fjell *et al.*, 2009).

As discussed by de Lima *et al.*, (2009) perhaps no other natural source on earth has evolved to such an extent to specifically interact with a plethora of medical relevant drug targets as venoms. Indeed the recent discovery of a new class of peptides with Dendroaspis venom which specifically target acid sensing channels and has an analgesic effect as strong as morphine, but with none of the associated side effects supports this view (Diochot *et al.*, 2012).

From the genomic analysis of *S. maurus palmatus* the peptide Smp43 was derived, exhibited good antimicrobial activity, especially against Gram positive organisms and exhibited extremely low haemolytic activity. Although it showed toxicity in the ATP assay it would be useful to re examine this toxicity against primary cells instead of an immortalised cell line due to changes in the membrane properties of these immortalised cells. Indeed, because of the membrane similarities between bacterial and cancer cells, the use of immortalised cell lines as a basis of peptide cytotoxicity needs to be discussed within the research field, as a whole as potential drug candidates may be overlooked on this basis of its inaccurate toxic effect.

The mechanisms of action of Smp24 and Smp43 have been examined, providing further insights into how AMPs interact with both prokaryotic and eukaryotic mimicking membranes. Smp43 was examined using Fast Scan AFM and represents one of the first studies of its kind to capture the effect of an AMP on hydrated lipid bilayers from initial attack to its end, and at the time of writing (October 2014) no published studies are available of its kind. Obviously, more work needs to be undertaken to fully elucidate its membrane disruptive mechanism, but it highlights the potential the technology has to redefine our understanding of an AMPS membrane disruptive properties. Future studies

to determine the peptides line active nature, the incorporation of cholesterol and cardiolipin into the membranes was well as increasing the acyl chain length would provide crucial information to distinguish between a possible aggregate carpet mechanism or a mechanism that requires insertion.

This possible aggregated mechanism seen with Smp43 highlights a cautionary point to be considered in the future widespread clinical use of membrane damaging AMPs. The aggregation of proteins onto a lipid bilayer is responsible for a number of devastating neuro degenerative diseases such as Alzheimer's and Parkinson's with the molecular mechanism of these diseases essentially the same as the possible aggregation mechanism of Smp43 (Eichner and Radford., 2011).

The potential of certain amyloid proteins, such as α -synuclein, to aggregate onto membranes can be driven by the presence of negative phospholipids within membranes such as PS, as the proteins cationic charge is neutralised by the anionic lipids allowing the other proteins to aggregate on to this seed protein (Terzi *et al.*, 1994). Based on these similarities the effect of administering AMPs systemically needs to be further elucidated. For example, what are the long term effects of AMPs either aggregating onto these enriched membranes or acting as "seed" proteins that could facilitate amyloid aggregation? Animal studies would be a good *in vivo* model to understand this question. However, both AFM and liposome leakage assays would be useful *in vitro* methods for determining changes in amyloid formation in the presence of AMPs.

Previous attempts to develop AMPs in the clinical setting have proven frustrating, with a number of peptides being rejected during the latter stages of clinical trials (Gordon., 2005). However, a recent commentary (Fox 2013) examined these failures and provided optimism for future AMP development. For example, pexiganan (Lamb 1998), a 22 residue peptide developed for the treatment of foot ulcers was stopped because of

manufacturing difficulties and changes in the clinical trial design, leading to a non-approval letter being issued (1999) due to deficiencies with US Chemistry Manufacturing & Controls. The United States Federal Drug Administration (FDA) also indicated that pexiganan was no more effective in treating foot ulcers than conventional antibiotics. Similarly plectasin (NZ2114) (Mygind *et al.*, 2005) developed by Novozymes for the treatment of Gram positive infections and licenced (2008) to Sanofi-Aventis was abandoned because of commercial rather than scientific reasons. In another example, omiganan (Sader *et al.*, 2004), which had good efficacy in inhibiting catheter associated infections, was rejected on the grounds of cost when it was demonstrated to show no clinical statistical difference when compared to the widely used povidone iodine. However recent acceptance of the lipopeptide, Daptomycin (2003) and the vancomycin derived Telavancin (2007), which have relatively low therapeutic indices compared with conventional β -lactams antibiotics, would suggest a possible change in regulating priorities. In this changing climate, pexiganan is re-entering clinical trials, as Locilex (Fox., 2013). Although, as argued by Echols. (2011) the impact of withdrawing telithromycin (Ketek) from the market in 2006 for use in bacterial sinusitis (ABS) and acute bacterial exacerbation of chronic bronchitis (ABECB) has had a dramatic effect on the approval of antimicrobial drugs, especially those of novel mechanism of action (Brenner *et al.*, 2006). Ketek was rejected on the basis of lack of efficacy against these two disease states compared with other antibiotics. However all, these of studies that had been done had been in full compliance with FDA guidelines on treating ABS and ABECB which has formed the basis of the majority of antimicrobial approvals. Therefore the confusion created by this decision has led to a number of other antibiotics being rejected or reassessed and a further flight of capital as drug companies and venture capitalists seek safer investments.

Whilst the process of approval still remains a stumbling block to antibiotic development, studies such as this in which potential drug candidates are indentified and characterised will remain valuable as future regulation will no doubt change and an understanding of novel drug candidates in the present will only aid drug development in the future.

On the basis of this increased optimism, the potential of developing AMPs into the clinical setting has potential. However, it seems a futile exercise to develop new anti infective agents if the way in which society views and uses antibiotics remains the same. Antibiotics should not be viewed as a commodity within healthcare. Not only do they provide a potentially lifesaving treatment option and improve our quality of life, they underpin a large array of treatment options for other disease states, for example, in immune suppressive regimes required for cancer treatment, organ transplant and prosthetic joint replacements.

Proper regulation of antibiotic use needs to be put in place on a global scale. Resistance mechanisms do not respect borders and increased global migration and more integrated transport systems will only enhance the spread of resistance. Therefore tighter regulation and administration of antibiotics in the healthcare setting, coupled with a decreased use within farming will be ineffective if only applied to certain parts of the world where regulation can easily be bypassed. For example, the use of antibiotics as a growth promoter in animal feed was banned within the European union (EU) in 2006, however the use of antibiotics still continued although the EU has since tightened the regulation allowing only for prescription only administration (Gilbert., 2011). Within the United States (US), similar restrictions have been implemented, however this is on a voluntary basis with drug companies encouraged to change their labels to require a prescription (Gilbert., 2012), and it remains to be seen if this strategy will have any

effect especially considering that agriculture within the US accounts for 80% of antibiotic use (Frieden., 2013). No such regulation has been imposed in other parts of the world, as examples, the unregulated use of antibiotics within Chinese pig farming (Zhu *et al.*, 2013) and shrimp production in South East Asia (Thuy *et al.*, 2011) have both been highlighted as areas of concern. Similarly, human antibiotic consumption in China is 10 times higher than that of the US per head of population with patient pressure and financial incentives for doctors to administer drugs being part of the problem. For example, 75% of patients with seasonal influenza are estimated to be prescribed antibiotics, and the rate of antibiotic prescription for inpatients is 80% (Li., 2014).

In light of the laissez-faire attitude towards antibiotic regulation and use in a number of highly populated areas of the globe, our understanding of the resistance mechanisms to AMPs needs to be further examined before any widespread administration is considered. Whilst pathogens have yet to develop resistance towards AMPs produced by our innate immune systems, the continued evolutionary process is dynamic, with both innate immunity and bacterial defence evolving, however, what will be the effect on this balance if widespread and unnatural levels of AMPs are present within the environment?

Evidence of the now ubiquitous nature of conventional antibiotics within our environments is abundant (Anderssen and Hughes., 2014) with low concentrations of these agents found within our water and soil systems. Although these concentrations are low they still have a role to play in the continued development of resistance. As highlighted by Anderssen and Hughes. (2014), these sub MIC environments allow for enrichment of resistant strains by providing a selective edge over susceptible colonies whose growth will be retarded. They also highlight the increased mutation rates of

bacteria exposed to sub-MIC antibiotic concentrations. Therefore the widespread release of an antibiotic, evolutionary related to a critical part of our innate immunity, needs to be investigated. For example, how altered are the peptides when they leave the body? In the presence of microorganisms found in water treatment systems and soil how long do they last and what effect do they have on these organisms?

Ultimately, better public dissemination of information regarding antibiotic resistance needs to occur. An understanding of how the routine of our daily lives is compounding the problem of resistance so that a social debate can take place and the mistakes of the past are not repeated. Combating antibiotic resistance will require a holistic approach, novel drug discovery, changes to the approval system, coupled with an increased global consensus and tighter regulation of administration to both patients and in agriculture are required.

The development of novel classes of antimicrobials will be a cornerstone of any concerted effort to tackle the problem. In this thesis the isolation of AMPs exhibiting low toxicity has been achieved from both scorpion and snake venom. It has highlighted how both a genomic and empirical approach can be used in drug discovery to successfully develop new AMPs and how venoms represent an underexploited source of new antimicrobials. A plethora of venoms have yet to be investigated, along with a range of other natural sources, and this study should be widened to examine these.

REFERENCES

- Abdel-Rahman MA, Quintero-Hernandez V, Possani LD. (2013). Venom proteomic and venomous glands transcriptomic analysis of the Egyptian scorpion *Scorpio maurus palmatus* (Arachnida: Scorpionidae). *Toxicon*. **74**:193-207.
- Ahmad I, Perkins WR, Lupan DM, Selsted ME, Janoff AS. (1995). Liposomal entrapment of the neutrophil-derived peptide indolicidin endows it with in vivo antifungal activity. *Biochim Biophys Acta*. **1237**(2):109-14.
- Akwar TH, Poppe C, Wilson J, Reid-Smith RJ, Dyck M, Waddington J, Shang D, Dassie N, McEwen SA. (2007). Risk factors for antimicrobial resistance among fecal *Escherichia coli* from residents on forty-three swine farms. *Microb Drug Resist*. **13**(1):69-76.
- Allen HK, Trachsel J, Looft T, Casey TA. (2014). Finding alternatives to antibiotics. *Ann N Y Acad Sci*. **1323**:91-100.
- Almaaytah A, Zhou M, Wang L, Chen T, Walker B, Shaw C. (2012). Antimicrobial/cytolytic peptides from the venom of the North African scorpion, *Androctonus amoreuxi*: biochemical and functional characterization of natural peptides and a single site-substituted analog. *Peptides* **35**: 291-299.
- Andersson DI, Hughes D. (2014). Microbiological effects of sublethal levels of antibiotics. *Nat Rev Microbiol*. **12**(7):465-78.
- Andrews JM. (2001). Determination of minimum inhibitory concentrations. *J Antimicrob Chemother*. **48** (1):5-16

- Angulo FJ, Nunnery JA, Bair HD. (2004). Antimicrobial resistance in zoonotic enteric pathogens. *Rev Sci Tech.* **23**(2):485-96.
- Angulo Y, Chaves E, Alape A, Rucavado A, Gutiérrez JM, Lomonte B. (1997). Isolation and characterization of a myotoxic phospholipase A2 from the venom of the arboreal snake *Bothriechis (Bothrops) schlegelii* from Costa Rica. *Arch Biochem Biophys.* **339**(2):260-6.
- Antonny B. (2011). Mechanisms of membrane curvature sensing. *Annu Rev Biochem.* **80**:101-23.
- Arouri A, Dathe M, Blume A. Peptide induced demixing in PG/PE lipid mixtures: a mechanism for the specificity of antimicrobial peptides towards bacterial membranes? *Biochim Biophys Acta* **1788**:650–9.
- Arpornsuwan T, Buasakul B, Jaresitthikunchai J, Roytrakul S. (2014). Potent and rapid antigonococcal activity of the venom peptide BmKn2 and its derivatives against different Maldi biotype of multidrug-resistant *Neisseria gonorrhoeae*. *Peptides.* **53** (3):15-20
- Ashrafuzzaman M, Andersen OS, McElhaney RN. (2009). The antimicrobial peptide gramicidin S permeabilizes phospholipid bilayer membranes without forming discrete ion channels. *Biochim Biophys Acta.* **1778**(12):2814-22.
- Bader MW, Navarre WW, Shiao W, Nikaido H, Frye JG, McClelland M, Fang FC, Miller SI. (2003). Regulation of *Salmonella typhimurium* virulence gene expression by cationic antimicrobial peptides. *Mol Microbiol.* **50**(1):219-30.
- Banigan JR, Mandal K, Sawaya MR, Thammavongsa V, Hendrickx AP, Schneewind O, Yeates TO, Kent SB. (2010). Determination of the X-ray structure

- of the snake venom protein omwaprin by total chemical synthesis and racemic protein crystallography. *Protein Sci.* **19**(10):1840-9.
- Basselin M, Robert-Gero M. (1998). Alterations in membrane fluidity, lipid metabolism, mitochondrial activity, and lipophosphoglycan expression in pentamidine-resistant *Leishmania*. *Parasitol Res.* **84**(1):78-83.
- Bayer AS, Schneider T, Sahl HG. (2013). Mechanisms of daptomycin resistance in *Staphylococcus aureus*: role of the cell membrane and cell wall. *Ann N Y Acad Sci.* **1277**:139-58.
- Bechinger B, Zasloff M, Opella SJ. (1993). Structure and orientation of the antibiotic peptide magainin in membranes by solid-state nuclear magnetic resonance spectroscopy. *Protein Sci.* **12**:2077-84.
- Bechinger B. (2009). Rationalizing the membrane interactions of cationic amphipathic antimicrobial peptides by their molecular shape. *Curr Opin Colloid Interf Sci.* **14**:349–55.
- Belokoneva OS, Satake H, Maltseva EL, Palmira NP, Villegas E, Nakajima T, Corzo G. (2004). Pore formation of phospholipid membranes by the action of two hemolytic arachnid peptides of different size. *Biochim Biophys Acta* **1664**:182-188.
- Belokoneva OS, Villegas E, Corzo G, Dai L, Nakajima T. (2003). The haemolytic activity of six arachnid cationic peptides is affected by the phosphatidylcholine-to-sphingomyelin ratio in lipid bilayers. *Biochim Biophys Acta.* **1617**(1-2):22-30 .
- Bertelsen K, Dorosz J, Hansen SK, Nielsen NC, Vosegaard T. (2012). Mechanisms of peptide-induced pore formation in lipid bilayers investigated by oriented ³¹P solid-state NMR spectroscopy. *PLoS One.* **7**(10):e47745

- Bigay J, Casella JF, Antony B. (2004). ArfGAP1 responds to membrane curvature through the folding of a lipid packing sensor motif. *EMBO J.* **24**:2244–2253.
- Bilwes A, Rees B, Moras D, Ménez R, Ménez A. (1994). X-ray structure at 1.55 Å of toxin gamma, a cardiotoxin from *Naja nigricollis* venom. Crystal packing reveals a model for insertion into membranes. *J Mol Biol.* **239**(1):122-36.
- Bina XR, Provenzano D, Nguyen N, Bina JE. (2008). *Vibrio cholerae* RND family efflux systems are required for antimicrobial resistance, optimal virulence factor production, and colonization of the infant mouse small intestine. *Infect Immun.* **76**(8):3595-605.
- Binnig G, Quate CF, Gerber C. (1986). Atomic force microscope. *Phys Rev Lett.* **56**(9):930-933.
- Bobone S, Bocchinfuso G, Park Y, Palleschi A, Hahm KS, Stella L. (2013). The importance of being kinked: role of Pro residues in the selectivity of the helical antimicrobial peptide P5. *J Pept Sci.* **19**(12):758-69.
- Bobone S, Roversi D, Giordano L, Zotti M, Formaggio F, Toniolo C, Park Y, Stella L. (2012). Lipid Dependence of Antimicrobial Peptide Activity is an Unreliable Experimental Test for Different Pore Models. *Biochemistry.* **51**(51):10124-6.
- Bommarius B, Sherman M, Kalman D, Cheng X.(2008). Production of Antimicrobial Peptides, World Pat. WO/2008/140582.
- Bontems F, Roumestand C, Gilquin B, Ménez A, Toma F. (1991). Refined structure of charybdotoxin: common motifs in scorpion toxins and insect defensins. *Science* **254**:1521-3.

- Borges A, Alfonzo M.J, García CC, Winand NJ, Leipold E, Heinemann SH. (2004). Isolation, molecular cloning and functional characterization of a novel beta-toxin from the Venezuelan scorpion, *Tityus zulianus*. *Toxicon* **43**:671-84.
- Botes DP, Viljoen CC. (1974). Purification of phospholipase A from *Bitis gabonica* venom. *Toxicon* **12**(6):611-9.
- Brandeli A, (2012). Nanostructures as promising tools for delivery of antimicrobial peptides. *Mini Rev. Med. Chem.* **12**(8):731e741.
- Brogden KA. (2005). Antimicrobial peptides: pore formers or metabolic inhibitors in bacteria? *Nat Rev Microbiol.* **3**(3):238-50.
- Budrikis Z, Costantini G, La Porta CA, Zapperi S. (2014). Protein accumulation in the endoplasmic reticulum as a non-equilibrium phase transition. *Nat Commun.* **5**:3620.
- Bui JM, McCammon JA. (2006). Protein complex formation by acetylcholinesterase and the neurotoxin fasciculin-2 appears to involve an induced-fit mechanism. *Proc Natl Acad Sci USA* **103**(42):15451-6.
- Calvete JJ. 2013. Snake venomomics: from the inventory of toxins to biology. *Toxicon.* **1**;75:44-62.
- Carmona G, Rodriguez A, Juarez D, Corzo G, Villegas E. (2013). Improved protease stability of the antimicrobial peptide Pin2 substituted with D-amino acids, *Toxicon* **32** (6): 456e466.
- Chan DI, Prenner EJ, Vogel HJ. (2006). Tryptophan- and arginine-rich antimicrobial peptides: structures and mechanisms of action. *Biochim Biophys Acta* **1758**(9):1184-202.

Chang CC, Tseng KH. (1978). Effect of crotamine, a toxin of South American rattlesnake venom, on the sodium channel of murine skeletal muscle. *Br J Pharmacol.* **63**(3):551-9.

Chastre J. (2008). Evolving problems with resistant pathogens. *Clin Microbiol Infect. Suppl* **3**:3-14.

Chen LW, Kao PH, Fu YS, Hu WP, Chang LS. (2011a). Bactericidal effect of *Naja nigricollis* toxin γ is related to its membrane-damaging activity. *Peptides.* **32**(8):1755-63.

Chen LW, Kao PH, Fu YS, Lin SR, Chang LS. (2011b). Membrane-damaging activity of Taiwan cobra cardiotoxin 3 is responsible for its bactericidal activity. *Toxicon* **58**(1):46-53.

Chen PC, Hayashi MA, Oliveira EB, Karpel RL. (2012). DNA-interactive properties of crotamine, a cell-penetrating polypeptide and a potential drug carrier. *PLoS One* **7**(11):e48913.

Chen Y, Guarnieri MT, Vasil AI, Vasil ML, Mant CT, Hodges RS. (2007). Role of peptide hydrophobicity in the mechanism of action of alpha-helical antimicrobial peptides. *Antimicrob Agents Chemother.* **51**(4):1398-406.

Chopra I, Schofield C, Everett M, O'Neill A, Miller K, Wilcox M, Frère JM, Dawson M, Czaplowski L, Urleb U, Courvalin P. (2008). Treatment of health-care-associated infections caused by Gram-negative bacteria: a consensus statement. *Lancet Infect Dis.* **8**(2):133-9.

Chopra I. (2013). The 2012 Garrod lecture: discovery of antibacterial drugs in the 21st century. *J Antimicrob Chemother.* **68**(3):496-505.

- Chopra, I. 2000. New drugs for the superbugs. *Microbiol. Today* **27**:4–6.
- Cociancich S, Goyffon M, Bontems F, Bulet P, Bouet F, Menez A, Hoffmann J, (1993). Purification and characterization of a scorpion defensin, a 4kDa antibacterial peptide presenting structural similarities with insect defensins and scorpion toxins. *Biochem Biophys Res Commun.* **194**:17-22.
- Cohen S. (1977). A strategy for the chemotherapy of infectious disease. *Science* **197**:431–432.
- Cole C, Barber JD, Barton GJ. (2008). The Jpred 3 secondary structure prediction server. *Nucl. Acids Res.* **36**(2): 197-201.
- Conde R, Zamudio FZ, Rodriguez MH, Possani LD. (2000). Scorpine, an anti-malaria and anti-bacterial agent purified from scorpion venom. *FEBS Lett.* **471**:165-168.
- Conley J. (1998). Controlling antibiotic resistance by quelling the epidemic of overuse and misuse of antibiotics. *Can Fam Physician.* **73**: 1780-4.
- Conlon JM, Prajeep M, Mechkarska M, Arafat K, Attoub S, Adem A, Pla D, Calvete JJ. (2014). Peptides with in vitro anti-tumor activity from the venom of the Eastern green mamba, *Dendroaspis angusticeps* (Elapidae). *J Venom Res.* **19**(5):16-21.
- Corona F, Martinez JL. (2013). Phenotypic resistance to bacteria. *Antibiotics* **2**:237-255.
- Coronado MA, Gabdulkhakov A, Georgieva D, Sankaran B, Murakami MT, Arni RK, Betzel C. (2013). Structure of the polypeptide crotamine from the Brazilian

- rattlesnake *Crotalus durissus terrificus*. *Acta Crystallogr D Biol Crystallogr*. **10**:1958-64.
- Corzo G, Escoubas P, Villegas E, Barnhjam KJ, He W, Norton RS, Nakajima T, (2001). Characterization of unique amphipathic antimicrobial peptides from venom of the scorpion *Pandinus imperator*. *Biochem. J.* **359**: 35–45.
- Costa BA, Sanches L, Gomide AB, Bizerra F, Dal Mas C, Oliveira EB, Perez KR, Itri R, Oguiura N, Hayashi MA. (2014). Interaction of the rattlesnake toxin crotamine with model membranes. *J Phys Chem B.* **118**(20):5471-9.
- Cotter PD, Hill C, Ross RP (2006). "What's in a name? Class distinction for bacteriocins". *Nature Reviews Microbiology.* **4**(2):777–88.
- Cruz VL, Ramos J, Melo MN, Martinez-Salazar J. (2013). Bacteriocin AS-48 binding to model membranes and pore formation as revealed by coarse-grained simulations. *Biochim Biophys Acta.* **1828**(11):2524-31.
- Dai C, Ma Y, Zhao Z, Zhao R, Wang Q, Wu Y, Cao Z, Li W. (2008). Mucroporin, the first cationic host defense peptide from the venom of *Lychas mucronatus*. *Antimicrob Agents Chemother.* **52**(11):3967-72.
- Dai L, Corzo G, Naoki H, Andriantsiferana M, Nakajima T. (2002). Purification, structure-function analysis, and molecular characterization of novel linear peptides from scorpion *Opisthacanthus madagascariensis*. *Biochem Biophys Res Commun.* **293**:1514-1522.
- Dai L, Yasuda A, Naoki H, Corzo G, Andriantsiferana M, Nakajima T. (2001). IsCT, a novel cytotoxic linear peptide from scorpion *Opisthacanthus madagascariensis*. *Biochem Biophys Res Commun.* **286**: 820-825.

Dathe M, Nikolenko H, Meyer J, Beyermann M, Bienert M. (2001). Optimization of the antimicrobial activity of magainin peptides by modification of charge. *FEBS Lett.* **501**(2-3):146-50.

Dathe M, Wieprecht T, Nikolenko H, Handel L, Maloy WL, MacDonald DL, Beyermann M, Bienert M. (1997). Hydrophobicity, hydrophobic moment and angle subtended by charged residues modulate antibacterial and haemolytic activity of amphipathic helical peptides. *FEBS Lett.* **403**(2):208-12.

Dauplais M, Neumann JM, Pinkasfeld S, Ménez A, Roumestand C. (1995). An NMR study of the interaction of cardiotoxin gamma from *Naja nigricollis* with perdeuterated dodecylphosphocholine micelles. *Eur J Biochem.* **230**(1):213-20.

Davlieva M, Zhang W, Arias CA, Shamooy Y. (2013). Biochemical characterization of cardiolipin synthase mutations associated with daptomycin resistance in enterococci. *Antimicrob Agents Chemother.* **57**(1):289-96.

De Groot AS, Rivera DS, McMurry JA, Buus S, Martin W. (2007). Identification of immunogenic HLA-B7 "Achilles' heel" epitopes within highly conserved regions of HIV. *Vaccine* **26** (24): 3059e3071.

de Oliveira Junior NG, e Silva Cardoso MH, Franco OL. (2013). Snake venoms: attractive antimicrobial proteinaceous compounds for therapeutic purposes. *Cell Mol Life Sci.* **70**(24):4645-58.

de Weille JR, Schweitz H, Maes P, Tartar A, Lazdunski M. (1991). Calciseptine, a peptide isolated from black mamba venom, is a specific blocker of the L-type calcium channel. *Proc Natl Acad Sci U S A.* **88**(6):2437-40.

Dean SN, Bishop BM, van Hoek ML. (2011). Natural and synthetic cathelicidin peptides with anti-microbial and anti-biofilm activity against *Staphylococcus aureus*. *BMC Microbiol.*:111e114.

Dempsey CE, Bazzo R, Harvey TS, Syperek I, Boheim G, Campbell ID. (1991). Contribution of proline-14 to the structure and actions of melittin. *FEBS Lett.* **281**(1-2):240-4.

Dennison SR, Wallace J, Harris F, Phoenix DA. (2005). Amphiphilic alpha-helical antimicrobial peptides and their structure/function relationships. *Protein Pept Lett.* **12**(1):31-9.

Department of Health. (2013). UK Five Year Antimicrobial Resistance Strategy 2013 to 2018. London: Whitehall.

Díaz C, Gutiérrez JM, Lomonte B. (1992). Isolation and characterization of basic myotoxic phospholipases A2 from *Bothrops godmani* (Godman's pit viper) snake venom. *Arch Biochem Biophys.* **298**(1):135-42.

Díaz C, Lomonte B, Zamudio F, Gutiérrez JM. (1995). Purification and characterization of myotoxin IV, a phospholipase A2 variant, from *Bothrops asper* snake venom. *Nat Toxins.* **3**(1):26-31.

Diaz P, D'Suze G, Salazar V, Sevcik C, Shannon JD, Sherman NE, Fox JW. (2009). Antibacterial activity of six novel peptides from *Tityus discrepans* scorpion venom. A fluorescent probe study of microbial membrane Na⁺ permeability changes. *Toxicon.* **54**: 802-817.

Diochot S, Baron A, Salinas M, Douguet D, Scarzello S, Dabert-Gay AS, Debayle D, Friend V, Alloui A, Lazdunski M, Lingueglia E. (2012). Black mamba venom peptides target acid-sensing ion channels to abolish pain. *Nature* **490**(7421):552-5.

- Dixon MC. (2008). Quartz crystal microbalance with dissipation monitoring: enabling real-time characterization of biological materials and their interactions. *J Biomol Tech.* **19**(3):151-8.
- Diz Filho EB, Marangoni S, Toyama DO, Fagundes FH, Oliveira SC, Fonseca FV, Calgarotto AK, Joazeiro PP, Toyama MH. (2009). Enzymatic and structural characterization of new PLA2 isoform isolated from white venom of *Crotalus durissus ruruima*. *Toxicon* **53**(1):104-14.
- Doley R, Kini RM. (2009). Protein complexes in snake venom. *Cell Mol Life Sci.* **66**(17):2851-71.
- Dorrer E, Teuber M. (1977). Induction of polymyxin resistance in *Pseudomonas fluorescens* by phosphate limitation. *Arch Microbiol.* **114**(1):87-9.
- Drider D, Fimland G, Héchard Y, McMullen LM, Prévost H. (2006). The continuing story of class IIa bacteriocins. *Microbiol Mol Biol Rev.* **70**(2):564-82.
- Drin G, Antonny B. (2010) Amphipathic helices and membrane curvature. *FEBS Lett.* **584**:1840–1847.
- Drin G, Casella JF, Antonny B. (2007). A general amphipathic α -helical motif for sensing membrane curvature. *Nat. Struct. Mol. Biol.* **14**:138–146.
- Drlica K, Zhao X. (2007). Mutant selection window hypothesis updated. *Clin Infect Dis.* **44**(5):681-8.
- Drolle E, Gaikwad RM, Leonenko Z. (2012). Nanoscale Electrostatic Domains in Cholesterol-Laden Lipid Membranes Create a Target for Amyloid Binding. *Biophysical J.* **103**(4): 27-29.

- D'Suze G, Sevcik C, Corona M, Zamudio FZ, Batista CVF, Coronas FI, Possani LD. (2004) Ardiscretin a novel arthropod-selective toxin from *Tityus discrepans* scorpion venom. *Toxicon* **43**: 263-272.
- Dubovskii PV, Lesovoy DM, Dubinnyi MA, Utkin YN, Arseniev AS. (2003). Interaction of the P-type cardiotoxin with phospholipid membranes. *Eur J Biochem.* **270**(9):2038-46.
- Duclohier H. (2004). Helical kink and channel behaviour: a comparative study with the peptaibols alamethicin, trichotoxin and antiamoebin. *Eur Biophys J.* **33**(3):169-74.
- Echols RM. (2011). Understanding the regulatory hurdles for antibacterial drug development in the post-Ketek world. *Ann N Y Acad Sci.* **1241**:153-61.
- Edgerton M, Koshlukova SE. (2000). Salivary histatin 5 and its similarities to the other antimicrobial proteins in human saliva. *Adv Dent Res.* 16-21.
- Eichner T, Radford SE. (2011). A diversity of assembly mechanisms of a generic amyloid fold. *Mol Cell.* **43**(1):8-18.
- Eisenberg D, Weiss RM, Terwilliger TC. (1984). The hydrophobic moment detects periodicity in protein hydrophobicity. *Proc Natl Acad Sci U S A.* **81**(1):140-4.
- El Jastimi R, Lafleur M. (1999). Nisin promotes the formation of non-lamellar inverted phases in unsaturated phosphatidylethanolamines. *Biochim Biophys Acta (BBA)*:1418:97-105.
- El Kirat K, Morandat S, Dufrêne YF. (2010). Nanoscale analysis of supported lipid bilayers using atomic force microscopy. *Biochim Biophys Acta.* **1798**(4):750-65.

- Epanand RF, Martinou JC, Montessuit S, Epanand RM, Yip CM. (2002). Direct evidence for membrane pore formation by the apoptotic protein Bax. *Biochem Biophys Res Commun.* **298**(5):744-9.
- Epanand RF, Wang G, Berno B, Epanand RM. (2009) Lipid segregation explains selective toxicity of a series of fragments derived from the human cathelicidin LL-37. *Antimicrob Agents Chemother* **53**:3705–14.
- Epanand RM, Epanand RF. (2009) Lipid domains in bacterial membranes and the action of antimicrobial agents. *Biochim Biophys Acta.* **1788**:289–94.
- Epanand RM, Rotem S, Mor A, Berno B, Epanand RF. (2008) Bacterial membranes as predictors of antimicrobial potency. *J Am Chem Soc.* **130**:14346–52.
- Epanand RM.. (1998) Lipid polymorphism and protein-lipid interactions. *Biochim Biophys Acta (BBA) – Rev Biomembr.* **1376**:353–68.
- Ernst RK, Guina T, Miller SI. (2001). *Salmonella Typhimurium* outer membrane remodeling: role in resistance to host innate immunity. *Microbes Infect.* **3**(14-15):1327-34.
- Falcao CB, de La Torre BG, Pérez-Peinado C, Barron AE, Andreu D, Rádis-Baptista G. (2014). Viperacidins: a novel family of cathelicidin-related peptides from the venom gland of South American pit vipers. *Amino Acids* **46**(11):2561-71.
- Falciani C, Lozzi L, Scali S, Brunetti J, Bracci L, Pini A. (2014). Sitespecific pegylation of an antimicrobial peptide increases resistance to *Pseudomonas aeruginosa* elastase. *Amino Acids* **46**(5): 1403e1407.

Fan K, Li H, Wang Z, Du W, Yin W, Sun Y, Jiang J. (2014). Expression and Purification of the Recombinant Porcine NK-lysin in *Pichia pastoris* and Observation of Anticancer Activity in Vitro. *Prep Biochem Biotechnol.* In Press.

Fan Z, Cao L, He Y, Hu J, Di Z, Wu Y, Li W, Cao Z. (2011). Ctriporin, a new anti-methicillin-resistant *Staphylococcus aureus* peptide from the venom of the scorpion *Chaerilus tricostatus*. *Antimicrob Agents Chemother.* **55**: 5220-9.

Fantner GE, Barbero RJ, Gray DS, Belcher AM. (2010). Kinetics of antimicrobial peptide activity measured on individual bacterial cells using high-speed atomic force microscopy. *Nat Nanotechnol.* **5**(4):280-5.

Farris C, Sanowar S, Bader MW, Pfuetzner R, Miller SI. (2010). Antimicrobial peptides activate Rcs regulation through the outer membrane lipoprotein RcsF. *J Bacteriol.* **192**(19):4894-903.

Fasoli A, Salomone F, Benedusi M, Boccardi C, Rispoli G, Beltram F, Cardarelli F. (2014). Mechanistic insight into CM18-Tat11 peptide membrane-perturbing action by whole-cell patch-clamp recording. *Molecules.* **19**(7):9228-39.

Fehlbaum P, Bulet P, Chernysh S, Briand JP, Roussel JP, Letellier L, Hetru C, Hoffmann JA. (1996). Structure-activity analysis of thanatin, a 21-residue inducible insect defense peptide with sequence homology to frog skin antimicrobial peptides. *Proc Natl Acad Sci USA* **93**(3):1221-5.

Fennell JF, Shipman WH, Cole LJ. (1968). Antibacterial action of melittin, a polypeptide from bee venom. *Proc Soc Exp Biol Med.* **127**(3):707-10.

Fernandez DI, Le Brun AP, Whitwell TC, Sani MA, James M, Separovic F. (2012). The antimicrobial peptide aurein 1.2 disrupts model membranes via the carpet mechanism. *Phys Chem Chem Phys.* **14**(45):15739-51.

Fernández L, Jenssen H, Bains M, Wiegand I, Gooderham WJ, Hancock RE. (2010). The two-component system CprRS senses cationic peptides and triggers adaptive resistance in *Pseudomonas aeruginosa* independently of ParRS. *Antimicrob Agents Chemother.* **56**(12):6212-22.

Fernandez-Reyes Ma, Di'az D, de la Torre BG, Cabrales-Rico A, Valle's-Miret M, Jimenez-Barbero Js. (2010). Lysine Ne-trimethylation, a tool for improving the selectivity of antimicrobial peptides. *J Med Chem.* **53**:5587-96.

Fjell CD, Jenssen H, Hilpert K, Cheung WA, Panté N, Hancock RE, Cherkasov A. (2009). Identification of novel antibacterial peptides by chemoinformatics and machine learning. *J Med Chem.* **52**(7):2006-15.

Fontell K. (1990) Cubic phases in surfactant and surfactant-like lipid systems. *Colloid Polym Sci.* **268**:264-85.

Fox JL. (2013). Antimicrobial peptides stage a comeback. *Nat. Biotechnol.* **31**(5),379e382.

Friedman L, Alder JD, Silverman JA. (2006). Genetic changes that correlate with reduced susceptibility to daptomycin in *Staphylococcus aureus*. *Antimicrob Agents Chemother.* **50**(6):2137-45.

Friedrich LV, White RL, Bosso JA. (1999). Impact of use of multiple antimicrobials on changes in susceptibility of gram-negative aerobes. *Clin Infect Dis.* **28**(5):1017-24.

Fromm & Hargrove. (2012). *Essentials of Biochemistry*. Berlin: Springer.

Fry BG, Scheib H, van der Weerd L, Young B, McNaughtan J, Ramjan SF, Vidal N, Poelmann RE, Norman JA. (2008). Evolution of an arsenal: structural and

- functional diversification of the venom system in the advanced snakes (Caenophidia). *Mol Cell Proteomics*. 7(2):215-46.
- Fuentes-Perez ME, Dillingham MS, Moreno-Herrero F. (2013). AFM volumetric methods for the characterization of proteins and nucleic acids. *Methods*. 60(2):113-21.
- Gajski G, Garaj-Vrhovac V. (2013). Melittin: a lytic peptide with anticancer properties. *Environ Toxicol Pharmacol*. 36(2):697-705.
- Galanth C, Abbassi F, Lequin O, Ayala-Sanmartin J, Ladram A, Nicolas P, Amiche M. (2009). Mechanism of antibacterial action of dermaseptin B2: interplay between helix-hinge-helix structure and membrane curvature strain. *Biochemistry* 48(2):313-27.
- Gao B, Xu J, Del Carmen Rodriguez M., Lanz-Mendoza H, Hernandez-Rivas R, Du W, Zhu S. (2010). Characterization of two linear cationic antimalarial peptides in the scorpion *Mesobuthus eupeus*. *Biochimie* 92: 350-359.
- García-Sáez AJ, Chiantia S, Salgado J, Schwille P. (2007). Pore formation by a Bax-derived peptide: effect on the line tension of the membrane probed by AFM. *Biophys J*. 93(1):103-12.
- Ghosh S, LaPara TM. (2007). The effects of subtherapeutic antibiotic use in farm animals on the proliferation and persistence of antibiotic resistance among soil bacteria. *ISME J*. 1(3):191-203.
- Giangaspero A, Sandri L, Tossi A. (2001). Amphipathic alpha helical antimicrobial peptides. *Eur J Biochem*. 268(21):5589-600.
- Gilbert N. (2011). Summit urged to clean up farming. *Nature* 478(7367):183

- Gilbert N. (2012). Rules tighten on use of antibiotics on farms. *Nature* **481**(7380):125.
- Giorgione JR, Huang Z, Epan RM. (1998) Increased activation of protein kinase C with cubic phase lipid compared with liposomes. *Biochemistry* **37**(8):2384-92.
- Gomes VM, Carvalho AO, Da Cunha M, Keller MN, Bloch C Jr, Deolindo P, Alves EW. (2005). Purification and characterization of a novel peptide with antifungal activity from *Bothrops jararaca* venom. *Toxicon* **45**(7):817-27.
- Gordon YL, Romanowski EG, McDermott AM. (2005). A review of antimicrobial peptides and their therapeutic potential as antiinfective drugs. *Curr. Eye Res.* **30**(7):505e515.
- Grant GA, Chiappinelli VA. (1985). kappa-Bungarotoxin: complete amino acid sequence of a neuronal nicotinic receptor probe. *Biochemistry* **24**(6):1532-7.
- Güell I, Cabrefiga J, Badosa E, Ferre R, Talleda M, Bardají E, Planas M, Feliu L, Montesinos E. (2011). Improvement of the efficacy of linear undecapeptides against plant-pathogenic bacteria by incorporation of D-amino acids. *Appl. Environ. Microbiol.* **77**(8): 2667e2675.
- Gunn JS, Ryan SS, Van Velkinburgh JC, Ernst RK, Miller SI. (2000). Genetic and functional analysis of a PmrA-PmrB-regulated locus necessary for lipopolysaccharide modification, antimicrobial peptide resistance, and oral virulence of *Salmonella enterica serovar typhimurium*. *Infect Immun.* **68**(11):6139-46.
- Guo X, Ma C, Du Q, Wie R, Wang L, Zhou M, Chen T, Shaw C. (2013). Two peptides, TsAP-1 and TsAP-2, from the venom of the Brazilian yellow scorpion, *Tityus serrulatus*: Evaluation of their antimicrobial and anticancer activities. *Biochimie.* **95**:1784-94.

- Gutiérrez JM, Lomonte B, Cerdas L. (1986). Isolation and partial characterization of a myotoxin from the venom of the snake *Bothrops nummifer*. *Toxicon* **24**(9):885-94.
- Gutiérrez JM, Ownby CL, Odell GV. (1984). Skeletal muscle regeneration after myonecrosis induced by crude venom and a myotoxin from the snake *Bothrops asper* (Fer-de-Lance). *Toxicon* **22**(5):719-31.
- Hachmann AB, Sevim E, Gaballa A, Popham DL, Antelmann H, Helmann JD. (2011). Reduction in membrane phosphatidylglycerol content leads to daptomycin resistance in *Bacillus subtilis*. *Antimicrob Agents Chemother.* **55**(9):4326-37.
- Hancock RE. (1997). Peptide antibiotics. *Lancet.* **349**(9049):418-22.
- Hancock RE. (1999). Host defence (cationic) peptides: what is their future clinical potential? *Drugs* **57**(4):469-73.
- Haney EF, Nathoo S, Vogel HJ, Prenner EJ. (2010). Induction of non-lamellar lipid phases by antimicrobial peptides: a potential link to mode of action. *Chem Phys Lipids* **163**:82–93.
- Harris F, Dennison SR, Phoenix DA. (2009). Anionic antimicrobial peptides from eukaryotic organisms. *Curr Protein Pept Sci.* **10**(6):585-606.
- Harrison PL, Abdel-Rahman MA, Miller K, Strong PN. (2014). Antimicrobial peptides from scorpion venoms. *Toxicon* **88**:115-37
- Hauser H, Pascher I, Pearson RH, Sundell S. (1981) Preferred conformation and molecular packing of phosphatidylethanolamine and phosphatidylcholine. *Biochim. Biophys. Acta* **650**: 21–51.
- Hayashi MA, Nascimento FD, Kerkis A, Oliveira V, Oliveira EB, Pereira A, Rádis-Baptista G, Nader HB, Yamane T, Kerkis I, Tersariol IL. (2008). Cytotoxic effects

of crotamine are mediated through lysosomal membrane permeabilization. *Toxicon* **52**(3):508-17.

He Q, Fu AY, Li TJ. (2015). Expression and one-step purification of the antimicrobial peptide cathelicidin-BF using the intein system in *Bacillus subtilis*. *J Ind Microbiol Biotechnol*. In Press.

Heath GR, Johnson BR, Olmsted PD, Connell SD, Evans SD. (2013). Actin assembly at model-supported lipid bilayers. *Biophys J*. **105**(10):2355-65.

Heath GR, Roth J, Connell SD, Evans SD. (2014). Diffusion in low-dimensional lipid membranes. *Nano Lett*. **14**(10):5984-8.

Heller WT, He K, Ludtke SJ, Harroun TA, Huang HW. (1997). Effect of changing the size of lipid headgroup on peptide insertion into membranes. *Biophys J*. **73**(1):239-44.

Herasimenka Y, Benincasa M, Mattiuzzo M, Cescutti P, Gennaro R, Rizzo R. (2005). Interaction of antimicrobial peptides with bacterial polysaccharides from lung pathogens. *Peptides*. **26**(7):1127-32.

Hernández-Aponte CA, Silva-Sanchez J, Quintero-Hernández V, Rodríguez-Romero A, Balderas C, Possani LD, Gurrola GB. (2011). Vejovine, a new antibiotic from the scorpion venom of *Vaejovis mexicanus*. *Toxicon* **57**:84-92.

Hickel A, Danner-Pongratz S, Amenitsch H, Degovics G, Rappolt M, Lohner K. (2008). Influence of antimicrobial peptides on the formation of nonlamellar lipid mesophases. *Biochim Biophys Acta* **1778**:2325–33.

- Hilliard JJ, Goldschmidt RM, Licata L, Baum EZ, Bush K. 1999. Multiple mechanisms of action for inhibitors of histidine protein kinases from bacterial two-component systems. *Antimicrob Agents Chemother.* **43**(7):1693-9.
- Holak TA, Engström A, Kraulis PJ, Lindeberg G, Bennich H, Jones TA, Gronenborn AM, Clore GM. (1988). The solution conformation of the antibacterial peptide cecropin A: a nuclear magnetic resonance and dynamical simulated annealing study. *Biochemistry* **27**(20):7620-9.
- Hritonenko V, Stathopoulos C. (2007). Omptin proteins: an expanding family of outer membrane proteases in Gram-negative *Enterobacteriaceae*. *Mol Membr Biol.* **24**(5-6):395-406.
- Huang HW. (2000). Action of antimicrobial peptides: two-state model. *Biochemistry.* **39**(29):8347-52.
- Huang Y, Huang J, Chen Y. (2010). Alpha-helical cationic antimicrobial peptides: relationships of structure and function. *Protein Cell* **1**(2):143-52.
- Huber R, Berendes R, Burger A, Luecke H, Karshikov A, (1992). Annexin V-crystal structure and its implications on function. *Behring Inst Mitt.* **91**:107-25.
- Hurley JH, Misra S, (2000) Signaling and subcellular targeting by membrane-binding domains. *Ann Rev Biophys Biomol Struct.* **29**:49–79.
- Hussain R, Siligardi G. (2010). Novel drug delivery system for lipophilic therapeutics of small molecule, peptide-based and protein drugs. *Chirality.* **22** (1):44-6.
- Jahn TR, Radford SE. (2008). Folding versus aggregation: polypeptide conformations on competing pathways. *Arch Biochem Biophys.* **469**(1):100-17.

- Jang SA, Sung BH, Cho JH, Kim SC. (2009). Direct expression of antimicrobial peptides in an intact form by a translationally coupled two-cistron expression system *Appl. Environ. Microbiol.* **75**:3980–3986.
- Jenssen H, Hamill P, Hancock RE. (2006). Peptide antimicrobial agents. *Clin Microbiol Rev.* **19**(3):491-511.
- Jerusalinsky D, Cerveñasky C, Peña C, Raskovsky S, Dajas F. (1994). Two polypeptides from *Dendroaspis angusticeps* venom selectively inhibit the binding of central muscarinic cholinergic receptor ligands. *Neurochem Int.* **20**(2):237-46.
- Jiang Z, Vasil A, Hale JD, Hancock RE, Vasil ML, Hodges RS. (2008). Effects of net charge and the number of positively charged residues on the biological activity of amphipathic alpha-helical cationic antimicrobial peptides. *Biopolymers* **90**(3):369-83.
- Jones S, Howl J. (2012). Enantiomer-specific bioactivities of peptidomimetic analogues of mastoparan and mitoparan: characterization of inverso mastoparan as a highly efficient cell penetrating peptide. *Bioconjug Chem.* **23**(1):47-56.
- Joubert FJ, Townshend GS, Botes DP. (1983). Snake Venoms. Purification, some properties of two phospholipases A2 (CM-I and CM-II) and the amino-acid sequence of CM-II and *Bitis nasicornis* (horned adder) venom. *Hoppe Seylers Z Physiol Chem.* **364**(12):1717-26.
- Kaduk C, Dathe M, Bienert M. (1998). Functional modifications of alamethicin ion channels by substitution of glutamine 7, glycine 11 and proline 14. *Biochim Biophys Acta.* **1373**(1):137-46.

Kaiser II, Gutierrez JM, Plummer D, Aird SD, Odell GV. (1990). The amino acid sequence of a myotoxic phospholipase from the venom of *Bothrops asper*. *Arch Biochem Biophys*. **278**(2):319-25.

Keller SL, Gruner SM, Gawrisch K. (1996) Small concentrations of alamethicin induce a cubic phase in bulk phosphatidylethanolamine mixtures. *Biochim Biophys Acta* **1278**:241–6.

Kini RM. (2003). Excitement ahead: structure, function and mechanism of snake venom phospholipase A2 enzymes. *Toxicon* **42**(8):827-40.

Kobayashi S, Chikushi A, Tougu S, Imura Y, Nishida M, Yano Y, Matsuzaki K. (2004). Membrane translocation mechanism of the antimicrobial peptide buforin 2. *Biochemistry* **43**(49):15610-6.

Kondejewski LH, Lee DL, Jelokhani-Niaraki M, Farmer SW, Hancock RE, Hodges RS. (2002). Optimization of microbial specificity in cyclic peptides by modulation of hydrophobicity within a defined structural framework. *J Biol Chem*. **277**(1):67-74.

Krabben L, Fassio A, Bhatia VK, Pechstein A, Onofri F, Fadda M, Messa M, Rao Y, Shupliakov O, Stamou D, Benfenati F, Haucke V. (2011). Synapsin I senses membrane curvature by an amphipathic lipid packing sensor motif. *J Neurosci*. **31**(49):18149-54.

Kramer NE, van Hijum SA, Knol J, Kok J, Kuipers OP. (2006). Transcriptome analysis reveals mechanisms by which *Lactococcus lactis* acquires nisin resistance. *Antimicrob Agents Chemother*. **50**(5):1753-61.

Kuhn-Nentwig L. (2003). Antimicrobial and cytolytic peptides of venomous arthropods. *Cell Mol Life Sci* **60**, 2651-68.

Kumarasamy KK, Toleman MA, Walsh TR, Bagaria J, Butt F, Balakrishnan R, Chaudhary U, Doumith M, Giske CG, Irfan S, Krishnan P, Kumar AV, Maharjan S, Mushtaq S, Noorie T, Paterson DL, Pearson A, Perry C, Pike R, Rao B, Ray U, Sarma JB, Sharma M, Sheridan E, Thirunarayan MA, Turton J, Upadhyay S, Warner M, Welfare W, Livermore DM, Woodford N. (2010). Emergence of a new antibiotic resistance mechanism in India, Pakistan, and the UK: a molecular, biological, and epidemiological study. *Lancet Infect Dis.* **10**(9):597-602.

Kupferwasser LI, Yeaman MR, Shapiro SM, Nast CC, Sullam PM, Filler SG, Bayer AS. (1999). Acetylsalicylic acid reduces vegetation bacterial density, hematogenous bacterial dissemination, and frequency of embolic events in experimental *Staphylococcus aureus* endocarditis through antiplatelet and antibacterial effects.. *Circulation.* **99**(21):2791-7.

Lam KL, Ishitsuka Y, Cheng Y, Chien K, Waring AJ, Lehrer RI, Lee KY. (2006). Mechanism of supported membrane disruption by antimicrobial peptide protegrin-1. *J Phys Chem B.* **110**(42):21282-6.

Lam KL, Wang H, Siaw TA, Chapman MR, Waring AJ, Kindt JT, Lee KY. (2012). Mechanism of structural transformations induced by antimicrobial peptides in lipid membranes. *Biochim Biophys Acta* **1818**(2):194-204.

Lamb HM, Wiseman LR. (1998). Pexiganan acetate. *Drugs* **56** (6), 1047e1052.

Latour FA, Amer LS, Papanstasiou EA, Bishop BM, van Hoek ML. (2010). Antimicrobial activity of the *Naja atra* cathelicidin and related small peptides. *Biochem Biophys Res Commun.* **396**(4):825-30.

Laure CJ. (1975). The primary structure of crotamine . *Hoppe Seylers Z Physiol Chem.* 1975 **356**(2):213-5.

Le Sage V, Zhu L, Lepage C, Portt A, Viau C, Daigle F, Gruenheid S, Le Moual H. (2012). An outer membrane protease of the ompT family prevents activation of the *Citrobacter rodentium* PhoPQ two-component system by antimicrobial peptides. *Mol Microbiol.* **74**(1):98-111.

Lee JH, Kim JH, Hwang SW, Lee KW, Yoon HK, Lee HS, Hong SS. (2000). High-level expression of antimicrobial peptide mediated by a fusion partner reinforcing formation of inclusion bodies *Biochem. Biophys. Res. Commun.*, **277**: 575–580.

Lee K, Shin SY, Kim K, Lim SS, Hahm KS, Kim Y. (2004). Antibiotic activity and structural analysis of the scorpion-derived antimicrobial peptide IsCT and its analogs. *Biochem Biophys Res Commun.* **323**:712-719.

Lee MT, Hung WC, Chen FY, Huang HW. (2005). Many-body effect of antimicrobial peptides: on the correlation between lipid's spontaneous curvature and pore formation. *Biophys J.* **89**:4006–16.

Lee QU. (2014). Use of cephalosporins in patients with immediate penicillin hypersensitivity: cross-reactivity revisited. *Hong Kong Med J.* **20**(5):428-36.

Lee SW, Foley E.J, Epstein JA. Mode of Action of penicillin: I. (1944). Bacterial growth and penicillin activity-*Staphylococcus aureus* FDA. *J. Bacteriol.* **48**:393–399.

Lei W, Zhang Y, Yu G, Jiang P, He Y, Lee W, Zhang Y. (2010). Cloning and sequence analysis of an *Ophiophagus hannah* cDNA encoding a precursor of two natriuretic peptide domains. *Toxicon* **57**(5):811-6.

Leontiadou H, Mark AE, Marrink SJ, (2006). Antimicrobial peptides in action. *J Am Chem Soc.* **128**(37):12156-61.

Lesovoy DM, Bocharov EV, Lyukmanova EN, Kosinsky YA, Shulepko MA, Dolgikh DA, Kirpichnikov MP, Efremov RG, Arseniev AS. (2009). Specific membrane binding of neurotoxin II can facilitate its delivery to acetylcholine receptor. *Biophys J.* **97**(7):2089-97.

Li A, Lee PY, Ho B, Ding JL, Lim CT. (2007). Atomic force microscopy study of the antimicrobial action of Sushi peptides on Gram negative bacteria. *Biochim Biophys Acta.* **1768**(3):411-8.

Li L, Cheng JX. (2008). Label-free coherent anti-stokes Raman scattering imaging of coexisting lipid domains in single bilayers. *J Phys Chem B.* **112**(6):1576-9.

Li Q, Zhao Z, Zhou D, Chen Y, Hong W, Cao L, Yang J, Zhang Y, Shi W, Cao Z, Wu Y, Yan H, Li W. (2011). Virucidal activity of a scorpion venom peptide variant mucroporin-M1 against measles, SARS-CoV and influenza H5N1 viruses. *Peptides* **32**:1518-25.

Li Y. (2011). Recombinant production of antimicrobial peptides in *Escherichia coli*: a review. *Protein Expr Purif.* **80**(2):260-7.

Li Y. (2014). China's misuse of antibiotics should be curbed. *BMJ.* **12**(348):g1083

Lim SS, Yoon SP, Park Y, Zhu WL, Park IS, Hahm KS, Shin SY. (2006). Mechanism of antibacterial action of a synthetic peptide with an Ala-peptoid residue based on the scorpion-derived antimicrobial peptide IsCT. *Biotechnol Lett.* **28**(18):1431-7.

Liu ZY, Xu T, Zheng ST, Zhang LT, Zhang FC. (2013). Studies on the properties of Cecropin-XJ expressed in yeast from Xinjiang silkworm. *Wei Sheng Wu Xue Bao.* **43**(5):635-41.

- Livermoore D. (2009). Has the era of untreatable infections arrived? *J Antimicrob Chemother.* **1**:i29-36.
- Llobet E, Tomás JM, Bengoechea JA. (2008). Capsule polysaccharide is a bacterial decoy for antimicrobial peptides. *Microbiology* **154**(12):3877-86.
- Lohner K, Latal A, Degovics G, Garidel P. (2001). Packing characteristics of a model system mimicking cytoplasmic bacterial membranes. *Chem Phys Lipids* **111**:177–92.
- Lomonte B, Gutiérrez JM. (1989). A new muscle damaging toxin, myotoxin II, from the venom of the snake *Bothrops asper* (terciopelo). *Toxicon* **27**(7):725-33.
- Lu S, Walters G, Parg R, Dutcher JR. (2014). Nanomechanical response of bacterial cells to cationic antimicrobial peptides. *Soft Matter.* **10**(11):1806-15.
- Ludtke SJ, He K, Heller WT, Harroun TA, Yang L, Huang HW. (1996). Membrane pores induced by magainin. *Biochemistry* **35**(43):13723-8.
- Ludtke SJ, He K, Wu Y, Huang HW. (1994). Cooperative membrane insertion of magainin correlated with its cytolytic activity. *Biochim Biophys Acta–Biomembr.* **1190**:181–4.
- Lysenko ES, Gould J, Bals R, Wilson JM, Weiser JN. (2000). Bacterial phosphorylcholine decreases susceptibility to the antimicrobial peptide LL-37/hCAP18 expressed in the upper respiratory tract. *Infect Immun.* **68**(3):1664-71.
- Majerle A, Kidric J, Jerala R. (2000). Production of stable isotope enriched antimicrobial peptides in *Escherichia coli*: an application to the production of a ¹⁵N-enriched fragment of lactoferrin J. *Biomol. NMR.* **18**:145–151.

- Mandelbrot BB, Vespignani A, Kaufman, H. (1995) Crosscut analysis of large radial DLA: departures from self-similarity and lacunarity effects. *Europhysics Letters* **32**:199-204.
- Mason AJ, Marquette A, Bechinger B. (2007) Zwitterionic phospholipids and sterols modulate antimicrobial peptide-induced membrane destabilization. *Biophys J.* **93**:4289–99.
- Matsuzaki K, Murase O, Fujii N, Miyajima K. (1996). An antimicrobial peptide, magainin 2, induced rapid flip-flop of phospholipids coupled with pore formation and peptide translocation. *Biochemistry* **35**(35):11361-8.
- Matsuzaki K, Nakayama M, Fukui M, Otaka A, Funakoshi S, Fujii N, Bessho K, Miyajima K. (1993). Role of disulfide linkages in tachyplesin-lipid interactions. *Biochemistry* **32**(43):11704-10.
- Matsuzaki K, Sugishita K, Ishibe N, Ueha M, Nakata S, Miyajima K, Epanand RM. (1998). Relationship of membrane curvature to the formation of pores by magainin 2. *Biochemistry* **37**(34):11856-63.
- Matsuzaki K, Yoneyama S, Fujii N, Miyajima K, Yamada K, Kirino Y, Anzai K. (1997). Membrane permeabilization mechanisms of a cyclic antimicrobial peptide, tachyplesin I, and its linear analog. *Biochemistry* **36**(32):9799-806.
- Mc Dermott W. (1958) Microbial persistence. *Yale J. Biol. Med.* **30**:257–291.
- McBride SM, Sonenshein AL. (2011). The *dlt* operon confers resistance to cationic antimicrobial peptides in *Clostridium difficile*. *Microbiology* **157**(5):1457-65.

- McDowell RS, Dennis MS, Louie A, Shuster M, Mulkerrin MG, Lazarus RA. (1992). Mambin, a potent glycoprotein IIb-IIIa antagonist and platelet aggregation inhibitor structurally related to the short neurotoxins. *Biochemistry* **31**(20):4766-72.
- McHenry AJ, Sciacca MF, Brender JR, Ramamoorthy A, (2012). Does cholesterol suppress the antimicrobial peptide induced disruption of lipid raft containing membranes? *Biochim Biophys Acta* **1818**(12):3019-24.
- McLaurin J, Franklin T, Chakrabarty A, Fraser PE. (1998). Phosphatidylinositol and inositol involvement in Alzheimer amyloid-beta fibril growth and arrest. *J Mol Biol.* **278**(1):183-94.
- McPhee JB, Lewenza S, Hancock REW. (2003). Cationic antimicrobial peptides activate a two-component regulatory system, PmrA-PmrB, that regulates resistance to polymyxin B and cationic antimicrobial peptides in *Pseudomonas aeruginosa*. *Mol. Microbiol.* **50**:205–217.
- Medalia O, Englander J, Guckenberger R, Sperling J. (2001). AFM imaging in solution of protein-DNA complexes formed on DNA anchored to a gold surface. *Ultramicroscopy* **90**(2-3):103-12
- Meier C, Wu Y, Pramanik G, Weil T. (2014). Self-assembly of high molecular weight polypeptide copolymers studied via diffusion limited aggregation. *Biomacromolecules* **15**(1):219-27.
- Melo MN, Ferre R, Castanho MA. (2009). Antimicrobial peptides: linking partition, activity and high membrane-bound concentrations. *Nat Rev Microbiol.* **7**(3):245-50.
- Mishra NN, Bayer AS. (2013) Correlation of cell membrane lipid profiles with daptomycin resistance in methicillin-resistant *Staphylococcus aureus*. *Antimicrob Agents Chemother.* **57**(2):1082-5.

Miteva M, Andersson M, Karshikoff A, Otting G. (1999). Molecular electroporation: a unifying concept for the description of membrane pore formation by antibacterial peptides, exemplified with NK-lysin. *FEBS Lett* **462**:155–8.

Miyashita M, Sakai A, Matsushita N, Hanai Y, Nakagawa Y, Miyagawa H. (2010). A novel amphipathic linear peptide with both insect toxicity and antimicrobial activity from the venom of the scorpion *Isometrus maculatus*. *Biosci Biotechnol Biochem.* **74**:364-369.

Moerman LFA, Bosteels S, Noppe W, Willems J, Clynen E, Schoofs L, Thevissen K, Tytgat J, Van Eldere J, van der Walt J, Verdonck F. (2002). Antibacterial and antifungal properties of alpha-helical, cationic peptides in the venom of scorpions from southern Africa. *Eur J Biochem.* **269**: 4799-4810.

Morita S, Weisendanger R, Meyer E, Giessibl F. (2002). Noncontact atomic force microscopy. Berlin: Springer.

Morris CJ, Beck K, Fox MA, Ulaeto D, Clark GC, Gumbleton M. (2012). Pegylation of antimicrobial peptides maintains the active peptide conformation, model membrane interactions, and antimicrobial activity while improving lung tissue biocompatibility following airway delivery. *Antimicrob. Agents Chemother.* **56**(6):3298e3308.

Mygind PH, Fischer RL, Schnorr KM, Hansen MT, Sonksen CP, Ludvigsen S, Raventos D, Buskov S, Christensen B, De Maria L, Taboureau O, Yaver D, Elvig-Jørgensen SG, Sørensen MV, Christensen BE, Kjaerulff S, Frimodt-Møller N, Lehrer RI, Zasloff M, Kristensen HH. (2005). Plectasin is a peptide antibiotic with therapeutic potential from a saprophytic fungus. *Nature* **437**(7061): 975e980.

- Nair DG, Fry BG, Alewood P, Kumar PP, Kini RM. (2007). Antimicrobial activity of omwaprin, a new member of the waprin family of snake venom proteins. *Biochem J.* **402**(1):93-104.
- Nannini E, Murray BE, Arias CA. (2010). Resistance or decreased susceptibility to glycopeptides, daptomycin, and linezolid in methicillin-resistant *Staphylococcus aureus*. *Curr Opin Pharmacol.* **10**(5):516-21.
- Nguyen KT, Le Clair SV, Ye S, Chen Z. (2009). Molecular interactions between magainin 2 and model membranes in situ. *J Phys Chem B.* **113**(36):12358-63.
- Nicolas P. (2009). Multifunctional host defense peptides: intracellular-targeting antimicrobial peptides. *FEBS Journal* **276**(22):6483-96.
- Nie Y, Zeng XC, Yang Y, Luo F, Luo X, Wu S, Zhang L, Zhou J. (2012). A novel class of antimicrobial peptides from the scorpion *Heterometrus spinifer*. *Peptides* **38**:389-94.
- Noinville S, Bruston F, El Amri C, Baron D, Nicolas P. (2003). Conformation, orientation, and adsorption kinetics of dermaseptin B2 onto synthetic supports at aqueous/solid interface. *Biophys J.* **85**(2):1196-206.
- Nomura K, Corzo G, Nakajima T, Iwashita T. (2004). Orientation and pore-forming mechanism of a scorpion pore-forming peptide bound to magnetically oriented lipid bilayers. *Biophys J.* **87**:2497-2507.
- Nomura K, Ferrat G, Nakajima T, Darbon H, Iwashita T, Corzo G. (2005). Induction of morphological changes in model lipid membranes and the mechanism of membrane disruption by a large scorpion-derived pore-forming peptide. *Biophys J.* **89**:4067-4080.

- Oguiura N, Boni-Mitake M, Affonso R, Zhang G. (2011). In vitro antibacterial and haemolytic activities of crotamine, a small basic myotoxin from rattlesnake *Crotalus durissus*. *J Antibiot.* **64**(4):327-31.
- Oppegård C, Rogne P, Emanuelsen L, Kristiansen PE, Fimland G, Nissen-Meyer J. (2007). The two-peptide class II bacteriocins: structure, production, and mode of action. *J Mol Microbiol Biotechnol.* **13**(4):210-9.
- Oren Z, Hong J, Shai Y. (1997). A repertoire of novel antibacterial diastereomeric peptides with selective cytolytic activity. *J. Biol. Chem.* **272**(23): 14643e14649.
- Osipov AV, Kasheverov IE, Makarova YV, Starkov VG, Vorontsova OV, Ziganshin RKh, Andreeva TV, Serebryakova MV, Benoit A, Hogg RC, Bertrand D, Tsetlin VI, Utkin YN. (2008). Naturally occurring disulfide-bound dimers of three-fingered toxins: a paradigm for biological activity diversification. *J Biol Chem.* **283**(21):14571-80.
- Otto M. (2009). Bacterial sensing of antimicrobial peptides. *Contrib Microbiol.* **16**:136-49.
- Ouberai MM, Wang J, Swann MJ, Galvagnion C, Guilliams T, Dobson CM, Welland ME. (2013). α -Synuclein senses lipid packing defects and induces lateral expansion of lipids leading to membrane remodeling. *J Biol Chem.* **288**(29):20883-95.
- Oukkache N, Chgoury F, Lalaoui M, Cano AA, Ghalim N. (2013). Comparison between two methods of scorpion venom milking in Morocco. *J Venom Anim Toxins Incl Trop Dis.* **19**(1):5.

Padilla E, Llobet E, Doménech-Sánchez A, Martínez-Martínez L, Bengoechea JA, Albertí S. (2010). *Klebsiella pneumoniae* AcrAB efflux pump contributes to antimicrobial resistance and virulence. *Antimicrob Agents Chemother.* **54**(1):177-83.

Páramo L, Lomonte B, Pizarro-Cerdá J, Bengoechea JA, Gorvel JP, Moreno E. (1998). Bactericidal activity of Lys49 and Asp49 myotoxic phospholipases A2 from *Bothrops asper* snake venom--synthetic Lys49 myotoxin II-(115-129)-peptide identifies its bactericidal region. *Eur J Biochem.* **253**(2):452-61.

Park CB, Kim HS, Kim SC. (1998). Mechanism of action of the antimicrobial peptide buforin II: buforin II kills microorganisms by penetrating the cell membrane and inhibiting cellular functions.. *Biochem Biophys Res Commun.* **244**(1):253-7.

Park CB, Yi KS, Matsuzaki K, Kim MS, Kim SC. (2000). Structure-activity analysis of buforin II, a histone H2A-derived antimicrobial peptide: the proline hinge is responsible for the cell-penetrating ability of buforin II. *Proc Natl Acad Sci USA* **97**(15):8245-50.

Park Y, Hahm KS. (2005) Antimicrobial peptides (AMPs): peptide structure and mode of action. *J Biochem Mol Biol.* **38**(5):507-16.

Parra-Lopez C, Baer MT, Groisman EA. (1993). Molecular genetic analysis of a locus required for resistance to antimicrobial peptides in *Salmonella typhimurium*. *EMBO J.* **12**(11):4053-62

Pathak N, Salas-Auvert R, Ruche G, Janna MH, McCarthy D, Harrison RG. (1995). Comparison of the effects of hydrophobicity, amphiphilicity, and alpha-helicity on the activities of antimicrobial peptides. *Proteins* **22**(2):182-6.

Peigneur S, Orts DJ, Prieto da Silva AR, Oguiura N, Boni-Mitake M, de Oliveira EB, Zaharenko AJ, de Freitas JC, Tytgat J. (2012). Crotonamine pharmacology

- revisited: novel insights based on the inhibition of KV channels. *Mol Pharmacol.* **82**(1):90-6.
- Peigneur, S, Sevcik, C, Tytgat, J, Castillo, C, D'Suze, G., (2012). Subtype specificity interaction of bactridines with mammalian, insect and bacterial sodium channels under voltage clamp conditions. *FEBS Journal* **279**:4025-38.
- Perron GG, Zasloff M, Bell G. (2006). Experimental evolution of resistance to an antimicrobial peptide. *Proc Biol Sci.* **273**(1583):251-6.
- Peschel A, Collins LV. (2001). *Staphylococcal* resistance to antimicrobial peptides of mammalian and bacterial origin. *Peptides* **22**(10):1651-9.
- Pfeifer Y, Cullik A, Witte W. (2010). Resistance to cephalosporins and carbapenems in Gram-negative bacterial pathogens. *Int J Med Microbiol.* **300**(6):371-9.
- Piantavigna S, McCubbin GA, Boehnke S, Graham B, Spiccia L, Martin LL. (2011). A mechanistic investigation of cell-penetrating Tat peptides with supported lipid membranes. *Biochim Biophys Acta.* **1808**(7):1811-7.
- Pieta P, Mirza J, Lipkowski J. (2012). Direct visualization of the alamethicin pore formed in a planar phospholipid matrix. *Proc Natl Acad Sci U S A.* **109**(52):21223-7.
- Pokorny A, Almeida PFF. (2004). Kinetics of dye efflux and lipid flip-flop induced by d-lysine in phosphatidylcholine vesicles and the mechanism of graded release by amphipathic, α -helical peptides. *Biochemistry* **43**:8846–57.
- Pokorny A, Birkbeck TH, Almeida PFF. (2002). Mechanism and kinetics of d-lysine interaction with phospholipid vesicles. *Biochemistry* **41**:11044–56.

- Polyakov P, Soussen C, Duan J, Duval JF, Brie D, Francius G. (2011). Automated force volume image processing for biological samples. *PLoS One* **6**(4):e18887.
- Porrero MC, Wassenaar TM, Gómez-Barrero S, García M, Bárcena C, Alvarez J, Sáez-Llorente JL, Fernández-Garayzábal JF, Moreno MA, Domínguez L. 2007. Detection of methicillin-resistant *Staphylococcus aureus* in Iberian pigs. *Lett Appl Microbiol.* **54**(4):280-5.
- Powers JP, Hancock RE. (2003). The relationship between peptide structure and antibacterial activity. *Peptides* **24**(11):1681-91.
- Pozo Navas B, Lohner K, Deutsch G, Sevcsik E, Riske KA, Dimova R, et al. (2005). Composition dependence of vesicle morphology and mixing properties in a bacterial model membrane system. *Biochim Biophys Acta* **1716**:40–8.
- Prenner EJ, Lewis RNAH, McElhaney RN. (1999). The interaction of the antimicrobial peptide gramicidin S with lipid bilayer model and biological membranes. *Biochim Biophys Acta* **1462**:201–21.
- Prenner EJ, Lewis RNAH, Neuman KC, Gruner SM, Kondejewski LH, Hodges RS, (1997) Nonlamellar phases induced by the interaction of gramicidin S with lipid bilayers. A possible relationship to membrane-disrupting activity. *Biochemistry* **36**:7906–16.
- Rádis-Baptista G, Kerkis I. (2011). Crotonamine, a small basic polypeptide myotoxin from rattlesnake venom with cell-penetrating properties. *Curr Pharm Des.* **38**:4351-61.
- Rádis-Baptista G, Moreno FB, de Lima Nogueira L, Martins AM, de Oliveira Toyama D, Toyama MH, Cavada BS, de Azevedo WF Jr, Yamane T. (2006).

- Crotacetin, a novel snake venom C-type lectin homolog of convulxin, exhibits an unpredictable antimicrobial activity. *Cell Biochem Biophys*. **44**(3):412-23.
- Rahaman A, Lazaridis T. (2014). A thermodynamic approach to alamethicin pore formation. *Biochim Biophys Acta*. **1838**(5):1439-47.
- Rajagopalan N, Pung YF, Zhu YZ, Wong PT, Kumar PP, Kini RM. (2007). Beta-cardiotoxin: a new three-finger toxin from *Ophiophagus hannah* (king cobra) venom with beta-blocker activity. *FASEB J*. **21**(13):3685-95.
- Rakowska PD, Jiang H, Ray S, Pyne A, Lamarre B, Carr M, Judge PJ, Ravi J, Gerling UI, Koksche B, Martyna GJ, Hoogenboom BW, Watts A, Crain J, Grovenor CR, Ryadnov MG. (2013). Nanoscale imaging reveals laterally expanding antimicrobial pores in lipid bilayers. *Proc Natl Acad Sci USA* **110**(22):8918-23.
- Ramanathan B, Davis EG, Ross CR, Blecha F. (2002). Cathelicidins: microbicidal activity, mechanisms of action, and roles in innate immunity. *Microbes Infect*. **4**(3):361-72.
- Rao XC, Li S, Hu JC, Jin XL, Hu XU, Huang JJ, Chen ZJ, Zhu JM. (2004). HuA novel carrier molecule for high-level expression of peptide antibiotics in *Escherichia coli* Protein Expr. Purif. **36**:11–18.
- Ratledge C, Wilkinson E SG. (1988) *Microbial lipids*, **3rd ed.**, vol. 1. London: Academic Press.
- Reißer S, Strandberg E, Steinbrecher T, Ulrich AS. (2014). 3D Hydrophobic Moment Vectors as a Tool to Characterize the Surface Polarity of Amphiphilic Peptides. *Biophysical Journal* **106**(11): 2385-2394.

- Richards SM, Strandberg KL, Conroy M, Gunn JS. (2012). Cationic antimicrobial peptides serve as activation signals for the *Salmonella Typhimurium* PhoPQ and PmrAB regulons in vitro and in vivo. *Front Cell Infect Microbiol.* **27**:2-102.
- Rizzi CT, Carvalho-de-Souza JL, Schiavon E, Cassola AC, Wanke E, Troncone LR. (2007). Crotonamine inhibits preferentially fast-twitching muscles but is inactive on sodium channels. *Toxicon* **50**(4):553-62.
- Rochet JC, Lansbury PT Jr. (2000). Amyloid fibrillogenesis: themes and variations. *Curr Opin Struct Biol.* **10**(1):60-8.
- Rodahl M, Höök F, Fredriksson C, Keller CA, Krozer A, Brzezinski P, Voinova M, Kasemo B. (1997). Simultaneous frequency and dissipation factor QCM measurements of biomolecular adsorption and cell adhesion. *Faraday Discuss.* **107**:229-46.
- Rodríguez A, Villegas E, Montoya-Rosales A, Rivas-Santiago B, Corzo G. (2014). Characterization of antibacterial and haemolytic activity of synthetic pandinin 2 variants and their inhibition against *Mycobacterium tuberculosis*. *PLoS One* **9**(7):e101742.
- Rodríguez A, Villegas E, Satake H, Possani LD, Corzo G. (2011). Amino acid substitutions in an alpha-helical antimicrobial arachnid peptide affect its chemical properties and biological activity towards pathogenic bacteria but improves its therapeutic index. *Amino Acids* **40**(1):61-8.
- Rokyta DR, Lemmon AR, Margres MJ, Aronow K.. (2012). The venom-gland transcriptome of the eastern diamondback rattlesnake (*Crotalus adamanteus*). *BMC Genomics* **16**:13:312.

Roversi D, Luca V, Aureli S, Park Y, Mangoni ML, Stella L. (2014). How many antimicrobial peptide molecules kill a bacterium? The case of PMAP-23. *ACS Chem Biol.* **9**(9):2003-7.

Rozek A, Friedrich CL, Hancock RE. (2000). Structure of the bovine antimicrobial peptide indolicidin bound to dodecylphosphocholine and sodium dodecyl sulfate micelles. *Biochemistry* **39**(51):15765-74.

Ruiming Z, Yibao M, Yawen H, Zhiyong D, Yingliang W, Zhijian C, Wenxin L. (2010). Comparative venom gland transcriptome analysis of the scorpion *Lychas mucronatus* reveals intraspecific toxic gene diversity and new venomous components. *BMC Genomics* **11**:452.

Rydberg HA, Kunze A, Carlsson N, Altgärde N, Svedhem S, Nordén B. (2014). Peptide-membrane interactions of arginine-tryptophan peptides probed using quartz crystal microbalance with dissipation monitoring. *Eur Biophys J.* **43**(6-7):241-53.

Saito HE, Harp JR, Fozo EM. (2014). Incorporation of Exogenous Fatty Acids Protects *Enterococcus faecalis* from Membrane-Damaging Agents. *Appl Environ Microbiol.* **80**(20):6527-38.

Samel M, Vija H, Kurvet I, Künnis-Beres K, Trummal K, Subbi J, Kahru A, Siigur J. (2013). Interactions of PLA2-s from *Vipera lebetina*, *Vipera berus berus* and *Naja naja oxiana* venom with platelets, bacterial and cancer cells. *Toxins (Basel).* **5**(2):203-23.

Samy RP, Kandasamy M, Gopalakrishnakone, P Stiles BG, Rowan EG, Becker D, Shanmugam MK, Sethi G, Chow VT. (2014). Wound healing activity and mechanisms of action of an antibacterial protein from the venom of the eastern diamondback rattlesnake (*Crotalus adamanteus*). *PLoS One* **9**(2):e80199.

Samy RP, Stiles BG, Gopalakrishnakone P, Chow VT. (2011). Antimicrobial proteins from snake venoms: direct bacterial damage and activation of innate immunity against *Staphylococcus aureus* skin infection. *Curr Med Chem.* **18**(33):5104-13.

Sánchez-Vásquez L, Silva-Sanchez J, Jiménez-Vargas JM, Rodríguez-Romero A, Muñoz-Garay C, Rodríguez MC, Gurrola GB, Possani LD. (2013). Enhanced antimicrobial activity of novel synthetic peptides derived from vejovine and hadrurin. *Biochim Biophys Acta* **1830**(6):3427-36.

Santamaría C, Larios S, Angulo Y, Pizarro-Cerda J, Gorvel JP, Moreno E, Lomonte B. (2005a). Antimicrobial activity of myotoxic phospholipases A2 from crotalid snake venoms and synthetic peptide variants derived from their C-terminal region. *Toxicon* **45**(7):807-15.

Santamaría C, Larios S, Quirós S, Pizarro-Cerda J, Gorvel JP, Lomonte B, Moreno E. (2005b). Bactericidal and antiendotoxic properties of short cationic peptides derived from a snake venom Lys49 phospholipase A2. *Antimicrob Agents Chemother.* **49**(4):1340-5.

Schittek B, Hipfel R, Sauer B, Bauer J, Kalbacher H, Stevanovic S, Schirle M, Schroeder K, Blin N, Meier F, Rassner G, Garbe C. (2001). Dermcidin: a novel human antibiotic peptide secreted by sweat glands. *Nat Immunol.* **2**(12):1133-7.

Selsted ME, Novotny MJ, Morris WL, Tang YQ, Smith W, Cullor JS. (1992). Indolicidin, a novel bactericidal tridecapeptide amide from neutrophils. *J Biol Chem.* **267**(7):4292-5.

- Sengupta D, Leontiadou H, Mark AE, Marrink SJ. (2008). Toroidal pores formed by antimicrobial peptides show significant disorder. *Biochim Biophys Acta*. **1778**(10):2308-17.
- Shafer WM, Qu X, Waring AJ, Lehrer RI. (1998). Modulation of *Neisseria gonorrhoeae* susceptibility to vertebrate antibacterial peptides due to a member of the resistance/nodulation/division efflux pump family. *Proc Natl Acad Sci USA* **95**(4):1829-33.
- Shai Y. (1999). Mechanism of the binding, insertion and destabilization of phospholipid bilayer membranes by alpha-helical antimicrobial and cell non-selective membrane-lytic peptides. *Biochim Biophys Acta* **1462**(1-2):55-70.
- Shin SY, Kang JH, Jang SY, Kim Y, Kim KL, Hahm KS. (2000). Effects of the hinge region of cecropin A(1-8)-magainin 2(1-12), a synthetic antimicrobial peptide, on liposomes, bacterial and tumor cells. *Biochim Biophys Acta* **1463**(2):209-18.
- Sieber M, Bosch B, Hanke W, Fernandes de Lima VM. (2014). Membrane-modifying properties of crotamine, a small peptide-toxin from *Crotalus durissus terrificus* venom. *Biochim Biophys Acta*. **1840**(3):945-50.
- Silver L. (2011). Challenges of Antibacterial Discovery. *Clin. Microbiol. Rev.* **24**(1):71-109.
- Silver LL, Bostian KA. (1993). Discovery and development of new antibiotics: the problem of antibiotic resistance. *Antimicrob Agents Chemother.* **37**(3):377-83.
- Smith VJ. (2011). Phylogeny of whey acidic protein (WAP) four-disulfide core proteins and their role in lower vertebrates and invertebrates. *Biochem Soc Trans.* **39**(5):1403-8.

- Snyder AB and Worobo RW. (2014). Chemical and genetic characterization of bacteriocins: antimicrobial peptides for food safety. *J Sci Food Agric.* **94**(1):28-44.
- St Pierre L, Earl ST, Filippovich I, Sorokina N, Masci PP, De Jersey J, Lavin MF. (2008). Common evolution of waprin and kunitz-like toxin families in Australian venomous snakes. *Cell Mol Life Sci.* **65**(24):4039-54.
- Strandberg E, Wadhvani P, Tremouilhac P, Dürr UH, Ulrich AS. (2006). Solid-state NMR analysis of the PGLa peptide orientation in DMPC bilayers: structural fidelity of 2H-labels versus high sensitivity of 19F-NMR. *Biophys J.* **90**(5):1676-86.
- Strandberg E., Deniz T., Ieronimo M., Kanithasen N., Wadhvani P, Ulrich A. (2007) Influence of C-terminal amidation on the antimicrobial and hemolytic activities of cationic α -helical peptides. *Pure Appl. Chem.* **79**(4):717-28.
- Straus SK, Hancock RE. (2006). Mode of action of the new antibiotic for Gram-positive pathogens daptomycin: comparison with cationic antimicrobial peptides and lipopeptides. *Biochim Biophys Acta.* **1758**(9):1215-23.
- Subbalakshmi C, Sitaram N. (1998). Mechanism of antimicrobial action of indolicidin. *FEMS Microbiol Lett.*; **160**(1):91-6.
- Sun Z, Zhong J, Liang X, Liu J, Chen X, Huan L. (2009). Novel mechanism for nisin resistance via proteolytic degradation of nisin by the nisin resistance protein NSR. *Antimicrob Agents Chemother.* **53**(5):1964-73.
- Sutherland I. (2001). Biofilm exopolysaccharides: a strong and sticky framework. *Microbiology.* **147**(1):3-9.

- Tachi T, Epand RF, Epand RM, Matsuzaki K. (2002). Position-dependent hydrophobicity of the antimicrobial magainin peptide affects the mode of peptide-lipid interactions and selective toxicity. *Biochemistry*. **41**(34):10723-31.
- Teixeira V, Feio MJ, Bastos M. (2012). Role of lipids in the interaction of antimicrobial peptides with membranes. *Prog Lipid Res*. **51**(2):149-77.
- Teixeira V, Feio MJ, Rivas L, De la Torre BG, Andreu D, Coutinho A. (2010) Influence of lysine Ne-trimethylation and lipid composition on the membrane activity of the cecropin A-melittin hybrid peptide CA(1–7)M(2–9). *J Phys Chem B* **114**:16198–208.
- Terzi E, Hölzemann G, Seelig J. (1994). Alzheimer beta-amyloid peptide: electrostatic interactions with phospholipid membranes. *Biochemistry* **33**(23):7434-41.
- Thuy HT, Nga le P, Loan TT. (2014). Antibiotic contaminants in coastal wetlands from Vietnamese shrimp farming. *Environ Sci Pollut Res Int*. **18**(6):835-41.
- Torres-Larios, A., Gurrola, G.B., Zamudio, F.Z., Possani, L.D., (2000). Hadrurin, a new antimicrobial peptide from the venom of the scorpion *Hadrurus aztecus*. *Eur. J. Biochem*. **267**:5023-5031.
- Tossi A, Sandri L, Giangaspero A. (2000). Amphipathic, alpha-helical antimicrobial peptides. *Biopolymers* **55**(1):4-30.
- Toyama MH, de Oliveira DG, Beriam LO, Novello JC, Rodrigues-Simioni L, Marangoni S. (2003). Structural, enzymatic and biological properties of new PLA(2) isoform from *Crotalus durissus terrificus* venom. *Toxicon* **41**(8):1033-8.

Trache A & Meininger GA. (2005). Atomic force-multi-optical imaging integrated microscope for monitoring molecular dynamics in live cells. *Journal of Biomedical Optics* **10**(6): 064023.

Tresset G. (2009). The multiple faces of self-assembled lipidic systems. *PMC Biophys.* **2**:3-14.

Tsargorodska A. (2007). Research and development in optical biosensors for determination of toxic environmental pollutants. PhD Thesis. Sheffield Hallam University: UK.

Tsubery H, Ofek I, Cohen S, Fridkin M. Structure activity relationship study of polymyxin B nonapeptide. *Adv Exp Med Biol.* **479**:219-22.

Tsukimori A, Nakamura I, Okamura S, Sato A, Fukushima S, Mizuno Y, Yamaguchi T, Matsumoto T. (2014). First case report of vancomycin-intermediate sequence type 72 *Staphylococcus aureus* with nonsusceptibility to daptomycin. *BMC Infect Dis.* **23**(14):459-65.

Uawonggul N, Thammasirirak S, Chaveerach A, Arkaravichien T, Bunyatratthata W, Ruangjirachuporn W, Jearranaipreame P, Nakamura T, Matsuda M, Kobayashi M, Hattori S, Daduang S. (2007). Purification and characterization of Heteroscorpine-1 (HS-1) toxin from *Heterometrus laoticus* scorpion venom. *Toxicon* **49**:19-29.

Uematsu N, Matsuzaki K. (2000). Polar angle as a determinant of amphipathic alpha-helix-lipid interactions: a model peptide study. *Biophys J.* **79**(4):2075-83.

Ulvatne H, Haukland HH, Samuelson Ø, Krämer M, Vorland LH.(2002). Proteases in *Escherichia coli* and *Staphylococcus aureus* confer reduced susceptibility to lactoferricin B. *J Antimicrob Chemother.* **50**(4):461-7.

Urban A, Eckermann S, Fast B, Metzger S, Gehling M, Ziegelbauer K, Rübsamen-Waigmann H, Freiberg C. (2007). Novel whole-cell antibiotic biosensors for compound discovery. *Appl Environ Microbiol.* **73**(20):6436-43.

Vamparys L, Gautier R, Vanni S, Bennett W F, Tieleman DP, Antony B, Etchebest C, Fuchs PF. (2013) Conical lipids in flat bilayers induce packing defects similar to that induced by positive curvature. *Biophys. J.* **104**:585–593.

Van den Bogaard AE, Stobberingh EE. (1999) Antibiotic usage in animals: impact on bacterial resistance and public health. *Drugs.* **158**(4):589-607.

Van Hal SJ, Paterson DL, Gosbell IB. (2011). Emergence of daptomycin resistance following vancomycin-unresponsive *Staphylococcus aureus* bacteraemia in a daptomycin-naïve patient--a review of the literature. *Eur J Clin Microbiol Infect Dis.* **30**(5):603-10.

Vanni S, Vamparys L, Gautier R, Drin G, Etchebest C, Fuchs PF, Antony B. (2013). Amphipathic lipid packing sensor motifs: probing bilayer defects with hydrophobic residues. *Biophys J.* **104**(3):575-84.

Veal WL, Yellen A, Balthazar JT, Pan W, Spratt BG, Shafer WM. (1998). Loss-of-function mutations in the mtr efflux system of *Neisseria gonorrhoeae*. *Microbiology* **144**(3):621-7.

Vidovic V, Prongidi-Fix L, Bechinger B, Werten S. (2009) Production and isotope labeling of antimicrobial peptides in *Escherichia coli* by means of a novel fusion partner that enables high-yield insoluble expression and fast purification *J. Pept. Sci.* **15**:278–284.

Viljoen CC, Botes DP, Kruger H. (1982). Isolation and amino acid sequence of caudoxin, a presynaptic acting toxic phospholipase A₂ from the venom of the horned puff adder (*Bitis caudalis*). **20**(4):715-37.

Von Delwig, A., Altmann, D.M., Isaacs, J.D., Harding, C.V., Holmdahl, R., McKie, N., Robinson, J.H., (2006). The impact of Glycosylation on HLADR1-restricted T Cell Recognition of Type II Collagen in a Mouse Model. **54**(2):482e491.

Vulfius CA, Gorbacheva EV, Starkov VG, Osipov AV, Kasheverov IE, Andreeva TV, Astashev ME, Tsetlin VI, Utkin YN. (2011). An unusual phospholipase A₂ from puff adder *Bitis arietans* venom--a novel blocker of nicotinic acetylcholine receptors. *Toxicon* **57**(5):787-93.

Wade D, Boman A, Wåhlin B, Drain CM, Andreu D, Boman HG, Merrifield RB. (1990). All-D amino acid-containing channel-forming antibiotic peptides. *PNAS* **87**(12):4761-65.

Wadhvani P, Epand RF, Heidenreich N, Bürck J, Ulrich AS, Epand RM. (2012). Membrane-active peptides and the clustering of anionic lipids. *Biophys J.* **103**(2):265-74.

Walsh F. (2014a). Antibiotic resistance: Cameron warns of medical 'dark ages'. (online). BBC news. Available at: <http://www.bbc.co.uk/news/health-28098838>. (Last accessed 1st March 2015).

Walsh F. (2014b). Antibiotics resistance 'as big a risk as terrorism' - medical chief. (online). BBC news. Available at: <http://www.bbc.co.uk/news/health-21737844>. (Last accessed 1st March 2015).

- Wang XJ, Wang XM, Teng D, Zhang Y, Mao RY, Wang JH. (2014). Recombinant production of the antimicrobial peptide NZ17074 in *Pichia pastoris* using SUMO3 as a fusion partner. *Lett Appl Microbiol.* **59**(1):71-8.
- Wang Y, Hong J, Liu X, Yang H, Liu R, Wu J, Wang A, Lin D, Lai R. (2008). Snake cathelicidin from *Bungarus fasciatus* is a potent peptide antibiotics. *PLoS One.* **16**(9):e3217.
- Wen YL, Wu BJ, Kao PH, Fu YS, Chang LS. (2012). Antibacterial and membrane-damaging activities of β -bungarotoxin B chain. *J Pept Sci.* **19**(1):1-8.
- Wieprecht T, Dathe M, Beyermann M, Krause E, Maloy WL, MacDonald DL, Bienert M. (1997). Peptide hydrophobicity controls the activity and selectivity of magainin 2 amide in interaction with membranes. *Biochemistry* **36**(20):6124-32.
- Wimley WC. (2011). Describing the mechanism of antimicrobial peptide action with the interfacial activity model. *ACS Chem Biol* **5**:905-17.
- Witten TA Jr, Sander LM. (1981). Diffusion-Limited Aggregation, a Kinetic Critical Phenomenon. *Phys. Rev. Lett.* **47**:1400.
- Witten TA Jr, Sander LM. (1983). Diffusion-limited aggregation. *Phys. Rev Lett.* **27**:5686.
- Won A, Khan M, Gustin S, Akpawu A, Seebun D, Avis TJ, Leung BO, Hitchcock AP, Ianoul A. (2011). Investigating the effects of L- to D-amino acid substitution and deamidation on the activity and membrane interactions of antimicrobial peptide anoplin. *Biochim Biophys Acta* **1808**(6):1592-600.
- Woodford 1, Livermore DM. (2009). Infections caused by Gram-positive bacteria: a review of the global challenge. *J Infect.* **59**(1):S4-16.

- Woodford N, Ellington MJ. (2007). The emergence of antibiotic resistance by mutation. *Clin Microbiol Infect.*13(1):5-18.
- World Health Organisation (WHO). (2014). ANTIMICROBIAL RESISTANCE Global Report on Surveillance. France: Paris.
- Wu M, Maier E, Benz R, Hancock REW. (1999). Mechanism of interaction of different classes of cationic antimicrobial peptides with planar bilayers and with the cytoplasmic membrane of *Escherichia coli*. *Biochemistry* **38**:7235–42.
- Wu S, Nie Y, Zeng XC, Cao H, Zhang L, Zhou L, Yang Y, Luo X, Liu Y. (2014). Genomic and functional characterization of three new venom peptides from the scorpion *Heterometrus spinifer*. *Peptides*,doi: 10.1016/j.peptides.2013.12.012.
- Wu T, Tang D, Chen W, Huang H, Wang R, Chen Y. (2013). Expression of antimicrobial peptides thanatin(S) in transgenic Arabidopsis enhanced resistance to phytopathogenic fungi and bacteria. *Gene*. **527**(1):235-42.
- Yamaguchi S, Huster D, Waring A, Lehrer RI, Kearney W, Tack BF, Hong M. (2001). Orientation and dynamics of an antimicrobial peptide in the lipid bilayer by solid-state NMR spectroscopy. *Biophys J*. **81**(4):2203-14.
- Yang SC, Lin CH, Sung CT, Fang JY. (2014). Antibacterial activities of bacteriocins: application in foods and pharmaceuticals. *Front Microbiol*. **26**(5):241.
- Yang SJ, Kreiswirth BN, Sakoulas G, Yeaman MR, Xiong YQ, Sawa A, Bayer AS. (2009). Enhanced expression of dltABCD is associated with the development of daptomycin nonsusceptibility in a clinical endocarditis isolate of *Staphylococcus aureus*. *J Infect Dis*. **200**(12):1916-20.

- Yeaman MR, Yount NY. (2003). Mechanisms of antimicrobial peptide action and resistance. *Pharmacol Rev.* **55**(1):27-55.
- Yi GS, Park CB, Kim SC, Cheong C. (1996). Solution structure of an antimicrobial peptide buforin II. *FEBS Lett.* **398**(1):87-90.
- Yonezawa A, Sugiura Y. (1992). Tachyplesin I as a model peptide for antiparallel beta-sheet DNA binding motif. *Nucleic Acids Symp Ser.* **27**:161-2.
- Yount NY, Kupferwasser D, Spisni A, Dutz SM, Ramjan ZH, Sharma S, Waring AJ, Yeaman MR.(2009). Selective reciprocity in antimicrobial activity versus cytotoxicity of hBD-2 and crotamine. *Proc Natl Acad Sci USA* **106**(35):14972-7
- Yuan W, Cao L, Ma Y, Mao P, Wang W, Zhao R, Wu Y, Cao Z, Li W. (2010). Cloning and functional characterization of a new antimicrobial peptide gene StCT1 from the venom of the scorpion *Scorpiops tibetanus*. *Peptides* **31**: 22-26.
- Zambidis ET, Scott DW. (1996). Epitope-specific tolerance induction with an engineered immunoglobulin. *Proc Natl Acad Sci USA* **93**(10):5019-24.
- Zanetti M. (2004). The role of cathelicidins in the innate host defenses of mammals. *Curr Issues Mol Biol.* **7**(2):179-96.
- Zasloff M. (1987). Magainins, a class of antimicrobial peptides from *Xenopus* skin: isolation, characterization of two active forms, and partial cDNA sequence of a precursor. *Proc Natl Acad Sci USA* **84**(15):5449-53.
- Zasloff M. (2002). Antimicrobial peptides of multicellular organisms. *Nature.* **415**(70): 389-95.
- Zeng XC, Corzo G, Hahin R. (2005). Scorpion venom peptides without disulfide bridges. *IUBMB Life* **57**: 13–21.

Zeng XC, Li WX, Peng F, Zhu ZH. (2000). Cloning and characterization of a novel cDNA sequence encoding the precursor of a novel venom peptide (BmKbpp) related to a bradykinin-potentiating peptide from Chinese scorpion *Buthus martensii* Karsch. *IUBMB Life* **49**: 207-210.

Zeng XC, Wang S, Nie Y, Zhang L, Luo X. (2012). Characterization of BmKbpp, a multifunctional peptide from the Chinese scorpion *Mesobuthus martensii* Karsch: gaining insight into a new mechanism for the functional diversification of scorpion venom peptides. *Peptides* **33**: 44-51.

Zeng XC, Wang SX, Zhu Y, Zhu SY, Li WX. (2004). Identification and functional characterization of novel scorpion venom peptides with no disulfide bridge from *Buthus martensii* Karsch. *Peptides* **25**: 143-150.

Zeng XC, Zhou L, Shi W, Luo X, Zhang L, Nie Y, Wang J, Wu S, Cao B, Cao H. (2013). Three new antimicrobial peptides from the scorpion *Pandinus imperator*. *Peptides* **45**:28-34.

Zhang M, Li MF, Sun L. (2014). NKLP27: a teleost NK-lysin peptide that modulates immune response, induces degradation of bacterial DNA, and inhibits bacterial and viral infection. *PLoS One* **9**(9):e106543.

Zhang T, Muraih JK, MacCormick B, Silverman J, Palmer M. (2014). Daptomycin forms cation- and size-selective pores in model membranes. *Biochim Biophys Acta* **1838**(10):2425-30.

Zhang T, Muraih JK, Tishbi N, Herskowitz J, Victor RL, Silverman J, Uwumarenogie S, Taylor SD, Palmer M, Mintzer E. (2014). Cardiolipin prevents membrane translocation and permeabilization by daptomycin. 2014. *J Biol Chem.* **289** (17):11584-91.

Zhao H, Gan TX, Liu XD, Jin Y, Lee WH, Shen JH, Zhang Y. (2008). Identification and characterization of novel reptile cathelicidins from elapid snakes. *Peptides* **(10)**:1685-91.

Zhao H, Mattila JP, Holopainen JM, Kinnunen PK. (2001). Comparison of the membrane association of two antimicrobial peptides, magainin 2 and Indolicidin. *Biophys J.* **81**(5):2979-91.

Zhao H, Rinaldi AC, Di Giulio A, Simmaco M, Kinnunen PK. (2002). Interactions of the antimicrobial peptides temporins with model biomembranes. Comparison of temporins B and L. *Biochemistry* **41**(13):4425-36.

Zhao H, Sood R, Jutila A, Bose S, Fimland G, Nissen-Meyer J, Kinnunen PK. (2006). Interaction of the antimicrobial peptide pheromone Plantaricin A with model membranes: implications for a novel mechanism of action. *Biochim Biophys Acta* **1758**(9):1461-74.

Zhao H, Tuominen EK, Kinnunen PK. (2004). Formation of amyloid fibers triggered by phosphatidylserine-containing membranes. *Biochemistry* **43**(32):10302-7.

Zhao Z, Hong W, Zeng Z, Wu Y, Hu K, Tian X, Li W, Cao Z. (2012). Mucroporin-M1 inhibits hepatitis B virus replication by activating the mitogen-activated protein kinase (MAPK) pathway and down-regulating HNF4 α in vitro and in vivo. *J Biol Chem.* **287**(36):30181-90.

Zhao Z, Ma Y, Dai C, Zhao R, Li S, Wu Y, Cao Z, Li W. (2009). Imcroporin, a new cationic antimicrobial peptide from the venom of the scorpion *Isometrus maculatus*. *Antimicrob Agents Chemother* **53**:3472-3477.

Zhou L, Narsimhan G, Wu X, Du F. (2014). Pore formation in 1,2-dimyristoyl-sn-glycero-3-phosphocholine/cholesterol mixed bilayers by low concentrations of antimicrobial peptide melittin. *Colloids Surf B Biointerfaces*. **123**:419-28.

Zhu S, Li W, Jiang D, Zeng X. (2000). Evidence for the existence of insect defensin-like peptide in scorpion venom. *IUBMB Life* **50**:57-61.

Zhu S, Tytgat J. (2004). The scorpine family of defensins: gene structure, alternative polyadenylation and fold recognition. *Cell Mol Life Sci* **61**:1751-1763.

Zhu X, Zhang L, Wang J, Ma Z, Xu W, Li J, Shan A. (2015). Characterization of antimicrobial activity and mechanisms of low amphipathic peptides with different α -helical propensity. *Acta Biomater*. In Press.

Zhu YG, Johnson TA, Su JQ, Qiao M, Guo GX, Stedtfeld RD, Hashsham SA, Tiedje JM. (2013). Diverse and abundant antibiotic resistance genes in Chinese swine farms. *Proc Natl Acad Sci USA* **110**(9):3435-40.

Zweytick D, Tumer S, Blondelle SE, Lohner K. (2008). Membrane curvature stress and antibacterial activity of lactoferricin derivatives. *Biochem Biophys Res Commun*. **369**:395-400.